The oxidative degradation of organic contaminants using a manganese oxide-containing mine waste

Catherine E. Dowding

The Oxidative Degradation of Organic Contaminants using a Manganese Oxide-containing Mine Waste

Catherine E. Dowding

A thesis submitted in partial fulfillment of the requirements for the degree of Doctor of Philosophy

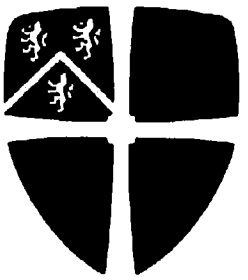

Durham University

School of Engineering
Durham University
November 2008

Abstract

Manganese oxide tailings material, a waste product generated during Mn ore extraction processes in South Africa, has been assessed in terms of its potential to oxidatively breakdown organic contaminants. Azo dyes and polycyclic aromatic hydrocarbons (anthracene) show oxidative interactions with the tailings, resulting in the formation of products which are more environmentally favourable than the parent compound.

Tailings samples from five mines were characterised to establish the redox reactivity of the material. Based on chemical and mineralogical data the tailings were grouped into the carbonate-rich Mamatwan type (MT) tailings (Mamatwan and Gloria mines), the Mn oxide-enriched Wessels type (WT) tailings (Wessels and Nchwaning mines) and the Mn oxide enriched Hotazel type (HT) tailings (Hotazel mine). The tailings are net-alkaline and non acid generating with a point of zero charge below pH 4. The average Mn oxidation state of the three tailings types ranges from 1.2 to 1.5 in the order HT>WT>MT. Despite a low surface area (1.5 to 6.4 $m^2.g^{-1}$) the tailings show a substantial (0.5 to 3.0%) 'easily' reducible, reactive Mn phase as well as a large pool of more recalcitrant dithionite-extractable Mn. Thus the tailings material displays both 'quick and slow release' oxidative capacity.

The oxidative decolorisation of acid azo dyes acid orange 7 (AO 7) and acid yellow 36 (AY 36) by the Mn tailings is highly pH dependent, with increased oxidation occurring at lower pH. The reaction mechanism for the oxidation of AO 7 by the tailings has many similarities to enzymatic degradation of the dye observed with white rot fungi. The reaction, initiated on the phenolic group, occurs via successive one electron transfers from the dye molecule to the Mn oxide. A series of radical reactions occur resulting in the asymmetrical cleavage of the azo bond and the generation of terminal reaction products 1,2 naphthoquinone and 4-hydroxybenzenesulfonate. Attenuated total reflectance Fourier transform infrared spectroscopy (ATR-FTIR) demonstrated that initial sorption of AO 7 is pH dependent and outer-sphere. A pronounced lag phase exists between the initial sorption of the dye to a Mn oxide surface and the initiation of oxidation. This lag phase can indicate that either the transfer of the initial electron is rate limiting or that correct orientation followed by inner-sphere complexation is necessary before oxidation can take place.

The reaction mechanism proposed for the oxidation of AY 36 is initiated at the amino moiety and proceeds via successive, one electron transfers from the dye to the Mn tailings. The reaction pathway involves the formation of a number of colourless intermediate products, some of which hydrolyse in a Mn oxide-independent step. The terminal oxidation products were observed to be *p*-benzoquinone and 3-hydroxybenzenesulfonate.

Light, both UV and ambient, and auxiliary compounds such as acetate buffer and salts did not reduce the decolorisation capacity of the tailings. Increased buffer strength enhanced decolorisation and addition of Na_2SO_4 in the presence of buffer increased the initial oxidation of AO 7. The decolorisation capacity of the Mn tailings showed durability with 90% colour removal observed 60 days after daily dye replenishment.

Drying anthracene-spiked Mn tailings, synthetic Mn oxide and calcite water slurries resulted in anthracene oxidation to anthraquinone (6-30% oxidation). Small but significant (4%) anthracene oxidation was also observed when anthracene spiked water was evaporated from quartz and a clean glass surface. No anthracene oxidation was apparent without the evaporation of water at pH > 5. The HT tailings oxidised up to 30% anthracene when dried, the most substantial oxidation took place below 5% gravimetric water content. Evaporation of anthracene-spiked cyclohexane slurries resulted in the same observed oxidation from both Mn tailings and calcite. It could not be established whether electron transfer was occurring between the Mn oxide phase of the tailings and the anthracene or whether the transformation was solely a surface mediated phenomenon with oxygen being used as the electron acceptor. Under fully hydrated conditions the Mn oxide tailings oxidised 75% of anthracene to anthraquinone at pH values less than 4.5. This would suggest that the Mn tailings can oxidise anthracene and sufficient mineral-contaminant contact can be achieved despite the low water solubility of the compound.

Declaration

I confirm that no part of the material offered has previously been submitted by myself for a degree in this or any other University. Where material has been generated through joint work, the work of others has been indicated.

Catherine E Dowding

Stellenbosch 3 November 2008

Acknowledgements

I would like to thank the following people and institutions for their greatly appreciated contribution to this PhD study:

My supervisor, Dr Karen Johnson, for her enthusiastic guidance and friendship and for her ability to always put things into perspective. My co-supervisor Tony Hutchings for his input during this study. Chris DeJager for his advice and stimulating conversation. Dr Filip Kielar, for his advice and giving up much of his time to help me with instruments.

My financial sponsors BHP Billiton, the Engineering and Physical Science Research Council of the United Kingdom and the South African National Research Foundation.

From the Geography department at Durham University, Frank Davies, Martin West. Amanda Hayten and Neil Tunstall, for their friendly assistance with analyses. Without the help these people and the Geography department much of this research would not have been possible.

From the Chemistry department at Durham University, Dr Sharon Cooper, for allowing me open access to the ATR-FTIR unit. Dr Mike Jones and Dr Lara Turner for LC-MS analysis and Professor David Parker for allowing me access to his UV-visible spectrometer.

In Engineering, my lab mates, Isolina Gonçalves, Janette Tourney and Zak Jarvis, for advice, assistance and baby sitting samples while I was away. Bernie McEleavey and Steve Richardson for assistance with many lab issues and my office mates and fellow postgraduate students for their friendship, stimulating conversation and fun in general!

Ritva Muhlbauer at BHP Billiton, for helping to organise field trips and for always assisting with any information that was needed for the study.

Helen Talbot at Newcastle University for spending many hours helping me with LC-MS analysis.

My family for their love and support and generally being so enthusiastic about manganese. Rob and Marina Clarke, not only for keeping the rusk tin full during the write-up, but also for the advice, encouragement and proof reading services.

Finally to my fiancé Sam Clarke, for embracing my enthusiasm for research and 'rocks', for enduring countless stories of instrument woes, for his invaluable help with document formatting and most of all for his continual encouragement, interest in my work and love.

Table of Contents

List of Figures

List of Tables

Abbreviations

AAS	-	Atiomic absorption spectroscopy
AO 7	-	Acid orange 7
AR 151	-	Acid red 151
AR 88	-	Acid red 88
ATR-FTIR	-	Attenuated total reflectance Fourier transform infrared
AY 36	-	Acid yellow 36
AY 9	-	Acid yellow 9
BET-N_2	-	Burnauer, Emmett and Teller-N_2
BS	-	Benzene sulfonate
CC	-	Calcite
CFSE	-	Crystal field stabilisation energy
DC	-	Dithionite-citrate
DDL	-	Double diffuse layer
DI	-	Deionised water
DOC	-	Dissolved organic carbon
DRIFT	-	Diffuse reflectance infrared Fourier transform
EC	-	Electrical conductivity
EC	-	Effective concentration
EDX	-	Energy dispersive x-ray
ESEM	-	Environmental scanning electron microscope
EU	-	European Union
GC/MS	-	Gas chromatography/mas spectroscopy
HAHC	-	Hydroxylamine Hydrogenchloride
4HBS	-	4-hydroxybenzenesulfonate
HOC	-	Hydrophobic organic compounds
HPLC	-	High pressure liquid chromatography
HQ	-	Hydroquinone
IP	-	Ionisation potential
IR	-	Infrared
IRE	-	Internal reflectance element
LC	-	Lethal concentration
LC-MS	-	Liquid chromatography mass spectroscopy
MO	-	Purchased Mn(III) oxide
MS	-	Mass spectrum
NQ	-	1,2 Napthoquinone
PAHs	-	Polycyclic aromatic hydrocarbons
PZC	-	Point of zero charge
QTZ	-	Quartz
S:L	-	Solid: liquid
[SA]	-	Surface area concentration
SOM	-	Soil organic matter
U.S. EPA	-	United states environmental protection agency
UK	-	United Kingdom
US	-	United States
UV	-	Ultraviolet
UV-vis	-	Ultraviolet-visible
XRD	-	X-ray diffraction

1. Introduction

1.1. Overview

The Kalahari Manganese Fields (KMF), situated in the Northern Cape Province of South Africa represent one of the largest Mn ore deposits in the world, holding up to 80% of the world's Mn reserves. The KMF is host to extensive Mn mining operations, involving both open pit and underground excavations. During the ore extraction process large volumes of fine, Mn oxide-containing tailings are produced. These fines are transported to large tailings dams where they are stored. Under the current South African waste classification system, Mn containing wastes are classified as 'Highly Hazardous' requiring stringent and expensive waste storage and disposal measures. A review conducted on the South African and various international waste classification systems is given in Appendix A. This review highlighted that South Africa's waste classification system is conservative in its approach to Mn containing wastes, with Mn rarely featuring as an element of concern in the EU, Canadian, Australian or US waste classification systems. Due to the local regulation of Mn-containing wastes the large stockpiles of Mn tailings are problematic for the mining companies, however, the oxidising capacity of these Mn oxide containing tailings may provide a valuable resource for the remediation of organically polluted soils and waters. Recycling and re-use of waste is considered a prime objective in waste minimisation practices. Thus finding a use for the stockpiled Mn tailings would form part of integrated waste management encouraged by the South African government's National Waste Management Strategy.

The oxidative breakdown of organic pollutants by Mn oxides is an area of growing interest due to the abundance of Mn oxides in the natural environment. The capacity for Mn oxides to sequester heavy metals in soils has been well established (Murray and Dillard, 1979; Manceau et al., 1987; Manceau et al., 1992; Manceau et al., 2003). For these reasons, Mn oxides have the potential to provide an all round remediation option for sites/waters showing both organic and metal contamination issues.

Manganese oxides are ubiquitous in soils and waters and thus viewed as a natural mediator of soil contamination (Sparks, 2003). Manganese oxides are rarely considered as a water treatment option, as sources of cheap Mn oxides have not previously been accessible. The

South African Mn mining waste consists of clean Mn oxide containing mine tailings which are net-alkaline, non-acid generating and low in trace elements, suggesting they would be suitable for sustainable cost-effective soil and water remediation. This project was initiated to establish the potential of the Mn oxide-containing tailings to act as soil and water remediation agents.

There are numerous types of organic contaminants. For this study acid azo dyes and polycyclic aromatic hydrocarbons (PAHs) were chosen as target contaminants. Azo dyes represent a highly soluble group of organic contaminants, which are problematic in water treatment and PAHs, represent a group of insoluble contaminants problematic in soils. Thus both hydrophilic, water-based and hydrophobic, soil-based contaminants are represented

1.2. Objectives

The overall aim of this project was to establish the capacity of the Mn oxide containing tailings (hereafter referred to as the Mn tailings) to oxidatively breakdown organic pollutants in soils and waters, focusing on acid azo dyes and PAHs. This was achieved by fulfilling the following research objectives:

i) Characterisation of the tailings in terms of their mineralogical, physical and chemical properties, with the aim of assessing their oxidative capacity

ii) Investigating the capacity of the Mn tailings to oxidatively decolorise acid azo dyes and elucidating the underlying reaction mechanisms

iii) Assessing reaction rates associated with Mn oxide mediated azo dye oxidation reactions

iv) Observing real time *in situ* oxidation of an azo dye by Mn oxides using ATR-FTIR.

v) Assessing the effect of auxiliary chemicals on dye decolorisation to determine if the Mn tailings provide a viable treatment option for the decolorisation of textile effluent.

vi) Investigating the capacity of the Mn tailings to oxidise anthracene, under hydrated and dehydrated conditions and establishing the effect of pH on anthracene oxidation.

vii) In addition to the research undertaken, the industrial partners required the generation of a comprehensive review on the regulation of Mn containing wastes. Thus an additional objective was to assess the characterisation of Mn containing wastes in the South African and various international waste management systems.

1.3. Mn oxide mining waste

1.3.1. Kalahari Mn fields

The KMF is situated 60 km northwest of Kuruman in the Northern Cape Province of South Africa (Figure 1-1). The Mn ores are hosted in rocks belonging to the Griqualand West Sequence (part of the Transvaal Supergroup) that occur along the western margin of the ancient Kaapvaal Craton (Viljoen and Reimold, 1999). The primary Kalahari Mn deposit is of sedimentary origin and interbedded with the iron formation from the Hotazel formation. Three Mn beds are present in the Hotazel formation, but only the lower one is extensively mined (Gutzmer and Beukes, 1996).

There are two main Mn ore types present in the KMF (Figure 1-1), the low-grade (30 to 39% wt Mn), diagenetic, carbonate-rich Mamatwan-type ore to the south east and the high-grade (>42% wt Mn), hydrothermally altered oxide-rich Wessels-type ore to the north west (Evans et al., 2001). The Hotazel outlier (Figure 1-1) represents a smaller third ore type and outcrops to the east of the KMF; it contains very high grade ore with a low carbonate content. Mamatwan and Gloria mines fall within the Mamatwan-type ore and Wessels and Nchwaning mines within the Wessels-type ore. Hotazel mine, situated on the Hotazel outlier is no longer operational.

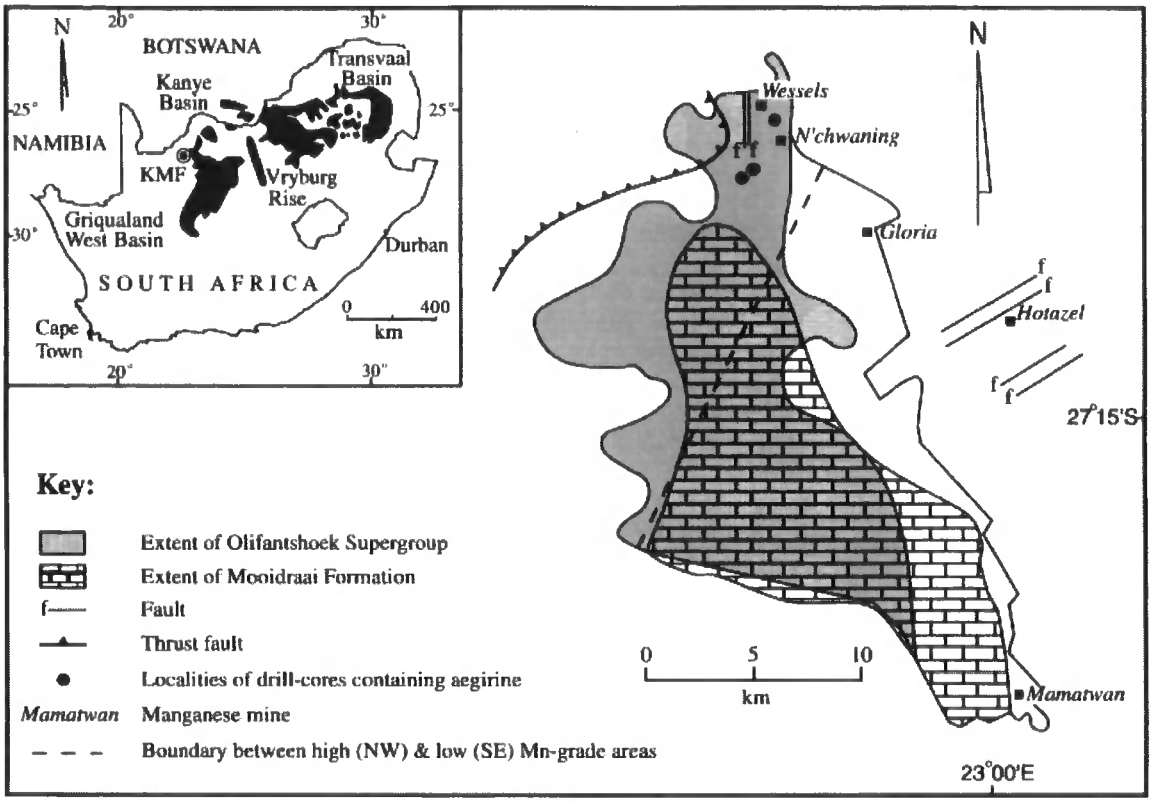

Figure 1-1 Map of South Africa showing geological formations relating to Kalahari Mn fields (KMF) and sampling locations at Mamatwan, Gloria, Wessels, Nchwaning and Hotazel mines taken from Tsikos and Moore (2005)

The tailings, produced during the ore extraction process, are of limited commercial use to the mining companies, due to their small particle size and slightly lower Mn content, and thus are regarded as a waste product of the mining operation. The fine tailings (<200 μm) are transported to tailings dams either in a water slurry (Wessels) or on a conveyor (Mamatwan). There are approximately 1.6 and 1.5 million tons of tailings stored in the Mamatwan and Wessels tailings dams, respectively. Hotazel mine is no longer in operation and the tailings are stockpiled in one of four dumps.

1.4. Regulation of Mn in waste in SA and internationally

A detailed review of Mn in waste and the environment can be found in Appendix A. This section provides only a short comparative summary of the South African, US and EU waste classification schemes.

1.4.1. Toxicological effects of Mn

Manganese is an essential element for physiological plant and human health with adverse health effects observed with Mn deficiencies as well as toxicities. The most common route of human exposure to Mn is through food ingestion. The United States Environmental protection agency (U.S.EPA) suggests an appropriate Reference Dose (RfD) of 10mg Mn/day (U.S.EPA, 1996). Other channels of exposure to Mn are through drinking Mn rich water, inhalation of Mn dust and ingestion of soil containing Mn compounds.

It is thought that inhalation of excessive amounts of Mn dust has the most serious adverse health effect, and at comparable doses it has been shown that more Mn reaches the brain following inhalation than following ingestion (Gianutsos and Murray, 1982; Dorman et al., 2002). Chronic inhalation of Mn containing particulate has been associated with nervous system disorders in a Parkinson-like disease known as manganism (Couper, 1837). In comparison Mn ingested orally has low toxicity and reports of adverse effects by this exposure route are rare (U.S.EPA, 2003).

1.4.2. Ecotoxicological effects of Mn

Ecotoxicological thresholds for Mn in water are lower than that those deemed safe for human consumption. An overall guidance value for the protection of 95% of marine species with 50% confidence was derived at 0.3 $mg.L^{-1}$. The guidance value for freshwater species in soft waters is 0.2 $mg.L^{-1}$ (Concise International Chemical Assessment Document, 2004). It is often the more conservative ecological thresholds that are used in the compilation of waste classification guidelines in South Africa.

There has been a recent announcement by the United Kingdoms' (UK) Environment Agency that there will be no Environmental Quality Standard for Mn for protected freshwaters because the ecotoxicological data is contradictory to what is seen in the natural environment – i.e. in certain streams elevated background Mn concentrations have shown no adverse effects on the ecosystem. Thus dissolved Mn is not a statutory driver in the UK Water Framework Directive.

1.4.3. Comparison of waste regulation schemes

The classification of Mn containing wastes differs significantly in the various international waste classification strategies. The 'Minimum requirements for the handling, classification and disposal of hazardous wastes' of South Africa are by far the most conservative with relation to Mn. The South African guidelines stipulate that the maximum amount of Mn that can be disposed of in a general purpose leachate-controlled landfill is 454.5 g/ha/month. Any waste stream that will exceed this dose will require disposal at a highly hazardous waste site.

According to the U.S.EPA, wastes are not classified as hazardous on the basis of their Mn content. Unlike the South African guidelines, the EU waste classification system recognises the importance of speciation when determining the classification of Mn for example $MnSO_4$ (soluble) is more conservatively classified than Mn oxide (insoluble). According to the risk phrase of $MnSO_4$ it is acutely toxic to aquatic organisms with long term toxicological effects. This corresponds to the LC_{50} of Mn falling between 1 and 10 $mg.L^{-1}$ (acutely toxic) and the fact that Mn^{2+} is soluble (long lived). With this classification it is recommended that the maximum amount of Mn as $MnSO_4$ allowed in a waste before it is termed hazardous is 9105 $mg.kg^{-1}$. Manganese dioxide has the risk phrases R20 and R22; Harmful: if inhaled or swallowed. According to the threshold for harmful materials, a waste would need to contain 25% MnO_2 for it to be classified as hazardous. The EU risk-based system recognises no ecotoxicological risk associated with MnO_2.

The Basel Convention (1992) is an international treaty designed to regulate the transport of hazardous waste between countries. Manganese is not included as a hazardous metal in the Basel Convention. The Convention has only established interim guidelines for assessing the generation of hazardous leachate from waste and does not include Mn in their list of hazardous leachate constituents.

In the light of international waste regulation schemes reviewed, the South African approach towards Mn appears conservative, despite it being based on universal ecotoxicological data. Since this ecotoxicological data has recently been called into question by the UK, there is a need for a review of South African waste legislation. At the time this study was conducted the South African waste guidelines were under review. The South African government has

expressed a need to incorporate a more globally harmonised approach to waste management, whilst keeping local conditions in consideration. This may result in relaxing the stringent regulation of Mn containing wastes. Manganese is a contentious element for many regulatory bodies due to its varying speciation, which dictates its ecotoxicological risk, and its natural abundance and varying background levels. A waste classification system resembling that of the EU, which considers element speciation, may provide a more rigorous and pragmatic approach to waste characterisation.

1.5. Persistent organic pollutants

Persistent organic pollutants (POPs) is a generic name for a group of organic compounds that are not easily degraded in the environment due to low solubility, low volatility and/or resistance to degradation (Andrews et al., 2004). Thus POPs encompass a wide range of organic compounds which can persist in soils, surface waters, ground waters, the atmosphere and the oceans. For the purposes of this investigation, which is the first to assess the oxidative capacity of the Mn tailings for remediation purposes, one highly-soluble, predominantly water-based contaminant group and one poorly-soluble, predominantly soil-based contaminant group have been targeted. Acid azo dyes were chosen as suitable water-soluble contaminants and PAHs have been targeted as insoluble organic contaminants.

Textile industries produce large volumes of wastewater polluted with dyes. It is estimated that between 10 and 15% of manufactured dyes are lost in wastewater streams (Zhao et al., 2005). Within the compounds manufactured as dyestuffs, azo dyes represent the largest class of dyes. The release of azo dyes into the environment is undesirable not only for obvious aesthetic reasons, but also because of the toxic and mutagenic properties of many dyes (Riu et al., 1997).

The removal of azo compounds from textile waste streams is a pertinent issue in water treatment. Many biotreatment technologies achieve the reductive cleavage of the azo bond, which generates a range of aromatic amines which are colourless but significantly more carcinogenic than the parent azo compound (Sweeney et al., 1994; Ge and Qu, 2003). Advanced oxidative techniques have been successfully employed to remove colour from waste effluents, however, these techniques are often expensive, thus the development of a

sustainable water treatment technique utilising the oxidising capacity of the Mn tailings waste is appealing. To the author's knowledge few researchers have studied the use of Mn oxides in the treatment of textile waste.

Polycyclic aromatic hydrocarbons have been highlighted as a health concern due to their chronic health effects (e.g. carcinogenicy); microbial recalcitrance; high bioaccumulation potential and low removal efficiency in traditional waste treatment processes (Herbes and Schwall, 1978; Bamforth and Singleton, 2005). Contamination of soils with PAHs is a major and widespread environmental problem. There are no simple remediation solutions for PAH breakdown. In this study the oxidation of anthracene, a three-ringed PAH, by the Mn tailings has been investigated. Anthracene is one of the priority contaminants listed by the U.S.EPA. It has been selected as a model PAH for this study, due to its low water solubility and the fact that it has the same arrangement of fused aromatic rings as the more complex carcinogenic PAHs (Alcalde et al., 2002). Oxidation of PAHs by Mn oxides has not been, to the author's knowledge, widely reported.

1.6. Structure of thesis

This thesis presents research conducted to assess the capacity of Mn oxide containing tailings to oxidatively breakdown organic contaminants. In presenting this work the thesis has been structured as follows:

- This Chapter presents an overview to the work in briefly describing; the geological setting of the KMF, the mining procedures which generate the tailings, a comparative summary of waste regulation with respect to Mn in the South African, US and EU waste characterisation systems and the rationale for choosing the two contaminant groups, acid azo dyes and PAHs

- Chapter 2 provides a review on Mn geochemistry focusing on Mn oxide mediated organic oxidation

- Chapter 3 reviews the chemistry of persistent organic pollutants in the environment. Azo dyes and PAHs are reviewed in terms of current treatment technologies and sorption and oxidation characteristics.

- Chapter 4 reviews experimental and analytical procedures used in previous studies on acid azo dyes and PAHs. It outlines the materials and methods used during the characterisation of the tailings and in the experimental design of the azo dye and PAH research.

- Chapters 5, 6 and 7 present the results and discussion of the tailings characterisation, the azo dye and PAH work, respectively

- Chapter 8 concludes the research and suggests further work.

2. Manganese geochemistry

Manganese is the twelfth most abundant element in the lithosphere comprising about 0.1% of the earth's crust (Dixon and White, 2002; Concise International Chemical Assessment Document (CICADS), 2004) and is second only to Fe as the most abundant heavy metal (Post, 1999). The Mn concentration in crustal rocks ranges from 350 to 2000 ppm (Kabata-Pendias and Pendias, 2001) and is generally highest in mafic rocks (Gilkes and McKenzie, 1988) and certain sedimentary rocks, such as dolomite. Manganese is present in minerals as Mn^{2+}, Mn^{3+} and Mn^{4+} ions. In primary minerals the dominant species is Mn^{2+}. Weathering and oxidation of primary minerals predominantly results in the formation of Mn^{4+} and Mn^{3+} oxide minerals. Manganese oxides are the most common Mn bearing minerals in surface environments.

Manganese oxides are one of the strongest natural oxidants in terrestrial geochemical systems. They are involved in redox cycles in soils and waters, which are essential to nutrient cycling, humification, metal sorption and contaminant fate and mobility. Chemical transformations caused by Mn oxides have become of increasing interest in fields of environmental geochemistry due to their control of biogeochemical cycles of many important contaminants such as Pb, Cr and many organic pollutants. Despite the low levels of Mn in natural soils (0.1%) they are highly reactive components forming an essential part of the soils' natural defence against contamination. This section describes some of the chemical, physical and mineralogical properties of natural Mn oxides pertaining to their reactivity in soils and waters.

2.1. Mn mineralogy of the KMF

Investigations into the mineralogy of the KMF have revealed up to 135 different minerals, 8 of which represent new mineral species and 59 of which are Mn bearing (Gutzmer and Beukes, 1996). Of these 59 Mn bearing minerals, the oxides (bixbyite, braunite, hausmannite, jacobsite, and manganite) and the carbonates (kutnahorite and rhodochrosite) dominate (Maynard, 2004). Supergene alteration of the deposits resulted in the formation of a number of MnO_2 phases, such as todorokite, lithiophorite, birnessite, hollandite and pyrolusite

(DeVilliers, 1965). Manganese oxides are assumed to be the reactive phase in terms of oxidative capacity and thus greater emphasis is given to the oxides.

2.1.1. Mn crystal chemistry

Manganese in surface environments is found in three valence states; Mn^{2+}, Mn^{3+} and Mn^{4+}. These ions are usually found in octahedral coordination with O^{2-}, OH^- or H_2O, although Mn^{2+} and Mn^{3+} may exist in tetrahedral and other coordination configurations. All five d-orbitals of Mn^{2+} are occupied in the high spin state so there is no crystal field stabilization energy (CFSE). The electron configuration for Mn^{3+} allows some CFSE, but probably more influential is the degenerate energy state of the $t_2g(3)$, eg(1) configuration that creates a Jahn-Teller distortion resulting in a difference in bond length between the equatorial and axial coordinated ligands. The Mn^{4+} ion has only one spin state in octahedral coordination and a large octahedral site preference energy, explaining why although its size is suitable for tetrahedral coordination, Mn^{4+} is solely found in an octahedral coordination state. The Mn oxides can accommodate Mn in all three of these oxidation states. Even the unstable Mn(III) ion seems to be stabilized in the structure of minerals.

2.1.2. Common Mn oxides

Manganese oxides contain Mn in the 2+, 3+ and 4+ oxidation state. Manganese oxides containing mainly the 4+ species are common in soil environments. The Mn octahedra in these Mn oxides can either be arranged in a tunnel or sheet structure. Some common MnO_2 minerals, that have previously been identified in the KMF are discussed below. Most of the MnO_2 minerals listed below are considered to be of supergene origin (DeVilliers, 1965; Gutzmer and Beukes, 1996)

Pyrolusite [(MnO_2)] has a tunnel structure with square cross sections that are one octahedron by one octahedron. The tunnels in pyrolusite are too small to accommodate cations thus the chemical composition deviates only slightly from pure MnO_2. Pyrolusite has been identified to be the primary product of surficial weathering of Mn minerals in the KMF (Gutzmer and Beukes, 1996).

Birnessite [(Na,Mg,Ca,Mn^{2+})Mn_7O_{14}] has a layer structure composed of sheets of edge-sharing MnO_6 octahedra alternating with planes of cations (mainly Ca, Mg, Na and Mn^{2+}). There are vacancies in one in every six MnO_6 octahedra within the sheet, with Mn^{2+} and Mn^{3+} ions situated between the sheets above and below these vacancies.

Lithiophorite [(Al,Li)$MnO_2(OH)_2$] has a layer structure like that of birnessite except that the interlayers between the MnO_6 octahedra consist of Al-hydroxy sheets containing Li in the octahedral vacancies. The cation sites in the Mn octahedral layer are fully occupied with two thirds of the sites occupied with Mn^{4+} ions and the remaining third occupied with Mn^{3+} ions.

Todorokite [(Na,Ca,K,Ba,Mn^{2+})$_2Mn_5O_{12}.3H_2O$] has a tunnel structure formed from triple chains of edge-sharing MnO_6 octahedra linked to form 3x3 tunnels which house Na, Ca, K, Ba, Sr and water molecules (Post and Bish, 1988). Todorokite has been identified to be one of the major alteration product of the hydrothermal Smartt event (Gutzmer and Beukes, 1996). Supergene origins have also been suggested for todorokite (DeVilliers, 1965).

Hollandite ($Ba_2Mn_8O_{16}$) and *romanechite* [(Ba,K,Mn,Ca)$_2Mn_5O_{10}$) have similar structures and often occur together as intergrowths. They have a tunnel structure consisting of a framework of double and triple chains of MnO_6 octahedra that enclose the tunnel. They are characterized by the presence of large cations (most commonly Ba) which occupy the tunnels (Dixon, 1988).

The lower oxides of Mn contain Mn primarily in the 2+ and 3+ oxidation states. The structures of these oxides will be discussed below

The MnOOH group consists of three polymorphs of which *manganite (γ-MnOOH)* is the most stable and most abundant in surface environments (Post, 1999). The remaining two polymorphs are feitknechtite and groutite. Manganite is isostructural with the tunnel forming pyrolusite, with the octaherdra containing Mn^{3+} ions and half the O atoms replaced by hydroxyl anions. Manganite is one of the dominant alteration products within the metamorphic zone of the KMF (Maynard, 2004).

Hausmannite [$Mn^{2+}(Mn^{3+})_2O_4$] has a spinel structure with Mn^{2+} occupying tetrahedral sites and Mn^{3+} occupying octahedral sites. Hausmannite forms a major component of the Hotazel

type ore, which underwent the largest degree of hydrothermal alteration (Gutzmer and Beukes, 1996).

2.1.3. Mn silicates and carbonates

Rhodochrosite [$MnCO_3$] is probably the most common Mn carbonate mineral found in surface environments. It is present in the Hotazel ore within vugs and as part of the carbonate rocks in the Mamatwan type ore (DeVilliers, 1965).

Kutnahorite [$CaMn(CO_3)$] is a Mn carbonate mineral which was originally proposed to be the Mn analog to dolomite (Frondel and Bauer, 1955), however, the composition of the natural phase is best described as a solid solution between $CaCO_3$, $MnCO_3$ and $MgCO_3$ (Bamforth et al., 2006). Kutnahorite is a major component of the Mamatwan type ore (Gutzmer and Beukes, 1996).

Braunite has been identified in two forms in the KMF. The ideal formula for braunite is [Mn^{2+} $(Mn^{3+})_6SiO_{12}$] which amounts to an SiO_2 content of 9.98 weight percent. A iron-rich braunite species, known as braunite II, has been identified in the KMF. Braunite II has the formula [$Ca(Mn^{3+}$ $Fe^{3+})_{14}SiO_{24}$] (Gutzmer and Beukes, 1996) and contains around 4.4 weight percent SiO_2 (DeVilliers, 1965). The cell dimension of Mn_2O_3 is not affected by Fe_2O_3 thus the two species cannot be distinguished by XRD analysis alone (DeVilliers, 1965). It is proposed that braunite II replaced type I braunite during the hydrothermal alterations (Kleyenstuber, 1984).

2.2. Redox properties

Manganese oxides are one of the most redox reactive constituents in soils and waters. The small particle size and large surface area of the oxides allows them to impart a greater influence on soil and water chemistry than would be expected by their relative abundance (Bartlett, 1988). Manganese oxides have been implicated in the removal of harmful free radicals in soils (Bartlett, 1999) and in non-microbial oxidation of NH_4^+ and NO_2^- to nitrate (Bartlett, 1981). Manganese oxides have been shown to act as catalysts for the breakdown and humification of organic matter (Shindo and Huang, 1984) and play an important role in the formation of topsoils (Bartlett and James, 1994) through their redox activity. Manganese

oxides have the capacity to oxidize inorganic ions such as U^{4+}, Se^{4+}, Cr^{3+}, As^{3+} and Co^{2+} and organic molecules such as phenols and aromatic amines. These interactions can be favourable, as in the case of many organics, As and Co, and unfavourable as in the case of Cr and U, which are rendered more mobile through oxidation. Table 2-1 gives a number of half-reactions important in the redox range of natural soils and waters. These are standard-state reactions and therefore not relevant to pH ranges and ion activities experienced in natural systems, however, it does illustrate the position of Mn oxides in a list of natural oxidants. The debate over whether Mn(III) or Mn(IV) oxides are the most redox active in soils has not been clearly resolved. Thermodynamically Mn(III) oxides would appear to be the strongest oxidants (Table 2-1), however, certain studies have shown a lower redox activity of manganite (γ-MnOOH) compared to birnessite (δ-MnO_2) (Zhang and Huang, 2003), while others have illustrated the increased oxidative capacity of manganite compared to birnessite (Xyla et al., 1992). The role of Mn(III) and Mn(IV) as the primary oxidant within a single mineral phase is also unclear, with some workers claiming a higher Mn(IV)/(III) ratio is more conducive to oxidation (Kim et al., 2002; Negra et al., 2005) and others suggest Mn(III) functions as the primary oxidant in Mn(III)/(IV) oxides (Nico and Zasoski, 2000; Nico and Zasoski, 2001). Due to the diverse nature of Mn oxides in terms of chemical composition, surface area and surface chemistry, drawing correlations between redox reactivity and Mn oxidation state probably cannot be achieved.

Table 2-1 Standard-state reduction potentials of some half reactions important in soil and aqueous chemistry taken from McBride (1994)

Reaction	E^0(volts)
$Mn^{3+} + e^- \Leftrightarrow Mn^{2+}$	1.51
$MnOOH(s) + 3H^+ + e^- \Leftrightarrow Mn^{2+} + 2H_2O$	1.45
$1/5\ NO_3^- + 6/5\ H^+ + e^- \Leftrightarrow 1/10N_2(g) + 3/5\ H_2O$	1.245
$½\ MnO_2(s) + 2\ H^+ + e^- \Leftrightarrow ½\ Mn^{2+} + H_2O$	1.23
$1/4\ O_2(g) + H^+ + e^- \Leftrightarrow ½\ H_2O$	1.229
$Fe(OH)_3(s) + 3H^+ + e^- \Leftrightarrow Fe^{2+} + 3H_2O$	1.057
$1/8\ S\ O_4^{2-} + 5/4\ H^+ + e^- \Leftrightarrow 1/8H_2S + 3/5\ H_2O$	0.303
$1/8\ CO_2\ (g) + H^+ + e^- \Leftrightarrow 1/8\ CH_4(g) + 1/4H_2O$	0.169

As can be seen from Table 2-1 hydrogen ions are involved in the transfer of electrons. The role pH plays in redox reactions is more meaningfully displayed in graphical form showing the relationship between pH and Eh for a certain element.

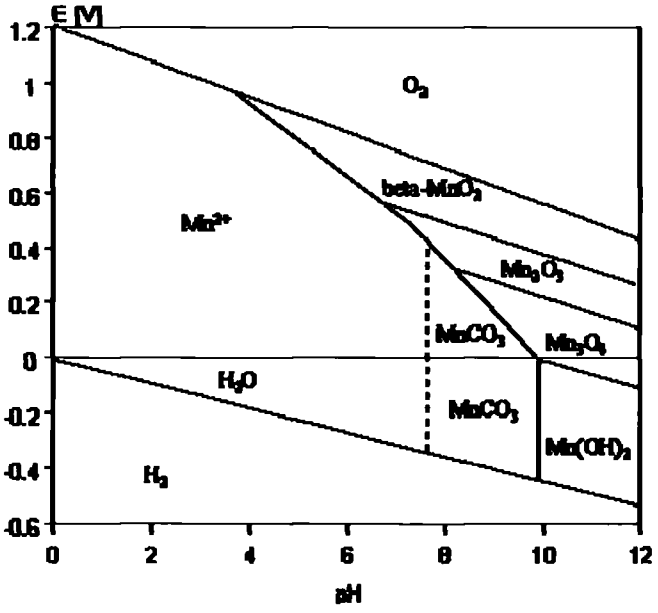

Figure 2-1 Eh-pH diagram showing soluble and solid forms of Mn under a range of pH and Eh conditions.

Figure 2-1 shows an Eh-pH diagram for Mn. This diagram can be used to predict the stability of Mn oxides under varying conditions of Eh and pH. Interpreted simply it shows the redox potentials of all Mn oxide phases increases with decreasing pH, thus Mn oxides are stronger oxidants under acidic conditions.

2.3. Mn mobility in soils and waters

Of the three valence forms of Mn in natural systems (Mn^{2+}, Mn^{3+}, Mn^{4+}) it is only Mn^{2+} that is found in measurable concentrations in solution. Thus solubility of Mn is largely controlled by redox processes. As seen from Table 2-1 when Mn (III)/Mn(IV) oxides are reduced soluble Mn^{2+} ions are produced. Water soluble Mn is an essential trace element in plants and soils but it can easily reach toxic quantities depending on the geochemical conditions. From Figure 2-1 it is apparent that soluble Mn^{2+} will occur under conditions of low pH and low Eh. Low Eh conditions arise in natural soils and waters when the amount of microbial substrates, primarily organic matter, exceeds the concentration of electron acceptors. Manganese oxides can also be abiotically reduced by organic compounds (Shindo and Huang, 1984). In soils Mn is generally mobilised from topsoils, where organic matter and microbial activity is most prolific, and redistributed down the rest of the profile. Manganese precipitation is often observed in saprolitic horizions where both Eh (low organic matter) and higher pH conditions favour oxidation. In lake sediments soluble Mn is present in the anoxic layers and precipitates out at the anoxic/oxic interface (Bartlett, 1999).

Mobilisation of Mn from Mn oxides does not always have to involve reduction. Under acid conditions the structure and chemistry of Mn oxides may be expected to undergo a change due to the acid lability of the mineral lattice (Murray, 1974). Banerjee and Nesbitt (2001) found that the release of Mn(II) from birnessite with decreasing pH, was not due to the reduction of Mn(IV) and Mn(III), but rather to the proton promoted release of Mn(II) that forms part of the birnessite structure. The mechanism involved being that suggested by Zinder et al. (1986) in which a proton attaches to an oxygen that bridges two metal ions and causes weakening and break up of the M-O-M bond. Manganese carbonate minerals such as rhodochrosite and kutnahorite contain Mn in its divalent state. Figure 2-1 shows $MnCO_3$

becomes unstable below pH 8, thus Mn carbonates can also be a substantial source of soluble Mn if the system that contains them begins to acidify.

An additional, but less recognised, factor which can influence the solubility of Mn in natural soils and waters is complexation of Mn ions by organic molecules. It has been shown that citrate can complex Mn (III) from β-MnOOH (Klewicki and Morgan, 1999) thus rendering soluble Mn complexes. Recent studies have shown the capacity of siderphores to complex, and solubilise Mn(III) ions from trivalent Mn minerals (Duckworth and Sposito, 2005; Duckworth and Sposito, 2007; Pena et al., 2007). Thus the role of Mn complexation by organic ligands needs to be considered in the solubilisation of Mn.

2.4. Surface properties

Manganese oxides display a pH-dependent surface charge. The pH for points of zero charge on common soil Mn oxides ranges from 1.5 for birnessite to 4.5 for hollandite (Healy et al., 1966), thus in all but acidic conditions these oxides will display a negatively charged surface. Manganite has had a point of zero charge (PZC) reported as 8.2 (Ramstedt et al., 2004), 6.2 (Xyla et al., 1992) and 1.5-4.5 (Murray, 1974), thus it would appear that in some Mn minerals the PZC is elusive. Measurement of PZC can be difficult when the PZC falls below the acid/redox stability of the mineral. This is the case in many Mn oxides and may account for reported failings of potentiometric tritrations for Mn oxide PZC determination (Murray, 1974).

2.5. Mn oxide mediated organic oxidation reactions

Activated (high surface area) Mn oxide is a well known selective oxidant used in organic synthesis reactions (Fatiadi, 1986). It was first used for the quantitative conversion of vitamin A to retinal (Ball et al., 1948) and since then its application as a selective oxidant has been extensive. In neutral media it is a mild oxidant capable of selectively oxidising saturated and unsaturated alcohols, phenols, polyhydroxy compounds, amines, hydrazines, hydrocarbons, heterocyclic compounds and various natural products (Fatiadi, 1986). The reaction mechanism usually involves electron transfer and the generation of free radicals (Bhatnagar and George, 1968; Fatiadi, 1986; Stone, 1987b; Ulrich and Stone, 1989; Laha and Luthy,

1990; Field et al., 1992), which can either be further oxidised to quinone species or take part in polymerisation reactions (Stone, 1987b). Free radicals can be generated either by the transfer of one electron to a metal centre or the abstraction of a hydrogen atom from the organic compound. An electron-rich compound, like toluene is likely to be oxidised by electron transfer while H-atom abstraction occurs in compounds that have weak C-H or O-H bonds (Bryant et al., 2002).

Stone and Morgan (1984a and b) undertook pivotal investigations into the oxidation of many naturally occurring organic compounds by Mn oxides. The steps they proposed for the oxidation of organic substrates are:

i) diffusion of organic substrate to the oxide surface,

ii) formation of a surface complex between sorbate and oxide,

iii) charge transfer within the surface complex,

iv) desorption of dissolved organic substrate,

v) movement of Mn^{2+} from crystal lattice to the adsorbed layer,

vi) desorption of Mn^{2+},

vii) diffusion of products away from the surface.

From their survey of Mn reduction by a variety of organics they concluded that saturated alcohols, aldehydes, ketones and carboxylic acids, except pyruvic and oxalic acids, showed no reactivity while catechols, hydroquinones, methoxyphenols and resorcinols reduced and dissolved Mn oxides. It was further established that reaction rates are not always proportional to redox potential with factors affecting surface complexation and electron transfer at the surface often being rate limiting.

Although sorption is considered a vital process in Mn oxide mediated oxidation reactions, no direct measurements have been reported due to the rapid reaction between the reductant and the oxidant (Xyla et al., 1992). Inner-sphere sorption has been postulated to occur before

oxidation occurs (Stone and Morgan, 1984a; Stone and Morgan, 1984b), although only one study has shown direct evidence for inner-sphere precursor complex formation (Gordon and Taube, 1962) . These workers provided evidence that during the oxidation of U(IV) by Mn oxides, the oxygen atoms in the UO_2^{2+} complex were derived from MnO_2.

The oxidation of phenols by Mn oxides has been well documented (Stone and Morgan, 1984b; Stone, 1987b; Ulrich and Stone, 1989; Petrie et al., 2002). The reaction is initiated by a one-electron transfer from the phenol to the metal centre to form a phenoxy radical (Waters, 1971). The radical species can then enter into a number of competitive pathways depending on pH and reductant concentration. The coupling of two radical species will result in dimer formation. Dimers are more susceptible to oxidation than monomers so polymerisation is often observed to be self-perpetuating (Stone, 1987b). Low reductant concentration and low pH favour further oxidation of the phenoxy radicals to phenoxenium ions, which in turn are subject to nucleophilic attack by water to form benzoquinone species (Waters, 1971). Oxidative coupling of phenolic compounds may be considered more beneficial than further oxidation to quinone species. The coupling of semiquinones results in the formation of stable humic acids, which is essentially a composting process (Huang, 2000). Coupling reactions require lower activation energy compared to electron transfer reactions (Chang and Allan, 1971), thus should be more kinetically favourable.

Functional group type and position on phenolic compounds influence the rate of oxidation by Mn oxides (Stone and Morgan, 1984a; Ulrich and Stone, 1989). Phenols with electron donating groups are stronger reducing agents than those with electron withdrawing groups and ortha and para substituted phenols are more reactive than their meta equivalents. This is thought to be a consequence of the π-electron donating capacity of para and ortho isomers, which facilitates resonance stabilisation of the phenoxy radical. In addition ortha and para isomers promote the formation of precursor inner-sphere mineral-organic complexes, which is a function of nucleophilicity of the phenolate ion (Ulrich and Stone, 1989).

Stone (1987) tried to quantify these observations in terms of the measurable chemical parameters; Hammett constants and half-wave potentials. In general the following observations were made: phenols with positive Hammett constants have electron withdrawing

substituents and high half-wave potentials and these phenols are the least reactive with Mn oxides; while substituted phenols with electron donating substituents have negative Hammett constants, low half-wave potentials and are the most reactive with Mn oxides. These correlations were relatively successful for meta and para substituted phenols, but ortha substituted phenols were less predictable, possibly due to steric hindrances.

Analogous studies with aromatic amines showed similar trends with respect to Hammett constants and half-wave potentials (Laha and Luthy, 1990; Klausen et al., 1997). Initial reaction rates for the oxidation of substituted aniline compounds correlates well with half-wave potentials and accordingly with Hammett constants. The strong correlation between half-wave potentials and initial reaction rates indicate that the transfer of the first electron from the aniline to the mineral controls the overall reaction rate (Klausen et al., 1997). The major reaction products of aniline oxidation were determined to be corresponding azobenzenes and aminodiphenylamines species of the various substituted aromatic amines, suggesting a head to head and/or head to tail coupling of two cation radicals.

Manganese oxide mediated oxidations are affected by pH, with oxidation of many polar organic compounds increasing with decreasing pH (Stone, 1987b; Ulrich and Stone, 1989; Laha and Luthy, 1990; Zhang and Huang, 2003; Zhang and Huang, 2005). In the oxidation of phenolic compounds the effect of pH on reaction rate showed a curved response with pH dependence being greater above pH 6 and constant below 4. Triclosan and chlorophene show increased oxidation at low pH (Zhang and Huang, 2003) as does aniline and its related compounds (Laha and Luthy,1990). The increased oxidation of organic compounds at low pH has been attributed to:

i) charging of the amide groups (eg. anilinium cation) resulting in electrostatic attraction to the oxide surface (Laha and Luthy, 1990);

ii) increased sorption of neutral phenolic groups;

iii) the decrease of the negative charge on MnO_2;

iv) the increased redox potential of the MnO_2/Mn^{2+} couple (Zhang and Huang, 2005); and

v) enhanced removal of Mn^{2+} from the oxide surface, exposing new reactive sites (Klausen et al., 1997).

The influence of co-solutes (organic ligands, Ca^{2+} and Mn^{2+} ions) on the initial and quasi-steady-state kinetics for the oxidation of substituted anilines by Mn oxides was investigated by Klausen et al. (1997). This study indicated that quasi-steady-state kinetics, as measured in an anaerobic mixed flow-through reactor, is significantly lower than initial reaction rates under identical conditions. This is attributed to the build up of Mn^{2+} ions, which block reactive sites and retard aniline oxidation. Autooxidation of Mn^{2+} by MnO_2 (Ross and Bartlett, 1981) may prevent this in aerobic conditions. Humic acids have been shown to retard oxidation suggesting that humic acids were reducing the oxide and generating Mn^{2+} ions (Klausen et al., 1997). Inhibition of phenol oxidation by phosphate ions (Stone and Morgan, 1984a) suggests that competition of ligand exchange sites may also be a contributing factor.

The effect of evaporation of moisture from mineral surfaces is note worthy. Drying is known to cause significant changes to the organic fractions of soils (Raveh and Avnimelech, 1978; Bartlett and James, 1980; Ross et al., 2001a). Drying soils results in an increase in the dissolved organic matter fraction and a concomitant increase in exchangeable Mn (Bartlett and James, 1980; Ross et al., 2001a). It has been suggested that drying results in oxidation of the organic matter by Mn oxides thus explaining the increase in soluble Mn and dissolved organic matter (Bartlett and James, 1979; Bartlett and James, 1980). This is based on the premise that drying results in a dramatic decrease of pH on the mineral surface, due to increased hydrolysis of surface cations (Mortland and Raman, 1968), which increases the reducibility of the organics. This increased acidity may allow reactions to occur which are not thought to be thermodynamically favourable within the environmental pH range (pH 4-9). The increased sorption of PAHs on dry mineral surfaces together with this drying phenomenon suggests that oxidation of PAHs during wetting and drying cycles could be an interesting avenue of research.

2.6. Mn biogeochemistry

Manganese biogeochemistry is an extensive field of research and largely lies beyond the scope of this review. Biogenic Mn oxides are claimed to be the most abundant and reactive Mn oxides in the environment (Tebo et al., 2004). Manganese oxidizing bacteria oxidize Mn(II) via a Mn(III)-complex intermediate to Mn(IV) oxides. The dominant Mn oxide that is formed is amorphous δ-MnO_2. Manganese oxidisers are usually found in environments where reduced Mn is available (Tebo et al., 2004). Thus the Mn tailings dams, which are highly oxidative in nature (high pH, high pe) are not likely to provide favourable conditions for Mn oxidizing bacteria. However, certain areas of the tailings dams contain ponded water and sparse vegetation, thus biogenic minerals and biological activity may be important to the geochemistry of these ponds. Elucidation of any biogeochemical interactions falls beyond the scope of this study.

One aspect of Mn biogeochemistry that has relevance to the current study is the oxidative properties of white rot fungi, which use a Mn(III) based oxidant to oxidise a host of xenobiotic compounds. Manganese plays a central role in the biological break down of lignin in woody material by white rot fungi (Gold et al., 1989; Wariishi et al., 1991; Hammel et al., 1993). The fungi produce an extracellular heme-iron enzyme called Mn peroxidase which preferentially oxidises Mn(II) to Mn(III). This highly reactive Mn(III) ion is stabilised by simple organic acid chelators, especially oxalate (Wariishi et al., 1988). The chelated Mn(III) acts as a diffusible low molecular weight oxidant capable of oxidising alkyl aromatic and phenolic substrates with weak C-H and O-H bonds, including lignin-type compounds (Valli and Gold, 1991; Reddy et al., 1998).

One of the characteristics of Mn peroxidases that generates continued interest is the fact that the Mn peroxidases are non-specific in the substrate they oxidise (Hammel et al., 1986; Field et al., 1992) enabling white rot fungi to oxidise a range xenobiotic organic compounds including chlorinated phenols, chloroanalines, pesticides, such as DDT, azo dyes and PAHs (Bumpus et al., 1985; Bumpus, 1989). Phenolic and amino-aromatic groups are the usual targets for oxidation by Mn(III)-chelates but certain non-phenolic aromatic substances like anthracene are subject to one-electron abstraction giving rise to aryl cation radicals.

The non-specific oxidative capacity of these white rot fungi have alerted researchers to their bioremediation potential of hazardous wastes (Hofrichter, 2002). For this to be a viable technology the enzyme would need to be produced in large volumes and be stable in the chemical conditions of the waste. Biotransformation of xenobiotic compounds by white rot fungi is generally a cometabolic process and therefore requires a primary substrate to sustain the organisms. It is often encountered that in wastewaters, such as textile effluents, fungi are unable to grow due to the lack of primary substrate (Vanhulle et al., 2008). Adding a primary substrate like molasses, increases the biological oxygen demand and can lead to unwanted biological activity, for example the microbial reduction of azo dyes to highly carcinogenic aromatic amines. If it were to be established that the Mn oxide phase of the tailings could achieve similar oxidative remediation goals, there would be a definite advantage to using an abiotic solid, as reactions would not be confined to environments which support fungus growth or enzyme stability. Since the tailings used in this study, contain a significant Mn(III) oxide phase they may provide an abiotic alternative white rot fungi.

3. Persistent organic pollutants

Organic pollutants persist in the environment if they are of low solubility, low volatility and/or resistant to degradation (Andrews et al., 2004). The processes that control the fate of organic pollutants in soils and waters can be divided into two general categories: processes that leave the structure of the molecule in tact (such as sorption) and those which transform the parent molecule into one or several compounds having a different chemical and physical behaviour (such as oxidation). Although transformation reactions are the focus of this study, obtaining mineral-organic contact is an essential pre-requisite to oxidation and thus organic sorption and oxidation reactions will both be reviewed in this section.

3.1. Sorption of organic compounds

Sorption of the organic molecule to the mineral surface is often a rate limiting factor in oxidation reactions. Compounds with hydrophilic functional groups will tend to be attracted or repelled from mineral surfaces depending mainly on the pH of the system and the type of charge on the mineral i.e. permanent or variable. Sorption of hydrophobic molecules usually occurs via partitioning and is less dependent on pH. Hydrophobic compounds tend to sorb preferentially to organic matter rather than charged mineral surfaces. This section briefly reviews sorption mechanisms of organic compounds with both hydrophilic and hydrophobic functional groups.

3.1.1. Polar organic molecules

Polar organic molecules are, in general, basic or acidic molecules which develop a charge through protonation and deprotonation, respectively. Bases become positively charged when they accept a proton to form a conjugate acid and will sorb readily onto permanently charged clay minerals. The uncharged conjugate acid will sorb weakly by physical sorption (interactions where bonding is not very energenic). The pK_a of the base and the pH of the solution are therefore paramount in determining the degree that a basic molecule will sorb (McBride, 1994).

Acid molecules become negatively charged when they lose a proton. Generally this occurs at a higher pH for phenolic groups than for carboxylic acid groups. For all acidic molecules sorption onto permanently charged minerals is positively correlated with pK_a. Negative charge generation results in electrostatic repulsion by negatively charged clay minerals and organic matter resulting in dissociated acid molecules being highly mobile at high pH. At pH values below the pK_a of the acid, only physical sorption of acid molecules is possible therefore sorption is inversely proportional to pH (Schwarzenbach, 1993).

Sorption of organic acids on variable charge minerals is more complicated. Generation of positively charged sites on the oxide, suitable for ligand exchange, and the generation of negatively charged organic ligands are oppositely correlated to pH. The pH equal to the pK_a of the organic acid is often found to be most favourable for adsorption (McBride, 1994).

Due to resonance stabilisation, position and type of functional groups on benzoic acids play an important role in charge generation and thus sorption behaviour. In the normal pH range of soils, pH 4-9, the carboxylic acid functional group is likely to be dissociated thus bonding constant becomes the discriminating factor in benzoic acid inner-sphere sorption. Any functional group which donates electrons to the benzoic acid, such as methyl groups, will create a stronger Lewis base than a benzoic acid with electron withdrawing groups like NO_2. Inner-sphere sorption of phenolic compounds is more complicated. Phenolic compounds usually have a pK_a that is higher than the pH of the soil. This means charge generation will be greatest for more acidic phenols, but stronger bases will be better Lewis bases and thus have a stronger bonding constant. As strong phenolic acids are seldom strong Lewis bases there has to be a trade off. Sorption data shows that dissociation of the phenolic acid is more important than the Lewis basicity of the phenolate (McBride, 1994).

Some weakly polar molecules like alcohols and amines can form weak hydrogen bonds or ion dipole attraction with waters of hydration surrounding cations on exchange sites of clays. However, these molecules compete weakly with the more abundant and stronger hydrogen bonds of water and are easily displaced and mobilised.

3.1.2. Nonpolar organic molecules

Sorption or partitioning of hydrophobic organic compounds (HOCs) to surfaces occurs as a result of weak solute-solvent interactions rather than specific sorbate-sorbent interactions (Means, 1995). Hydrophobic compounds cause a local ordering of water molecules, which decreases the entropy of the system and force molecules out of solution and onto weakly hydrating or uncharged surfaces. This is known as the 'iceberg' effect (Frank and Evans, 1945). Larger molecules will tend to disturb more water molecules and therefore will be more prone to being forced out of solution than smaller molecules. Thus water solubility is inversely proportional to molecular size and accordingly inversely proportional to sorption of nonpolar compounds to soils. The hydrophobicity of a compound is commonly measured by the octonal/water partitioning coefficient (K_{ow}) which is defined as the concentration of an organic compound in octanol to its concentration in water after equilibrating with the two solvents.

The partitioning coefficient (K_p) is defined as the concentration of sorbed species on the solid phase (C_s) to concentration in the aqueous phase (C_{aq}) as given by:

$$K_p = \frac{C_s}{C_{aq}}$$

In natural soils and waters sorption of HOCs is usually proportional to the organic matter content (Chiou et al., 1983) thus it is common to normalize the K_p to a function of the total organic carbon content (f_{oc}). This normalised organic carbon coefficient (K_{oc}) is calculated as:

$$K_{oc} = \frac{K_p}{f_{oc}}$$

For HOCs the K_{ow} is often found to correlate with the K_{oc} of a particular soil or sediment (Chiou et al., 1983) although complicating factors such as organic matter composition (i.e. aromatic vs. aliphatic) and dissolved organic carbon make correlations more difficult and often inaccurate (Krauss and Wilcke, 2001).

Sorption of HOCs onto mineral surfaces can be influenced by organic or biogenic coatings. The sorption of HOCs onto kaolinite and hematite surfaces has been shown to be proportional to the amount and aromatic nature of the humic coatings (Murphy et al., 1990). Sorption of HOCs to biofilms, which are often intimately associated with mineral surfaces, has only received limited attention. The emulsifying properties of extracellular polymeric substances, which are produced to bind biofilms, have been implicated in the decrease in K_p of certain soils contaminated with PAHs (Dohse and Lion, 1994). Although the Mn tailings are considered to be an inorganic material, cognisance must be made of organic and biological coatings which may influence HOC sorption behaviour however, a detailed investigation of biogenic material falls outside the scope of this study.

Sorption is a necessary precursor step for oxidation (Stone and Morgan, 1984a) and both inner-sphere and outer-sphere sorption can precede an oxidation step (Stone, 1986). Inner-sphere sorption can only be possible for organics which have polar functional groups. Compounds without Lewis base functional groups (like PAHs) cannot directly coordinate with a metal centre. Once an organic molecule has sorbed onto a mineral surface thermodynamic and kinetic parameters will then determine whether electron transfer will occur between the mineral and the organic molecule.

3.2. Thermodynamic predictions of organic oxidation reactions

Thermodynamic data allows a first approximation as to whether an organic compound can be spontaneously oxidised by an oxidant, however, due to kinetic constraints and sorption limitations some thermodynamically spontaneous reactions may not occur at a significant rate. Thermodynamics is important, however, in establishing which reactions are theoretically possible.

The Gibbs free energy of a redox reaction, ΔG^0, can be calculated from:

$$\Delta G^o = -nF(E^0_{ox} - E^0_{red}) \qquad (3.1)$$

Where n is the number of electrons transferred, F is Faraday's constant and E^0_{ox} and E^0_{red} are the standard-state redox potentials of the oxidant and reductant, respectively. If E^0_{ox} - E^0_{red}

(ΔE^0) is positive, that is if the redox potential of the oxidant is more positive than the reductant, the reaction is spontaneous. The following reactions show the reduction of manganese (III/IV) oxides together with their standard redox potential (E^0) as given by Stone (1987):

$$\gamma\text{-MnOOH(s)} + 3H^+ + e^- \leftrightarrow Mn^{2+}(aq) + 2H_2O \qquad E^0 = 1.50\ V \quad (3.2)$$

$$\tfrac{1}{2}MnO_2(s) + 2H^+ + e^- \leftrightarrow \tfrac{1}{2}Mn^{2+}(aq) + H_2O \qquad E^0 = 1.23\ V \quad (3.3)$$

Theoretically any organic molecule with an E^0 less that 1.5 V should be oxidized by manganite (γ-MnOOH) and any organic with an E^0 lower that 1.23 V should be oxidized by MnO_2. Equation 3.1 uses standard-state redox potentials which are calculated at pH 0 using a concentration of 1M for reactants and products. Such conditions are not realistic for environmental conditions where oxidant and reductant concentrations are significantly lower and the pH range is between 4 and 9. The Nernst equation can be used to translate the E^0 potential of a half reaction into a redox potential (Eh) relevant to environmental conditions. The Nernst Equation is given by:

$$Eh = E^o + \frac{0.0592}{n}\log\frac{(OM)}{(RM)} \qquad (3.4)$$

where RM and OM are the activity products of reduced and oxidized molecules, respectively. For this equation to be valid the electrons must appear on the left hand side of the equation. These derived E_h values can then be substituted into Equation 3.1 to calculate the Gibbs free energy in the environmental system.

Sequential removal of electrons from organic compounds often results in each electron transfer step having its own E_h (Neta, 1981). It is often observed that the formation of an organic radical has a higher E_h than the subsequent oxidation to a species with an even number of electrons (Scharzenbach et al., 1993). For example, the E_h for the oxidation of hydroquinone to the free radical species, semiquinone, is 0.46 V compared to 0.01 V for the oxidation of semiquinone to benzoquinone. Consequently the first step of a two electron transfer is often rate-limiting (Scharzenbach et al, 1993). This is of great importance for many oxidation reactions, for example the oxidation of azo dyes by white rot fungi peroxidases is

known to occur via a series of one electron transfers (Goszczynski et al., 1994; Spadaro and Renganathan, 1994; Chivukula et al., 1995; Lopez et al., 2004; Zille et al., 2005).

3.3. Azo dyes

Industries which use and manufacture azo dyes are highly polluting. Azo dyes released into the environment without proper treatment represents 15% of global dye production, that is 150 tonnes per day (Bandara et al., 1999a). A variety of effluent treatment options are available, but many are expensive and only partially effective, thus colour removal from effluents emanating from textile, photographic, paper and food industries remains a pertinent issue in waste water treatment.

Major classes of synthetic dyes include anthraquinoid, triarylmethane and azo dyes. The latter category is the most common group of synthetic dyes. Azo dyes have great structural variations and the highly conjugated molecular structure allow π-π^* transitions within the UV-visible region (Zille et al., 2005) resulting in their characteristic array of colours.

Acid dyes are a group of azo dyes which are used in the dying of wool, nylon and silk. Acid dyes contain one or more sulfonic acid group, which have a low pKa ($\pm$ 1). These dyes are applied in an organic buffer, usually acetate, with a pH between 4 and 5. Within this pH range the amino group of the fabric is protonated, and is electrostatically attracted to the negative sulfonate group of the azo dye molecule which is still negative at this pH. Uptake of the dye onto the fibre is controlled by the addition of leveling agents, usually NaCl and Na_2SO_4 (Muthukumar and Selvakumar, 2004). Thus in addition to dyes, textile effluents also contain a number of auxiliary compounds, like salts and organic acids, which add to the contaminant load. Due to their high solubility, and potential to contaminate ground and drinking water supplies, acid dyes are of high environmental concern (Riu et al., 1997). They are recalcitrant by design, having to resist light, chemical bleaching, water, sweat and microbial attack, making treatment of textile effluent a problematic issue in waste water treatment. Currently there is no single, economically attractive treatment that can effectively decolorise dyes (dos Santos et al., 2007).

3.3.1. Dye treatment techniques

A range of physio-chemical processes such as flocculation-coagulation, adsorption, oxidation-ozonation and biological reduction are commonly used as treatment methods for dye-containing effluent (Pekkuz et al., 2008). Coagulation and flocculation are effective at removal of certain azo dyes, however, this method is only effective over a limited pH range. Coagulants and flocculants add to the total dissolved solids in the effluent and sludge generation causes problematic disposal issues (Banat et al., 1996). Adsorption is made difficult by the high solubility of many azo dyes, and concentrates rather than eradicates the contaminants. Anaerobic treatment causes rapid decolorisation but generally generates breakdown products which are more carcinogenic than the parent molecules (dos Santos et al., 2007). Advanced oxidation processes such as ozonation (Muthukumar and Selvakumar, 2004), Fentons reagents (Gutowska et al., 2007) and photo-catalysis using UV radiation (Bandara et al., 1999b; Muruganandham and Swaminathan, 2006; Sleiman et al., 2007) have shown the capacity to oxidatively decolorise dye solutions. The major drawbacks of AOP are the high input and running costs in addition to their limitation to low-concentration waste waters (Andreozzi et al., 1999). Dye loading becomes a particular problem in any treatment technology making use of UV radiation, as many dye containing waste waters are dark in colour (Bandara et al., 1999b).

Dye-containing effluents are only slightly decolorised by conventional biological waste water treatments (Shaul et al., 1991) with the important exception of white rot fungi (Wesenberg et al., 2003). Numerous studies have shown the capacity of lignin and Mn peroxidases to oxidatively decolorise a number of dye compounds (Pasti-Grigsby et al., 1992; Goszczynski et al., 1994; Spadaro and Renganathan, 1994; Chivukula et al., 1995; Lopez et al., 2004; Pizzigallo et al., 2004; Zille et al., 2005; Lu and Hardin, 2006). As discussed in Section 2.6, Mn(III) complexes are one of the non-specific oxidants responsible for the capacity of white rot fungi to oxidatively decolorise azo dyes.

3.3.2. The use of Mn oxides in azo dye treatment.

Research into the potential of using Mn oxides to oxidatively decolorise azo dyes is still in its infancy. Only two studies could be identified that investigated the decolorisation of azo dyes

(acid red B and direct light red F3B) using Mn oxides (Liu and Tang, 2000; Ge and Qu, 2003) and two additional studies have probed the use of Mn oxides to catalyse electrochemical decolorisation processes (Liu and Qu, 2002; Wang et al., 2006). The reaction between dye compounds and Mn oxides is enhanced at low pH, which has been attributed to the generation of positive charge on the oxide surface, as well as the increased oxidative capacity of the Mn oxide itself at lower pH (Liu and Tang, 2000; Ge and Qu, 2003). Increased dye decolorisation was observed after the addition of $NaNO_3$ to the Mn oxide containing reaction solution and was attributed to the compaction of the diffuse double layer, which would improve dye-mineral contact (Liu and Tang, 2000). Conversely, Ge and Qu (2003) observed a decrease of decolorisation with the addition of NO_3^-, Cl^- and SO_4^{2-}, which was ascribed to competition of these anions with the dye molecule for sorption sites on the oxide surface. Sonication has been shown to greatly enhance the decolorisation reaction, through increasing the surface area of the Mn oxide and generating H_2O_2 which regenerates fresh Mn oxide surfaces (Ge and Qu, 2003).

These two studies have focused on the decoloristion of selected dyes, but little is known in terms of the sorption reactions, reaction kinetics, reactive pathways and reaction intermediates and products in the interactions between azo dyes and Mn oxides. Oxidation has been considered an attractive technology for treating dye waste water (Zhao et al., 2007) and affordable technologies are necessary for water treatment in developing countries, thus investigating the use of natural Mn oxides, occurring as mining waste, for dye water treatment is appealing.

3.3.3. Oxidative reaction mechanisms

The two aforementioned studies (Liu and Tang, 2000; Ge and Qu, 2003) gave no details about the reaction mechanisms involved in Mn oxide mediated dye decoloration. However, there is the likelihood that Mn oxide decolorisation reactions may follow a chemical pathway similar to that of lignin or Mn peroxidase mediated dye oxidation. Thus these reaction mechanisms have been reviewed.

Manganese or lignin peroxidase initiated oxidative reaction mechanisms have been proposed for a number of sulfonated azo dyes. Despite different dyes being used in the various

investigations, similar reaction pathways have been suggested for all of the oxidation reactions (Goszczynski et al., 1994; Spadaro and Renganathan, 1994; Chivukula et al., 1995; Lopez et al., 2004). The azo bond has been reported to undergo either symmetrical (Goszczynski et al., 1994; Lopez et al., 2004) or asymmetrical (Goszczynski et al., 1994; Spadaro and Renganathan, 1994; Chivukula et al., 1995; Lopez et al., 2004) cleavage. Both mechanisms involve successive one-electron transfers initiated on either a phenolic or amino moiety. Symmetric cleavage results via the formation of an imiunium ion on one of the azo N atoms followed by nucleophilic attack, by a water molecule and consequent cleavage of the azo bond (Goszczynski et al., 1994). Asymmetrical cleavage, which seems to be the most frequently observed mechanism, occurs when the carbocation is situated on the C atom bearing the azo bond. Nucleophilic attack, by a water molecule, results in the formation of an unstable tetrahedral complex which breaks down to yield quinone and phenyldiazene type compounds (Spadaro and Renganathan, 1994; Chivukula et al., 1995). Goszczynski et al. (1994) proposed symmetric cleavage of the azo bond would result in nitro or quinone monoimine compounds. These workers also established that symmetric cleavage could result in the same products as asymmetric cleavage if reduction of the nitro group occurred.

3.3.4. Sorption of azo dyes

Manganese oxide mediated oxidation reactions are preceded by a sorption step (Stone and Morgan, 1984a). Thus the mechanism of dye sorption to the oxide surface will be an important precursor reaction. Sorption of azo dyes to oxide surfaces have been studied mainly in investigations involving photo-catalysts like titanium and iron oxides (Bauer et al., 1999; Bandara et al., 1999a; Bourikas et al., 2005). Sorption of the dye onto an oxide surface can be understood in electrostatic terms taking into account surface species on oxide and the pH-dependent charge characteristics of the azo dye. Acid azo dyes have a number of functional groups which can undergo pH-dependent charging. The sulfonate group has a pKa_1 of approximately 1 (Bandara et al., 1999a) and thus is essentially always deprotonated under experimental conditions. Other functional groups on azo dyes undergo protonation above this pH. Acid yellow 36, for example, has a secondary amine group which has a pKa_2 of 2.3 (Sleiman et al., 2007) and methyl orange has a tertiary amine group with a pKa_2 of 3.4 (Oakes and Gratton, 1998). Acid orange 7 has a phenolic group on the naphthalene ring,

which has a pKa_2 of 11 (Bandara et al., 1999a) so this dye is essentially negatively charged under all but extremely acid conditions. Thus the charge characteristics of every dye are different, except for the fact that they all contain a negatively charged sulfonate group.

The sorption of AO 7 on the Ti oxide surfaces has been found, without exception, to increase with decreasing pH (Bandara et al., 1999a; Konstantinou and Albanis, 2004; Bourikas et al., 2005) with a notable increase of sorption occurring below pH 7 due to the formation of $TiOH_2^+$ species (Bandara et al., 1999a; Bourikas et al., 2005). Similar pH-dependent effects have been found for sorption of dyes on other metal oxides, with a rapid onset of sorption occurring as the pH drops below the PZC of the oxide (Bandara et al., 1999a; Wu et al., 2005). Similarly, positive charge generation of the oxide surface has been proposed to be a influencing factor contributing to increased oxidation of azo dyes by Mn oxides observed at low pH (Liu and Tang, 2000; Ge and Qu, 2003).

From the various FT-IR investigations into the sorption of AO 7 onto Ti oxide surfaces, it has been proposed that inner-sphere sorption occurs between the sulfonate group of the dye and the metal centre (Bauer et al., 1999; Bandara et al., 1999a; Bourikas et al., 2005). The observations in these studies of electrostatic attraction may also support outer-sphere interactions rather than chemical bonding (Eggleston et al., 1998).

Sorption was not investigated in the two aforementioned Mn oxide dye decolorisation studies (Liu and Tang, 2000; Ge and Qu, 2003), however, Ge and Qu (2003), observed decreased decolorisation potential in the presence of SO_4^{2-} ions which led these authors to propose sorption occurred via the sulfonate group of the dye.

3.3.5. Reaction kinetics

Reactions occurring at the water-mineral interface, are usually preceded by a sorption step resulting in reaction kinetics that are more complex than solution based reactions. The Langmuir-Hinshelwood kinetics model accounts for sorption and includes parameters such as equilibrium concentration and partitioning coefficient in the kinetic equation. This kinetic model has been used with mixed success to describe the kinetics of a number of photo-catalytic studies involving Ti oxides (Bandara et al., 1999a; Konstantinou and Albanis, 2004;

Muruganandham and Swaminathan, 2006; Sleiman et al., 2007). When investigating photo-catalysed reactions it is possible to gather sorption information before the light-dependent reaction is initiated (Bandara et al., 1999b; Muruganandham and Swaminathan, 2006; Sleiman et al., 2007). In the case of Mn oxides, sorption studies are difficult to characterise due to the rapid reaction of the reductant on the oxide surface (Xyla et al., 1992; Matocha et al., 2001). For this reason many kinetic studies involving Mn oxides have based kinetic calculations on the generation of Mn^{2+} and not solely on the disappearance of the reductant (Stone and Morgan, 1984a; Stone and Morgan, 1984b; Stone, 1987a; Stone, 1987b; Laha and Luthy, 1990; Xyla et al., 1992; Klausen et al., 1997; Matocha et al., 2001). It has to be taken into consideration however, that kinetic measurements, based solely on Mn^{2+} release, have limitations in that Mn^{2+} once released through reduction can be re-adsorbed onto the mineral surface.

3.3.6. Background information on acid orange 7

Acid orange 7 (AO 7), also commonly known as Orange II, has been used as a model acid azo dye by a number of workers (Bauer et al., 1999; Bandara et al., 1999b; Lopez et al., 2004; Bourikas et al., 2005; Lu and Hardin, 2006). It displays the 'core-structure' of a number of commercial dyes and thus has similar physiochemical properties of the more complex dye compounds (Coen et al., 2001). The numerous investigations on AO 7 have resulted in extensive chemical and structural information being available for the dye, which provides a good platform to gather an understanding of reactions between the tailings materials and azo dye compounds.

Acid orange 7 is subjected to intramolecular hydrogen bonding tautomeric interactions between the oxygen of the naphthyl group and the β-hydrogen of the corresponding azo linkage (Stylidi et al., 2003) as shown in Figure 3-1. Thus AO 7 can exist in either the azo or the hydroazo form. In aqueous solutions the hydroazone form is the most favourable (Stylidi et al., 2003).

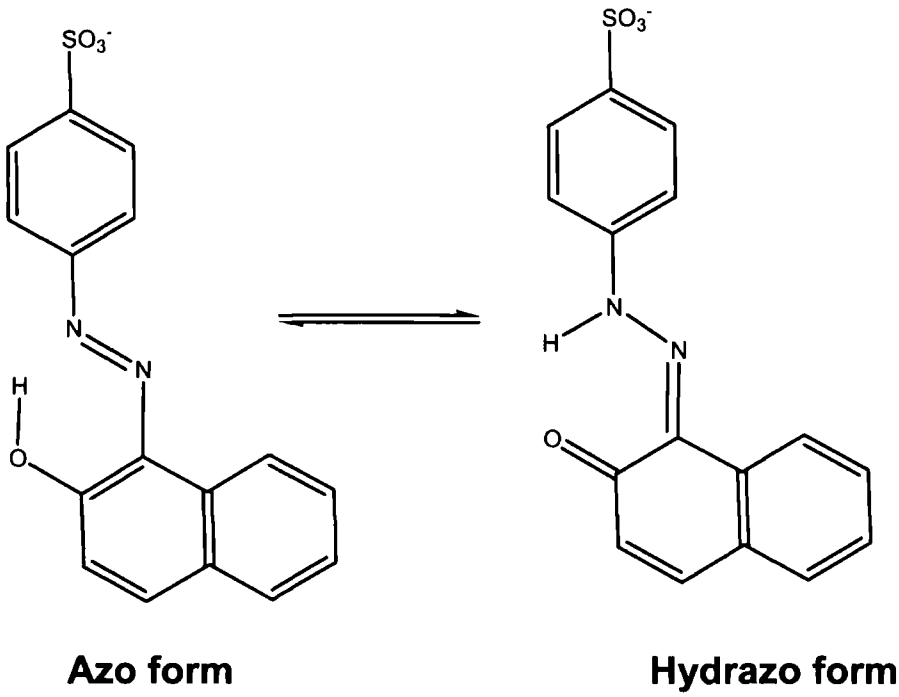

Figure 3-1 Tautomeric forms of AO 7 in solution

The oxidative breakdown of AO 7 has been investigated in numerous studies (Chivukula et al., 1995; Lopez et al., 2004; Zille et al., 2005; Lu and Hardin, 2006). Apart from Lopez et al. (2004) where both cleavage mechanisms were reported, asymmetric cleavage is most frequently observed. Asymmetrical cleavage of the azo bond results in the formation of 1,2-naphthaquinone and (4-sulfophenyl)diazene (Chivukula et al., 1995). The latter product is unstable and can undergo oxidation by oxygen to generate an unstable phenyldiazene radical which in turn forms a sulfophenyl radical through the loss of N_2. The fate of this sulfophenyl radical differs depending on the chemical environment (Chivukula et al., 1995). Phenyl radicals can only abstract a hydrogen radical from the medium and cannot react with oxygen (Russell and Bridger, 1963), however, when a sulfonate substituent is present the reactivity of the radical towards oxygen can change and sulfophenyl hydroperoxides can be generated (Chivukula et al., 1995). These phenyl radicals can also undergo coupling reactions with other breakdown products (Zille et al., 2005) or undergo hydrolysis to generate hydroxybenzenesulfonate (Lopez et al., 2004). The symmetrical cleavage of AO 7 has been reported to generate 4-aminobenzenesulfonate and 1-amino-2-naphthol (Lopez et al., 2004). A range of oxidation products have been identified for other azo dyes (Goszczynski et al.,

1994; Spadaro and Renganathan, 1994; Chivukula et al., 1995) but all products can be rationalised by either symmetrical or asymmetrical cleavage pathways.

Further enzyme catalysed coupling reactions between unreacted dye and the breakdown products can result in polymerisation, which can again generate coloured solutions (Zille et al., 2005). Prolonged contact between the enzymes and reaction products can be problematic for water cleanup purposes. Surface-mediated oxidations would therefore have the distinct advantage over enzymatic systems in this instance as rapid removal of breakdown products from the reactive surface may be achievable.

3.3.7. Background information on acid yellow 36

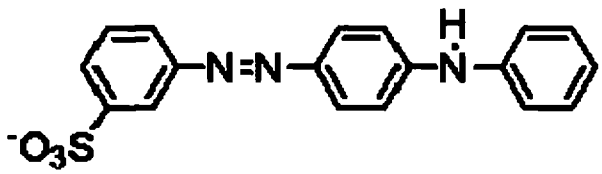

Figure 3-2 Structure of acid yellow 36 (AY 36)

Acid yellow 36 (AY 36), also known as metanil yellow, is an acid azo dye that has found wide use in a number of industries including tannery, paper, cosmetic, textile, soap and polish manufacturing. It is also used as a pH indicator and in the determination of trace amounts of Mo(IV). Despite AY 36 being a non-permitted food colorant it is still widely used in sweet meat, ice creams, soft drinks and a coating for tumeric (Mittal et al., 2008). Due to its wide use it is a common contaminant in waste waters emanating from such industries. Acid yellow 36 is an amine containing dye (Figure 3-2). Amine containing dyes are known to be carcinogenic, due to their oxidative metabolism in the gut, even without cleavage of the azo bond (Brown and Devito, 1993). Ingestion of the dye has been shown to cause a number of human disorders and has been implicated in tumor producing effects (Mittal et al., 2008). Despite this, there are a limited number of studies investigating degradation of AY 36 and only two could be found that demonstrate oxidative breakdown (Shigwedha et al., 2006; Sleiman et al., 2007). Decolorisation in these aforementioned studies was achieved via photo-catalytic oxidation using Ti oxides and only the latter study suggests a tentative reaction

mechanism. There is no information on the oxidation of AY 36 either enzymatically or by Mn oxides.

3.4. Polycyclic aromatic hydrocarbons

Polycyclic aromatic hydrocarbons are a ubiquitous product of hydrocarbon combustion under reducing conditions, thus there are both natural and anthropogenic sources of PAHs. Major anthropogenic sources include fossil fuel combustion, metallurgical processes and the manufacture of creosote and bitumen. They are of high concern in the environment as many of them are toxic, mutagenic and/or carcinogenic to micro-organisms as well as to higher systems, including humans. Their low water solubility and strong partitioning into soil organic matter (SOM) hinders bioremediation techniques which are more effective when the contaminant is soluble and therefore bioavailable (Zhang et al., 1995).

There is a wealth of research focusing on the removal of PAHs from soils using various physical, chemical and biological techniques. Physical techniques include incineration (Long, 1993) and thermal desorption (Kopinke and Remmler, 1995). These techniques have their limitations due to their high capital costs and large associated carbon footprints. Chemical treatment of PAHs using advanced oxidative processes is another treatment option but requires the use of expensive oxidising agents such as peroxide and permanganate (Brown et al., 2003). These oxidising techniques are also frequently unsuccessful in soil treatment due to the hydroxyl radicals being scavenged by natural organic matter before the target compound can be oxidised.

Bioremediation in the form of microbial degradation of PAHs has been well documented (Mihelcic and Luthy, 1988; Gray et al., 1994; Willumsen et al., 1997; McNally et al., 1998) but as mentioned above most bacteria require a soluble substrate (Zhang et al., 1995) which makes this form of bioremediation difficult. Oxidative breakdown of PAHs has been achieved by white rot fungi via Mn(III)-organic complexes which serve as easily diffusible, non-specific oxidants (Field et al., 1992; Wariishi et al., 1992), however, PAH solubility is still a problem and maximum oxidation is achieved only when water miscible solvents are used in reactions (Eibes et al., 2005).

There are very few reports of abiotic interactions between PAHs and soil minerals. Pyrene degradation has been observed when birnessite was gently ground with PAH contaminated soil (Napola et al., 2006). Other reports of abiotic interactions between Mn oxides and PAHs have not shown any positive reaction (Daly, 1907; McNally et al., 1998).

3.4.1. Sorption of PAHs onto mineral surfaces

Polycyclic aromatic hydrocarbons are HOCs and PAH-mineral sorption is governed by factors discussed in section 3.1.2, thus only a brief mention is given to PAH-mineral interactions in this section.

Whilst PAH-mineral interactions are considered to be subordinate to PAH-SOM interactions in controlling the mobility of PAHs, under low organic soil conditions sorption onto the mineral phase is competitive. In hydrated mineral systems it is the hydrophobicity of the PAH which is considered to be the most important factor driving the partitioning of the PAH onto mineral surfaces, although solution chemistry, like pH and ionic strength can have a limited influence (Schlautman and Morgan, 1994). Ionic strength can influence organic-mineral interactions in a number of ways. Increasing the ionic strength of a solution can have an effect on HOCs known as 'salting out' whereby the solubility of HOCs decreases and accordingly their partitioning into the solid phase increases (Means, 1995; Tremblay et al., 2005). Ionic strength and pH influence charge generation on mineral surfaces, which also influences PAH sorption (Schlautman and Morgan, 1994).

Murphy et al. (1990) compared sorption of anthracene on hematite and kaolinite in hydrated systems with and without humic coatings. Sorption to both mineral phases was very low compared to the humic coated minerals but between the two uncoated minerals kaolinite showed the highest partitioning coefficient, which was interpreted as being a function of the larger area of basal siloxane and gibbsite sheets, which are more hydrophobic than the ionizable hydroxyl groups of hematite. Despite this it has been established that mineral surface area is the most important mineral characteristic when it comes to PAH sorption (Schlautman and Morgan, 1994).

Sorption of PAHs onto mineral surfaces has been shown to be inversely proportional to the moisture content of soils (Chiou and Shoup, 1985). Karimi-Lotfabad et al. (1996) reported sorption of PAHs to the mineral phase of dried soils and a pure montmorillonite clay. Rewetting reduced mineral sorption and increased partitioning into organic matter. This was interpreted as increased competition by water molecules for sorption sites on the mineral surface. Similar observations have been made during investigations of volatile and semi-volatile organic compound sorption onto clay mineral and quartz surfaces (Goss, 1992; Goss, 1993). These studies by Goss established that at humidity levels equating to less than monolayer water coverage of the mineral surface, sorption coefficients were high and decreased exponentially as the exposed mineral surfaces were progressively hydrated. The enhanced sorption of hydrophobic organic compounds on dried mineral surfaces, suggests that moisture content should be considered during investigations of mineral-PAH interactions.

3.4.2. Oxidation of PAHs

Removal of an electron from an aromatic molecule, involves transfer of a π-electron from the position of highest charge density to the metal centre. Ionization potential (IP) quantifies the ease with which this π-electron is removed. For PAHs, IP is an important indicator of bio- and carcinogenic activity as ionisation is necessary prior to binding to cellular macromolecules (Cremonesi et al., 1992). Ionization potential has been determined for a number of PAHs, but standard redox potentials are difficult to obtain due to the irreversible redox behaviour of many PAHs. Formal E^0 can be determined empirically for certain condensed PAHs, like anthracene, which display reversible behaviour if radical stabilising electrolytes are utilised. Using this technique, Cremonesi et al. (1992) determined the E^0 of anthracene to be 1.26 V and the ionization potential to be 7.43 eV. The heterogenous composition of natural Mn oxide minerals and mixed oxidation states make thermodynamic calculations difficult, however, according to Equations 3.2 and 3.3 it would appear that oxidation of anthracene by MnOOH is spontaneous whilst the reaction with MnO_2 is not. Using free energies of formation, McFarland and Sims (1991) calculated a negative ΔG for the reaction of anthracene and MnO_2 thus there appears to be some disparity in

thermodynamic data, which is not unexpected considering the variable composition of Mn oxides.

Microbial mineralisation of organic contaminants can only occur sustainably if the microbe's metabolic needs are catered for by exothermic reactions which need to yield enough energy to support growth as well as fulfil microbial cell maintenance requirements. A thermodynamic framework was established by McFarland and Sims (1991), in which energy yields were calculated for heterotrophic PAH metabolism using a variety of terminal electron acceptors. According to their study complexed Mn^{4+} ions showed the highest energy yield followed by O_2, NO_3^-, Fe^{3+} ions , MnO_2, FeOOH, SO_4^{2-} and CO_2. Manganese (III) hydroxides or complexed Mn^{3+} ions, arguably more prevalent in natural systems than Mn^{4+} ions (Dion and Mann, 1946), were not considered in this study. From the energy yield calculations of McFarland and Sims (1991) it would appear that oxidation of anthracene is thermodynamically favourable using Mn oxides as a terminal acceptor, but would not be a competitive substrate in the presence of aliphatic or alcoholic substrates. In reality biodegradation of PAHs is often hindered by their poor aqueous solubility and strong partitioning into the organic phase (Manilal and Alexander, 1991; Volkering et al., 1992; Weissenfels et al., 1992).

It has been demonstrated that, with a few exceptions, PAHs with an IP $\leq$7.55 eV can be oxidised by lignin and Mn peroxidases (Hammel et al., 1986). Up to 100% anthracene removal by Mn peroxidases has been reported when water miscible solvents are used to increase anthracene solubility (Eibes et al., 2005). One oxidation pathway of anthracene has been shown to proceed via anthraquinone to phthalic acid (Hammel, 1995). Other studies have suggested that anthraquinone is the dead-end product of anthracene oxidation by certain peroxidases (Field et al., 1992; Bezalel et al., 1996). The hydroxylation of anthracene is thought to occur via radical formation followed by nucleophilic attack by water molecules (Hammel et al., 1986). The alternative polymerisation and humification pathway, has also been observed (Bogan et al., 1999). Generation of anthraquinone or further breakdown products is considered beneficial as these metabolites are more bioavailable and can be further degraded by bacteria (Mueller et al., 1989). Polymerisation and humification reduces the mobility of the PAH and these humified products have a reduced genotoxicity compared

to the parent compounds (Bogan et al., 1999) thus both oxidation pathways can be considered beneficial.

Oxidation of PAHs on the surface of clay minerals has been reported (Karimi-Lotfabad et al., 1996). The decreased recovery of added anthracene from both soils and pure montmorillinite clay was accompanied by the appearance of certain higher molecular weight compounds. Loss of anthracene was greatest for dry samples, and increasing the moisture content significantly increased anthracene recovery. It was suggested that this oxidation of anthracene occurred through one electron transfer to transition metals on the exchange sites of clays. Their study is one of a few studies which reports abiotic oxidation of PAHs.

4. Material and methods

4.1. Review of experimental and analytical techniques: Azo dyes

4.1.1. Infrared spectroscopy

Infrared spectroscopy has frequently been used to probe sorption and oxidation reactions of dyes on Ti, Al and Fe oxide surfaces (Vinodgopal et al., 1996; Bauer et al., 1999; Bandara et al., 1999a; Bandara et al., 1999b; Lucarelli et al., 2000; Stylidi et al., 2003; Bourikas et al., 2005). The majority of these studies have used diffuse reflectance infrared Fourier transform (DRIFT) spectroscopy. This allows a 'snap shot' view before and after the reaction has taken place, but cannot provide kinetic or dynamic information. Another limitation of the DRIFT technique arises from the need for samples to be dried after the reaction has taken place. Drying has been shown to change co-ordination of sorbed compounds (Hug, 1997; Eggleston et al., 1998; Dowding, 2004), as well as surface acidity (Mortland and Raman, 1968; Dowding et al., 2005). Thus artefacts may arise in data interpretation (Eggleston et al., 1998).

Attenuated Total Reflectance Fourier Transform Infrared spectroscopy (ATR-FTIR) has the benefit of allowing real time surface analysis in a fully hydrated system and thus is a powerful *in-situ* technique. It has found applications in probing oxidation (Parikh et al., 2008) and sorption (Hug, 1997; Eggleston et al., 1998) reactions at the mineral-water interface. It has been shown to be particularly well suited in discerning between inner- and outer-sphere sorption of compounds on mineral surfaces (Hug, 1997; Eggleston et al., 1998; Johnson et al., 2005), through the splitting, shifting and formation of new IR peaks.

There are also many limitations with ATR-FTIR. The spectral range is limited to wavenumbers above 850 cm^{-1} for Ge crystals and 750 cm^{-1} for ZnSe crystals. Zinc selenide crystals are the most frequently used due to their low cost and high penetration depth but their operational pH is limited to between 7 and 9. Germanium crystals have a wider operational pH (1 to 12), but a lower penetration depth (0.2 μm) which reduces the sensitivity. Achieving *in-situ* data requires coating the crystal with a thin clay layer following the technique of Hug (1997). Controlling clay film thickness can be very difficult and therefore the technique is not

well suited to quantitative assessment. Despite these shortcomings the qualitative information can provide valuable insight into reaction kinetics and mechanisms.

4.1.2. Analytical techniques

Due to their chromaphoric properties, Ultraviolet-visible (UV-vis) spectroscopy, is a useful tool for analysing azo dyes. Percentage decolorisation is a commonly used parameter in dye removal studies and is calculated using the following equation:

$$\% \text{ decolorisation} = (1\text{-}AA/AB) \times 100$$

Where AA is the absorbance after and AB is the absorbance before the reaction, measured at the at the visible region λ_{max} of the dye (Lu and Hardin, 2006).

High Pressure Liquid Chromatography (HPLC) combines chromographic separation with UV-vis analysis and is a common tool for the qualitative and quantitative analysis of azo dyes and their breakdown products. The draw back of this technique is product identification is very difficult unless standards of compounds are run, which requires certain knowledge of reaction products. This makes identification of unknown compounds difficult.

Liquid-chromatography mass spectrometry (LC-MS) combines chromagraphic separation followed by MS analysis. It has been identified as the technique of choice for environmental monitoring of dyes because of its high sensitivity and ability to obtain structural information on unknown compounds (Rafols and Barcelo, 1997). Sulfonated azo dyes are non-volatile thus MS with conventional electron ionisation cannot be used (Holcapek et al., 1999). Electrospray ionisation is a soft ionisation technique which is well suited for ionic dyes with high molecular weight. The sulfonic group is strongly acidic and is completely dissociated in aqueous solution thus negative ion mode is much more sensitive than positive ion mode for the analysis of azo dyes (Rafols and Barcelo, 1997). In tandem with soft ionisation techniques, in-source collision induced dissociation or multiple MS $(MS)^n$ using an ion trap analyser aids in the structural identification of dyes (Holcapek et al., 2001) and unknown reaction products. For this reason LC-MS has been the central technique used in the analysis of oxidative breakdown products of dyes (Goszczynski et al., 1994; Lopez et al., 2004; Zille et al., 2005; Lu and Hardin, 2006).

4.2. Review of experimental and analytical techniques: PAHs

4.2.1. Spiking techniques

One of the biggest hurdles in reacting PAHs with mineral phases is achieving contact between the hydrophobic organic molecule and the mineral surface. Difficulties in achieving homogenous distribution of PAHs in soil for use in sorption/desorption studies has resulted in a number of investigations into soil spiking procedures (Murdoch et al., 1997; Reid et al., 1998; Brinch et al., 2002; Doick et al., 2003). One approach is to add aqueous solutions of PAHs at or below the PAH water solubility limit (Murphy et al., 1990; McNally et al., 1998). Due to the very low solubility of PAHs (e.g. anthracene solubility = 0.07mg.L^{-1}) this results in low loading and low solid/liquid ratios being used to reach the required concentrations. Using water as the carrier medium has distinct advantages however, as it is likely to be most representative of environmental conditions, will favour hydrophobic partitioning onto the mineral surface and will be the medium in which Mn oxides will react with the PAH. Other workers have employed organic solvents like dichloromethane, acetone, ethanol, methanol and toluene (Karimi-Lotfabad et al., 1996; Fisher et al., 1997; Reid et al., 1998; Northcott and Jones, 2001; Brinch et al., 2002) as carrier mediums to apply PAHs to soils. These solvents greatly increase the solubility of the PAH and thus may achieve greater surface contact and distribution of the PAH on the solid phase, however, biofilms, microbial populations (Brinch et al., 2002; Doick et al., 2003) and hydrophobic partitioning maybe affected by solvents. It is also questionable how applicable such HOC delivery is to environmental conditions. An investigation into a number of spiking procedures was undertaken by Reid et al. (1998). It was established that the spiking protocol which gave the most homogeneous distribution of the PAH involved a single spiking/rehydration operation conducted on a dried soil. This involves spiking a volume of water (sufficient to rehydrate a dried soil to the required moisture content), and then blending with the dried soil.

Mechanochemical techniques have recently been employed to overcome poor contaminant/mineral contact (Pizzigallo et al., 2004; Napola et al., 2006). Grinding of solid phenanthrene with soil resulted in better contact and breakdown than grinding soil with phenanthrene dissolved in acetone (Napola et al., 2006).

4.2.2. Extraction techniques

Extraction of HOCs from polluted soils is generally considered to be more difficult than extracting HOCs from a clean soil which has been recently spiked, due to the shorter exposure time of contaminant and solid in spiked samples (Lopez-Avila et al., 1995). In addition extraction from mineral phases, like the tailings, should be easier than from soils, which usually have significant organic matter content.

Soxhlet extraction (U.S.EPA Method 3540) is a rigorous and effective extraction technique. It involves continuous extraction of a sample with aliquots of clean solvent. Disadvantages of this technique are the large volumes of solvent used, long extraction periods and the use of specialised soxhlet glassware which limits the number of simultaneous extractions. Extraction by ultra sonication (U.S.EPA Method 3550b) involves sonicating a sample in a chosen extraction solvent. It is a less rigorous extraction technique, but is rapid and requires no specialised glassware so multiple samples can be extracted simultaneously. Microwave assisted extraction is an attractive alternative to soxhlet extraction as it gives the same efficiency but is significantly faster (Lopez-Avila et al., 1995; Flotron et al., 2003).

Greater extraction efficiency of pesticides has been achieved for polar organic solvents compared to non-polar solvents (Chiou and Shoup, 1985), which is thought to result from polar molecules displacing HOCs from mineral surfaces (Chiou and Shoup, 1985).

4.2.3. Analytical techniques

Analysis of extracts can be achieved by means of HPLC (U.S.EPA Method 8310) equipped with a fluorescence or UV detector or GC/MS (U.S.EPA Method 8270c). A distinct disadvantage of using GC/MS is that high molecular weight polymers can not be detected. Karimi-Lotfabad et al. (1996) detected anthracene polymeric oxidation products qualitatively using thin layered chromatography.

Due to the photo-active nature of many PAHs, fluorescence and UV-visible spectroscopy provide quick, easy and sensitive analytical tools. Fluorescence and UV absorption spectroscopy can be used to quantify PAH concentrations in waters due to the extinction

coefficient and quantum yields being the same in ethanol and water. This allows ethanol based calibration standard curves to be used to determine the concentration of aqueous anthracene solutions. Using this technique detection limits of 0.03 $\mu g.L^{-1}$ have been achieved for anthracene (Schwarz and Wasik, 1976).

4.3. Collection of tailings materials

Tailings samples were collected from Wessels, Nchwaning, Mamatwan, Gloria and Hotazel mines. Wessels and Nchwaning mines are found to the north of the KMF, Gloria mine is situated to the north east and Mamatwan mine lies on the south east tip of the KMF (Figure 1-1). The Hotazel mine lies on the Hotazel outlier to the east of the KMF (Figure 1-1). Mining operations have ceased on the Hotazel mine but the other 4 mines are all fully operational. The waste material, generated during the ore extraction process is graded into different size fractions and the fine material is transported to tailings dams where it is stored.

Samples were collected from the fine tailings (<200 μm) stockpiled on the tailings dams of Wessels and Mamatwan mines. At the time of sampling water was ponded in both tailings dams with reeds, grasses and trees surrounding the ponded area (Figure 4-1 a and c). An iridescent, oily looking scum, which shattered when disturbed, was present on the surface of the ponded water of the Wessels tailings dam. Composite samples of the Wessels and Mamatwan tailings were collected from the dry areas of the tailings dams. The Hotazel tailings are stockpiled in four dumps. Grass has established an intermittent covering of the largely dry dumps (Figure 4-1 d). Composite samples of the four dumps were collected from boreholes drilled at an earlier date by the BHP Billiton mine staff. Similarly composite samples were collected from cores drilled into the Nchwaning and Gloria tailings dams by the ASSMANG mine staff.

Samples were sealed in polyethylene sample bags and couriered to the Durham University. On arrival samples were well mixed and sieved through a 2 mm sieve. This material was then used for further analysis.

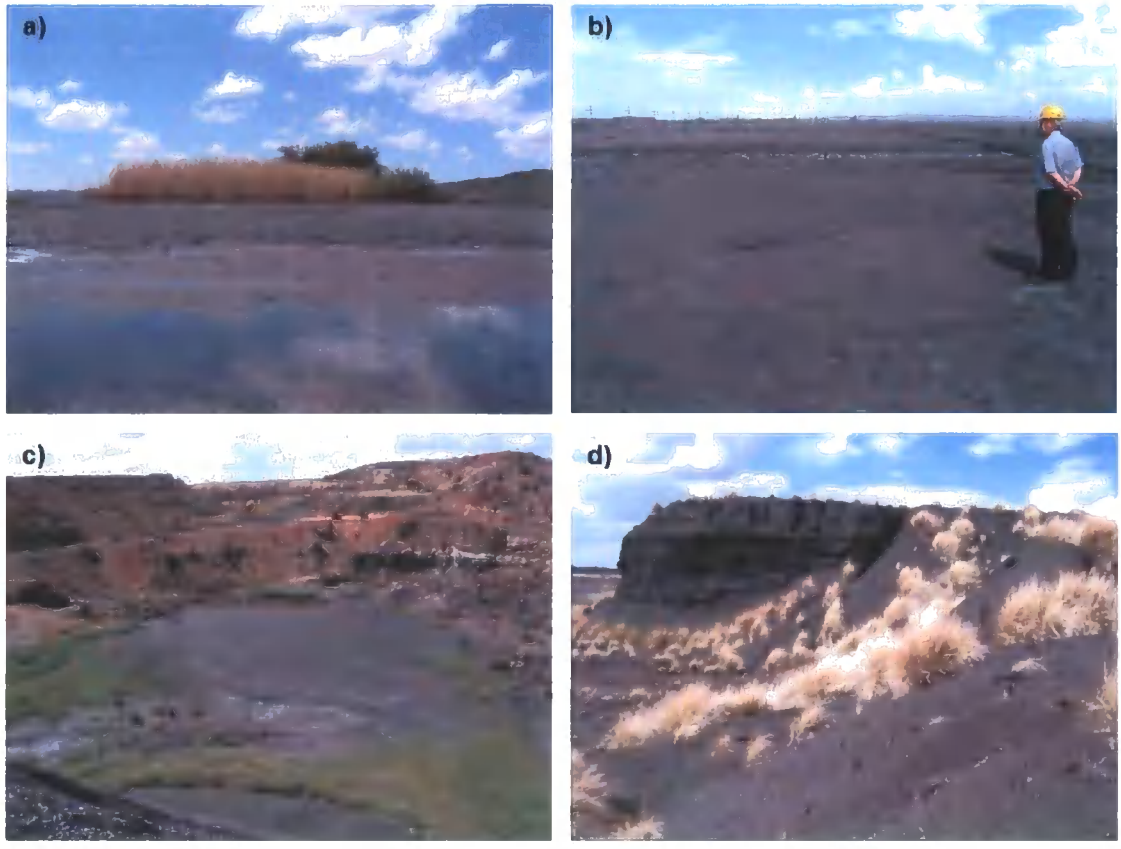

Figure 4-1 Photographs of a) ponded area of Wessels tailings dam, b) Nchwaning tailings dam, c) Mamatwan tailings dam and d) one of four dumps at Hotazel

Tailings from the Wessels and Nchwaning mines originate from the same ore body, known as Wessels type (WT) ore and tailings from Gloria and Mamatwan mines originate from the Mamatwan type (MT) ore. The Hotazel tailings originate from yet another ore type, Hotazel (HT) ore. The tailings of all five mines were characterised to establish any similarities between the tailings produced from the same ore type.

4.4. Synthetic Mn oxides and control minerals

Manganite was synthesized following the method of McArdell et al (1998). A 2 L solution of 60 mM $MnSO_4$ was heated to 60°C. To this, 41 mL of 8.8 M H_2O_2 was added followed by the slow addition of 600 mL of 0.2 M NH_4OH. This solution was stirred at 95 °C for 6 hours and then allowed to cool overnight. The clear supernatant was siphoned off and the remaining

slurry centrifuged to concentrate the mineral phase. The mineral phase was washed and sonicated 10 times to remove excess salts. The mineral phase was then freeze dried. X-ray diffraction, ESEM and IR were used to confirm the formation of manganite.

Quartz (QTZ) and calcite (CC) (Derbyshire limestone; TRUCAL 6) powders (<63 μm) were obtained from Tarmac. The purity of these minerals was verified in an earlier study (Bamforth et al., 2006). Manganese (III) oxide (Mn_2O_3) was purchased from Sigma-Aldrich and is referred to as purchased Mn oxide throughout the thesis.

4.5. General laboratory equipment and chemicals used

Unless specified the following laboratory equipment was used: an AND analytical balance (120 x 0.0001 g resolution) (A & D weighing, Japan), a Yellow line OS 10 Basic reciprocal shaker (IKA, Germany), a Decon F5200b sonic bath, (Decon Laboratories, UK) a MSE Harrier 15/80 centrifuge (MSE, UK) and a Metrohm 785 titrino, (Metrohm, Switzerland) for pH measurement (2 decimal places).

All chemicals, unless specified, were reagent grade. Potassium chloride, analysis grade ammonium acetate, sodium hexametaphosphate (calgon solution), sodium dithionite, and sodium citrate were purchased from Fisher Scientific. Analysis grade hydroxylamine hydrogenchloride (HAHC) and hydroquinone (HQ) were purchased from Acros organics. Deionised (DI) water was obtained from a Purite Select water deioniser (Resistance 14 Ω).

Acid yellow 36 (AY 36), acid orange 7 (AO 7), acid yellow 9 (AY 9), acid red 88 (AR 88) and acid red 151 (AR 151) were obtained from Sigma and used without further purification. 1,2 Naphthaquinone, 4-hydroxybenzenesulfonic acid, benzenesulfonate and *p*-benzoquinone were purchased from Arcos organics. Glacial acetic acid was purchased from Fisher Scientific and sodium acetate was purchased from Sigma –Aldrich.

Anthracene (98%) and anthraquinone (96%) were obtained from Arcos organics and used without prior purification. Cyclohexane (HPLC grade) and acetonitrile (HPLC grade) were obtained from Fisher scientific.

4.6. Wet chemistry methods

4.6.1. Clay extraction

Clay extraction for XRD analysis was achieved as follows: 10 g tailings were weighed out into a 500 mL centrifuge vessels, 50 mL DI was added followed by 1 mL 1% calgon solution. The samples were shaken for 40 minutes on a reciprocal shaker. The slurry was then passed through a 53 μm sieve prior to centrifugation at 1000 rpm for 5 minutes. The supernatant was decanted and a few drops of 0.5 M $MgCl_2$ added. The suspension was allowed to settle overnight. The clear supernatant was siphoned off and the remaining concentrate was used for analysis. A few drops from each of the clay concentrates were added to ceramic tiles and the excess moisture removed through suction. The clay coated tiles were then allowed to dry overnight before XRD analysis.

The clay fraction of HT tailings was collected for PZC determinations by clay dispersion. A 15 g HT sample was weighed into a 500 mL measuring flask and 500 mL DI water added. The pH of the slurry was adjusted to pH 11 by adding a few drops of 5 M NaOH. The measuring cylinder was shaken and placed in a sonic bath for 1 hour. This process was repeated four times after which the sample was left to settle overnight. The suspended clay particles were siphoned off into a beaker. The clay suspension was titrated to pH 4 using 0.1 M HCl and centrifuged at 3000 rpm for 5 minutes. The clear supernatants were decanted and the remaining mineral phase washed several times with DI until the clay phase began to disperse. This dispersed clay was used in the electrokinetic mobility, potentiometric and flocculation determinations.

4.6.2. pH and electrical conductivity (EC)

Samples were prepared for pH analysis in DI, using a solid:liquid (S:L) ratio of 1:2.5. The pH was measured using a Satorius Professional Meter PP-50. The EC of the tailings was measured in DI using a Mettler Delta 350 conductivity meter. Samples were prepared for EC analysis in DI using a S:L of 1:10. These same samples were used for the analysis of soluble cations and anions.

4.6.3. Mn oxidation state

The average oxidation state of the material was determined iodometrically (Murray et al., 1984). Briefly, 30 mL of DI water was added to 10 mg of sample. To this 1 mL of iodide solution (4 M NaI + 5 M NaOH) and 1 mL 8 M H_2SO_4 was added to the slurry and allowed to react for 10 minutes. The iodine was titrated with standardised 0.01 M $Na_2S_2O_3$ using starch as an indicator. Manganese and Fe concentrations were determined in the solution using atomic absorption spectroscopy (AAS) and the O/Mn as MnO_x ratio was then calculated using the following formula:

$$x = 1 + \frac{1}{2}\left[\frac{Ox - Fe_t}{Mn_t}\right]$$

Where Ox is total oxidising equivalents, Fe_t is total Fe equivalents and Mn_t is total moles of Mn.

4.6.4. Sequential extraction

Water soluble and exchangeable Mn were determined following the methods of Gambrell (1996). Water soluble Mn was determined by reacting the tailings with DI using a 1:10 solid:liquid (S:L) ratio. The DI was equilibrated with the tailings for 30 minutes by shaking on a reciprocal shaker set at 250 rpm. The supernatants were filtered through 0.2 μm syringe filters prior to analysis using AAS. Exchangeable Mn content was determined in the same manner replacing DI with either 1 M KCl , or pH 7 1M NH_4OAc. The reducible fraction was determined by sequential extractions using a series of reducing agents as shown and referenced in Table 4-1. Two washings were performed per extractant, with the final S:L ratio being 1:250. For these extractions the tailings were used without prior grinding (i.e. the < 2 mm fraction). The total reducible Mn content was determined by reacting finely ground material (< 63 μm) with sodium dithionite in a sodium citrate buffer. Metal concentrations were determined using AAS.

Table 4-1 Sequential extraction methods

Method	Reference
0.2% hydroquinone in 1M pH7 NH4OAc	Gambrell and Patrick (1982)
Acidified (0.01M HNO3) hydroxylamine hydrogenchloride	Chao (1972)
0.3 M Sodium citrate; 2g Sodium dithionite	Holmgren (1967)

Samples were submitted to Analytical and Environmental Services (Howden, UK) for aqua regia extraction. All acid extractable metals were digested by an oxidising mixture of concentrated nitric acid and hydrochloric acid and refluxed for 3 hours. The digests were then clarified by filtration and the concentration of the metals determined by inductively coupled plasma spectroscopy.

4.6.5. Point of zero charge

An attempt was made to measure the PZC of the tailings materials using a potentiometric approach (Hunter, 1981). Sodium chloride was used as the indifferent electrolyte at concentrations of 0.01, 0.1 and 1.0 M. Tailings material (5 g) were placed into polyethylene bottles and 50 mL of NaCl solution added. Each of the slurries, were treated with either 0.1 M NaOH or HCl and allowed to equilibrate on a reciprocal shaker overnight. A settling period of 30 min was allowed before pH was measured.

Potentiometric titrations using the untreated tailings were unsuccessful, due to their considerable carbonate content. Large quantities of acid were necessary to achieve low pH values, which resulted in unacceptable increases in ionic strength and volume. Thus potentiometric titrations were attempted using only the clay fraction of the HT tailings. Potentiomentric titrations were conducted using the same electrolyte concentrations given above. A 2 mL aliquot of clay slurry was added to 10 mL of electrolyte solution, and the pH adjusted between 1 and 10 using standardised 0.1 M NaOH and HCl and the volume made up to 15 mL with DI water. Equilibration and pH measurement were conducted as described above. Electrokinetic mobility was determined using a ZetaPlus Zeta potential analyser (Brookhaven Instruments Corporation, USA). Samples were prepared for electrokinetic mobility determination by pipetting a 0.02 mL aliquot of clay suspension into 40 mL of 0.1

M KCl. The pH of the dilute suspensions were adjusted (pH 1-9) using 0.01M HCl or NaOH and the final volume made up to 50 mL by adding 0.01 M KCl solution. The flocculation procedure involved suspending 2 mL of the clay slurry in 12 mL 0.01 M KCl and adjusting the pH of each sample to a pH between 9 and 1 using 0.1 M NaOH or HCl. The volume in all samples was made up to 15 mL. The suspensions were shaken and allowed to settle overnight. Visual observations of flocculation were made and the final pH of the suspensions measured.

4.6.6. Biological activity screening

Gram stains were conducted on the surface scum from the ponded area of the the Wessels tailings dumps. A microscope slide was washed in ethanol and a drop of sterile water added. A small scraping of the surface scum was added to the sterile water. The Gram positive and Gram negative stains were then added and the slide heated. A few drops of crystal violet were added, and the slide washed. This was repeated with iodine and sophronine. The latter was only exposed to the slide for 5 seconds. The slide was then allowed to dry and observed under a microscope using an oil immersion lense (1000 x magnification).

4.7. Analytical techniques

4.7.1. XRD and ESEM

X-ray diffraction analysis was performed on a XPERT-PRO diffractometer system using CoKα radiation generated at 40 kV and 35 mA from 3.5 to 60° 2θ using a 0.017 step size.

Environmental Scanning Electron Microscope (ESEM) images were taken using a FEI XL30 ESEM field emission gun. Unground powder samples were placed in the sample chamber and examined at various magnifications. Elemental analysis was achieved by Electron Dispersive X-ray (EDX) Spectroscopy.

4.7.2. Particle size and surface area

Particle size was measured using a Beckman Coulter LS 13320 Laser Diffraction Particle Size Analyser. Samples were prepared by dispersing 0.4 g of sample in 20 mL DI water and adding 0.5 mL of calgon solution.

Surface area of the tailings was determined by means of BET-N_2 analysis using a Micromeritics Tristar porosity analyser. The samples were not ground prior to analysis.

4.7.3. Solution analysis

Anions and cations were analysed by ion chromatography using a DIONEX DX-500 unit. Samples were prepared by filtering solutions through 0.45 μm membrane filters into 5 mL vials. Any dilutions were performed using 18.2 mΩ deionised water. The instrument was calibrated using an eight multi-element calibration standard (made from 1000 ppm AccuSPEC stock solutions, SCP science) every 20 samples.

Anions were run using an IonPAC AS17A (2 mm) column at 30°C, using a KOH eluent (5mM grading to 35 mN over 20 minutes) with a flow rate of 0.5 $mL.min^{-1}$. Cations were run using an IonPac CS16 (3 mm) column at 35°C using 30 mN H_2SO_4 (isocratic for 25 minutes). An ED40 ECD detector was used for both anion and cation analysis.

Metals were analysed by atomic absorption spectroscopy using a Varian SpectrAA 220FS atomic absorption spectrometer. Manganese was determined at 403.1 nm using a 0.2 nm slit width calibration range: 0.5 –60 ppm. Samples were filtered through 0.2 μm membrane filters prior to analysis.

4.7.4. UV-visible spectroscopy

UV-visible spectra of samples were obtained using a Varian Cary 50 UV-spectrometer, fitted with a fibre optic probe. For azo dye analysis the wavelength range was set between 200 to 600 nm. Dye concentrations were determined by measuring the absorbance at λ_{max} in the visible region for each dye for a set of standard solutions and plotting a calibration curve (1.3×10^{-6} M to 1.7×10^{-4} M).

Percentage decolorisation is a commonly reported parameter in this study and is calculated as:

$$\% \text{ decolorisation} = (1 - AB/AA) \times 100$$

where AB is absorbance at the λ_{max} before reaction and AA is the absorbance at the same wavelength after the reaction.

4.7.5. High pressure liquid chromatography

High pressure liquid chromatography was conducted using a Perkin Elmer Series 200 fitted with a Genesis, C-18 column (4.6 mm x 250 mm) containing 4 μm packed particles (Alltech, Deerfield, Germany). Acetonitrile and a 0.03 M, pH 7.7 ammonium carbonate buffer were used as eluents. The pump program was set as follows, isocratic 20% acetonitrile: 80% buffer held for 2 min; grading to 100% acetonitrile over 10 min and held at 100% for 7 minutes. The wavelengths on the detector were set at 254 nm and the λ_{max} for each dye. Dye concentrations were determined from peak area-concentration curves, plotted for a series of concentration standards (1.3×10^{-6} M to 1.1×10^{-4} M).

For the analysis of anthracene and anthraquinone the same HPLC system was used. The pump programme was as follows: 50% water and 50% acetonitrile held for 2 minutes grading to 100% acetonitrile over 10 minutes and held isocratic for 2 minutes, returning to starting conditions over 3 minutes. The injection volume was 190 μL and the flow rate was 1 $mL.min^{-1}$. The wavelengths on the detector channels were set at 254 nm and 272 nm. Concentrations were determined by running a series of anthracene and anthraquinone standards which were used to plot peak area-concentration calibration curves (2.8×10^{-6} to 2.8×10^{-5} M).

4.7.6. Liquid chromatography-mass spectrometry

For liquid chromatography mass spectroscopy (LC-MS) analysis of breakdown products, 0.14 and 0.28 mM dye solutions were reacted at pH 4 for an hour in the same manner described in Section 4.8.3. Two dye concentrations were used in the LC-MS analysis, for sensitivity reasons as well as for the observation of any potential coupling products (Zille et

al., 2005). LC-MS was conducted on two different systems depending on instrument availability.

In the first system reversed-phase HPLC was accomplished using a Surveyor HPLC system (ThermoFinnigan, Hemel Hempstead, UK) fitted with a Genesis, C-18 column (4.6 mm x 250 mm) containing 4 μm packed particles (Alltech, Deerfield, Germany). Separation was achieved at ambient temperature with a flow-rate of 1 mL min^{-1} and the following gradient profile: 80% water and 20% acetonitrile (0 min, hold for 2 min); 100% acetonitrile (at 12 min), then isocratic to 16 min, returning to the starting conditions in 1 min and stabilising for 8 min.

LC-MS^n was performed using a Finnigan LCQ ion trap mass spectrometer equipped with an electrospray ionization interface (ESI) source operated in positive or negative ion mode. LC-MS settings were as follows: capillary 250°C, spray voltage 4.5 kV, sheath gas flow 80 and auxiliary gas 20 (arbitrary units). In positive ion mode the capillary voltage 3V and Tube lens offset 50V, in negative ion mode Capillary voltage -19 V and Tube lens offset -60 V. LCQ instrument parameters were selected using an automated tune facility on a direct infusion of 1000 ppm AY 36 stock solution on the protonated molecular ion, m/z 354 ($[M+H]^+$) or deprotonated molecule, m/z 352 ($[M-H]^-$) .

LC-MS^n analysis was carried out in data-dependent mode with two scan events: SCAN 1 – full mass spectrum, m/z 100-800; SCAN 2: data-dependent MS^2 spectrum of the most intense ion from SCAN 1. Detection was achieved at an isolation width of m/z 4.0 and fragmentation with normalised collisional dissociation energy of 50% and an activation Q value (parameter determining the m/z range of the observed fragment ions) of 0.25.

On-line UV-vis absorbance spectra (200-600 nm) were recorded using a Surveyor photodiode array (PDA). Three additional channels were recorded at specific wavelengths: Channel A 254 nm, Channel B 434 nm, Channel C 484 nm.

In the second system reversed-phase HPLC was accomplished using a Surveyor HPLC system (ThermoFinnigan, Hemel Hempstead, UK) fitted with a Phenomenex, C-18 column (2.00 mm x 150 mm) containing 3 μm packed particles. Separation was achieved at ambient

temperature with a flow-rate of 1 $mL.min^{-1}$ and the following gradient profile 95% water and 5% acetonitrile (0 min, hold for 5 min) grading to 95% acetonitrile and 5% water over 30 min), returning to the starting conditions in 1 min and stabilising for 8 min.

LC-MS was performed using a ThermoFinnigan LTQ ion trap mass spectrometer equipped with an electrospray ionization interface (ESI) source operated in positive or negative ion mode. LC-MS settings were as follows: capillary 275°C, spray voltage 4.0 kV, sheath gas flow 10 and auxiliary gas 2 (arbitrary units). In positive ion mode the capillary voltage 25 V and Tube lens offset 100 V, in negative ion mode Capillary voltage -9 V and Tube lens offset -100 V.

The major difference in the two systems described above, is the first system allowed secondary fragmentation patterns to be obtained of the most intense ion detected in the initial MS, while in the second system only one initial MS could be obtained.

4.7.7. Attenuated total reflectance Fourier transform infrared spectroscopy (ATR-FTIR)

Attenuated total reflectance Fourier transform infrared spectroscopy was performed using a Thermo Electron Nexus FTIR fitted with a liquid-N_2 cooled MCT detector and a Horizontal ATR flow-through assembly (PIKE Technology) containing a germanium (Ge) internal reflectance element (IRE). The Ge IRE was chosen over the more common Zinc Selenide IRE due to wider operating pH range (1-12). Omnic 32 software was used for all spectral processing.

4.8. Experimental design: Azo dyes

Throughout this study the term control relates to samples prepared in precisely the same manner as the treatments but omitting the tailings material. A blank sample refers to a sample prepared in precisely the same manner as the treatments, omitting the dye solution. In certain, specified, cases calcite or quartz controls have been included, i.e. calcite or quartz substituted for tailings material. When no acidification is involved calcite has been chosen as a control

due to the large calcite fraction present in the tailings. When acidification is involved quartz has been used as a control. Unless specified all samples were prepared in triplicate.

Due to the similarities of the Wessels and Nchwaning tailings and the Gloria and Mamatawn tailings, azo dye decolorisation experiments were not carried out on all five tailings but rather a representative of each ore type i.e. Wessels type (WT), Mamatwan type (MT) and Hotazel type (HT). Due to the large carbonate phase of the MT tailings and the surface scum present on the WT tailings, HT tailings were used in the bulk of the dye experiments.

4.8.1. Screening of five acid azo dyes

Five azo dyes, acid yellow 9 (AY 9), acid red 88 (AR 88), acid red 151 (AR 151), acid yellow 36 (AY 36) and acid Orange 7 (AO 7) were reacted with the HT tailings in a pH 4 acetate buffer using a batch procedure. Reactions with AY 36 and AO 7 were repeated for the WT and MT tailings. Dye stock solutions at a concentration of 0.14 mM were prepared in a 0.2 M, pH 4 acetate buffer. A 40 mL volume of stock solution was added to 2 g of tailings material, weighed out into 50 mL centrifuge tubes. These suspensions were agitated on a reciprocal shaker set at 250 rpm. At various time intervals, specified in the corresponding figures, samples were removed and centrifuged at 3000 rpm for 5 minutes. The supernatants were analysed using UV-visible spectrometry.

4.8.2. Abiotic vs biotic interactions?

Batch experiments were carried out using autoclaved HT tailings material. The tailings were autoclaved for 1 hour at 121°C in a 2100 Classic, Clinical Autoclave, Prestige Medical and kept in sterilized containers. Samples were manipulated with sterilised implements to avoid contamination. Batch experiments were conducted as described above but stock solutions were made up in DI. The batch experiments were repeated using both synthetic manganite and purchased Mn oxide. Calcite and dye solutions containing no solid phase were included as controls. The purpose of the calcite control was to indicate any sorption onto the calcite surface, raise the pH of the in accordance with the tailings and to establish any coagulation tendency of the dyes. Samples were placed on a reciprocal shaker set at 250 rpm and reacted

for 45 days. At various time intervals, specified in the corresponding figures, the samples were centrifuged and the supernatant analysed using UV-visible spectroscopy.

4.8.3. pH treatments

The effect of pH was established by reacting the tailings with AO 7 and AY 36 at pH 9; 7; 5; 4 and 3. Samples were prepared by weighing 2 g tailings material into 50 mL centrifuge tubes and adding 20 mL DI. The pH of this slurry was adjusted and held constant by addition of 0.1 M HCl using an autotitrator. Once the desired pH was reached 2 mL of 1000 ppm dye stock solution (prepared in DI water) was added to the suspension and allowed to react with the tailings for 1 hr. All volumes were adjusted using DI to a final S:L ratio of 1:20. Samples were shaken for 10 seconds, centrifuged and the supernatants filtered before analysis with, UV-visible spectroscopy, HPLC and AAS.

4.8.4. Investigation of further reactions involving azo dye breakdown products

AO 7 and AY 36 breakdown products; 1,2 naphthoquinone (NQ), 4-hydroxybenzenesulfonate (4HBS) and *p*-benzoquinone were reacted with the tailings in a pH 4 acetate buffer following the batch method described in Section 4.8.1.

To observe the hydrolysis reaction of the 366 isomers in real time, the tailings were reacted with AY 36 at pH 3 for 20 minutes and then filtered through a 0.2 μm filter in order to remove all Mn oxide material. The absence of Mn(III) complexes was verified by a negative tetramethylbenzidine test (Bartlett, 1999). The filtrate was immediately placed in a cuvette and a UV-vis spectrum collected every 10 min for 130 minutes and thereafter every 60 mins for 17 hrs. After 17 hrs the filtrate was added to 2 g tailings and reacted for 24 hrs at pH 3 after which the suspension was filtered and the filtrate analysed by UV-vis spectroscopy.

4.8.5. Initial reaction rates and orders

Reaction rates and orders were determined by continuous stirring reactions using the initial rate method described by Lasaga (1981). The general experimental design was as follows: AO 7 and AY 36 stock solutions were prepared in 0.2 M acetate buffers adjusted to pH 4, 5

and 6. A volume of 250 mL dye stock or blank (acetate buffer alone) solution was added to a 500 mL flask and stirred at 50 rpm using a magnetic stirrer. The reaction was initiated by adding the tailings to the stirred solution. Aliquots of 5 mL were extracted at increasing time intervals and filtered through syringe membrane filters (0.2 μm). The shortest practical sampling time interval was 30 seconds, which includes the residence time in the syringe. The filtrates were analysed by AAS, UV-vis spectroscopy and HPLC to determine concentrations of soluble Mn, dye and breakdown products. Soluble Mn concentrations in the blanks and treatments were used to calculate $[Mn]_{diss}$ which is an operational function, as employed by Stone and Morgan (1984a) and Laha and Luthy (1990), and is the amount of Mn not retained on the filter and represents the Mn concentration beyond that measured in the blank solutions. Reactions conducted at pH 4 were repeated in the dark and under UV radiation (100 mW, 365 nm). The reaction progression of AY 36 oxidation was followed using data from the pH 4 batch experiment.

The order of the initial reaction rate was determined with respect to the tailings surface area concentration [SA], dye concentration and pH. The order with respect to available tailings surface area was determined by varying the [SA] between 4.8 and 48 $m^2.L^{-1}$ while the pH and dye concentration were held constant at pH 4 and 0.14 mM, respectively. Similarly, the order with respect to dye concentration was determined by varying the dye concentration between 0.07 and 0.70 mM while the pH was maintained at pH 4 and the [SA] held constant at 48 $m^2.L^{-1}$. The initial rate was calculated over the first few time intervals when reaction concentrations would be close to initial conditions.

4.8.6. ATR-FTIR experiments

The ATR experiments were conducted following the procedure outlined by Hug (1997) whereby the IRE is coated with a clay film. Reflectance techniques have inherently low sensitivity, thus it is important to use a clay with as higher surface area as possible. For this purpose synthetic manganite (prepared as described in Section 4.4) was used in all ATR-FTIR experiments. The final concentration of the dye in contact with the manganite film needed to be below the infrared detection limit for aqueous species on the IRE used (Duckworth and Martin, 2001; Borda et al., 2003) permitting any dye detected to be

considered surface-bound. This means valuable information can be obtained about dye sorption.

A 1 g/L suspension of manganite was prepared in a 30:70 water:ethanol solution. This suspension was used to create a thin clay film on the Ge IRE by pipetting a 2 mL aliquot onto the crystal and allowing to dry. The final surface area of manganite on the crystal was approximately 0.028 m^2.

The dry clay film was re-hydrated in the flow cell with 0.5 mL DI water adjusted to pH 4 and a background scan was collected of the fully hydrated clay. All subsequent scans were ratioed against the hydrated-clay background, allowing peak intensity due the sorbed compound to be observed. A 0.28 mM AO 7 solution was prepared in DI water and the pH adjusted to 2.3, 2.7, 3.0, 3.5, 4.0 and 6.0 by the addition of 0.01M HCl. At the start of the reaction 0.5 mL of the dye solution was injected into the flow cell, thus the final concentration of dye in contact with the clay was 0.14 mM. This concentration was confirmed to be below the infrared detection limit for aqueous species on the IRE used in the present ATR-FTIR system. This permitted any dye solution detected to be considered surface-bound. A set of control spectra (as above but without the clay film) and blanks (pH adjusted DI water injected onto the clay film with no dye) were collected. Scans were displayed within 10 seconds of the dye being injected into the cell. During the reaction period spectra were collected every minute using 64 co-added scans at 4 cm^{-1} resolution. Standard spectra of pH adjusted (2.3 to 6.0) 25 mM solutions of AO 7 were collected on a clean Ge crystal.

4.8.7. Effects of acetate buffer concentration

Batch experiments were carried out using pH 4 acetate buffers of varying strengths. Acetate buffers having concentrations of 100, 200 and 500 mM were prepared using glacial acetic acid and sodium acetate. Dye stock solutions were added to the buffer solutions to give a final dye concentration of 0.14 mM. The dye solutions were added to 2 g of tailings materials to a final S:L ratio of 1:20. Purchased Mn(III) oxide, was included in the experiment due to significant pH drift observed with the tailings material. The centrifuge tubes were sealed and placed on a reciprocal shaker set at 250 rpm. After two hours reaction time the samples were

centrifuged and the supernatants analysed using UV-vis spectroscopy. The pH of the samples were measured before being replaced on the shaker. Samples were analysed daily for a week.

4.8.8. Effect of salt type and concentration

The influence of salt type and concentration was determined with and without acetate buffer. Batch experiments similar to those described in Section 4.8.7 were employed except that solutions of NaCl and Na_2SO_4 at three concentrations 30, 100 and 500 mM (in either DI or a 0.2 M, pH 4 acetate buffer) were used to make up 0.14 mM stock solutions of AY 36 and AO 7.

4.8.9. Quasi-continuous flow batch experiments

Quasi 'continuous flow' reactions were conducted by sequentially reacting fresh dye solution with a single measure of tailings over 60 days. Acetate buffer solutions (100 mM, pH 4) containing 0.14 mM AO 7 and AY 36 were prepared. The tailings were weighed out into 15 mL centrifuge tubes and the mass of the tube plus dry tailings recorded. The dye solution was added to the centrifuge tubes to obtain a S:L ratio of 1:10. These tubes were placed on a reciprocal shaker for 24 hrs. The samples were then centrifuged at 2500 rpm and the supernatant carefully decanted and filtered through 0.45 μm filters. Care was taken not to disturb the tailings during decanting. Fresh dye solution was then added to the remaining slurry. Separate experiments, where the solution was added gravimetrically, showed that the amount of dilution of fresh dye by the entrained solution was negligible, so pipetting fresh solution was considered appropriate. These samples were then replaced on the shaker. The continual replenishment procedure was repeated for 60 days. The filtrates were analysed for dye concentration using UV-vis spectrometry and for Mn concentration using AAS.

4.9. Experimental design: PAHs

Throughout this study the following definition of control is used: A control is treated in the same manner as the treatments omitting any mineral phase. Originally quartz and calcite were intended to serve as mineral controls but it was observed that these mineral phases were

reactive during drying reactions and thus could not be used as controls but have been included in the results.

Unless specified all samples and controls were prepared in triplicate.

4.9.1. Drying experiments

Quartz, calcite, purchased Mn oxide, WT, MT and HT tailings were used in the drying experiments. Samples were spiked with anthracene using the minimal solvent, single step rehydration/spiking procedure as described by (Reid et al., 1998). Briefly, 0.4 mL DI was added to acid washed amber vials. A 7 μL aliquot of anthracene stock solution ($4g.L^{-1}$ made up in acetone) was added to the water, and 1 g of mineral sample immediately stirred in with a glass spatula to make a moist crumbly paste. The control consisted of adding the spike to water but omitting any mineral phase. Half the samples were sealed using Teflon lined caps and half the samples were lightly covered in foil to omit light while allowing slow air-drying. These samples were then left for 7 days. On a separate set of HT samples this procedure was repeated but at various time intervals the drying samples were weighed and sealed to prevent further moisture loss.

The above procedure was repeated on oven-dried (104° C overnight) calcite and HT samples, except that the 0.4 mL of water was replaced by 10 mL cyclohexane. In half the samples the cyclohexane was allowed to evaporate while an identical set were sealed to prevent evaporation. Mixing of the latter samples was achieved by placing them on a reciprocal shaker, set at 250 rpm for the 7 day period.

4.9.2. pH experiments

The pH experiments were conducted in a series of 0.2 M acetate buffers prepared at pH 3, 4, 5 and 6. The HT tailings and quartz (1 g) were weighed into acid washed amber bottles and 20 mL of the acetate buffer solutions added. These suspensions were shaken for 30 min before the pH of the supernatants were measured. The pH values in the quartz samples were within 0.05 units of the original pH while pH in the tailings treatment showed a slight drift, especially in the pH 6 buffer, which is on the margin of the acetate buffering range. Although

the use of acetate to buffer reactions at pH 6 may be questionable, it was decided that it would be better to treat all samples with the same organic buffer to avoid differences in anthracene solubility. The data was plotted according to the final pH of the suspension. Samples were spiked with a 10 μL aliquot of anthracene stock, sealed with Teflon caps and shaken on a reciprocal shaker (250 rpm) for 5 days. The process was repeated spiking, the samples with an anthraquinone spike.

A separate pH experiment was conducted in DI. A 1 g tailings sample was added to an amber glass bottle followed by 10 mL DI. A 10 μL anthracene spike was added. The slurry was titrated to and maintained at pH 4 using an autotitrator dispensing 0.1 M HCl.

4.9.3. Anthracene/anthraquinone extraction procedures

Extraction of anthracene and the oxidation product, anthraquinone, was achieved using a simple sonication method. The anthracene extraction efficiency using this technique was >89% for hydrated samples thus it was deemed sufficient for the current investigation.

Due to reports that extraction of hydrophobic compounds from dried soils using non-polar extractants is inefficient (Chiou and Shoup, 1985) a range of extraction solvents (cyclohexane, cyclohexane plus water, methanol and acetonitrile) were trialed for anthracene and anthraquinone recovery from dried tailings and calcite samples. Anthracene recovery did not differ with the type of solvent used, however, anthraquinone recovery was very dependent on solvent type. Reduced recovery of anthraquinone was observed when extracted directly with cyclohexane (80%), while efficient recovery (100%) was observed when water was added to the dry tailings prior to extraction with cyclohexane (Figure 4-2). Equally efficient recoveries were obtained in the polar solvents, methanol and acetonitrile. Separation of the mineral phases from methanol and actetonitrile through filtration proved difficult, thus the mixed cyclohexane and water extraction procedure, described below, was used for all the experiments.

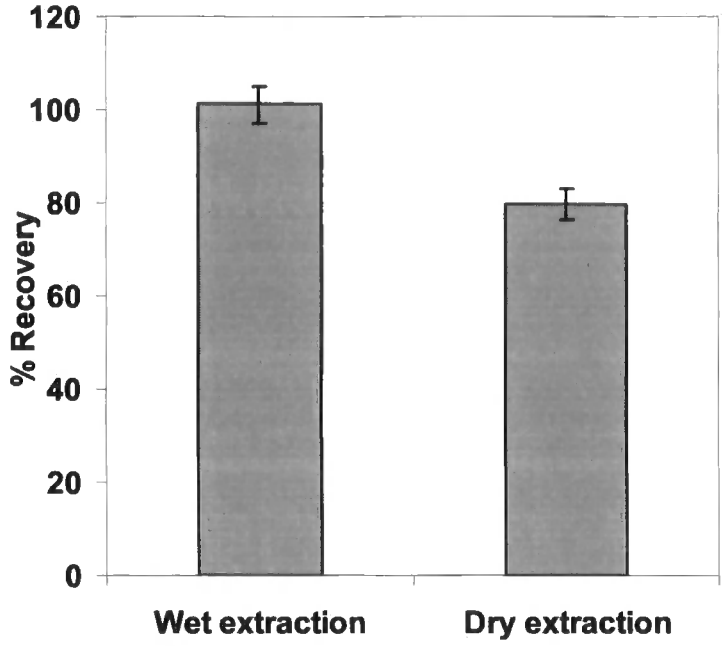

Figure 4-2 Percentage recovery of anthraquinone in cyclohexane with (wet extraction) and without (dry extraction) the addition of water prior to extraction in cyclohexane.

Both dry and moist samples were extracted in the same manner. A volume of 10 mL water was added to the spiked samples followed by 10 mL cyclohexane. The samples were sealed with Teflon line caps and placed in a sonic bath for 2 hrs. The samples were then shaken on a reciprocal shaker set at 250 rpm for 24 hours. Cyclohexane was separated from the water and solid phases using Fisherbrand phase separation paper. Filtered extracts were collected in amber vials for UV and HPLC analysis.

Samples reacted in cyclohexane were sonicated and shaken. No water was added to these samples.

Extraction of anthracene and anthraquinone from acetate suspensions was achieved by the addition of 10 mL cyclohexane, followed by the sonication and shaking routine described above.

4.10. Statistical analysis

Significance testing (t-test) was perfomed using Microsoft Excel (1 tailied; unequal variance). Evaluation of slope significance in the kinetic analysis was conducted using equations provided in Appendix D.

5. Results and Discussion: Characterisation of the tailings materials

5.1. Physical and Mineralogical properties

5.1.1. Mineralogy

The mineralogy of the KMF has been well characterized (DeVilliers, 1965; Kleyenstuber, 1984; Gutzmer and Beukes, 1996), thus an extensive investigation into the mineralogy of the tailings was not necessary. The clay phase of the tailings is likely to be the most reactive in geochemical reactions, thus a brief mineralogical survey was conducted of the clay fraction extracted from tailings. X-ray diffraction patterns of the sedimented clay fraction of all five tailings are given in Appendix B.

The XRD patterns shown in Appendix B show broad, poorly defined peaks, despite the analysis being performed on the clay fraction of the tailings. This problem is commonly encountered during XRD surveys of Mn minerals (Taylor et al., 1964). Calcite (3.00; 2.10; 2.29 Å) was present in all tailings as was braunite ($Mn^{2+}Mn^{3+}{}_6SiO_{12}$) (2.72; 2.14; 2.35 Å). Bixbyite [$(Mn^{3+},Fe^{3+})_2O_3$] has similar d-spacings as braunite (2.72 and 2.14 Å) thus it was difficult to discern between these two minerals. Both have been identified in the KMF (Gutzmer and Beukes, 1996). Manganese (IV) oxides, birnessite (7.27; 3.57; 2.44 Å) and todorokite (9.57; 2.40; 2.39 Å) are present in all the tailings. A d-spacing of 3.10 Å was observed in the traces of the Wessels and Hotazel type tailings, which may correspond to the major peak of hollandite [$Ba(Mn^{4+}, Mn^{2+})_8O_{16}$]. It is possible that the HT tailings may also contain lithiophorite [$(Al, Li)Mn^{4+}O_2(OH)_2$] (4.71; 9.43; 2.37 Å) another Mn(IV) oxide. Hausmannite (Mn_3O_4) was identified in all tailings samples (2.49; 2.77 Å) Manganite (3.40; 2.62 Å) was observed in the WT and HT tailings but could not be identified in the MT tailings. Kutnahorite [$CaMn(CO_3)_2$] (2.92; 1.81; 1.84 Å) was only identified in the MT tailings. The most intense rhodochrosite d-spacing of 2.84 Å was also identified in the MT tailings. Jacobsite is known to occur in the MT tailings (Gutzmer and Beukes, 1996) but its major peak at 2.56 Å was not observed in this study.

The results in this study reiterate the findings of previous analyses on the mineral composition of the ore bodies. The Wessels and Nchwaning tailings are essentially the same in mineralogical makeup as are the Gloria and Mamatwan samples. Qualitatively the HT tailings do not differ substantially from the WT tailings, however relative proportions of the minerals may be different. The HT and WT tailings show a mineralogy comprising mainly of braunite and a mixture of Mn(III/IV) oxides, while the MT tailings contain braunite, Mn(III/IV) oxides and kutnahorite. It expected that the WT and HT tailings would be more powerful oxidising agents than the MT tailings due to the enrichment of Mn oxides in these ore types.

The ESEM images of the WT and MT tailings are shown in Figure 5-1. The two images of the MT tailings are taken at two different locations. In the first image (Figure 5-1a) the large crystal in the centre shows the typical calcite cleavage pattern. The more amorphous material surrounding the calcite crystal has a chemical composition of Si, Ca and Mn which may relate to a braunite mineral phase. The MT tailings appear to have a finer mineral structure than that of the WT tailings sample with needle-like minerals visible in the former (Figure 5-1b). These minerals may represent kutnahorite crystals, as EDX gives an elemental composition of Ca, Mn, O and C (Figure 5-1b). The large particles shown in the WT sample (Figure 5-1c) have an elemental composition indicative of Mn oxides (Ca Mn O). The finer material viewed in the same image shared this chemical composition (data not shown). The highly crystalline structures identified in the ESEM images correlate largely with carbonate minerals, while the Mn oxide phase appears slightly less crystalline. Another observation that can be made from these images is the apparent low surface area of the materials, which correlates to the BET-N_2 surface area discussed in Section 5.1.2.

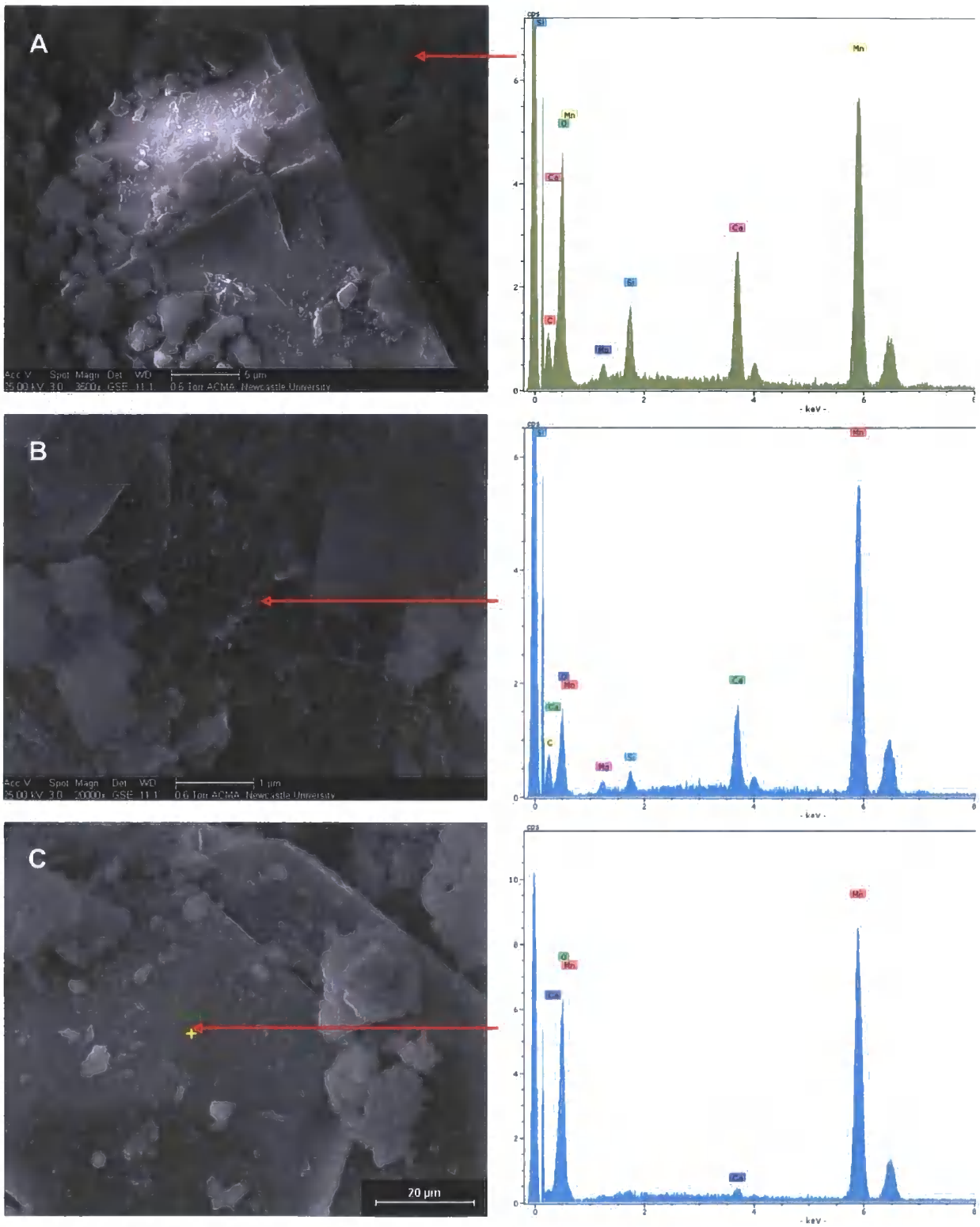

Figure 5-1 ESEM images and EDX plots of Mamatwan (A and B) and Wessels tailings (C)

5.1.2. Particle size and surface area

Table 5-1 Particle size and surface areas for the Wessels, Nchwaning, Gloria, Mamatwan and Hotazel tailings

		--------WT------		---------MT-------		---HT----
		Wessels	**Nchwaning**	**Gloria**	**Mamatwan**	**Hotazel**
Particle size (mm)	**Unit**					
Sand (2-0.063)		36.7	28.6	39.1	15.7	83.3
Silt (0.063-0.0039)	**%**	45.9	56.1	42.1	61.7	11.2
Clay (<0.0039)		17.4	15.3	18.8	22.6	5.5
Surface Area	$m^2.g^{-1}$	1.2	2.0	4.0	6.4	2.4

Particle size and surface area data are given in Table 5-1. Apart from HT tailings, which show a coarser texture, the particle size of tailings material is dominated by the silt size fraction (39-63μm). The WT (Wessels and Nchwaning) tailings have clay fractions of between 15 and 17% and the MT (Gloria and Mamatwan) tailings have clay fractions of between 19 to 23%. Hotazel type tailings have a very low clay fraction (6%). The tailings are the product of milling and crushing processes, which differ from mine to mine thus correlations between tailings type and particle size may not be relevant, however, the finer texture of the MT tailings may be a result of the softer mineral (carbonate-rich) composition of the ore. The HT tailings are visibly coarser than the other tailings and were produced during earlier mining operations, thus the crushing technique that generated these tailings may have been different to the more recently produced WT and MT tailings.

The BET-N_2 surface areas (Table 5-1) of all the tailings are very low (1.2 to 6.4 $m^2.g^{-1}$). The MT tailings have the highest surface areas (4 to 6.4 $m^2.g^{-1}$). The WT tailings have disproportionately low surface areas (1.2 to 2.0 $m^2.g^{-1}$), relative to that of the HT tailings (2.4 $m^2.g^{-1}$) considering their substantially higher clay fractions. Again it is hard to draw any conclusions about the differences in surface areas of the tailings due to the different ore crushing processes utilized in the different mining operations.

5.2. Chemical properties

The pH, electrical conductivity, anion and cation data for all five tailings are given in Table 5-2. The pH of the tailings (8.5 to 9.7) falls in the alkaline to highly alkaline range. A pH above 8.5 falls outside the range of $CaCO_3$ equilibria (McBride, 1994) and may indicate the presence of sodium carbonate minerals. The Wessels tailings have the highest soluble cation and anion concentrations, and accordingly the highest EC (284 mS/m). The soluble cations and anions in the HT and WT tailings are low and they show low conductivities (42 to 120 mS/m). The tailings are transported to the dams via process water, thus the chemical composition of a water extract may not reflect the chemistry of the actual tailings. Salt precipitates were observed in isolated patches of the Wessels and Nchwaning tailings dams. BHP Billition mine staff suggested that these were salt precipitates that formed as a result of transporting the tailings in the hard process water. Unfortunately a sample of this water was not collected.

Table 5-2 pH (S:L 1:2.5) , electrical conductivity (EC) soluble anions and cations (S:L 1:10) for Wessels, Nchwaning, Gloria, Mamatwan and Hotazel tailings (BD = below detection limit)

		----------WT----------		---------MT----------		---HT---
	Units	**Wessels**	**Nchwaning**	**Gloria**	**Mamatwan**	**Hotazel**
pH (H_2O)		9.43	8.8	8.78	8.33	8.63
EC	mS/m	284	44	42	120	60
Cations	**$mg.L^{-1}$**					
Li^+		BD	BD	BD	BD	BD
Na^+		72.5	12.6	11	21.2	5.48
NH_4^+		16.6	17.1	BD	0.1	BD
K^+		4.98	1.56	0.38	0.99	0.12
Mg^{2+}		35.3	4.91	4.05	13.3	5.39
Ca^{2+}		39.8	13.9	11.3	27.4	29.8
Anions	**$mg.L^{-1}$**					
F^-		0.52	0.5	0.28	0.69	0.36
Cl^-		91.9	6.29	11.3	37.8	8.38
NO_2^-		BD	BD	0.01	0.01	0.01
Br^-		BD	0.01	0.07	0.16	0.15
SO_4^{2-}		195.5	43	21.8	51.5	47.3
NO_3^-		145.7	58.5	3.9	54.7	35.4
PO_4^{3-}		0.18	0.09	0.03	0.31	0.03

5.2.1. Tailings Reactivity

Table 5-3 shows the oxidative properties, total Mn and reactive Mn phases of all five tailings. The O/Mn ratio indicates the net oxidation state of the material. These ratios range from 1.2 to 1.5 which suggests that the Mn oxidation state within the tailings is between 2+ and 3+. A mixture of Mn(II) and Mn(IV) minerals may also give a similar oxidation state. The higher the oxidation state the more oxidising power the material is expected to have. The HT tailings have the highest oxidation state (O/Mn = 1.5) which is expected from the high Mn oxide content of the ore. The MT type tailings have the lowest oxidation states (O/Mn = 1.2 to 1.3), indicative of the higher proportion of Mn carbonates in this ore type.

Table 5-3 Oxidation state, total extraction and sequential extraction data for the Wessels, Nchwaning, Mamatwan, Gloria and Hotazel tailings.

		----------WT---------		----------MT----------		--HT--
	Units	**Wessels**	**Nchwaning**	**Mamatwan**	**Gloria**	**Hotazel**
O/Mn ratio		1.36	1.29	1.26	1.21	1.46
Total extraction						
DC Mn	%	42.57	33.70	20.29	27.84	33.31
DC Fe	%	5.51	6.57	1.84	2.28	6.58
Sequential extraction						
Water soluble	$mg.kg^{-1}$	0.10	0.40	0.05	BD	BD
Exchangeable Mn (KCl)	$mg.kg^{-1}$	1.90	1.40	4.25	3.45	1.95
NH_4OAc (pH 7)	$mg.kg^{-1}$	66.00	145.50	1317.50	1976.00	39.50
Hydroqinone	%	1.81	0.54	2.02	1.24	2.96
HAHC	%	4.23	2.67	3.73	4.04	4.76
DC	%	8.14	8.20	8.49	6.04	5.75
Total	%	14.18	11.41	14.24	11.32	13.47

The sequential extraction results (Table 5-3) show Mn release after treatment with increasingly aggressive extractants. In order of increasing reactivity with Mn oxides the extractants used were: DI water; 1M KCl; pH 7, 1M ammonium acetate (NH_4OAc); 0.2% hydroquinone (HQ); hydroxylamine hydrogenchloride (HAHC) and dithionite-citrate (DC). The last three extractants are reducing agents. Reaction with hydroquinone, a mild reducing agent, gives an indication of the easily reducible and reactive Mn phase (Bartlett and James, 1979; Gambrell and Patrick, 1982). Hydroxylamine hydrogenchloride is a stronger reducing agent which is expected to reduce Mn oxides selectively over iron oxides (Chao, 1972; Tokashiki et al., 1986; Tokashiki et al., 2003; Neaman et al., 2004). Dithionite-citrate is an extremely strong reductant and is used to estimate total Mn and Fe oxide concentrations in a material (Holmgren, 1967).

Water soluble Mn is low in all samples which is expected in such alkaline conditions. Extraction with 1 M KCl traditionally gives an indication of exchangeable metals. The Mn concentration in the KCl extract is substantially higher than the water extract. While this may be interpreted as representing the proportion of exchangeable Mn, the higher ionic strength of

the KCl solution could alter ion activities sufficiently to cause dissolution from Mn carbonate minerals. Extraction in pH 7 ammonium acetate (NH_4OAc) is used as another measure of exchangeable Mn (Gambrell and Patrick, 1982). The Mn release in this extractant is surprisingly high, especially in the MT-tailings (1317 and 1976 $mg.kg^{-1}$). The HT and WT tailings also release large concentrations of Mn, from an extractant supposedly specific for exchangeable cations. The reason for this inflated Mn release in the neutral acetate is not known. One possibility could be the formation of Mn-acetate complexes in the strong (1 M) acetate solution.

The hydroquinone (HQ) extractable Mn content of the tailings (Table 5-3) is high (0.5 to 3.0%). The reactive hydroquinone extractable Mn phase has been shown to represent the most favourable electron acceptors for microbes (Guest et al., 2002). Hydroxylamine hydrogenchloride is supposed to remove Mn oxides selectively from Fe oxides. As can be seen from the data in Table 5-3 not all Mn was removed with this extractant, which may be a result of the slow dissolution rate of highly crystalline particles. Large concentrations of Mn were released in the DC extract which is an aggressive reducing agent and should remove all remaining Mn oxides. The cumulative Mn concentrations of the sequential extraction fell well short of the total Mn extraction in DC. The total extraction was performed on finely ground (<63 μm) tailings whereas the sequential extraction was performed on the unaltered tailings (< 2 mm). The difference in particle size may account for the large disparity between the total and sequential extractions. The total DC extracts should represent the total reducible Mn phase present in the tailings. The extraction process does not involve acidification (pH approximately 7) (Holmgren, 1967), thus Mn carbonate minerals should not be dissolved. The Wessels tailings has the highest DC extractable Mn content (42.6%) followed by Nchwaning (33.7%) and Hotazel (33.3%) tailings. The MT tailings show a lower reducible Mn content of 20 to 28%. The high HQ and DC extractable contents of the tailings suggest that the material will have 'quick' and 'slow' release oxidising capacity.

The redox properties of braunite are not well documented. Tephroite ($MnSiO_4$), another Mn silicate has shown the capacity to polymerise hydroquinone (Shindo and Huang, 1985). Thus braunite may exhibit similar redox properties and it is possible that some of the reducible Mn originates from the braunite phase.

Correlation between the chemical reactivity of Mn oxides and any single parameter is hampered through the compositional, crystallinity, chemical and structural variations of natural Mn oxide minerals. For example, Bartlett and James (1979) found a direct correlation between HQ extractable Mn and net Cr oxidising capacity of soils, whilst Negra et al. (2005) found a better correlation between Cr oxidising capacity and HAHC extractable Mn. The role of oxidation state in redox reactivity has also not been clarified, with some authors suggesting Mn(III) functions as the primary oxidant (Xyla et al., 1992; Nico and Zasoski, 2000; Nico and Zasoski, 2001) whilst other authors suggest greater redox activity is observed at higher Mn(IV)/Mn(III) ratios (Kim et al., 2002; Negra et al., 2005). From these contrasting studies it would appear that each system needs to be studied individually to determine the parameters correlating best to reactivity.

5.2.2. Total elemental composition

Results of the total elemental analysis as determined in an aqua regia extract are provided in Table 5-4. If these tailings are to be applied as a treatment to soils and waters it is important to know their trace element composition. Considering, the metal-scavenging capacities of many Mn oxides (McKenzie, 1980), the levels of trace elements in the tailings are relatively low in comparison to a range of world wide means for soils (McBride, 1994). One exception is Pb, which is present in the HT and WT tailings at 110 and 140 $mg.kg^{-1}$; respectively. These Pb levels are higher than the worldwide mean for soils (10-84 $mg.kg^{-1}$), but well below the U.S.EPA soil screening guideline for Pb (270 $mg.kg^{-1}$). The South African government has drawn up a set of guidelines used to determine the threshold levels of certain metals permitted in sewage sludge that will be applied to agricultural land (Water Research commission report TT262/06). The trace elements in the tailings all fall well below these threshold values (Table 5-4). Thus applications of the tailings to a soil would not add unacceptable levels of trace elements, provided of course that the target soil is not acidic (pH<5) which would reduce the stability of the Mn phases.

The major element analysis (Table 5-4) shows Mn contents of 42% for the WT tailings, 30-32% for the MT tailings and 38% for the HT tailings. Again the similarities between the Gloria and Mamatwan tailings and the Nchwaning and Wessels tailings are apparent in their

elemental compositions. The different values obtained for aqua regia extractable Mn and DC extractable (reducible) Mn (Table 5-3) is probably accounted for by carbonate bound Mn.

Table 5-4 Total element analysis of the five tailings samples as determined in an aqua regia extract presented together with the range of world wide soil means of certain elements as taken from McBride (1994) and the guidelines for permissible metal concentrations for sewage sludge applied to agricultural land in South Africa (taken from Water Research commission report TT262/06)

		---------WT----------		---------MT--------		--HT--		
	Unit	**Wessels**	**Nchwaning**	**Mamatwan**	**Gloria**	**Hotazel**	**SA Sewage sludge guidelines***	**Range of worldwide means for soils**
Major elements								
Mn	%	42.0	42.0	32.0	30.0	38.0		
Fe	%	11.0	10.0	4.3	3.8	14.0		
Al	%	0.17	0.22	0.22	0.22	0.29		
Ca	%	4.6	3.7	12.0	9.3	3.6		
Trace elements								
Hg	$mg.kg^{-1}$	0.16	<0.06	0.20	0.10	0.10	15	0.02-0.41
As	$mg.kg^{-1}$	22.0	32.0	7.7	7.8	20.0	40	2.2-25
Be	$mg.kg^{-1}$	<0.1	1.0	0.3	0.3	0.9	-	1.2-2.1
Cd	$mg.kg^{-1}$	0.4	0.4	<0.2	<0.2	0.6	40	0.06-1.1
Cr	$mg.kg^{-1}$	7.0	11.0	20.0	5.0	42.0	1200	7-221
Cu	$mg.kg^{-1}$	89.0	40.0	10.0	3.0	41.0	1500	6-80
Pb	$mg.kg^{-1}$	140.0	140.0	3.0	11.0	110.0	300	10-84
Mo	$mg.kg^{-1}$	5.3	5.4	5.4	5.5	5.9	-	39450
Se	$mg.kg^{-1}$	<0.2	<0.2	<0.2	<0.2	<0.2	-	0.05-1.27
Ag	$mg.kg^{-1}$	<0.8	<0.8	<0.8	<0.8	<0.8	-	0.03-8
Th	$mg.kg^{-1}$	<1.0	<1.0	<1.0	<1.0	<1.0	-	0.02-2.8

5.2.3. Mn stability in an acetate buffer

Much of the experimental work conducted in this study involved the use of acetate buffers to control pH. Manganese release from the tailings would be expected when exposed to an acetate buffer solution for several reasons:

i) Mn carbonate minerals dissolve under acid conditions releasing soluble Mn;

ii) Mn^{2+}, housed in the mineral lattice of Mn oxides, may be released through proton promoted dissolution;

iii) the redox stability of Mn oxides decreases at low pH (<5) and

iv) there may be limited complexation and dissolution of solid phase Mn by acetate ligands.

The stability of the Mn tailings was assessed in a pH 4, 0.2 M acetate buffer. The results are shown in Figure 5-2. Large concentrations of Mn are released in all the tailings, however, the MT tailings released more than twice as much Mn as the WT and HT tailings. The larger release of Mn from the MT tailings can be accounted for by the high $MnCO_3$ fraction of this ore type. The extremely high Mn release from the MT tailings would make it problematic in the treatment of any acidic (pH< 5) soils and waters.

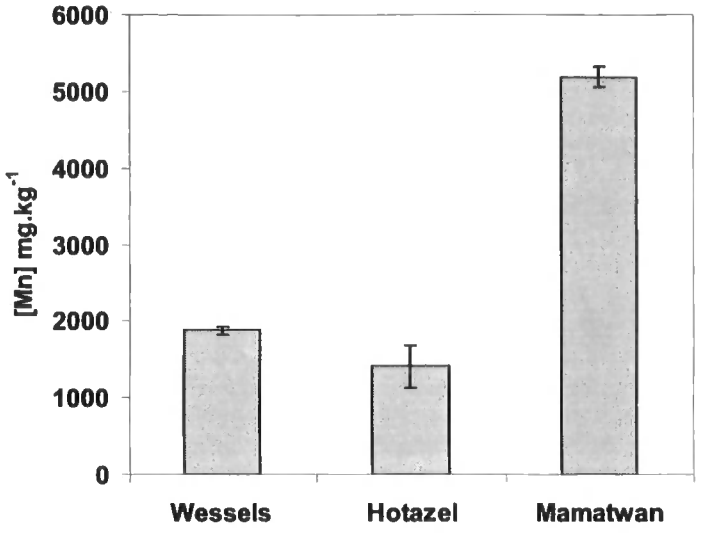

Figure 5-2 Manganese release from Wessels type, Hotazel type and Mamatwan type tailings in a 0.2 M actetate buffer.

5.2.4. Point of zero charge

Attempts to determine the surface charge of the tailings materials potentiometricaly were unsuccessful both on the whole tailings (< 2mm) and the clay fraction. The PZC is often below pH 3 for many Mn oxide minerals (Murray, 1974). A large amount of acid was necessary to adjust the pH of the tailings to low pH values, due to the large alkali buffering capacity of the tailings, and this resulted in alterations of ionic strength. Electrokinetic mobility determinations on the clay phase also failed to yield a discrete value for PZC. This may result from the differences in particle size and charge properties of the individual mineral types.

Due to the failure of these two methods, a flocculation technique was employed and visual observation made to determine the pH at which the clay phase began to flocculate (Figure 5-3). Amiphoteric oxides have been shown to aggregate near the pH of their PZC (Wiese and Healy, 1975; Tombacz et al., 2001) where the electrostatic repulsion between the particles is negligible. This may be expected to be a discrete point for a single mineral phase, but for a mineral compilation like the tailings flocculation might be expected to occur over a range of pH. This may explain why the aggregation of the Hotazel clay phase occurs in the pH range <

4. From this evidence we can infer that the PZC of the HT tailings is close to pH 3.5, but may not be represented by a discrete pH, but rather a pH range. The alkali dispersion needed to separate the clay fraction could not be achieved in the WT and MT tailings, thus determination of the PZC for these tailings could not be achieved, however, a similar PZC can be assumed based of the similarities of the Mn oxides present in the tailings.

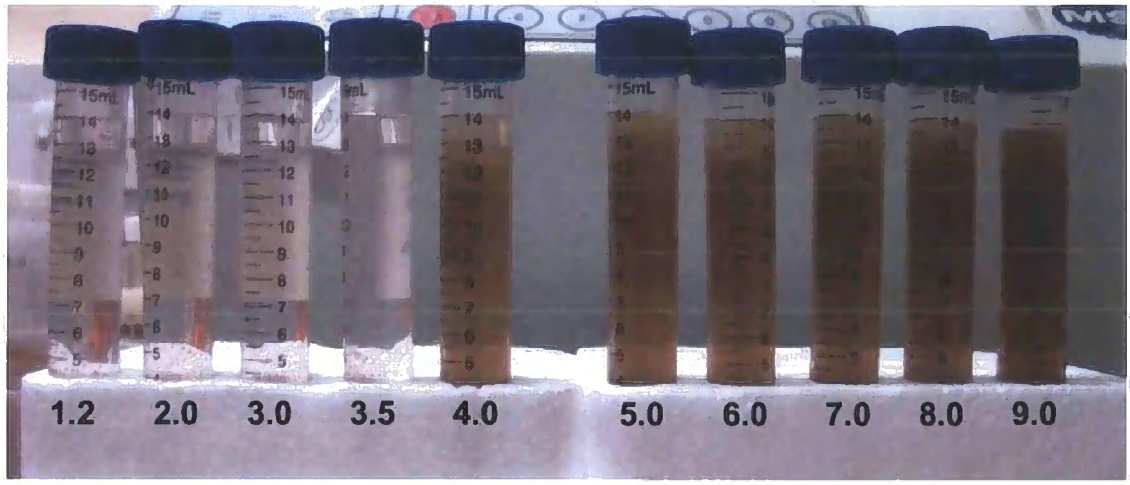

Figure 5-3 Series of pH adjusted clay solutions extracted from the Hotazel tailings allowed to settle overnight

5.3. Biological activity

During the collection of samples it was observed that parts of the Wessels and Mamatwan tailings dams had ponded water, which supported reeds, grasses and a number of other vegetation types (see Figure 4-1). The Hotazel dumps are dry but at the time of sampling (December 2005) were sparsely populated with grass tufts (Figure 4-1d). Thus it is probable that bacterial communities may be associated with the tailings. There was a visible surface scum on the ponded water of the Wessels tailings dam at the time of sampling and on wetting, the Wessels tailings forms an iridescent layer on the surface of added water, which is commonly associated with biofilms (K. Johnson pers. comm.). A scraping of this iridescent layer was placed on a glass slide and a Gram stain performed. Although some bacteria sized particles retained the pink stain, they had irregular shapes, which would be uncharacteristic for bacteria. Further biological investigations fell outside the scope of the current study, but in a separate investigation on the tailings material, polymerise chain reaction assays showed

the presence of bacterial populations (Goncalves et al., 2007). This latter study also established that there was more microbial diversity in the Wessels tailings than the Mamatwan tailings.

5.4. Characterisation of synthetic manganite

X-ray diffraction, infrared spectroscopy and scanning electron microscopy were used to characterise the synthetic manganite. The XRD pattern is shown in Appendix C (Figure C-1). The d-distances agree well with those reported for manganite (3.40; 2.64; 1.78; 2.42; 1.67 Å) (Dixon and White, 2002). The ESEM image of the freeze dried manganite (Appendix C, Figure C-2) show the typical needle morphology associated with manganite (Xyla et al., 1992). Surface area of the manganite, from the BET analysis, was determined to be 28 $m^2.g^{-1}$ which correlates well with the synthetic manganite in other studies (Xyla et al., 1992). The PZC as determined by electrophoretic mobility was pH 4.

6. Results and discussion: Oxidative decolorisation of acid azo dyes

6.1. Screening of five acid azo dyes

Five azo dyes, acid yellow 9 (AY 9), acid red 88 (AR 88), acid red 151 (AR 151), acid yellow 36 (AY 36) and Acid Orange 7 (AO 7) were screened for decolorisation reactivity with the HT tailings in a pH 4 acetate buffer. The structures of these azo dyes are given in Figure 6-1.

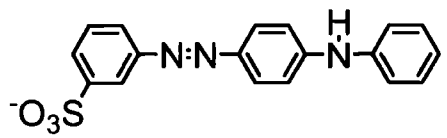

Acid yellow 36
3-(4-Anilinophenylazo) benzenesulfonate

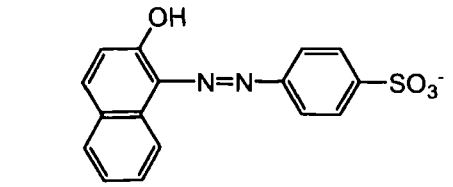

Acid orange 7
4-[(2-hydroxy-1-naphthyl)azo]benzenesulfonate

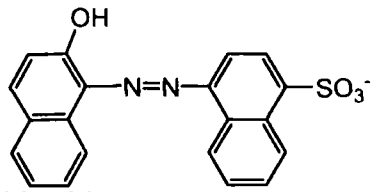

Acid red 88
4-(2-Hydroxy-1-naphthylazo)-1-naphthalenesulfonate

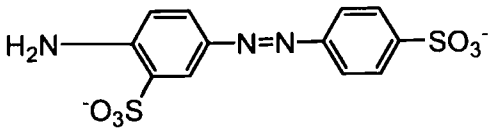

Acid yellow 9
4-Amino-1,1'-azobenzene-3,4'-disulfonate

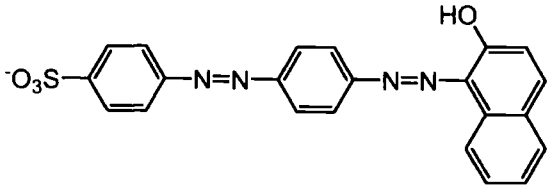

Acid Red 151
4-(4-(2-hydroxynaphthalenylazo)phenylazo)benzenesulphonate

Figure 6-1 Structures of acid dyes acid yellow 36, acid orange 7, acid red 88, acid yellow 9 and acid red 151.

Figure 6-2 shows the percentage decolorisation and corresponding UV-visible spectra collected at various intervals during the reaction period. All UV-Vis spectra, including blanks (acetate buffer) and controls showed saturated absorbance below 230 nm. This was assumed to represent absorption from the acetate buffer. There is no colour removal of AY 9 when reacted with the HZ tailings (Figure 6-2a). Acid yellow 9 is one of the most recalcitrant of the azo dyes and shows limited biodegradability (Pasti-Grigsby et al., 1992). The resistance of this dye to degradation is assumed to be a result of the arrangement of substituents within the azo dye (Pasti-Grigsby et al., 1992). The reaction of AR 88 with the Mn tailings is rapid with 93% decolorisation achieved within 2 hours (Figure 6-2b). Acid red 88 contains 2 naphthalene rings. Azo dyes with naphthalene rings are reported to be more susceptible to oxidation than their benzene equivalents due to the electron donating properties of the second ring (Mokrini et al., 1997) which may explain the rapid colour removal of AR 88 in the current investigation. After 2 hours of reaction time the UV-vis spectrum of AR 88 shows a loss of absorbance in the visible region and an increase of absorbance in the UV region. This would suggest that the molecular structure of AR 88 has changed after reaction with the HT Tailings. Acid red 151 showed 93% decolorisation after reacting with the tailings for 2 hours. However, the control solution for AR 151, in which the tailings were omitted, showed 75% decolorisation after 2 hours and a red precipitate was observed in the reaction vessel. Thus AR 151 was precipitating and/or flocculating in the 0.2 M acetate buffer solution. Evaluation of the UV spectra collected during the reaction of AR 151 with the tailings (Figure 6-2c) would suggest that colour removal in the tailings treatment is not solely due to precipitation, because despite there being a nearly complete removal of absorbance in the visible region, a peak still remains in the UV region after 2 hours. With continual reaction the λ_{max} of this peak shifts to a lower wavelength and is still present after 28 days of reaction. Acid Yellow 36 and AO 7 both lose absorbance in the visible region and form new peaks in the UV region after treatment with the tailings (Figure 6-2d and e, respectively). These new peaks in the UV region suggest transformation reactions are occurring with these dyes.

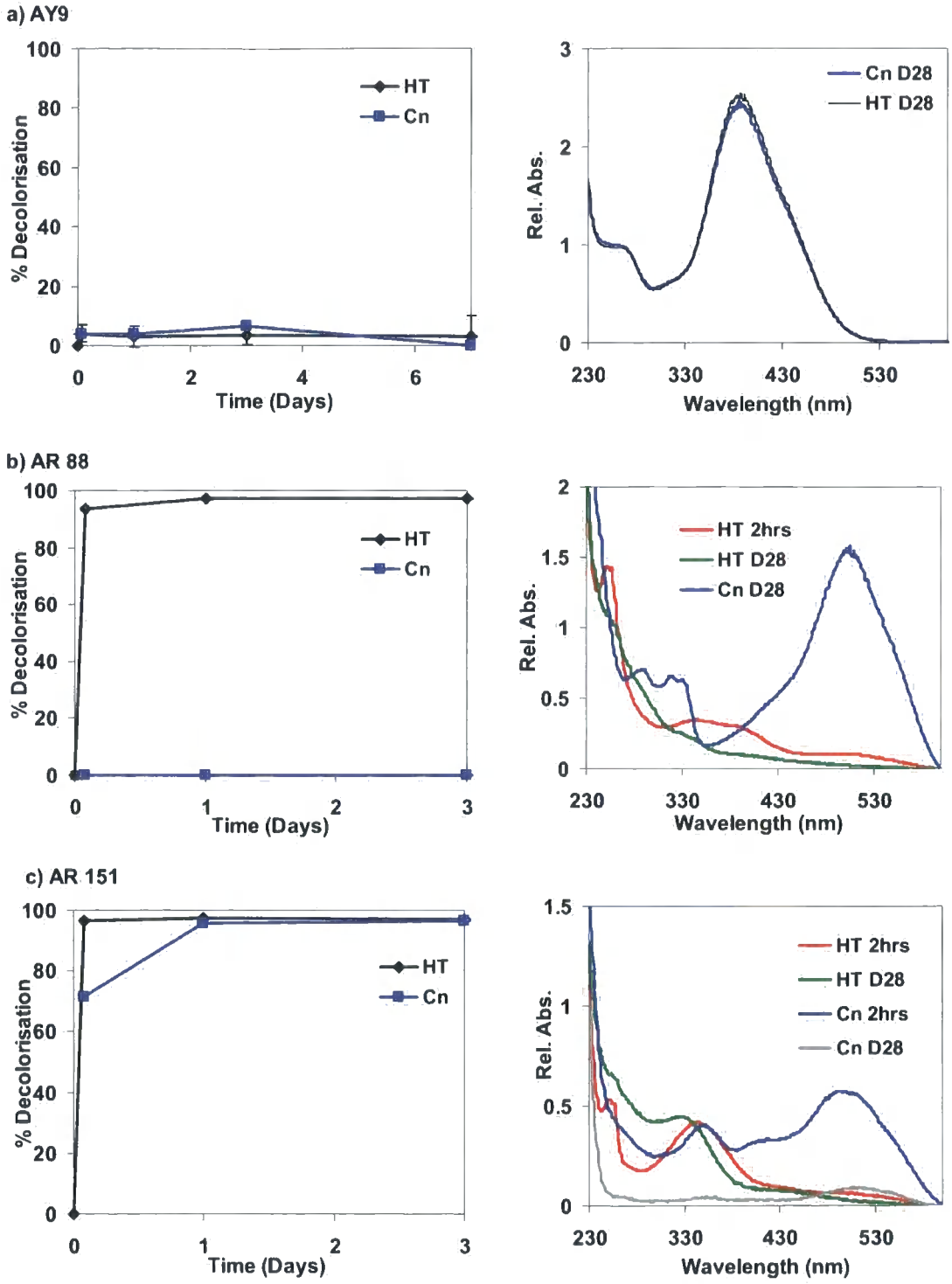

Figure 6-2 Percentage decolourisation of a) AY 9; b) AR 88, c) AR 151, d) AY 36 and e) AO 7 and associated UV-visible spectra collected at intervals (2 hours and 28 days (D28)) during the reaction with HT tailings. (Note: scales are not all the same)

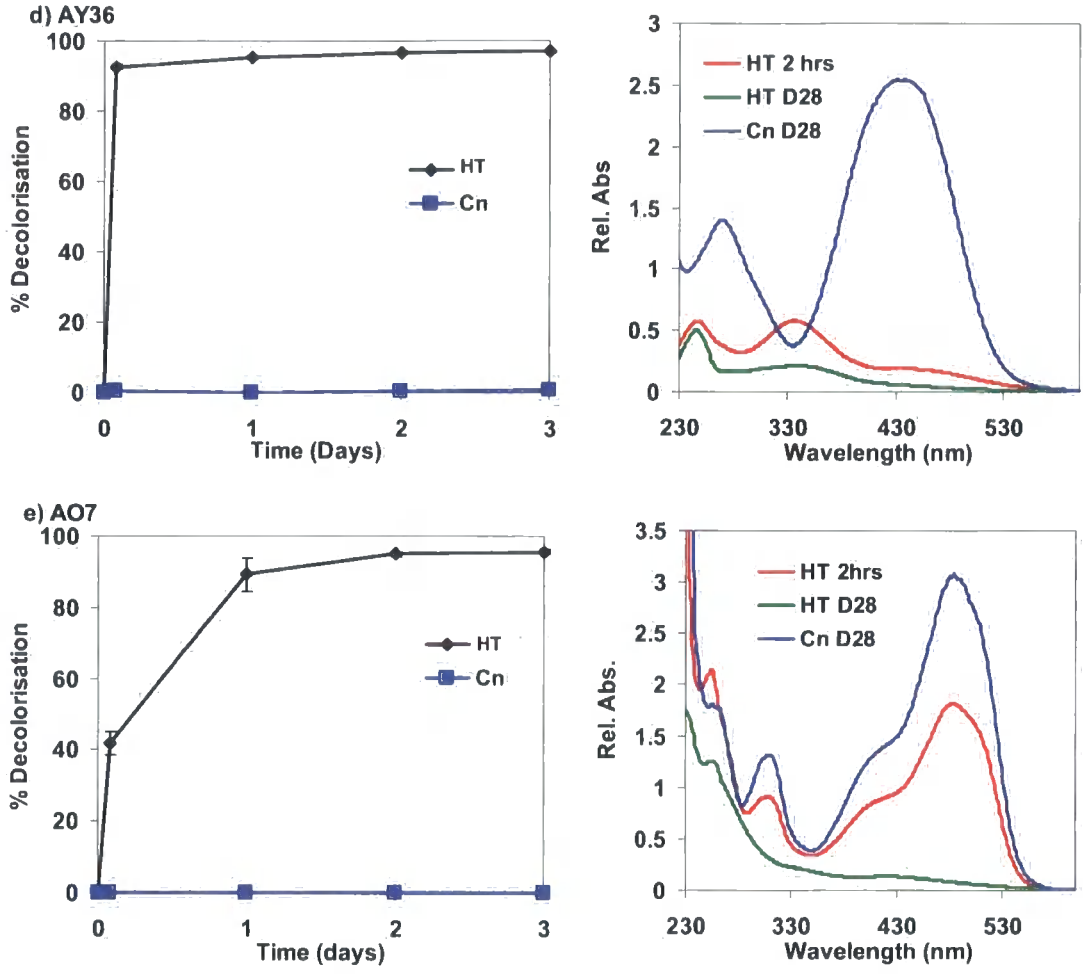

Figure 6.2. Continued.

These results suggest that 4 of the 5 azo dyes screened are decolorised when reacted with the Mn oxides. To obtain detailed information on all dyes would fall outside the scope of this study, thus AO 7 and AY 36 were selected for the reasons stated in Sections 3.3.6 and 3.3.7.

6.2. Dye decolorisation potential of all ore types

Acid orange 7 and AY 36 were reacted with MT, WT and HT tailings, in a pH 4 acetate buffer, to compare the decolorisation potential of the three tailings types. The results, shown in Figure 6-3, suggest all three tailings types remove colour from both dye solutions, but the MT tailings are less efficient than the WT and HT tailings. The pH values of the supernatants after 1 hour reaction was 5.4, 4.4 and 4.3 for the MT, WT and HT tailings, respectively. As

will be shown in Sections 6.4.1 and 6.6.1 the decolorisation reaction is strongly dependent on pH, which may explain the poorer decolorisation capacity observed for the MT tailings. No difference could be observed in the decolorisation capacity of the WT and HT tailings for AY 36 with 89% colour removal achieved in the first 2 hours. The WT tailings displayed better initial color removal efficiency for AO 7 compared to the HT tailings, however, no difference could be observed between the WT and HT tailings after 9 hours reaction time (90% AO 7 decolorisation).

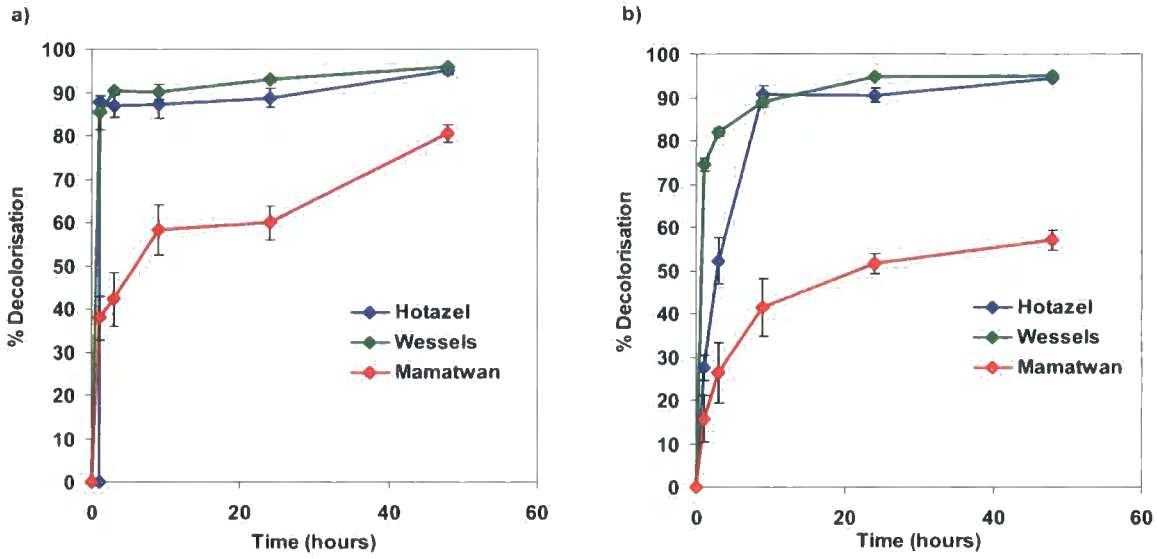

Figure 6-3 Percentage decolorisation of a) AY 36 and b) AO 7 after reaction of Hotazel, Wessels and Mamatwan-type tailings with the dyes in a pH 4 acetate buffer.

Despite the WT tailings showing the highest initial colour removal capacity, handling of the tailings in the laboratory was difficult due to the formation of a surface scum whenever the tailings were hydrated. The HT tailings were used for further analysis of the dye interactions.

6.3. Abiotic vs biotic interactions?

The HT tailings are stored in large dumps that are sparsely vegetated, thus there is the likelihood of biological life associated with the tailings. The involvement of bacteria in redox reactions is well known, so it was necessary to establish whether the reaction between the dye and the tailings was an abiotic or biotic interaction. To achieve this the HT tailings were

autoclaved prior to reaction with the dyes. Although the autoclaved material was assumed to be free of living organisms, biotic material, such as dead cells, may still have been present. The reaction was carried out at the ambient pH of the tailings without addition of buffer. Due to the high carbonate fraction in the tailings calcite was used as a control to establish any reaction carbonate may have with the dyes. The calcite was not autoclaved. The results are shown in Figure 6-4.

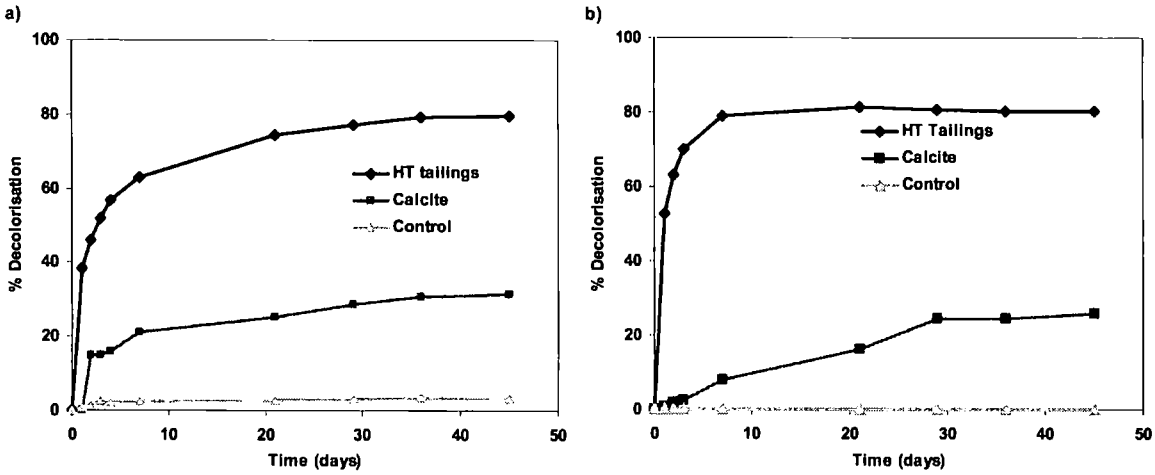

Figure 6-4. Percentage decolorisation of a) AO 7 and b) AY 36 reacted with autoclaved tailings and calcite as a function of time.

Colour removal was observed in the calcite control (up to 30% for both dyes) which may be a result of sorption as it was observed that the white colour of the calcite turned coloured over the reaction period. The decolorisation is far more pronounced in the tailings treatments with 80% decolorisation achieved over the 45 day period for both dyes.

In separate experiments the two dyes were reacted with synthetic manganite and a purchased Mn(III) oxide, both of these Mn oxides decolorised AY 36 and AO 7 (data not shown). Thus decolorisation is observed in autoclaved tailings materials and synthetic Mn oxides (expected to be devoid of any bacteria). This is by no means exhaustive evidence that the interactions between the dyes and the Mn tailings are abiotic, but with the limited data available it would appear that it is mainly a chemical reaction that is taking place. To elucidate the chemical interactions between the acid dyes and the Mn tailings the decolorisation mechanisms were investigated for AO 7 and AY 36.

6.4. Oxidative breakdown of acid dye AO 7

Removal of colour from solution can either be as a result of sorption reactions or transformation of the parent molecule to colourless breakdown products. The aim of this section was to establish the processes involved in colour removal of AO 7 when reacted with the tailings.

6.4.1. pH treatments

The pH range in this investigation spanned from pH 3 to pH 9. This pH range was chosen because the pH of the tailings is close to pH 9 and acid dyes are applied in organic acid buffers thus textile effluents are often acidic. A set of controls (pH adjusted AO 7 solutions) were assessed by UV-vis spectroscopy to establish any pH-related colour changes or flocculation of the original dye over this pH range. No pH-dependent wavelength shifts or concentration differences were observed in the UV-vis spectra of the controls (Figure 6-5a).

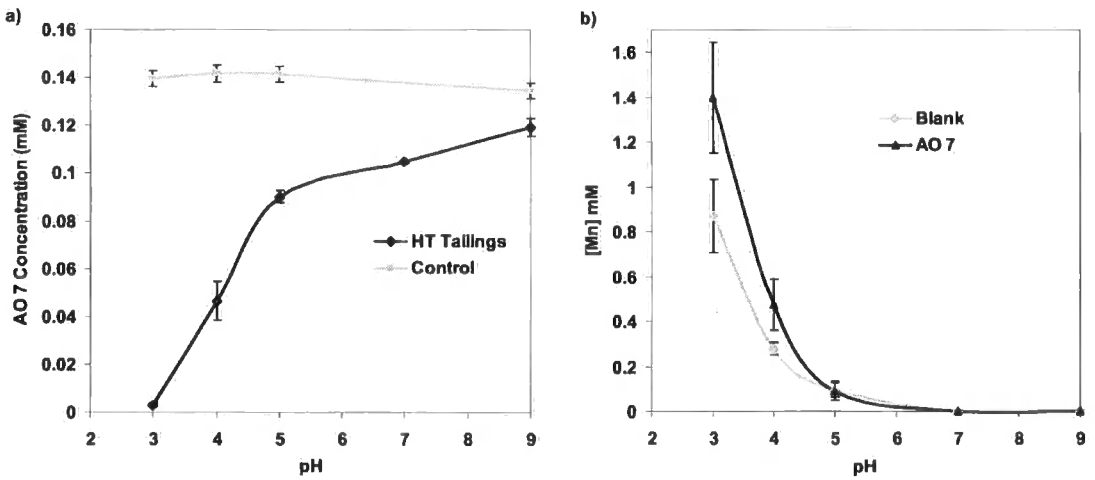

Figure 6-5 Concentration (mM) of a) AO 7 and b) soluble Mn after reacting the HT tailings with the dye at pH 3, 4, 5, 7 and 9 presented with Mn release from pH adjusted blank samples.

A plot of AO 7 concentration against time for samples reacted with the Mn tailings for 1 hour at pH 3, 4, 5, 7 and 9 is given in Figure 6-5a. The concentration of AO 7 in solution decreases as a function of pH when reacted with the tailings. The removal of the dye is most pronounced below pH 5, and increases linearly with further pH decrease and almost complete

removal of colour is achieved at pH 3 (95% decolorisation) after the 1 hour reaction period. Soluble Mn concentrations were measured in the decolorised dye solutions as well as in a series of pH adjusted blank solutions containing no dye (Figure 6-5b). In both the blank and treatment solutions soluble Mn concentrations were below detection limit above pH 7, but at lower pH soluble Mn increases exponentially. This pH-dependent Mn release from the blank samples is expected and can originate through a number of factors including, dissolution of Mn carbonate minerals, reductive dissolution of Mn oxides as the redox stability of the oxides decreases and/or release of Mn(II) ions housed in the mineral lattice via proton promoted dissolution (Zinder et al., 1986). There is large variation in the Mn release both in the blank and the dye treatment. Even at pH 3 the Mn released in the dye treatment was not significantly greater than the blank ($P = 0.059$). The reason for this large variation most likely stems from the heterogenous nature of the tailings as it was noted that different acid volumes and reaction times were needed to obtain the starting pH conditions.

The UV-vis spectra measured at each pH are given in Figure 6-6. A successive decrease in the λ_{max} of the visible region (484 nm) is observed as the pH is lowered, and a new peak at 250 nm is evident in the lower pH treatments, which suggests that colour removal may involve alteration rather sorption alone.

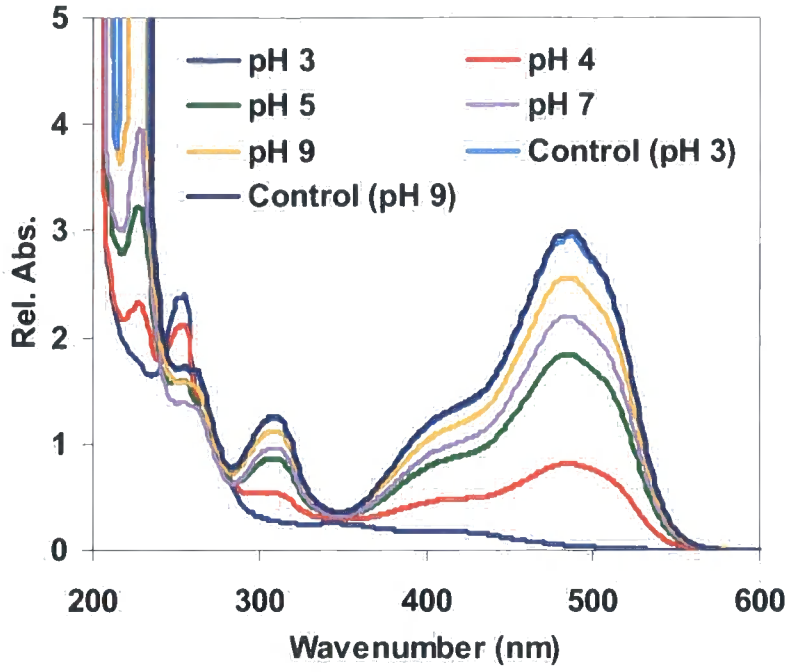

Figure 6-6 UV-visible spectra measured after reaction of AO 7 with the HT tailings at pH 3, 4, 5, 7 and 9 for 1 hr, presented with controls adjusted to pH 3 and pH 9

Further analysis with HPLC was conducted to establish whether oxidative or sorptive reactions were responsible for the progressive increase in decolorisation in increasingly acidic solutions. Chromatograms are shown in Figure 6-7.

During the HPLC study two peaks (3.6 min and 13.8 min) were identified in all chromatograms, including blanks, controls and de-ionised water. The peak at 3.6 min was identified as being a solvent peak while the peak at 13.8 min was identified as being a plastisizer, thus these peaks will be ignored in the subsequent discussion.

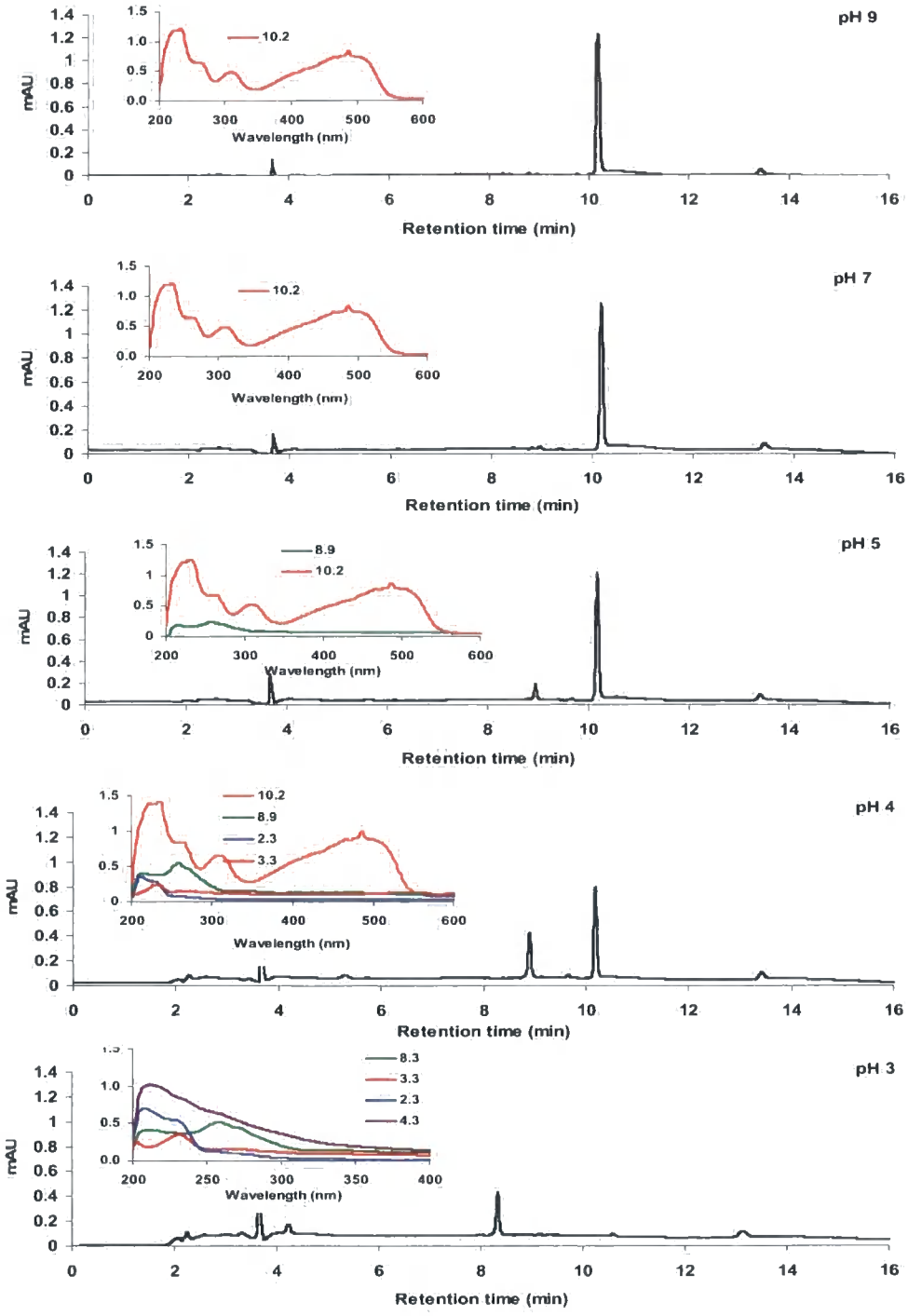

Figure 6-7 Chromatograms of AO 7 solutions after reaction with the tailings at pH 9, 7, 5, 4 and 3 for 1 hour. UV-Vis spectra corresponding to peaks at the various retention times shown in the insets. (Note not all scales are the same)

Chromatograms of the pH 9 and 7 samples contain only one peak at 10.2 min which has a UV-vis spectrum corresponding to that of the parent dye. In the pH 5 treatment another peak at 8.9 min, is evident and in the pH 4 treatment two additional peaks at 2.3 and 3.3 min occur together with the 8.9 min and parent dye peak. At pH 3 there is no evidence of the parent dye molecule. Despite a shorter retention time the peak at 8.3 min has the same UV spectrum as the 8.9 min peaks of the higher pH treatments. A peak at 4.3 min, has a UV-vis spectrum showing a broad absorption band in both the visible and UV region. This may represent one of the coupling products identified in the LC-MS study described below. All the new peaks observed in the chromatograms correspond to compounds absorbing in UV region.

1,2 Napthoquinone (NQ), 4-hydroxybezenesulfonate (4HBS) and benzenesulfonic acid (BS) have been identified as breakdown products in the oxidation of AO 7 by the enzyme laccase (Lopez et al., 2004; Lu and Hardin, 2006). Standard solutions of NQ, 4HBS and BS were analysed for comparison with the observed UV spectra. When the NQ standard was analysed with HPLC immediately after preparation, two peaks (Rt 8.9 and 11 min) were evident on the chromatogram. After the sample stood for 24 hours, only one peak at 8.9 min was observed. Lopez et al. (2004) observed similar peaks in their NQ standards and assigned it to a quinone-hydroquinone equilibrium. As the samples in Figure 6-7 were run 24 hours after filtration the NQ standards were treated in the same manner.

The UV spectra of the NQ, 4HBS and BS standards are given in Figure 6-8 along with UV spectra observed in the chromatogram from the pH 3 treatment. The UV spectra and retention times of the NQ and 4HBS standards compare well with the 8.3 (8.9 in the higher pH treatments) and 3.3 minute peaks, respectively, suggesting that these compounds are breakdown products of AO 7 oxidation by the Mn tailings. The BS standard, although having a comparable retention time did not have a UV spectrum fitting that of the 2.3 min peak and thus its formation as a product cannot be confirmed by HPLC analysis.

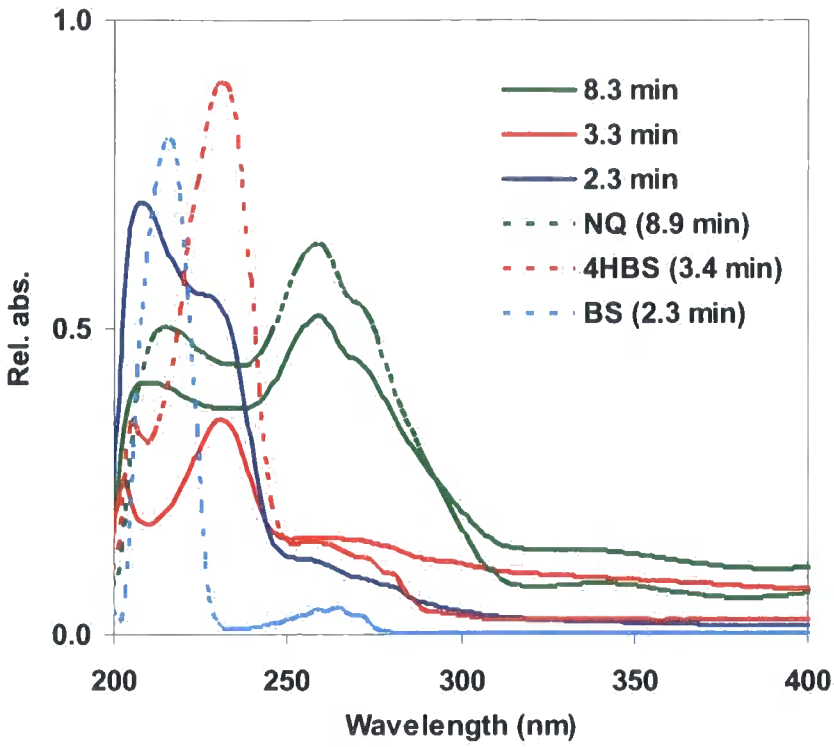

Figure 6-8 UV spectra corresponding to retention times 2.3, 3.3 and 8.3 minutes observed in the pH 3, AO 7 treatment compared to 1,2 naphthoquinone (NQ), 4-hydroxybenzenesulfonate (HBS) and benzenesulfonate (BS) standards. Retention times of the standards are given in parenthesis.

From the above data is it clear that the dye is reacting with the Mn tailings to produce breakdown products and the reaction is enhanced as the pH is lowered. The influence of pH in the reaction between organic molecules and Mn oxides has been well established, with a decrease in pH facilitating oxidation of various organic compounds (Stone, 1987a; Ulrich and Stone, 1989; Laha and Luthy, 1990; Zhang and Huang, 2003; Zhang and Huang, 2005). These workers have attributed the increased oxidation of organic compounds by Mn oxides at lower pH to:

i) the decrease of the negative charge on the Mn oxide surface;

ii) positive charging of the organic molecule resulting in electrostatic attraction to the oxide surface;

iii) the increased redox potential of the MnO_2/Mn^{2+} couple; and

iv) enhanced removal of Mn^{2+} from the oxide surface, exposing new reactive sites (Klausen et al., 1997).

It is likely one or more of these pH-dependent influences are playing a role in the reaction between AO 7 and the Mn tailings. As established in Section 5.2.4 the Mn tailings have a PZC below 4. As the pH is lowered the charge on tailings will become less negative. Thus the repulsion between the negatively charged azo dye and the negatively charged Mn oxide surface will diminish as the pH drops. The measured PZC indicates the point where the overall charge, comprising of individual contributions from the different mineral phases, is equal to zero. Although the net charge is zero only below pH 4, individual mineral phases may have a positive charge at a substantially higher pH. Thus the negative azo dye molecules may preferentially sorb to mineral phases within the tailings that are positively charged. Decreasing the pH will increase the proportion of positively charged phases and thus more reactive sites become available for the adsorption of the dye thereby increasing dye-mineral contact and accordingly, oxidation.

Ionic speciation of AO 7 across the pH range was described by (Bandara et al., 1999a). Acid orange 7 has a pKa_2 of 11.4, corresponding to the deprotonation of the napthanol group, and there is little contribution of this deprotonated species below pH 8. The pKa_1, corresponding to protonation of the sulfonate group is 1, therefore in the pH range of this study (3 to 9) the molecule will be negatively charged. This implies that any electrostatic attraction between the dye and the Mn oxide surface will be dependent on charge generation on the oxide surface. Sorption of AO 7 on other oxides (Ti, Fe and Al oxides) has been shown to commence once the pH is lowered sufficiently to generate $M\text{-}OH_2^+$ groups on the oxide surface and increases linearly below the PZC of the oxide (Bandara et al., 1999a).

The pH-dye concentration curve for AO 7 after reaction with the tailings is linear between 5 and 3 and no plateau is reached within this pH range (Figure 6-5a). For samples reacted without pH adjustment (i.e. pH = 9.0), 60% decolorisation was achieved in 1 week and 80% decoloristion was achieved after 45 days (Figure 6-4a). At this pH electrostatic repulsion between the dye and the negatively charged Mn oxide surface may hinder dye-mineral

interactions. The fact that decolorisation of the dye occurs at pH 9, albeit slowly, implies that the pH dependence may have kinetic as well as thermodynamic influences.

6.4.2. Reaction and polymerisation products determined by LC-MS

Identification of reaction products was attempted using LC with tandem $MS(MS)^n$. The mass spectral data is summarised in Table 6-1. Compound (V), measured in negative ion mode, represents the parent dye molecule (m/z: 327). Figure 6-9 shows the fragmentation pattern of the parent dye molecule, which is in good agreement with the fragmentation observed by Lopez et al. (2004) for AO 7.

Four AO 7 degradation products were identified using LC-MS analysis. In addition to 4HBS and NQ (compounds I and IV, respectively) observed in the HPLC investigation, two additional products (compounds II and III) were identified. Compound II has been interpreted as being the coupling product of BS and NQ. Similarly the next eluting compound (compound III) has been identified as the polymerisation product of 4HBS and NQ. Comparable polymerisation products have been identified during enzymatic oxidation of AO 7 (Zille et al., 2005).

Table 6-1. Mass spectra data of AO 7 degradation products

Compound No.	Retention time (min)	Mode	MS m/z (% relative intensity)	MS^2 (% relative intensity)
I*		ES-	173(100); 198(80); 196(70); 137(36)	NA
II	3.73	ES-	313(100); 314(22); 315(10); 329(5)	285(100); 249(17); 257(5); 233(7)
III	3.94	ES-	329(100); 173(90); 411(40); 287(34);	301(100); 285(52); 302(30); 273(7)
IV*		ES+	159(100); 191(45); 181(31)	NA
V	7.65	ES-	327(100); 500(10); 329(5)	171(100); 247(12); 156(10)

* Compounds I and IV were identified using the second LC-MS system described in the methods section thus retention times have not been not reported.

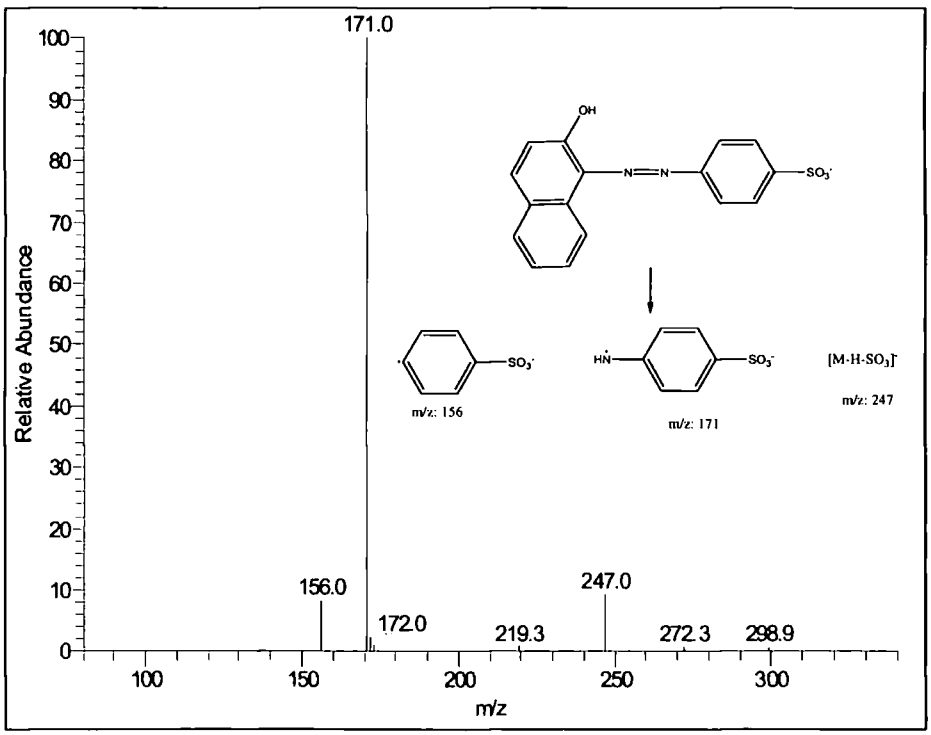

Figure 6-9 Ion products as identified in the MS^2 of the 327 m/z peak, representing the fragmentation pattern of AO 7.

The proposed reaction mechanism of AO 7 oxidation by the Mn tailings is given in Scheme 1. The mechanism appears to be essentially the same as that proposed for peroxidase degradation mechanisms (Chivukula et al., 1995; Lopez et al., 2004; Zille et al., 2005; Lu and Hardin, 2006). Electron transfer from the phenolic group to the Mn oxide generates a phenoxy radical which undergoes resonance rearrangement and additional electron transfer to generate a carbocation on the C-1 carbon of the naphthol ring. Nucleophilic attack by water generates an unstable tetrahedral complex resulting in the cleavage of the C-N bond yielding 1,2-naphthoquinone (Compound IV) and (4-sulfophenyl)diazene. Although the latter compound was not detected in the current study, possibly due to its instability, it has been identified by Lopez et al. (2004). Unstable diazene derivatives readily oxidise in the presence of oxygen or metal ions to generate unstable phenyldiazene radicals (Huang and Kosower, 1968). These phenyldiazene radicals in turn lose the azo linkage as N_2 to yield a phenyl radical (Kosower et al., 1969) or undergo hydrolysis to form 4-hydroxybenzenesulfonate (Compound I) (Lopez et al., 2004). The phenyl radical can abstract a hydrogen radical from its surroundings to generate a stable phenyl compound (Spadaro and Renganathan, 1994) or take part in coupling reactions with other oxidation products (Zille et al., 2005). Benzenesulfonate was not detected in the mass spectra or HPLC study, however, a coupling product of benzenesulfonate and NQ was detected (Compound II), suggesting the latter process occurs. An alternate or additional pathway for the phenyl radical involves further oxidation followed by nucleophilic attack of water generating 4-hydroxybenzenesulfonate (Compound I).

This reaction mechanism suggests the asymmetric cleavage of the azo bond. While the same reaction products can be generated through symmetric cleavage of the azo bond, the reaction pathway involves reduction steps (Goszczynski et al., 1994), which are not likely to occur in the oxidative environment provided by the Mn oxides.

According to the above mechanism three successive electron transfers are involved. In section 5.2.1 it was established that the net oxidation state of the HT tailings was 3+, and the mineralogy showed a predominance of Mn(III) oxides. If this were the case the reaction would have a dye: Mn(III) reaction stiochiometry of 1:3 and 3 moles of Mn^{2+} would be expected to be generated from the breakdown of 1 mole of AO 7.

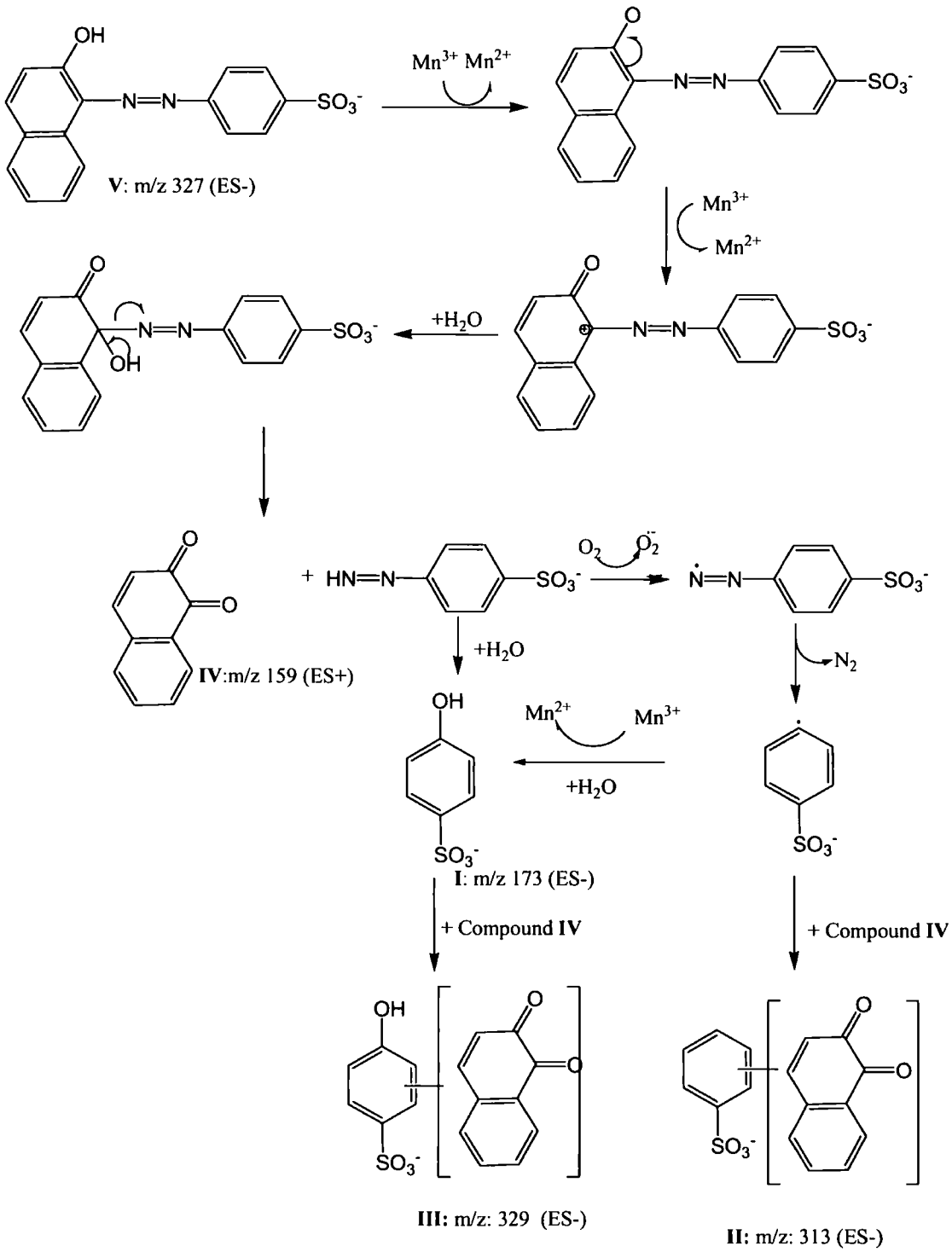

Scheme 1 Proposed mechanism for the oxidation of AO 7 by the Mn tailings

To assess the correlation between dye decolorisation and Mn release, AO 7 was reacted with the tailings for 18 hrs in a pH 4 acetate buffer. Aliquots were collected periodically and analysed for dye and Mn content. The relationship between percentage decolorisation and $[Mn]_{diss}$ (Mn release additional to that of the blank), is given in Figure 6-10a. There is an initial increase in dye decolourisation without concomitant Mn release, but after this, further decolorisation is proportional to $[Mn]_{diss}$. The initial colour decrease, without simultaneous Mn release suggests the dye is adsorbing to the tailings prior to the oxidation reaction. It is also interesting to correlate the concentration of AO 7 as a function of $[Mn]_{diss}$ after the first sampling interval (i.e. not including the initial rapid dye removal) (Figure 6-10b). A linear correlation exists (R^2= 0.99) with a gradient of -0.32 giving an AO 7: Mn(III) reaction stoichiometry of 1:3 as suggested by the reaction mechanism above.

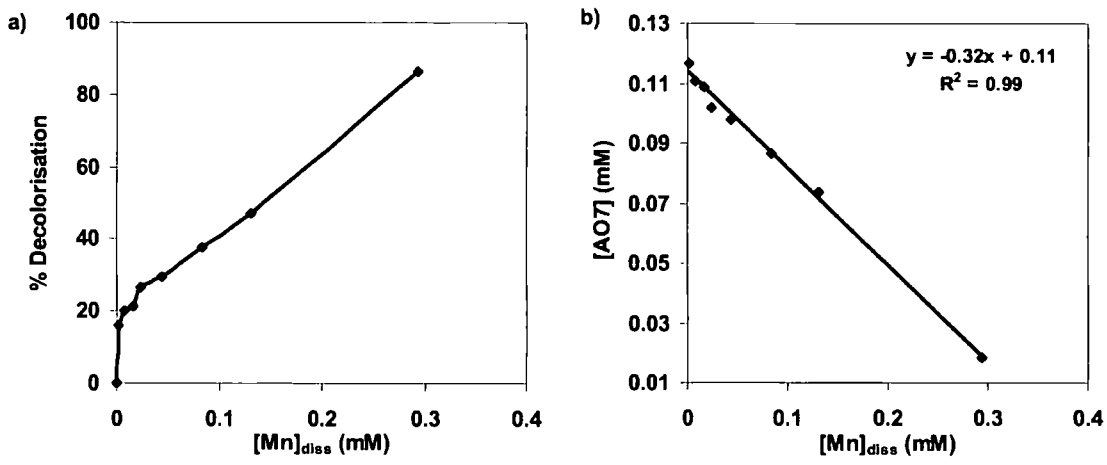

Figure 6-10 a) Percentage decolorisation of AO 7 plotted against $[Mn]_{diss}$ for a 0.14 mM AO 7 solution reacted with the HT tailings (S:L 1:50) in a pH 4 acetate buffer over 18 hours and b) AO 7 concentration as a function of $[Mn]_{diss}$ excluding the first sampling interval (after 0.5 min)

To establish whether 4HBS and NQ are the terminal products in the reaction, these 2 compounds were reacted with the tailings in a pH 4 buffer. The concentration of 4HBS reacted with the tailings was not significantly lower (P = 0.39) than the control after 28 days reaction time (Figure 6-11a), suggesting sorption and transformation of this compound is minimal in the presence of the tailings. This is in contrast to enzymatic treatment of 4HBS which showed a 70% removal of this compound (Lopez et al., 2004). The concentration of NQ decreases with time in both the control and the tailings treatment. A brown precipitate

was observed in the NQ control which may suggest that coupling reactions were occurring in the pH 4 acetate medium. When NQ was reacted with the tailings the concentration-time curve displayed the same shape as the control but the concentrations were consistently lower (Figure 6-11b). Analysis of the filtrates by UV and HPLC showed no evidence that transformation of NQ had occurred after 28 days of reaction, thus the difference between the concentration in the control and the tailings treatment may relate to sorption. It is thus assumed that these two compounds and their coupling products are the final products of AO 7 oxidation and complete mineralization of the dye is not possible using the Mn tailings under the current experimental conditions. 1,2 Naphthoquinone is a coloured product which explains why total colour removal was never achieved.

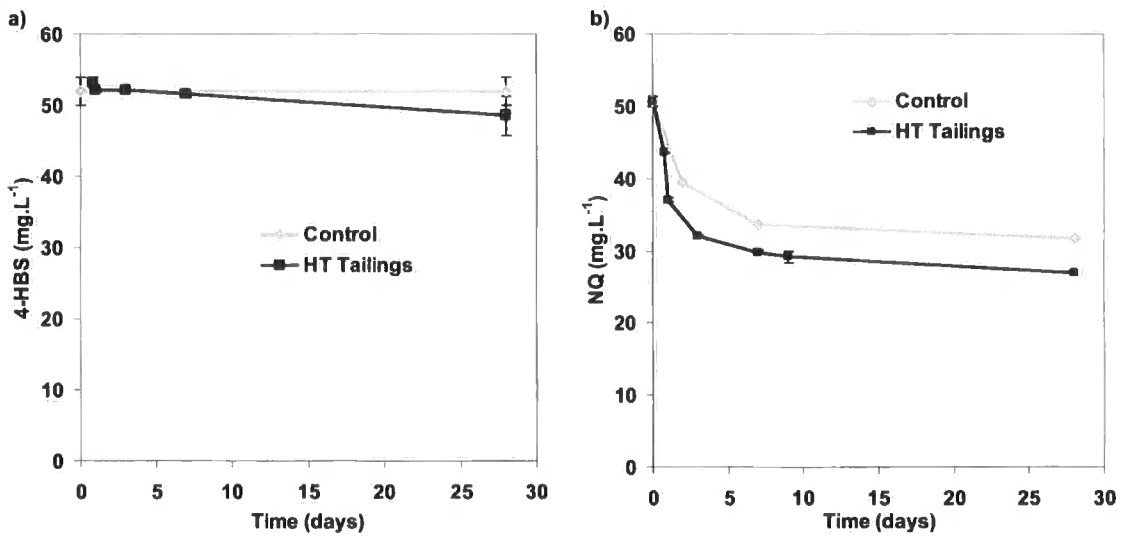

Figure 6-11 Concentration of a) 4 hydroxybenzenesulfonic acid (4HBS) and b) 1,2 naphthoquinone (NQ) as a function of time in the absence (control) and presence of the HT tailings. Certain error bars may be smaller than data points.

6.4.3. Reaction rates and orders

As shown above, the mechanism for the oxidative breakdown of AO 7 by the Mn tailings follows a multi-step reaction, involving a few short-lived reaction intermediates. An attempt was made to determine the rate and order of the reaction. Most kinetic studies use simple model systems involving only one mineral phase. Due to the complex nature and heterogeneity of the tailings the rates and orders here must be taken as tentative. To

determine the rate of the reaction both dye removal and reductive dissolution of the Mn tailings were considered. As mentioned above $[Mn]_{diss}$ represents Mn release additional to Mn dissolution observed in the blank solution. Raw data can be found in Appendix D.

Reactions were carried out at pH 4, 5 and 6. At pH 5 and 6 the Mn released in the dye treatments did not differ substantially from the Mn released in the blank solutions over the 4 hours reaction period (data not shown). Due to time constraints these reactions could not be repeated over longer time periods. Figure 6-12 shows the change in AO 7 concentration and $[Mn]_{diss}$ over time for the pH 4 treatment. There is an initial sharp decrease in AO 7 concentration in the first 30 seconds of the reaction, after which dye removal slows down. This initial dye decrease is not reciprocated by a similar sharp increase in $[Mn]_{diss}$ (Figure 6-12b), which could suggest that sorption is responsible for the initial removal of dye from solution, or that Mn release from the solid phase is delayed.

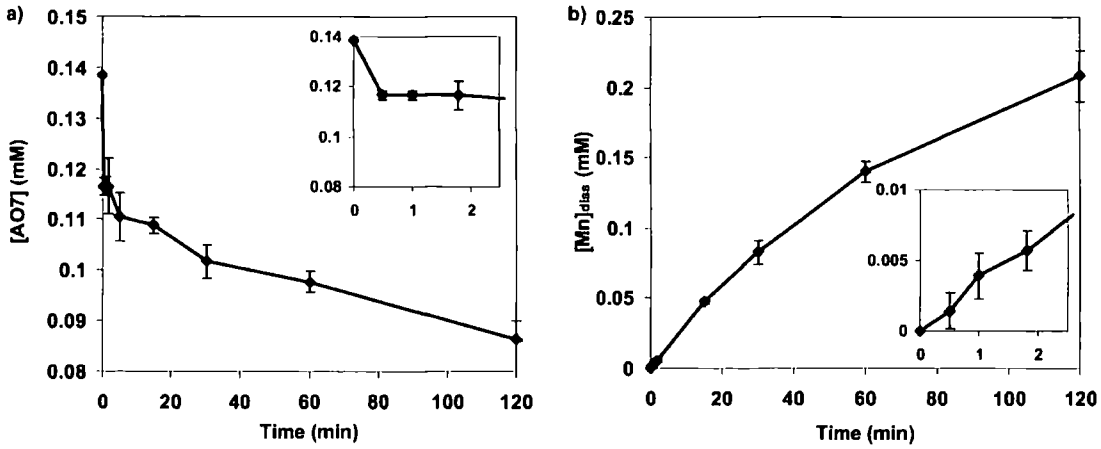

Figure 6-12 Plots of a) AO 7 concentration and b) $[Mn]_{diss}$ as a function of time. Insets display enlarged scale over the initial sampling interval. Initial dye concentration = 0.14 mM, [SA] = 48 $m^2.L^{-1}$, pH 4.

Ideally in kinetic studies one would like to investigate both Mn release and AO 7 disappearance. However, assessing AO 7 removal would involve incorporating sorption considerations into the kinetics equations as in the Langmuir–Hinshelwood equation. This has been achieved for dye decolorisation reactions involving photo-catalysts where sorption parameters such as equilibrium concentrations and distribution coefficients can be obtained before the light-dependent reaction is initiated (Bandara et al., 1999b; Muruganandham and

Swaminathan, 2006; Sleiman et al., 2007). In the case of Mn oxides, sorption studies are difficult due to the rapid reaction of the reductant on the oxide surface (Xyla et al., 1992). For this reason, rate calculations have been confined to $[Mn]_{diss}$ as done for a number of Mn oxide mediated organic oxidation reactions (Stone and Morgan, 1984a; Stone and Morgan, 1984b; Laha and Luthy, 1990; Xyla et al., 1992; Matocha et al., 2001).

Using $[Mn]_{diss}$, the initial rate, calculated for the reaction between the tailings and a 0.14 mM AO 7 solution at pH 4, normalised for surface area is 3.8 x 10^{-6} $mol.s^{-1}.m^{-2}$. A plot of NQ concentration as a function of time is given in Figure 6-13. The initial rate of NQ generation was determined as 2.5 x 10^{-6} $mol.s^{-1}.m^{-2}$. Thus the rates of Mn^{2+} generation and NQ formation are of the same magnitude suggesting that once initiated, the complete oxidation to NQ occurs rapidly. This is further demonstrated in the ATR study discussed later.

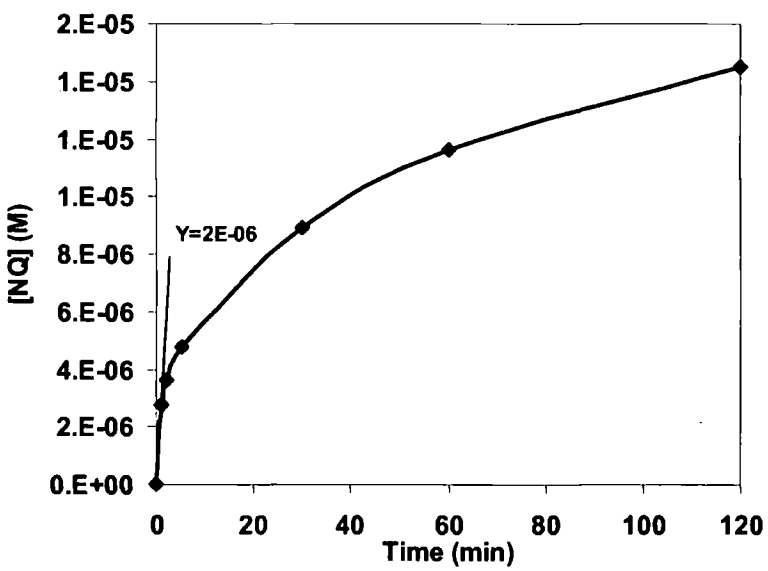

Figure 6-13 Concentration of NQ generated over time after reacting the tailings with a 0.14 mM AO 7 solution at pH 4.

The reaction order was determined using the initial rate method of Lasaga (1981). Figure 6-14a shows $[Mn]_{diss}$ as a function of time for three surface area concentrations at a constant dye concentration and pH. The ln (initial rate) vs. ln[SA] plot given in Figure 6-14b is linear (R^2>0.95) with a slope of 1.19 ± 0.08 (not significantly different to 1 at a 5% confidence level (t = 3.4; f = 2)), indicating a pseudo-first-order dependence on [SA]. This result is expected

for surface-dependent reactions. Calculation of the experimental rate constant (k_{exp}) is usually achieved using the following equation:

$$\ln([MnO_x]_0-[Mn^{2+}]_{diss})-\ln([MnO_x]_0) = - k_{exp}t$$

Where $[MnO_x]_o$ is the starting Mn oxide concentration and t is time. To calculate the k_{exp} by this method the concentration of MnO_x needs to be known. This is not possible for a heterogeneous material like the Mn tailings, thus only pseudo rate constants (k') were calculated. The pseudo-first order rate coefficient with respect to surface area, shown by the y-intercept of the ln (initial rate)-ln[SA] (Appelo and Postma, 2005) is 1.8 x 10^{-6} s^{-1}.

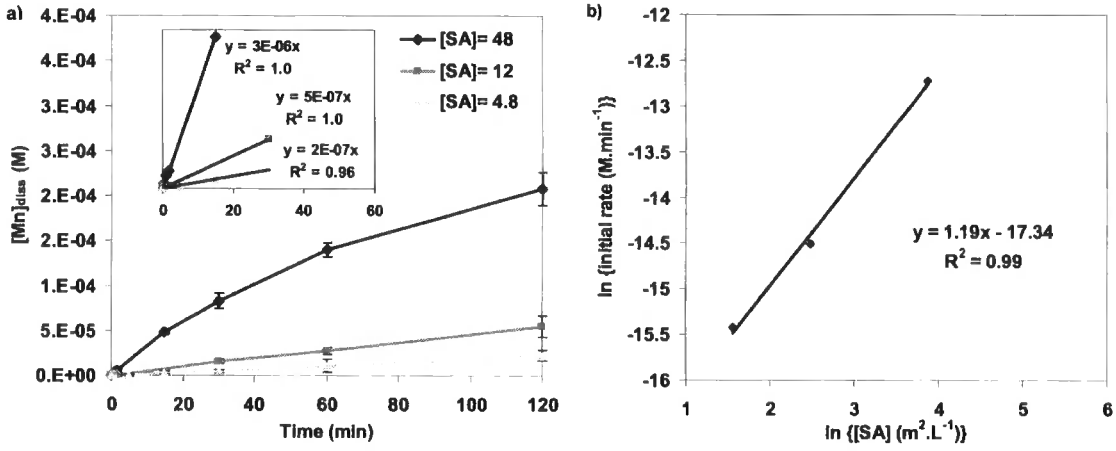

Figure 6-14 Plots of a) $[Mn]_{diss}$ as a function of time for three surface area concentrations ([SA]) with inset showing initial rate plots for the three curves and b) ln(initial rate) vs ln[SA]

Figure 6-15a shows $[Mn]_{diss}$ as a function of time for three AO 7 concentrations reacted at constant [SA] and pH. A 10-fold increase in dye concentration only results in a 4-fold increase in reaction rate. This would suggest that dissolution rate is dependent on surface coverage and the availability of surface sites limits the rate at higher dye concentrations.

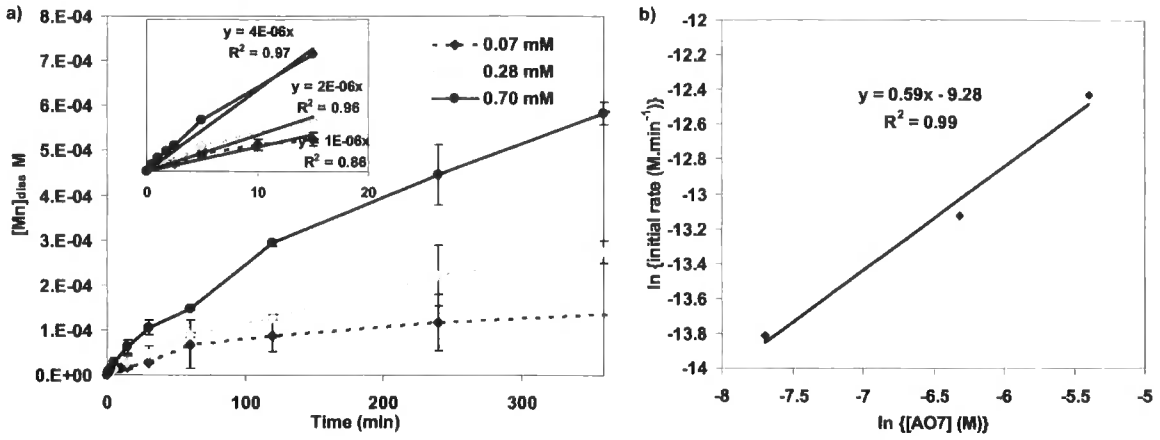

Figure 6-15 Plots of a) $[Mn]_{diss}$ as a function of time for three AO 7 concentrations ([AO 7]) with inset showing initial rate plots for dye concentrations and b) ln(initial rate) vs ln[AO 7]

The plot of ln (initial rate) vs ln [AO 7] (Figure 6-15b) gives a straight line (R^2=0.99) with a slope of 0.6 ± 0.07 (significantly different to 1 at a confidence level of 5% (t = 8.3; f = 2)). This fractional rate order would suggest that there are some rate limiting factors involving residence time on the Mn tailings surface i.e. either precursor complex formation, electron transfer or removal of the reaction products from the surface are the rate limiting factors. In certain Mn oxide mediated organic oxidations the transfer of the first electron has been observed to be the rate limiting step (Klausen et al., 1997; Khan et al., 2004; Kumar and Khan, 2005). In such cases fractional rate orders with respect to the reductant have been reported (Khan et al., 2004; Kumar and Khan, 2005). As will be shown in the results from the ATR study (Section 6.5), a lag phase occurs between initial sorption of the dye to the surface and the initiation of oxidation. This would explain the fractional order with respect to dye concentration observed here.

6.5. Sorption and oxidation of AO 7 measured using ATR-FTIR.

Interactions between AO 7 and Mn oxides were probed with ATR-FTIR in order to obtain real time *in-situ* information. As discussed in Section 6.4.3 information pertaining to sorption of the reductant onto the oxidant surface can be difficult to obtain due to the rapid reaction between the two. The ability to scan the sample rapidly makes ATR suitable for this purpose. One of the limitations of ATR is poor sensitivity, thus a high surface area sorbent is

necessary to allow sufficient sorbate to be detected. The low surface area and complex nature of the tailings made ATR experiments difficult. Manganite (γ-MnOOH) is present in the WT and HT tailings. Synthetic manganite was therefore thought a suitable Mn oxide to use in the ATR experiments. Details of the synthesis and characterisation of the manganite can be found in Sections 4.4 and 5.4, respectively. The IR spectrum of the synthetic manganite is shown in Figure 6-16. The observed bands correlate well with those reported for manganite (2083; 1151; 1116 and 1086 cm^{-1}) (Kohler et al., 1997).

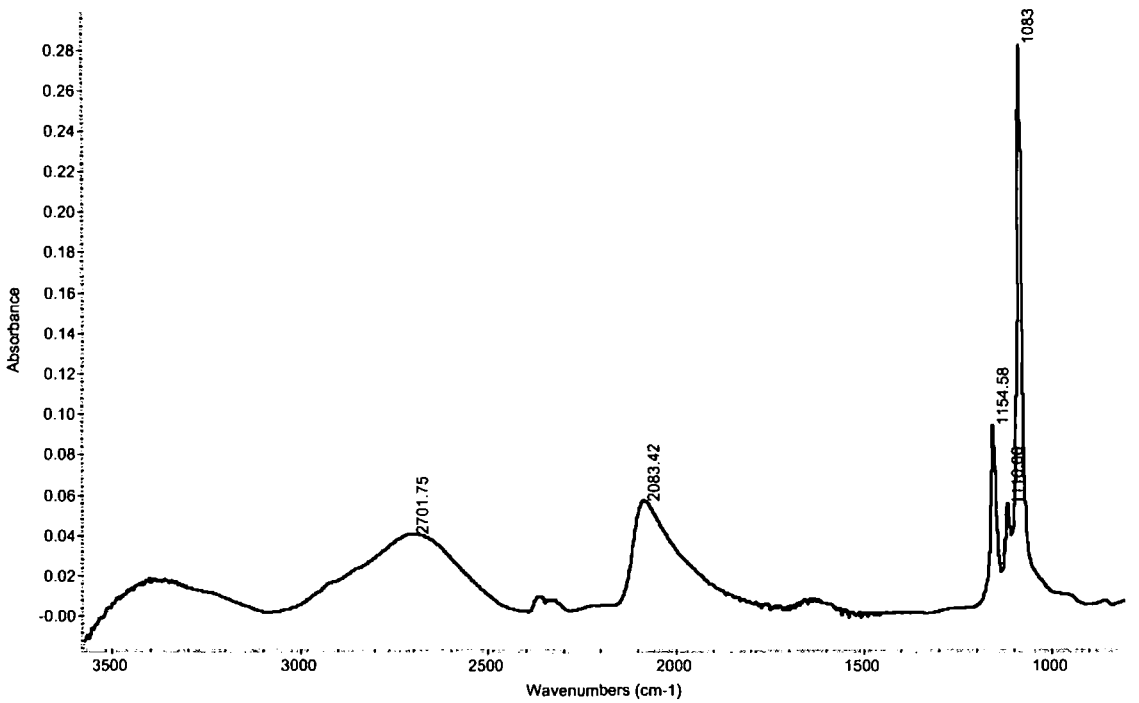

Figure 6-16 IR spectrum of manganite

6.5.1. Sorption of AO 7 to the manganite surface

The IR spectrum of a 25 mM AO 7 standard is shown in Figure 6-17. Interpretation of IR spectra can often be difficult and inconsistent absorption band assignments have been made for azo dyes by previous workers. The azo-hydrazone tautomerism of AO 7 often leads to conflicting interpretation of IR spectra due to the fact that the analytical useful group vibrations are intermixed with those of aromatic rings (Bauer et al., 1999).

Due to reasons related to symmetry the intensity of the azo bond vibrations in the IR region are low, however, substitutents *para* to the azo group significantly enhance the vibrational intensity (Vinodgopal et al., 1996). Assignments of the azo bond have been made at 1429 and 1454 cm^{-1} (Li et al., 2006). Vinodgopal et al. (1996) assigned the peak at 1500 cm^{-1} to the azo bond or an aromatic C=C vibration which is sensitive to the azo bond. This band has also been assigned to the N-H bend of the hydrazone form of AO 7 (Bauer et al., 1999; Zhang et al., 2005; Li et al., 2006). Bandara et al (1999a) has proposed that the peak intensity of the 1500 cm^{-1} peak is too high to be assigned to the N=N group, and proposes a weak band at 1452 cm^{-1} to represent the azo bond, while Bauer et al. (1999) assigns this band to one of the phenyl ring vibrations. Absorption bands at 1620, 1529, 1568, 1555 and 1454 cm^{-1} have been attributed to aromatic skeletal vibrations (Vinodgopal et al., 1996). The small band at 1420 cm^{-1} has been assigned to the OH bending vibration and the band at 1255 cm^{-1} to the C-O-H stretching vibration (Vinodgopal et al., 1996; Lucarelli et al., 2000). In their study Bauer et al. (1999) assigned the band at 1124 cm^{-1} to the symmetric stretching (υ_s) of the SO_3 group and the band at 1180 cm^{-1} to the asymmetrical (υ_{as}) stretching of the SO_3 group. Bourikas et al. (2005) assigned symmetric and asymmetric stretching of the SO_3 group at 1198 and 1304 cm^{-1}, respectively while Sperline et al. (1994) assigned bands at 1209 and 1177 cm^{-1} to asymmetric stretching of the SO_3 group. Stylidi et al. (2003) observed a peak at 1572 cm^{-1} in a powdered sample of AO 7, this was reported to represent the C=O group of the hydrazone form. Disappearance of this peak on sorption was interpreted as inner-sphere coordination of this group with a titanium oxide. From Figure 6-17 it is clear that no 1572 cm^{-1} peak exists in the aqueous AO 7 species. Considering the numerous conflicting band assignments in the literature interpretation of the IR spectrum of AO 7 can only be tentative. The current work differs from all the previous IR studies involving AO 7, which were limited to dry powdered samples, in that IR spectra presented here represent aqueous solutions. For this reason IR bands may be shifted in relation to published values.

In the sorption experiments AO 7 was added to a clay film in concentrations that were below the detection limit for aqueous species on the ATR unit. This was validated by adding a 0.14 mM AO 7 solution to the clean Ge crystal and collecting a series of spectra. No peaks were evident (data not shown) thus it can be accepted that any peaks observed, at this concentration, will represent AO 7 sorbed to the mineral surface.

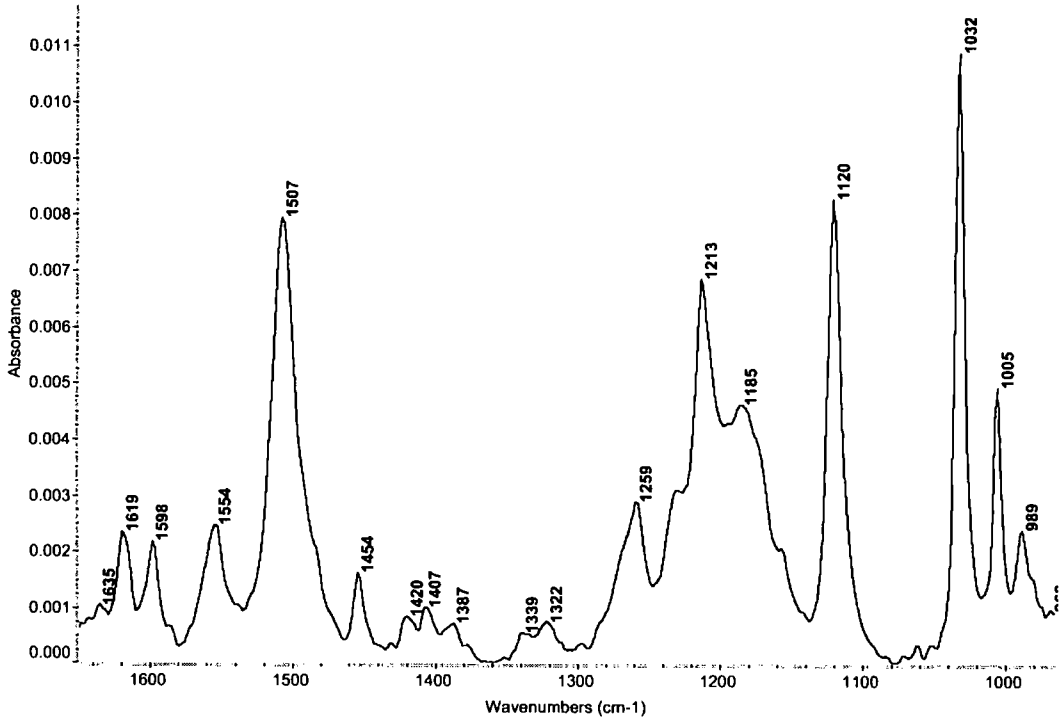

Figure 6-17 Infrared spectrum of a 25 mM AO 7 solution on a clean Ge IRE

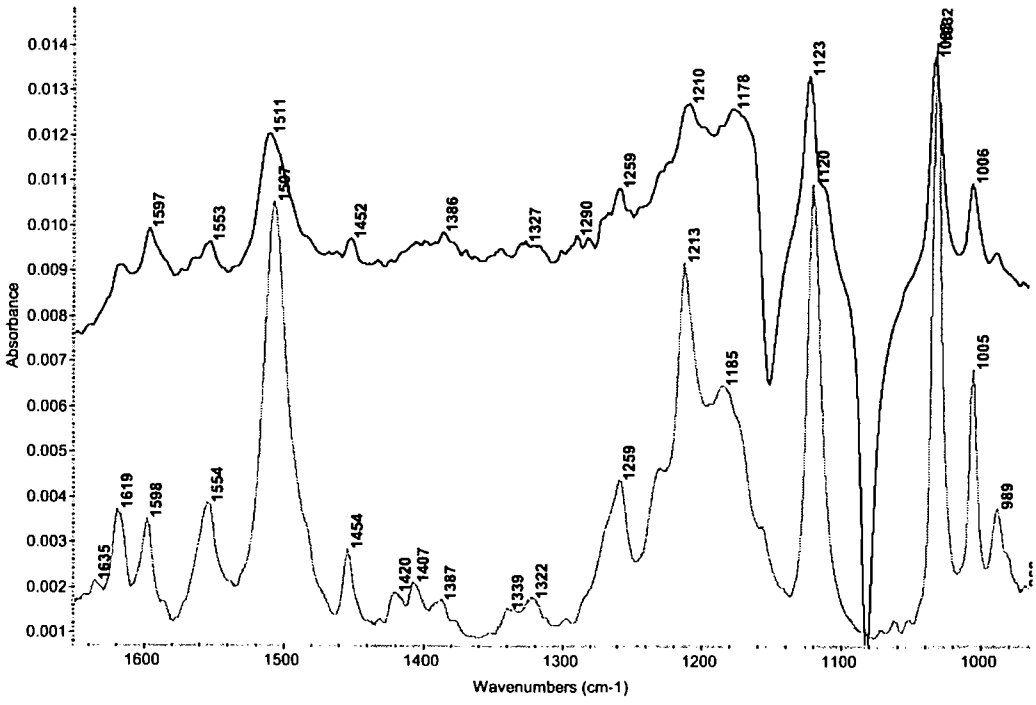

Figure 6-18 IR Spectra of a 25 mM AO 7 standard solution (grey) and 0.14 mM AO 7 sorbed onto the manganite surface (black). Spectra not to scale.

Figure 6-18 shows an IR spectrum of a 0.14 mM, pH 2.5 AO 7 solution sorbed onto the manganite surface, measured 60 seconds after dye addition, along with a spectrum of a 25 mM standard adjusted to the same pH. The large negative peaks observed in the sorbed sample relate to rapid dissolution of manganite (manganite peaks shown in Figure 6-16) after the addition of acidic AO 7 solution. The IR spectrum of adsorbed AO 7 shows slight peak shifts for certain absorption bands but largely a close resemblance to the standard aqueous solution can be observed. The shift observed in the 1507 cm^{-1} peak was inconsistent in repeat experiments.

Changes in the sulfonate group bands have been used to provide important clues about the sorption of AO 7 to a number of mineral surfaces (Stylidi et al., 2003). In the current study, interpretation of these bands is difficult due to the negative absorbance of the manganite peaks. To remedy this, an IR spectrum was collected of a manganite film to which 0.01M HCl had been added. This spectrum, which only shows manganite dissolution was subtracted from the AO 7 spectrum in Figure 6-18. The subtraction result is shown in Figure 6-19. The IR spectrum of the sorbed AO 7 species show slight band shifts compared to that of the aqueous sample. The peak at 1185 cm^{-1} shifts to 1177 cm^{-1} and the 1213 cm^{-1} peak shifts to 1211 cm^{-1} and shows a slight decrease in intensity. These two bands are proposed to represent the asymmetric stretching mode of the SO_3 group (Sperline et al., 1994). In work using diffuse reflectance infrared Fourier transform (DRIFT) spectroscopy to probe sorption of AO 7 on Fe and Ti oxides, major changes have been observed in the symmetric and asymmetric stretching bands of the sulfonate group (Bauer et al., 1999; Bandara et al., 1999a; Bourikas et al., 2005). In these investigations it was observed that the 1185 cm^{-1} band disappeared after the dye had been sorbed onto the mineral surface. Based on this, these workers proposed that the sulfonate group forms an inner-sphere complex with the Ti and Fe metal ions. All the above mentioned studies used DRIFT spectroscopy, a technique which requires reacted samples to be dried prior to analysis. Drying can cause significant changes in the ligand coordination (Hug, 1997; Eggleston et al., 1998; Dowding, 2004) and surface pH (Mortland and Raman, 1968; Dowding et al., 2005), thus it is valuable to obtain sorption data from an aqueous medium, where no drying related artefacts should be present. The IR spectrum of AO 7 sorbed to manganite does not show a relative decrease in intensity of the 1185 cm^{-1} just a shift in peak position (Figure 6-19). Inner-sphere complexation significantly alters the

symmetry of molecules resulting in substantial changes in their IR bands, whereas electrostatic or physio-sorbed species do not show large spectral changes relative to that of the aqueous species (Hug, 1997). The symmetry of the sulfonate group is lowered when the O groups coordinate directly with a metal centre, and it is anticipated that the doubly degenerate vibrations will be split into two (Nakamoto, 1997). Despite shifts observed in some of the bands of sorbed AO 7 in the present study, inner-sphere sorption would be expected to have a more substantial affect on the IR spectrum. Bauer et al. (1999) investigated sorption of AO 7 onto Ti and Zn oxides. These workers observed that the $\upsilon_{as}(SO_3)/\upsilon_s(SO_3)$ peak ratio changed from 0.2 in the IR spectrum of the isolated AO 7 sample to 0.87 in the IR spectrum of the inner-sphere species. For Zn oxide, the difference between the sorbed and isolated IR spectra and the $\upsilon_{as}(SO_3)/\upsilon_s(SO_3)$ ratio was much smaller (0.03), leading them to conclude AO 7 was weakly associated with the Zn oxide surface. Applying this ratio to the current data gives 0.5 for the aqueous species compared with 0.4 for the sorbed AO 7 species (Figure 6-19), which suggests there isn't a great change in relative peak height intensities. From the evidence obtained here it is proposed that the sulfonate group of AO 7 initially sorbs to the manganite surface via a predominantly outer-sphere, electrostatic association rather than through a direct inner-sphere complex as suggested for other oxides in earlier studies.

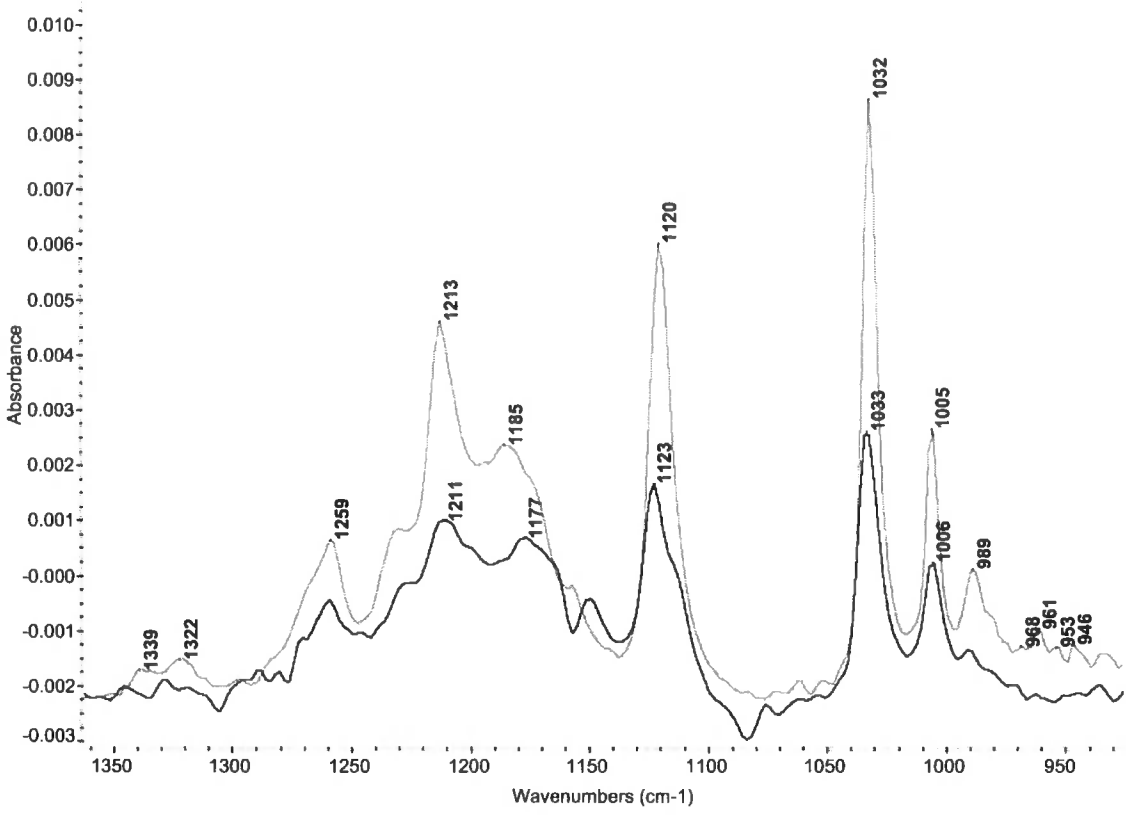

Figure 6-19 IR spectrum of sorbed AO 7 (black) after removing negative manganite dissolutions peaks through subtraction of a manganite blank presented with a 25 mM standard AO 7 solution (grey).

Bauer et al. (1999) proposed that the C=O group of the AO 7 hydrazone tautomer forms an inner-sphere complex with the Ti metal during sorption of AO 7. Evidence for this was given as disappearance of the 1570 cm^{-1} peak, observed in the IR spectrum of the isoloated compound (powdered AO 7), once the dye had sorbed to the surface. The IR spectrum of the aqueous AO 7 species (Figure 6-18), shows no peak at 1570 cm^{-1} thus this peak may only be present in the dehydrated AO 7 powder sample. No conclusive evidence of initial inner-sphere sorption between the C=O group and the manganite surface can be found, although this is the group through which oxidation of the dye is initiated.

The experimental design used in this study is such that only molecules that are sorbed onto the clay surface can be observed, thus it is expected that peak intensity would indicate the degree of dye sorption on the mineral surface. To establish the effect of pH on AO 7 sorption, dye solutions adjusted to pH 2.3, 2.7, 3.0, 3.5, 4.0 and 6.0 were added to manganite clay films

and IR spectra collected. Sorption was observed by comparing the intensity of the peak at 1036 cm^{-1} for the pH adjusted solutions. This peak was chosen because it fell outside the range of the manganite dissolution bands, thus no subtraction was necessary, and the band has been assigned to benzene mode 1 and υ_{as} (SO_3), neither of which are redox reactive or pH sensitive in the chosen range. Figure 6-20 shows the IR spectra collected 1 minute after addition of pH adjusted AO 7 dye solutions to the clay film. Each spectrum represents the average of 64 co-added scans. During data collection it was evident that sorption is rapid as peaks were observed in the initial scans i.e. 10 seconds after dye addition.

Sorption clearly increases as the pH of the added AO 7 solutions decreases (Figure 6-20). Lowering the pH below 4 results in the most dramatic increase in sorption. It has been established, in the pH investigation (Section 6.4.1) and by other workers (Bauer et al., 1999; Bandara et al., 1999a; Bourikas et al., 2005), that the interaction between AO 7 and the Mn oxide surface is largely electrostatic, thus pH dependent sorption is rational. Acid orange 7 is negatively charged in the pH ranged investigated (pK_a = 1). Decreasing the pH will increase the proportion of positively charged sites (PZC =pH 4) on the manganite, thereby increasing the number of AO 7 molecules attracted to the oxide surface and increasing the intensity of the IR peaks. The use of manganite in this study, means precisely the same pH-sorption relationship may not apply to the more complex tailings. The additional mineral phases present in the tailings may result in increased sorption at higher pH due to the non-discrete charge properties of the material. As mentioned earlier this data can only give qualitative information but it provides insight into sorption behaviour between an oxidant and a reductant which is inherently difficult to observe and to the author's knowledge this is one of the first observations of its kind.

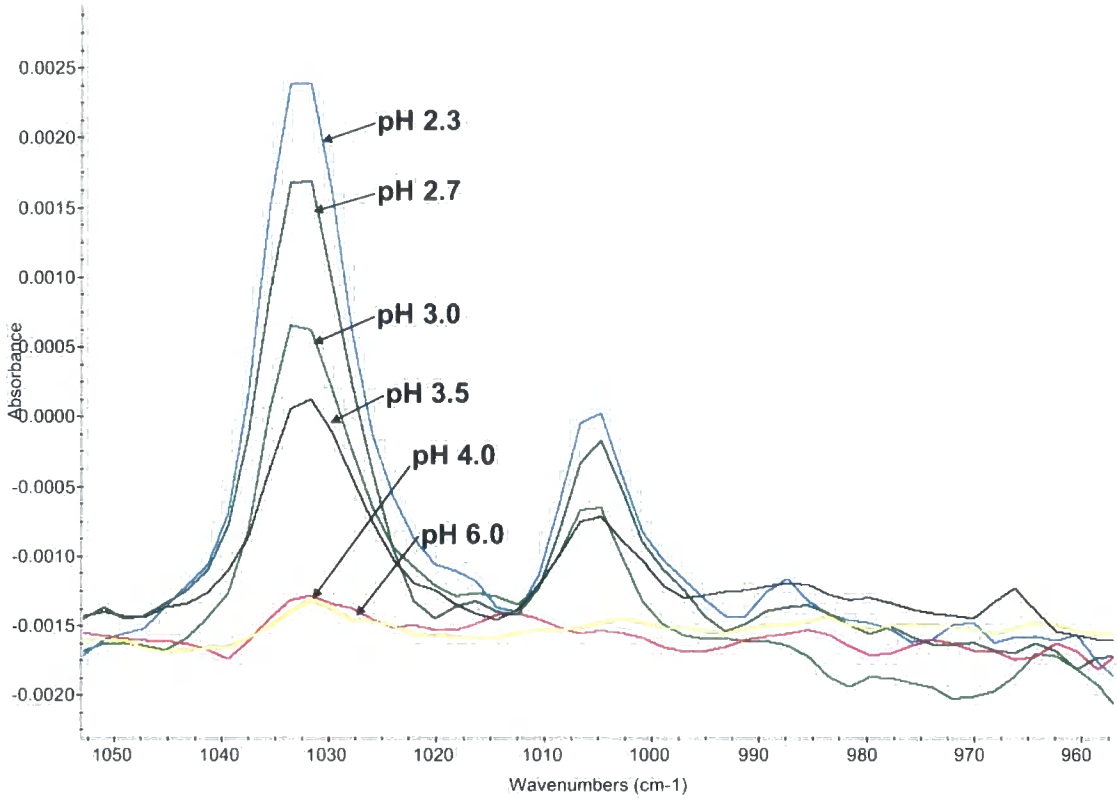

Figure 6-20 IR spectra of pH adjusted AO 7 solutions collected 1 min after injection onto a manganite coated Ge crystal.

6.5.2. Oxidation reactions

To probe the oxidation reaction between AO 7 and the manganite in real time, IR spectra were continually collected over the reaction period. As discussed above the lower pH treatments showed the most intense IR peaks, thus for sensitivity reasons oxidation reactions were conducted at pH 2.7. Figure 6-21 shows a series of spectra collected every minute throughout the duration of the experiment. The peak at 1507 cm^{-1} has either been associated directly with the azo bond (Vinodgopal et al., 1996), a bond sensitive to changes in the azo bond (Vinodgopal et al., 1996), or the bending mode of N-H bond of the hydazone form (Bauer et al., 1999; Zhang et al., 2005; Li et al., 2006), so oxidation would be expected to cause substantial changes to this peak. Thus this region of the IR spectrum will be considered in detail as it is also not subject to the negative manganite dissolution bands.

As established above, sorption of the dye onto the oxide surface occurs rapidly giving rise to the IR spectrum labelled 1 minute (Figure 6-21). Little change occurs in the spectra for the first 7 minutes, apart from a very slight increase in the 1507 cm^{-1} peak intensity. At 8 minutes the peak starts to decrease in intensity and over the following four minutes there is a dramatic decrease in the 1507 cm^{-1} peak and a concomitant increase in a new peak at 1468 cm^{-1}. After 13 minutes the peak at 1468 cm^{-1} reaches a maximum intensity and no further change in spectra was observed during the following 5 hours. The peak at 1213 cm^{-1} shows a similar kinetic trend with a definite lag period between sorption and the initiation of spectral changes. All peaks assigned to AO 7 show a progressive loss in intensity after 8 minutes.

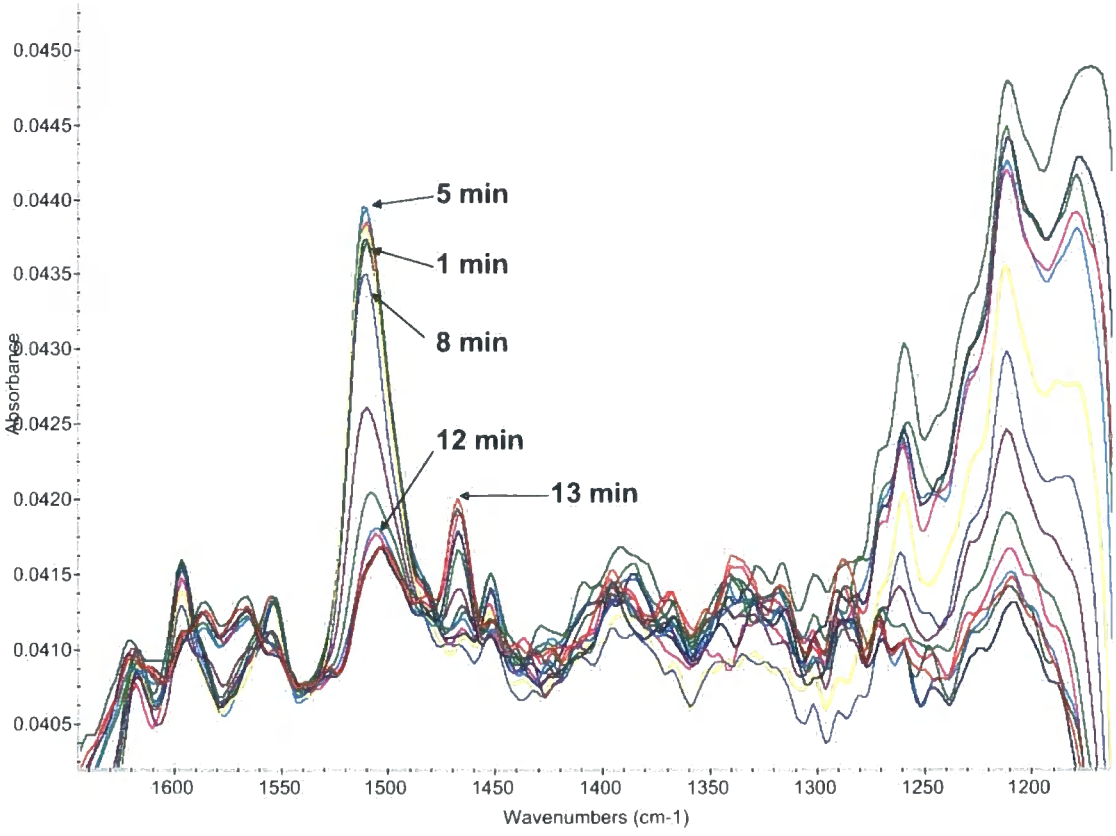

Figure 6-21 Sequence of IR spectra collected during the oxidation of AO 7 by the manganite

In Section 6.4.2 it was shown that NQ and 4HBS are the oxidation products of the Mn tailings mediated oxidation of AO 7. To identify any IR bands associated with these compounds in the 13 minute spectrum (Figure 6-21), standard solutions of NQ and 4HBS were added to a manganite clay film and IR spectra collected. Figure 6-22 shows the 13

minute IR spectrum together with the standard NQ and 4HBS spectra. The new peaks at 1467, 1398, 1366, 1318 and 1285 cm^{-1} coincide directly with that of the NQ standard. The peak at 1503 cm^{-1} coincides with the 4HBS peak, thus it would appear that both these products are present on the manganite surface after 13 minutes.

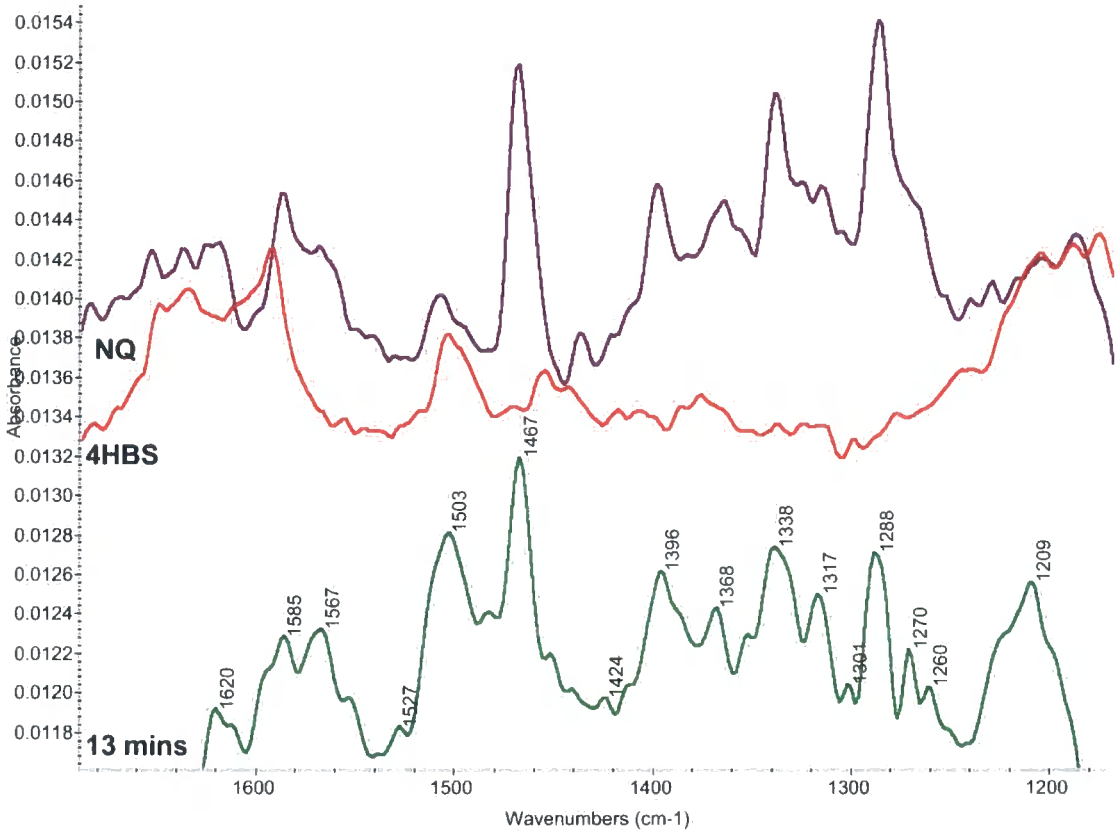

Figure 6-22 IR spectra of AO 7 after 13 min reaction with the manganite (green), presented with IR spectra of naphthoquinone (purple) and 4-hydroxybenzenesulfonate (red) sorbed onto the manganite surface.

The sudden decrease in intensity of the 1507 cm^{-1} peak was accompanied by increased manganite dissolution over the same period (Figure 6-23). Dissolution starts as soon as the acidic solution is added to the manganite film but dissolution would appear to accelerate during the period of substantial change in the AO 7 peaks, as observed in the 1036 cm^{-1} peak (Figure 6-23). To establish if loss of intensity of the AO 7 peaks was purely a result of decreased Mn oxide surface a reacted sample of manganite was rinsed with water before the addition of fresh dye solution. Addition of fresh dye produced exactly the same peaks, at the

same intensity as those observed in the first reaction thus decrease in peak intensity was not a result of diminishing oxide surface. Therefore it was assumed that the removal of AO 7 from the surface was due to a chemical interaction.

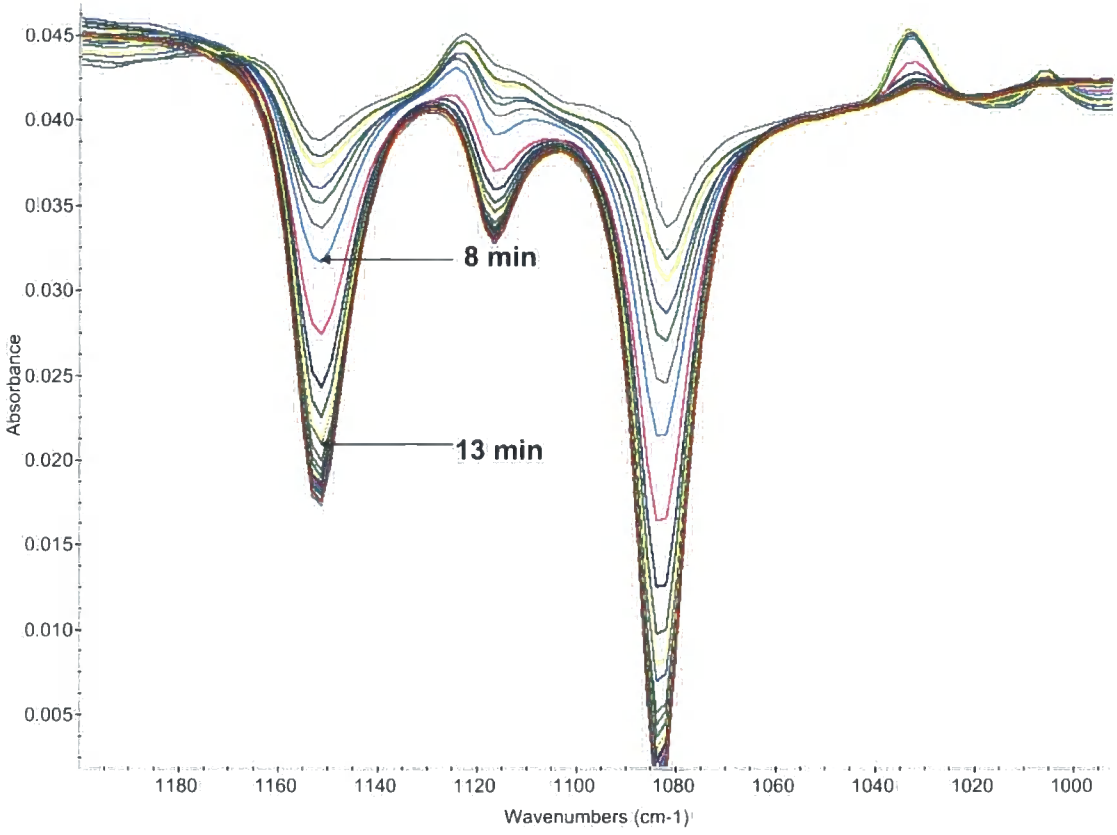

Figure 6-23 IR absorption bands showing manganite dissolution collected during the oxidation of AO 7 by manganite (data collected over 1 hour).

The data from the ATR study provides valuable insight in to the oxidation of AO 7 by Mn oxides. Sorption has been shown to be pH-dependent with enhanced sorption occurring at lower pH. Sorption occurs extremely rapidly at low pH and thus is not likely to be a rate limiting step in the oxidation reaction under acid conditions (pH < 4). The IR data would suggest that sorption of AO 7 onto the manganite surface is outer-sphere, as the IR spectrum of the sorbed species has a strong resemblance to the aqueous species. There is the chance that an inner-sphere complex may occur between the C=O group of the hydrazone tautomer and the Mn oxide but no conclusive evidence for this could be obtained from this data. Two scenarios are presented to explain the time lag observed before the apparent onset of

oxidation of AO 7. One possibility relates to the transfer of the first electron being the rate limiting factor. If this is the case subsequent electron transfer to form 1,2 naphthoquinone is rapid (the formation of the 1468 cm^{-1} peak appeared concomitant with decrease in the 1507 cm^{-1} peak). A concerted two-electron transfer has also been proposed for MnO_2 mediated organic oxidations (Perez-Benito et al., 1996), however, this is not likely to be the case for MnOOH. The second scenario involves rapid electrostatic sorption of the dye to the oxide surface followed by a time lag for the orientation and inner-sphere coordination between the C-OH group and the Mn oxide, after which electron transfer is rapid. Both scenarios would explain the rapid structure breakdown observed in the IR spectra after the 7 minute time lag. The rate limiting factor in the oxidative decolorisation of direct light red F3B dye by Mn oxides was shown to be interface reactions (Liu and Tang, 2000). The ATR evidence presented here supports this observation.

There was no evidence that NQ was removed and replaced by fresh AO 7 on the mineral surface. Analysis of the supernatant after the IR experiment showed only a slight decrease in AO 7 concentration suggesting there was sufficient AO 7 concentration remaining to still react with the Mn oxide. It should be noted that the solution was not stirred and thus all processes were diffusion controlled. Removal of reaction products from the oxide surface could be another rate limiting factor. Electron transfer and removal of breakdown products has been observed to be the rate limiting factors of Mn oxide mediated oxidation of 1,2 naphthodiol (Whelan and Sims, 1995). These workers, however, assumed that inner-sphere electron transfer occurred.

A number of valuable insights have come from this ATR investigation. Firstly, it has been shown that initial sorption of the dye to the Mn oxide is rapid, outer-sphere and pH dependent. Secondly a time lag has been observed from the time when the dye initially sorps onto the surface until the onset of oxidation. This suggests that either some kind of activation energy barrier needs to be overcome or there is a time consuming inner-sphere sorption step prior to electron transfer. Thirdly once initiated, complete oxidation to NQ and 4HBS is virtually instantaneous. Finally it has been shown that removal of products from the surface does not occur readily. All of the above observations support the finding of a fractional rate

order with respect to AO 7 dye concentration. To the author's knowledge this is the first direct observation of surface mediated dye oxidation.

6.6. Mechanistic study of acid yellow 36 oxidation

Acid yellow 36 is an amine containing dye and unlike AO 7 there is little information pertaining to the oxidative decolourisation of the dye. This section addresses the mechanism involved in the decolorisation reaction shown in Section 6.2.

6.6.1. pH treatments

As with AO 7, AY 36 decolorisation reactions were investigated within the pH range 3 to 9. To establish pH-dependent colour and flocculation stability of AY 36 a set of pH adjusted controls were prepared. Figure 6-24 shows UV-visible spectra collected from a series of pH adjusted (pH 3-9) solutions of AY 36. No changes were observed between pH 4 and 9, however, the pH 3 solution showed a slight darkening in colour evident by a slight bathochromic shift in the visible spectrum (Figure 6-24) as well as a slightly lower absorbance at 434 nm (the λ_{max} in the visible region for AY 36). This colour change is related to protonation of the amino group (pKa = 2.3 (Sleiman et al., 2007)). The pH 3 AY 36 solution did not show any evidence of flocculation. Due to the slight change in λ_{max} in the pH 3 solution all treatments were compared to control solutions adjusted to the same pH.

The concentration of AY 36 after reaction with the tailings is plotted as a function of reaction pH (Figure 6-25a). As the pH is lowered there is a substantial decrease in AY 36 concentration, with the most notable change occurring between pH 7 and 5. Below pH 5, AY 36 removal showed a lower response to pH decrease. Release of Mn into solution was measured for a series of pH adjusted blank solutions (no dye added) as well as the reacted dye solutions (Figure 6-25 a). Below pH 7 soluble Mn concentrations in the dye treatments are significantly higher ($P = 0.016$ at pH 5; $P<0.01$ at pH<5) than the blank solutions. This would imply that, below pH 7, Mn dissolution is enhanced by the presence of the dye. It is assumed that the difference in Mn concentration between the blank and the reacted sample represents dye-related Mn release. This Mn concentration is 4-times higher than the original dye concentration, which implies a Mn:Dye reaction-stoichiometry greater than one.

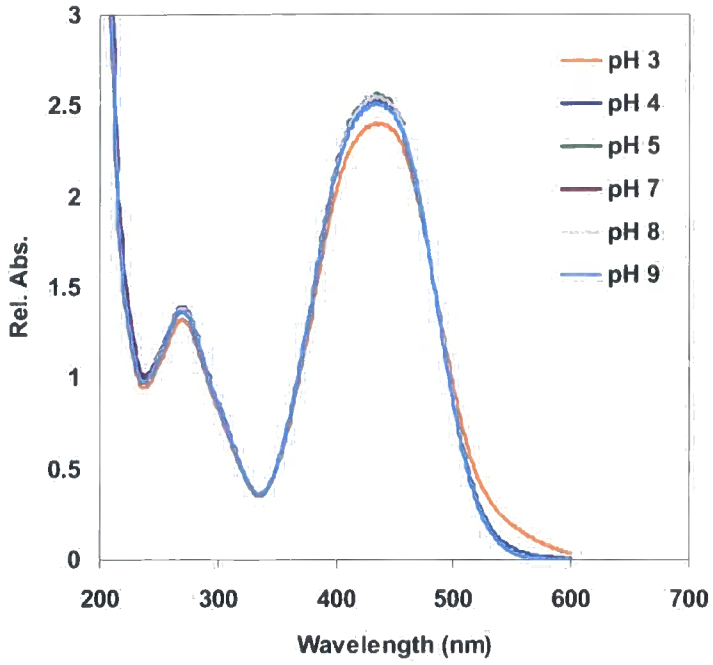

Figure 6-24 UV-visible spectra of 0.14 mM, pH adjusted AY 36 solutions

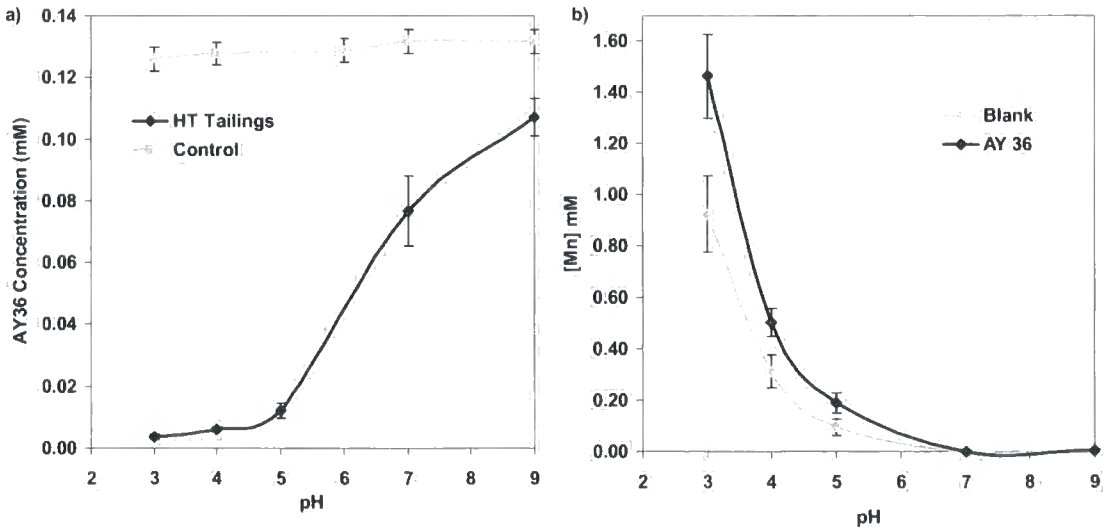

Figure 6-25 Concentration (mM) of a) AY 36 and b) soluble Mn after reacting the HT tailings with the dye at pH 3, 4, 5, 7 and 9 presented with Mn release from pH adjusted blank samples.

The UV-vis spectra measured at each reaction pH are shown in Figure 6-26. For comparison controls at pH 3 and 9 have been included. At pH 9 and 7 a progressive decrease in intensity is observed in the treatments compared to the pH 9 control. At pH 5 and 4 the spectra show a substantial loss in absorbance in the visible region, accompanied by the formation of new peaks at 335, 395 and 245 nm. At pH 3 the peaks at 335 and 395 nm disappear while the peak at 245 nm increases in intensity. The appearance of new peaks concomitant with the decrease in the 434 nm peak would suggest that the dye is reacting with the Mn tailings rather than solely being adsorbed. The disappearance of the 335 and 395 nm peaks at pH 3 would suggest that the compounds having these peaks are further degraded.

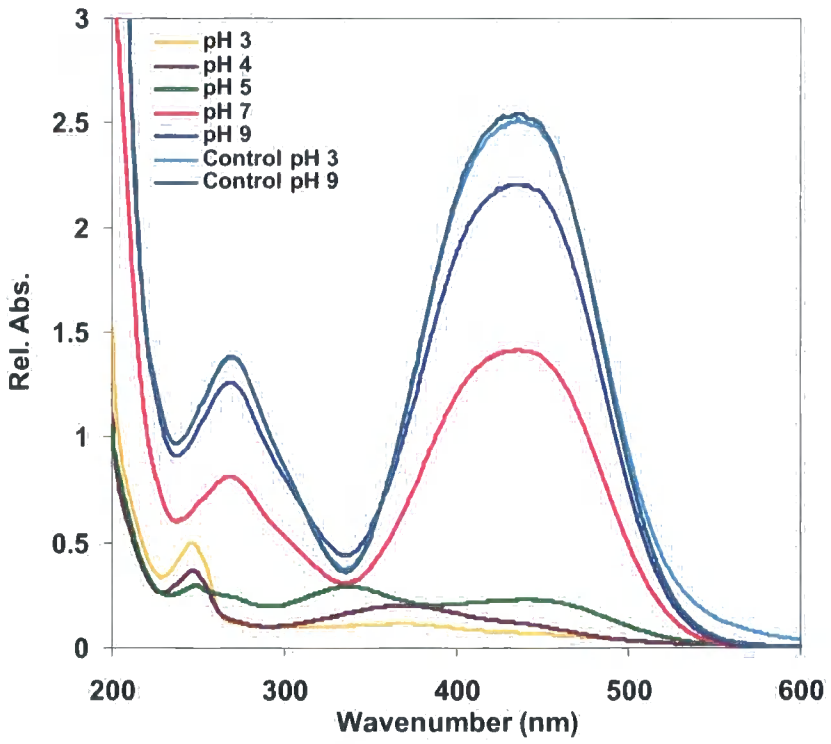

Figure 6-26 UV-visible spectra measured after reaction of the dye with the tailings at pH 3, 4, 5, 7 and 9 for 1 hour presented together with control AY 36 solutions adjusted to pH 3 and pH 9.

The filtered pH-treated samples were analysed with HPLC to obtain a better understanding of intermediate and product formation during the decolorisation reaction. The chromatograms of the samples are shown in Figure 6-27. All chromatograms, including the blank (not shown) show a solvent peak at 3.6 min and a peak at 13 min that corresponds to a phthalate

plasticizer. The peak at 11 min, representing the parent dye compound (λ_{max} : 434 nm) , shows a progressive decrease in intensity down the pH series and is absent from the pH 3 chromatogram. In the pH 9 and 7 treatments a peak at 10 min is evident which has a λ_{max} at 335 nm. The retention times of this peak and the parent dye peak are slightly shorter in the pH 5 sample (9.5 and 10.6 min, respectively) and three additional peaks are present at 9.7, 7.7 and 7.2 min having λ_{max} at 340, 395 and 246 nm, respectively. In the pH 4 treatment the relative intensity of the 9.8 min peak (9.5 min in the pH 5 chromatogram) has decreased, while that of 7.4 min peak (7.2 min in the pH 5 chromatogram) has increased. Finally in the pH 3 sample all peak intensities have decreased while the 7.1 min peak (7.2 min in the pH 5 chromatogram) has increased in intensity. The reaction mechanism for oxidation of this dye is largely unknown so product identification was not possible from the UV spectra.

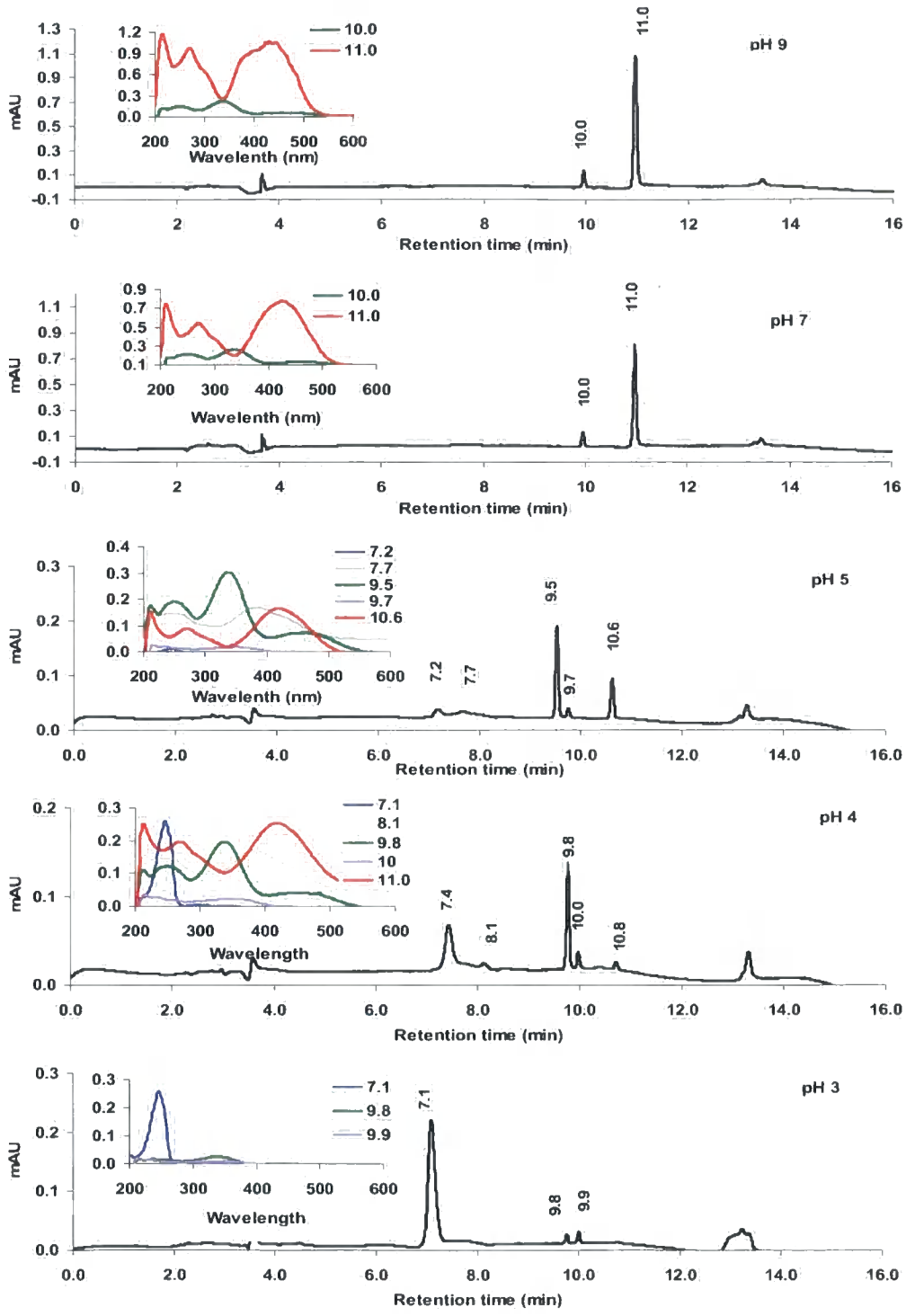

Figure 6-27 Chromatograms of AY 36 solutions after reaction with the tailings at pH 9, 7, 5, 4 and 3 for 1 hour. UV-Vis spectra corresponding to peaks at the various retention times shown in the insets. (Note not all scales are the same)

From this data it would appear that the reaction pH has a pronounced influence on the AY 36 decolorisation reaction and product formation. The role of pH in intermediate product formation will be discussed in the following section, however, from this data it can be established that removal of the parent dye increases with decreasing pH and thus it would appear that decreasing the pH increases oxidation of the dye by the tailings materials. As discussed in Section 6.4.1, lowering the reaction pH has been shown to enhance organic oxidations by Mn oxides, through increased electrostatic attraction, increased redox potential and enhanced removal of Mn^{2+}. Charge behaviour of AY 36 differs to that of AO 7 in that protonation of the N-groups occurs below pH 3 (pK_a 2.3), thus at pH 3 a proportion of the N groups would be protonated, accounting for the darkening of the colour of the pH 3 control (Figure 6-24). However, the most significant pH response in AY 36 oxidation was observed to occur below pH 7 and the response to pH lessened below pH 5, thus it would appear that increasing the positive charge on the dye molecule is not the primary cause of pH-dependent AY 36 oxidation. As discussed for AO 7, the positive charging of the oxide surface may play a role in increasing the dye-mineral contact and therefore oxidation. It is interesting to observe the difference in pH-dependence between the two dyes. Oxidation of AY 36 shows the largest response to pH between pH 7 and 5 (Figure 6-25a) while with AO 7 oxidation responses to pH only occur below pH 5 (Figure 6-5a) and this response is linear with further decreases in pH. If sorption was the only factor influencing oxidation it would be expected that the two dyes would show a similar pH-dependence considering that both dyes are predominantly negatively charged in the experimental range. The increased oxidation of AY 36 below pH 7, which is well above the PZC of the tailings (PZC < 4), may indicate that the pH-dependence of the reaction is not solely related to sorption. It also indicates the oxidation of AY 36 is less dependent on H^+ concentration than AO 7.

6.6.2. Identification of reaction products and proposed reaction mechanism

Identification of reaction products and intermediates formed during the reaction of AY 36 with the tailings was attempted using LC-MS. The molecular ions and ion products are summarized in Table 6-2. The retention times reported for the LC-MS analysis are different for those reported in the HPLC analysis as the samples were run without a buffer, due to

excessive salt crusting on the ion transfer tube. Retention times in the first LC-MS system were not consistent for repeat runs, the reason for this may be related to the fact that the buffer solution had to be omitted. Other workers conducting chromatographic studies of azo dyes have also experienced retention time shifts (Lopez et al., 2004).

Table 6-2 Mass spectra data of AY 36 and degradation products

Compound No.	Retention time (min)	Mode	MS m/z (% relative intensity)	MS^2 m/z (% relative intensity)
I	2.25	ES-	173(100); 113(21); 174(10); 275(10); 369(10)	N/A
II	3.59	ES-	276(100); 286(44); 171(20)	156(100); 215(10); 158(7)
II*	-	ES+	278(100); 198(35); 239(17); 149 (140)	N/A
IV**	4.82	ES-	366(100); 367(20); 540(20); 173(6)	302(100); 156(30); 274(7);
III**	5.76	ES-	366(100); 367(18); 540(10); 708 (7)	156(100); 338(50) 274(45);
V	7.57	ES-	458(100); 459(50); 460(20); 171(15); 173(10)	402(100); 156(60); 338(30); 430(10)
VI	8.01	ES-	352(100)	156(100); 260(15); 324(18)
VII	9.35	ES+	352(100)	275(75), 203(100)

*This compound was identified using the second LC-MS system described in the methods section thus the retention time has not reported

** These samples do not follow in numerical order due to conflicting eluting orders found in the HPLC data (run with buffer) and LC-MS data (run without buffer)

The fragmentation pattern of the parent molecule (compound VI), detected in negative ion mode is shown in Figure 6-28. Fragmentation of AY 36 (m/z = 352) occurs via rearrangement loss of N_2 from the azo group (M^- - 28) which is typical of a number of azo dyes (Holcapek et al., 2007). Further fragmentation involves loss of either the SO_2 (M^--28-64) or diphenylamine (M^- - 28-168) group.

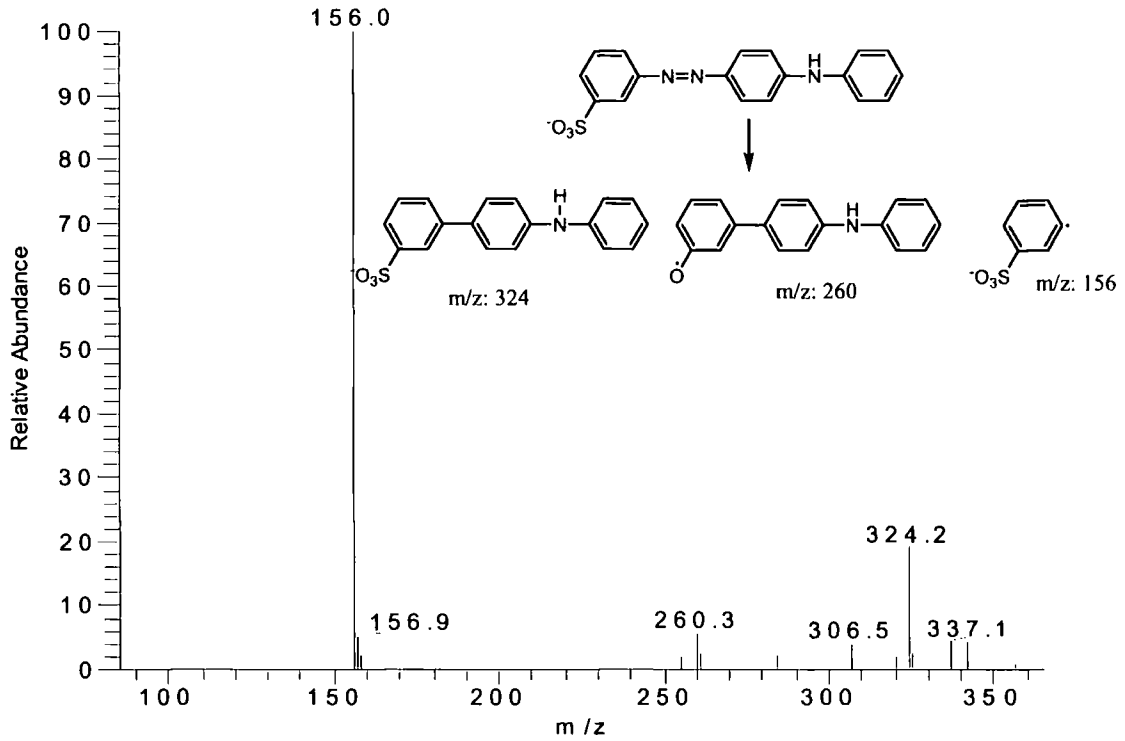

Figure 6-28 Ion products as identified in the MS^2 of the ES- 352 peak, representing the fragmentation pattern of AY 36

A total of six compounds were observed in the negative MS scan mode (Table 6-2) and two in the positive scan mode. In ion negative mode only 2 compounds (I and II) were identified which had m/z values less than the parent compound. Compound I (m/z: 173) was detected in both LC-MS systems, however, the signal was very weak in the first system so no MS^2 could be obtained. Compound II was detected in negative (m/z: 276) and positive ion (m/z: 278) mode. Compounds (III; IV and V) all had m/z ratios higher than the parent compound, which would suggest that alteration, but not necessarily breakdown of the parent compound was occurring. Photo-oxidation of methyl orange has also been shown to generate products with higher molecular weights than the parent dye (Baiocchi et al., 2002). The earlier elution of compounds III, IV and V, compared to the parent molecule, would suggest an increase in the polarity of the altered compounds (Table 6-2). Compounds III and IV appear to be isomers having the same m/z value of 366, but having different retention times, fragmentation patterns and slightly different λ_{max} (Figure 6-29). These isomers eluted in different orders in the HPLC and LC-MS studies, this could be a consequence of buffer omission in the LC-MS

study as mentioned above. The proposed structures for these isomers, as well as the other identified compounds, are given in Scheme 2. It is not possible to state with certainty which isomer corresponds with which UV spectrum (Figure 6-29), but for reasons to be discussed later, compounds III and IV have been assigned the structures in Scheme 2. Compound VII, identified in positive ion mode, has a m/z of 352, and could not be assigned a structure.

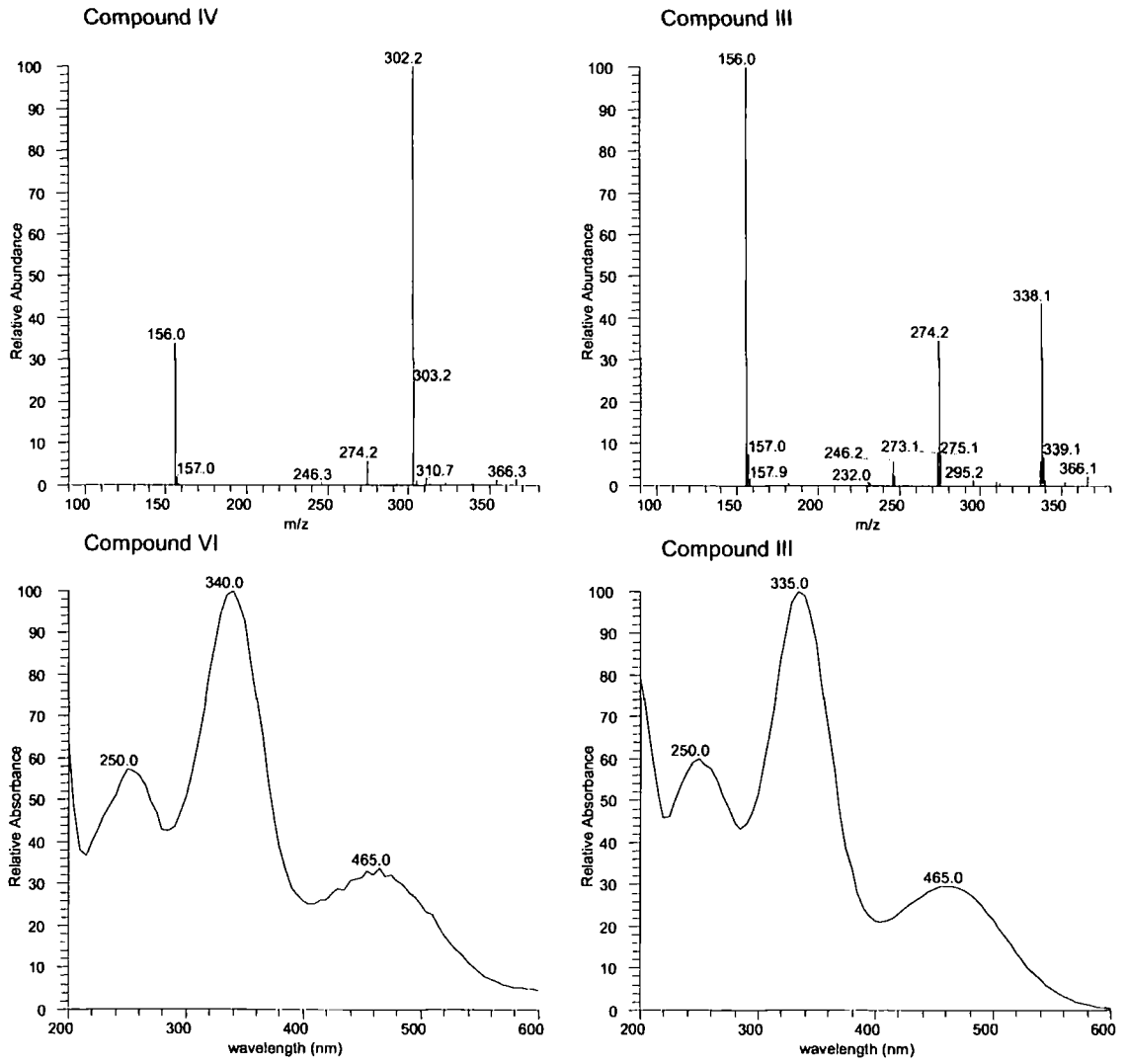

Figure 6-29 MS^2 and UV-vis spectra of m/z 366 isomers (Compounds IV and III) observed in the treated AY 36 solutions

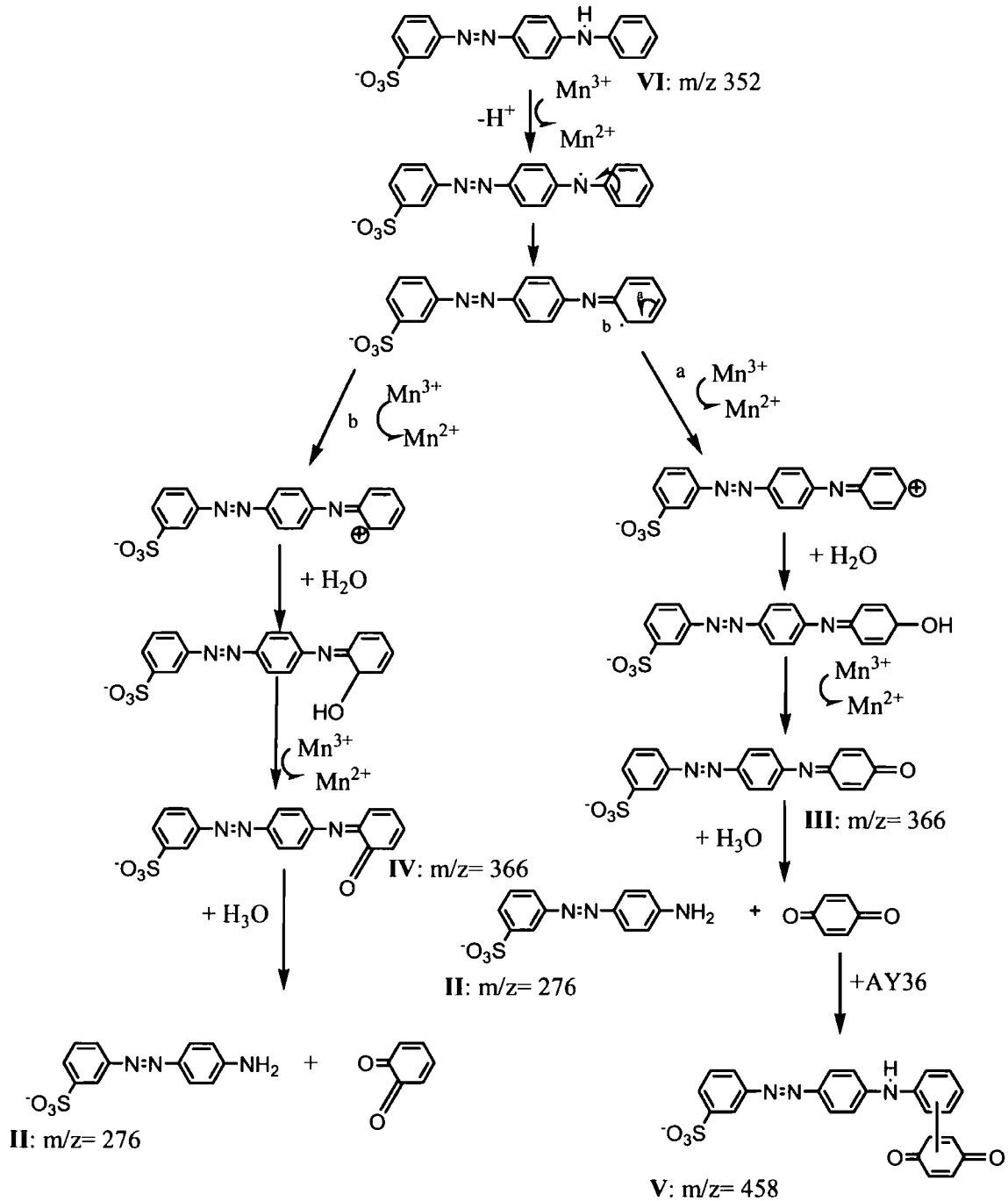

Scheme 2 Proposed reaction mechanism for the oxidation of AY 36 by Mn tailings

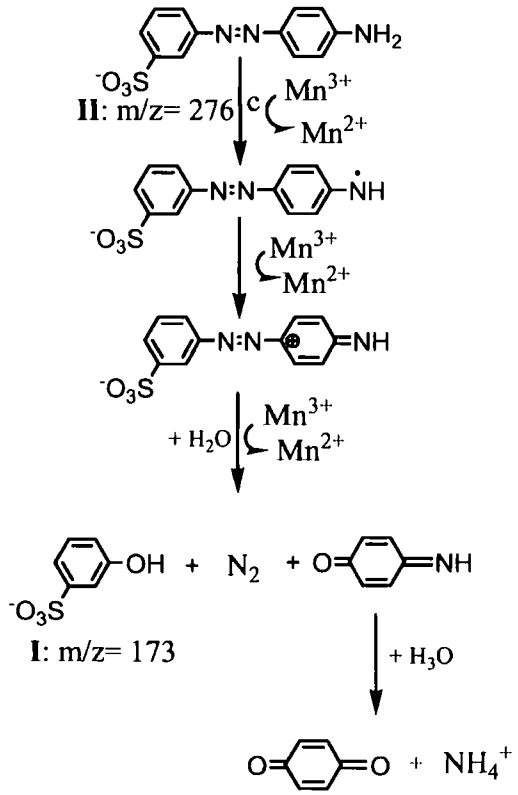

Scheme 2 Continued (reaction pathway c)

Structures were assigned to the compounds identified in the LC-MS study and a reaction mechanism for the oxidation of AY 36 by the Mn tailings has been proposed in Scheme 2. A one electron transfer is initiated on the amine nitrogen, which is expected to have a higher electron density than the azo N atoms (Oakes and Gratton, 1998). Resonance rearrangement and additional one electron transfer results in carbocations forming at either the ortha or para positions of the aromatic ring. These carbocations undergo rapid nucleophilic attack by water molecules to generate hydroxyl groups. Due to the electron withdrawing effect of the sulfonate group, the carbocation and subsequent hydroxylation is expected to occur on the phenyl group attached to the amine group (Sleiman et al., 2007) via pathway a or b (Scheme 2). The phenolic group is further oxidized to generate a quinone moiety in either the ortha or para positions giving rise to the 366 m/z isomers (Compounds III and IV). This reaction pathway is similar to that described for the oxidation of diphenylamine to N-phenyl-p-benzoquinoneimine (Balon et al., 1993).

Hydrolysis of N-phenyl-*p*-benzoquinoneimine to form amine and *p*-benzoquinone has been shown to occur below pH 4 (Balon et al., 1993). Thus it is proposed that compound III undergoes hydrolysis to form compound II (3-('4-anilinoazo)-benzenosulfonic acid) and *p*-benzoquinone when the pH is lowered. Similar hydrolysis of compound IV would generate compound II and *o*-benzoquinone. Neither of these benzoquinone isomers could be identified in the LC-MS investigation but the UV spectrum and retention time of a *p*-benzoquinone standard matched the UV spectrum of the 7.2 min peak of the pH 3 treatment (Figure 6-30). Unfortunately a standard of *o*-benzonquinone could not be obtained, but the λ_{max} for *o*-benzoquinone is reported at 390 nm (Mentasti et al., 1975), thus the 7.2 min product is likely to represent *p*-benzoquinone. Identification of *p*-benzoquinone presents evidence for the proposed reaction mechanism and suggests that pathway a is the most favourable.

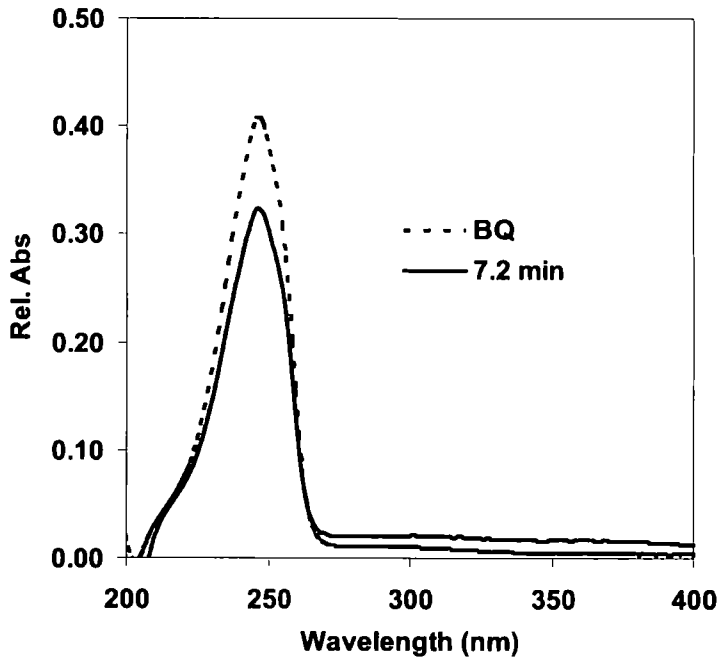

Figure 6-30 UV spectrum of AY 36 degradation product eluting at 7.2 min and a *p*-benzoquinone standard (BQ)

Compound II has a UV spectrum which corresponds to that of the 8.1 peak in the pH 4 chromatogram (Figure 6-27). Compound II is expected to undergo further oxidation, via pathway c (Scheme 2) which will eventually cleave the molecule at the azo group to form

compound I and *p*-benzoquinone. A peak was never observed for compound I in the HPLC data and the highly soluble compound possibly eluted with the solvent peak as observed in the LC-MS analysis.

The formation of *p*-benzoquinone, which itself has a light brown colour, as a final product would explain why 100% decolorisation was not achieved even at pH 3. *p*-Benzoquinone was reacted with the Mn tailings to observe if further breakdown was possible. No decrease in *p*-benzoquinone concentration was observed after reaction with the tailings for 8 days (Appendix E; Figure E-1), thus in terms of water treatment with the tailings *p*-benzoquinone and 3-hydroxybenzenesulfonate can be regarded as the terminal oxidation products. Compound VI, was identified as a polymerisation product of the parent compound and *p*-benzoquinone (Scheme 2). This product was more abundant in the 0.28 mM treatment, which would be expected due to the higher concentration of parent molecule. Similar polymerisation products have been identified to form during enzymetic oxidation of AO 7 and methyl orange (Zille et al., 2005). It is proposed that the parent molecule in these coupling products will eventually undergo oxidation by the tailings. The formation of coupling products may be avoided if contact time between the tailings and dye solution is optimised to reduce the chance of coupling reactions between radicals and unreacted dye molecules.

The mechanism proposed by Sleiman et al. (2007) for the titanium oxide-induced photo-oxidation of AY 36 is different to that described here and involves direct hydroxyl attack on the phenyl group, rather than oxidation of the amine group. According to their study it was proposed that hydroxyl attack on the phenyl group attached to the amine group results in cleavage of the azo bond generating diphenylamine and benzenesulfonate. Hydroquinone was identified and proposed to oxidize to *p*-benzoquinone. Total mineralisation of the azo dye was reported for photo-oxidation. Complete mineralisation was not observed in the current investigation within the pH range investigated.

According to the above mechanism the hydrolysis of the isomers should be independent of the Mn tailings. To verify this a filtered sample of AY 36, reacted with the tailings in a pH 4 acetate buffer for 1 hour, was analysed immediately (within 1 hr) and 24 hours after filtration.

The absence of any Mn(III)-complexes or colloidal Mn oxide in the filtrate was confirmed by a negative tetramethylbenzidine test (Bartlett, 1999). The two chromatograms are presented in Figure 6-31.

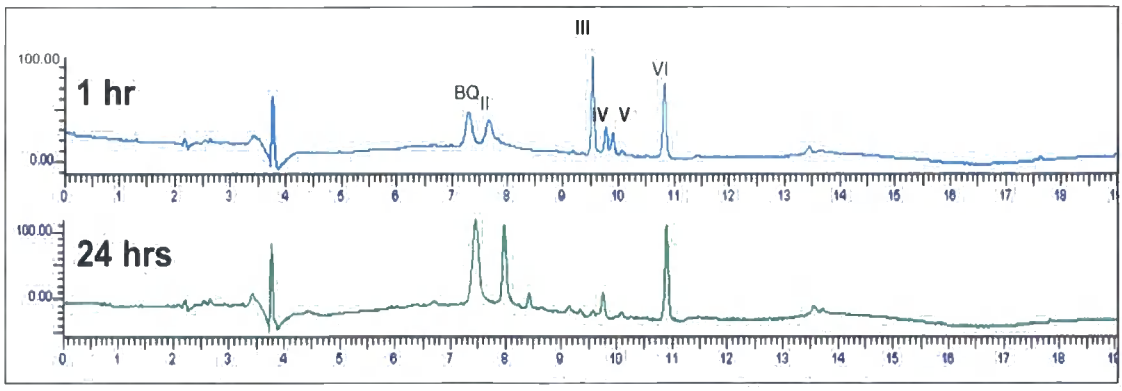

Figure 6-31 Chromatograms of a filtered solution of AY 36, reacted with the tailings for 60 min in a pH 4 buffer, analysed 1 and 24 hrs after the reaction. Compound numbers correspond to products in Table 6-2 (BQ = *p*-benzoquinone)

The chemical composition of the filtrate changes with time, with the *p*-benzoquinone peak increasing while the peaks labeled III and IV, representing the 366 isomers, change in their absolute and relative proportions. From Figure 6-31 it is evident that the earlier eluting isomer (compound III) is initially present in higher proportion than the later eluting isomer (compound IV). The earlier eluting isomer is nearly completely removed after 24 hrs, suggesting that this isomer is the most unstable. Both the position and stability of the carbocation will play a role in determining the most favourable isomer. The carbocation ion is likely to be more stable in the *ortha* position, but steric hindrances may make the *para* isomer the most kinetically favourable. A tentative suggestion is made then that the *para* isomer (compound III) is the most abundant and most reactive isomer. This is supported by the findings that oxidation of diphenylamine has been shown to produce N-phenyl-*p*-benzoquinoneimine (Balon et al., 1993), and the fact that only *p*-benzoquinone was detected as a reaction product. It is assumed that compound IV will undergo the same hydrolysis reaction but concentrations of *o*-benzoquinone may have been below the detection limit. The chromatograms in Figure 6-31 show that the composition of the filtrate changes substantially

over 24 hours in the absence of the Mn tailings which supports the proposal that hydrolysis of the N-phenyl-*p*-benzoquinoneimine group is independent of Mn oxide.

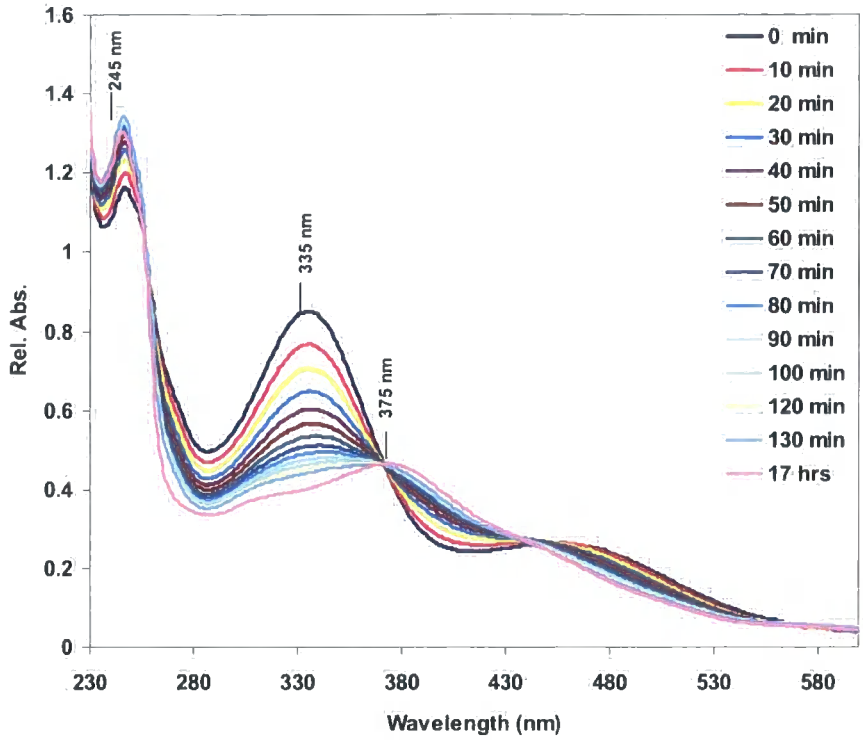

Figure 6-32 UV-vis spectra of a filtered solution of AY 36 after reaction with the Mn tailings for 20 min at pH 3 showing the hydrolysis of the first eluting isomer.

To observe the hydrolysis reaction in real time UV spectra were collected every 10 minutes of a filtered AY 36 solution reacted with the tailings for 20 minutes i.e. just after the 366 isomers had formed (Figure 6-32). The peak at 335 nm represents the first eluting isomer (compound III). This peak shows a progressive decrease and bathochromic shift to 375 nm (Compound II) while the peak at 245 nm (*p*-benzoquinone) progressively increases. The UV-vis spectrum of the filtrate collected 17 hrs later shows only a marginal increase in the 375 nm peak (Figure 6-32), which suggests that the hydrolysis reaction effectively happens within the first 2 hours after the reaction. At this stage the filtered solution was added to fresh Mn tailings and reacted at pH 3 for 24 hours after which it was filtered and a UV-vis spectrum collected (Figure 6-33). The peak at 375 nm decreases after the reaction with the tailings

while the *p*-benzoquinone peak increases. This provides evidence for reaction pathway c and cleavage of the azo bond.

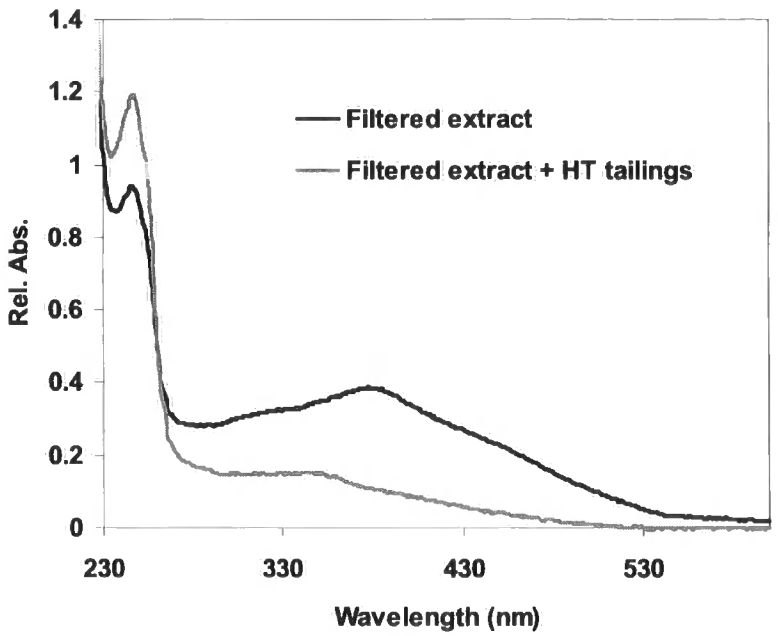

Figure 6-33 UV-vis spectra of hydrolysis products (shown in Figure 6-32) in the supernatant before (Filtered extract) and after reaction with HT tailings (Filtered extract + HT)

6.6.3. Reaction progression

In Section 6.6.2 a reaction mechanism is proposed which involves a series of intermediate products; thus it is important to understand the progression of this reaction in relation to the decolorisation of AY 36. For this purpose sub-samples were abstracted at various time intervals from a reaction vessel in which AY 36 was reacting with the tailings in a pH 4 acetate buffer. Chromatograms of these sub-samples are shown in Figure 6-34 while Figure 6-35 gives percentage decolorisation measured over time. After 0.5 minute of reaction time the AY 36 peak has halved in intensity compared to the control but only a trace amount of compound III can be identified; this correlates with the 45% decolorisation observed (Figure 6-35).

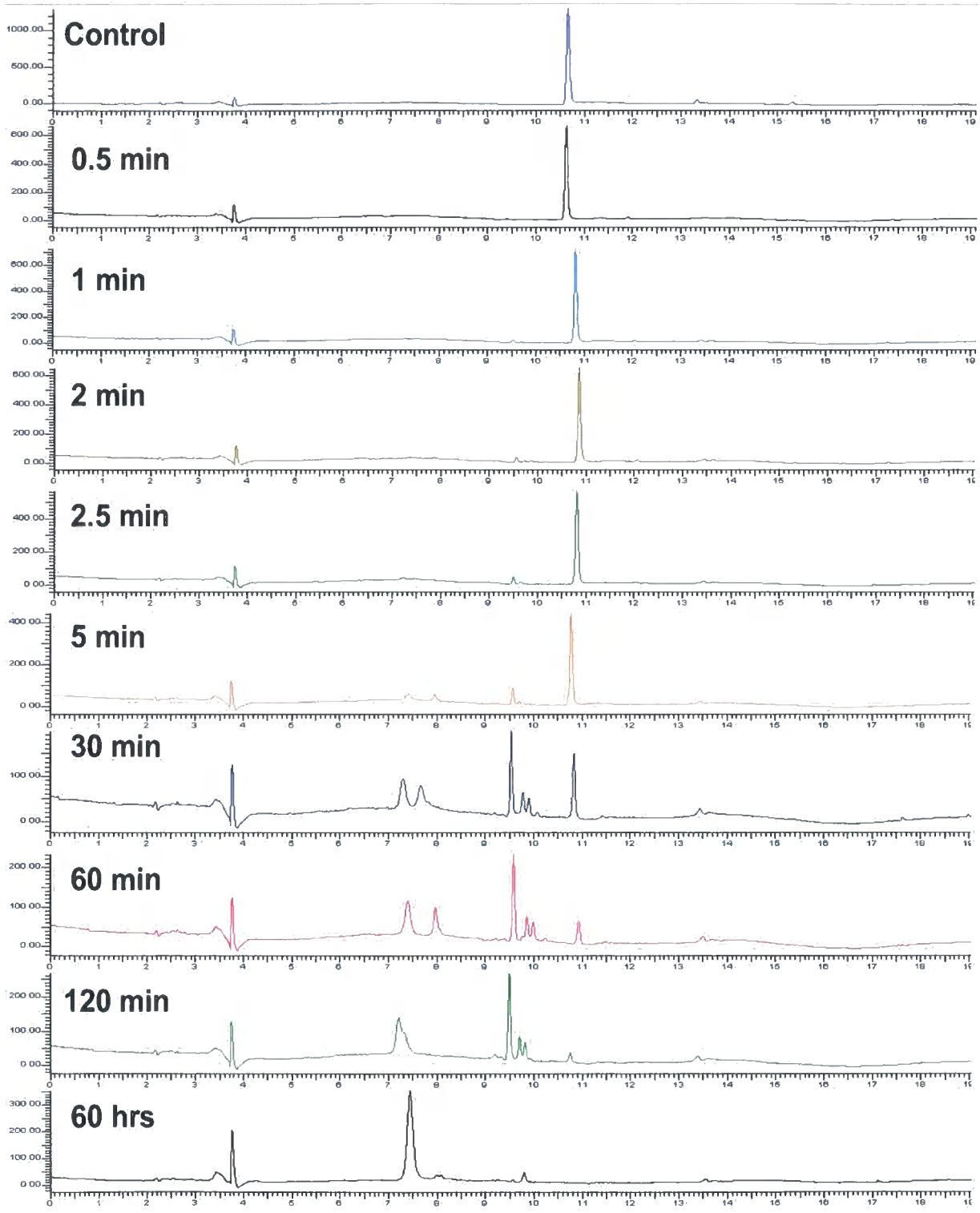

Figure 6-34 Sequence of chromatograms showing chemical composition changes during the reaction of AY 36 with the HT tailings in a pH 4 acetate buffer (Note scales are different).

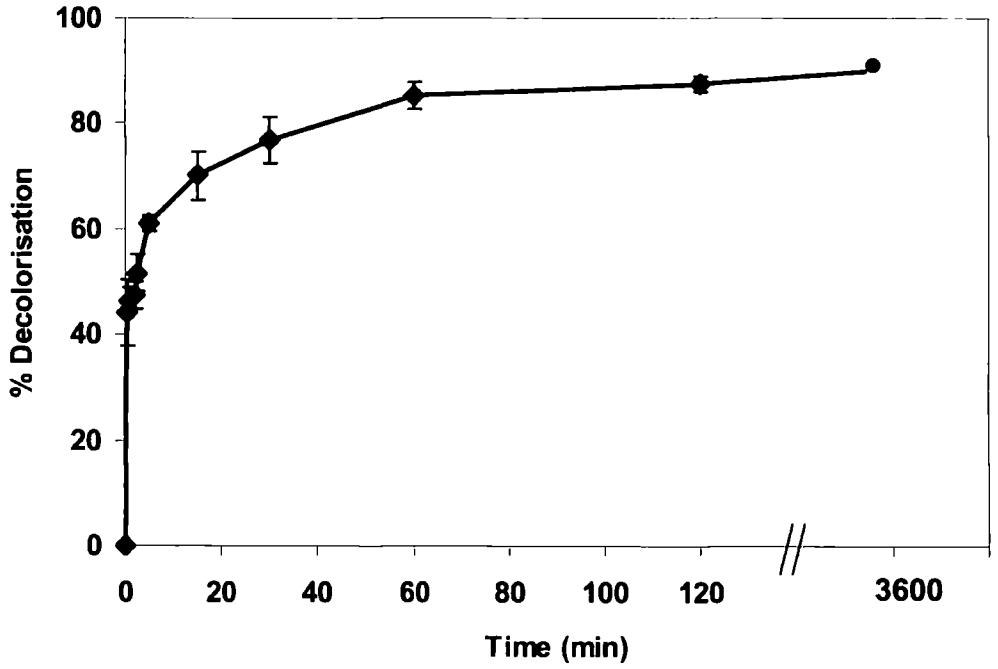

Figure 6-35 Percentage decolorisation of AY 36 as a function of time for samples analysed by HPLC in Figure 6-34

The substantial decrease in dye concentration and decolorisation without an equivalent increase in product peaks would suggest that sorption of the dye onto the tailings surface is responsible for this initial concentration and colour decrease; however, it is also possible that the disparity between AY 36 removal and product formation could relate to the retention of products on the tailing surface. After 1 minute, compound III increases in intensity and after 2 minutes peaks representing compounds III, IV and V can be observed. *p*-Benzoquinone and compound II start appearing after 5 mins. These products increase as the reaction time proceeds while the AY 36 peak concomitantly decreases and decolorisation increases, reaching 86% at 120 min. From this data it is evident that nearly complete decolorisation of the solution coincides with the formation of the 366 isomers even though these compounds still contain an intact azo bond. It would appear that oxidation of the amine group shifts the visible absorbance of the molecule to lower wavelengths. A similar finding was observed for the oxidation of methyl orange where oxidation of the tertiary amine resulted in loss of absorbance in the visible range despite the azo bond staying intact (Oakes and Gratton, 1998).

After 60 hours, most of the intermediate products have disappeared and *p*-benzoquinone dominates the chromatogram (Figure 6-34) (compound I could not be identified from the HPLC study, for reasons discussed in Section 6.6.2) suggesting that the reaction has followed pathway c. Despite complete cleavage of the azo bond, only 91% decolorisation was obtained at 60 hours. This relates to the fact that *p*-benzoquinone itself is light brown in colour.

Dye-related Mn dissolution ($[Mn]_{diss}$) was measured throughout the reaction period and is plotted as a function of percentage AY 36 decolorisation (Figure 6-36). The initial increase in AY 36 decolorisation is not matched by a proportional increase in $[Mn]_{diss}$, which again suggests that this initial colour removal is a result of sorption of the dye onto the tailings surface. After the initial decolorisation increment further colour removal is proportional to increases in $[Mn]_{diss}$, until decolorisation stabilises at 80%. After this the decolorisation gradually increases to 90% while $[Mn]_{diss}$ increases disproportionately. The generation of *p*-benzoquinone probably accounts for the more gradual colour loss after 80% decolorisation. The inset in Figure 6-36 shows AY 36 disappears at the point that the decolorisation curve starts to flatten (0.1 mM $[Mn]_{diss}$). The continual Mn release after the flattening of the curves representing decolorisation and removal of AY 36 may indicate that some colorless intermediates are reacting with Mn tailings. This would add further support to reaction pathway c as it has been shown that the hydrolysis of compounds III and IV (via reaction pathways a and b) is independent of the Mn tailings.

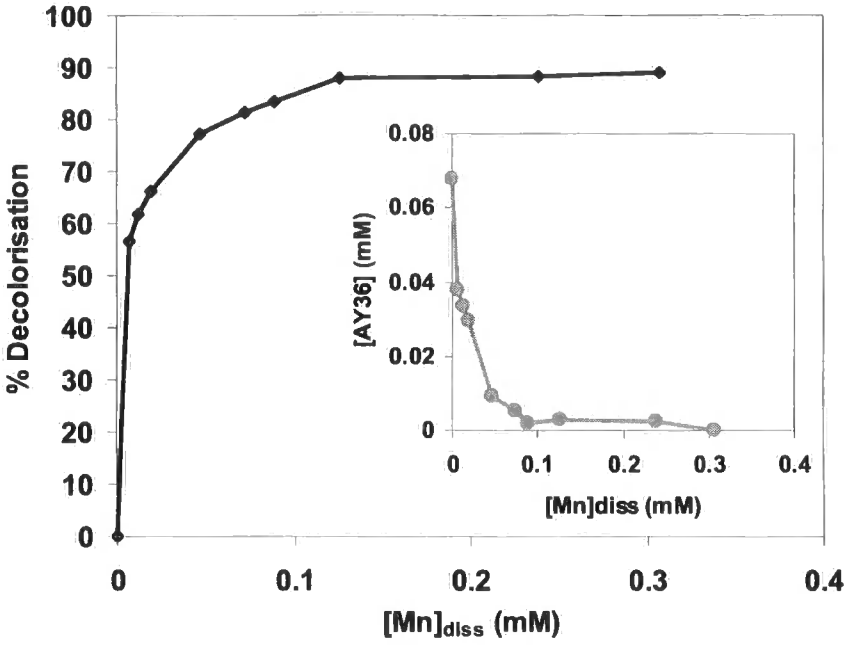

Figure 6-36 Percentage decolorisation of AY 36 plotted against $[Mn]_{diss}$ (Mn released after subtraction from blank) for a AY 36 solution reacted with the tailings (S:L 1:50) in a pH 4 acetate buffer. Inset shows AY 36 concentration vs $[Mn]_{diss}$.

6.6.4. Reaction rates and order

As established in the previous section the reaction between the Mn tailings and AY 36 involves a multi-stage pathway involving successive electron transfers and reactive intermediates. The hydrolysis of the N-phenyl-*p*-benzoquinoneimine moiety is independent of oxidation thus overall reaction kinetics are likely to be complex. Further complications such as the heterogeneity of the tailings and carbonate buffering make kinetic approximations difficult. Thus the initial rates and orders calculated here are tentative and relate to the initial decolorisation reaction i.e. the oxidation of the amine group.

Batch experiments were used to monitor Mn dissolution ($[Mn]_{diss}$) and dye concentration over time (Mn release data provided in Appendix D). Figure 6-37 presents $[Mn]_{diss}$ and AY 36 concentration as a function of time during the reaction of AY 36 with the tailings at pH 4. Nearly 50% dye removal is observed after 30 seconds of reaction time, after which the dye concentration decreases more gradually (Figure 6-37a). The dissolution of Mn, on the other

hand, shows a more linear increase over the initial 5 minutes (Figure 6-37b). As mentioned in section 6.6.3 the disparity between the decrease in dye concentration and $[Mn]_{diss}$ would suggest that sorption may be responsible for the initial sharp decrease in dye concentration. As mentioned in section 6.4.3 sorption data is not easily obtainable for Mn oxide mediated oxidation reactions, thus only $[Mn]_{diss}$ was considered for rate calculations.

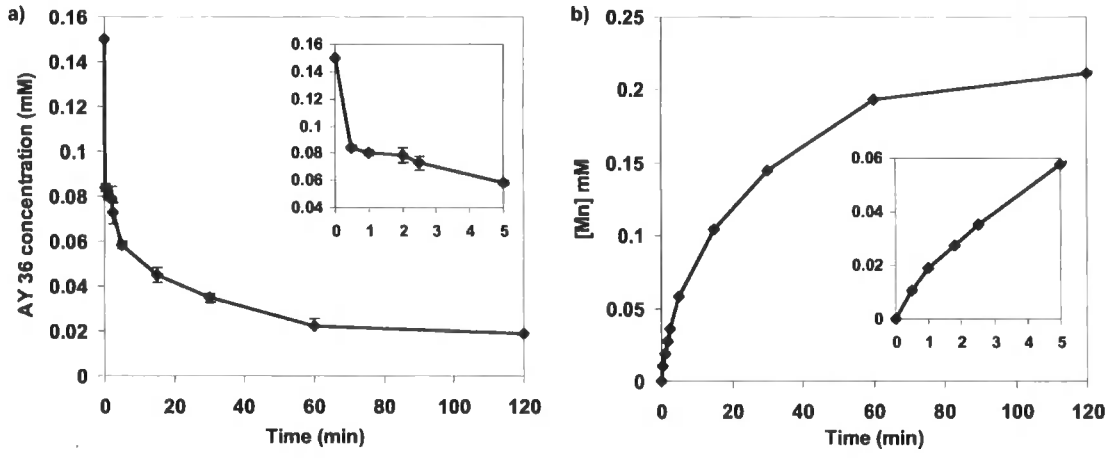

Figure 6-37 Plots of a) AY 36 concentration and b) $[Mn]_{diss}$ as a function of time. Initial dye concentration = 0.14 mM, [SA] = 48 $m^2.L^{-1}$, pH 4. Insets display enlarged scale over the initial sampling interval.

Rate order was determined using the initial rate method (Lasaga, 1981). The rate order with respect to pH was determined at pH 4, 5 and 6 while keeping other reaction conditions ([AY 36] and [SA]) constant. This pH range was chosen as textile effluents containing acid dyes are usually discharged in an organic acid medium, buffered around this pH range. The pH of the reaction appears to have a large influence on reaction rate with the initial rate (normalized to surface area) at pH 4 determined to be 2.5 x 10^{-5} $mol.s^{-1}.m^{-2}$ while at pH 6 the rate is an order of magnitude lower at 1.0 x 10^{-6} mol. $s^{-1}.m^{-2}$. The order with respect to pH is 0.7 ± 0.003 (significantly different to 1 at a confidence level of 5% (t = 156; f = 2)) and appears not to change within the experimental range (Figure 6-38). Similar fractional rate orders for pH have been reported for the oxidation of aromatic amines (Laha and Luthy, 1990) and other organic compounds oxidised by Mn oxides (Zhang and Huang, 2003). The strong dependence of the reaction rate on pH can be a result of increased sorption of the dye to the mineral surface (via electrostatic attraction), or enhanced electron transfer. Protons are required for

the reduction of Mn oxides and the release of Mn^{2+} ions from the mineral lattice. All of these factors are likely to influence the reaction rate.

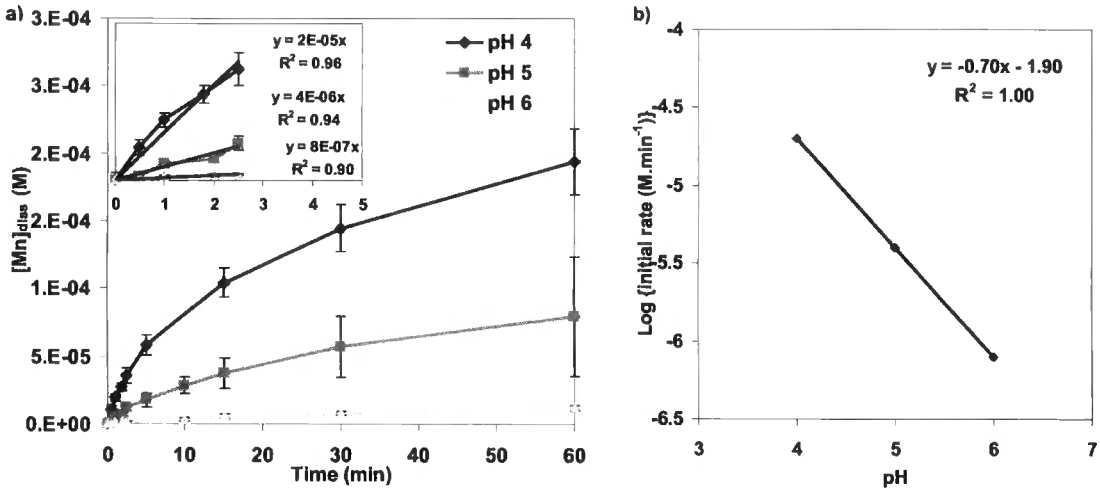

Figure 6-38 Plots of a) $[Mn]_{diss}$ (M) as a function of time at pH 4, 5 and 6 with inset showing initial rate plots for the three curves and b) log(initial rate) vs pH for the oxidation of AY 36

Figure 6-39a shows $[Mn]_{diss}$ as a function of time and the initial rate for three surface area concentrations at constant dye concentration and pH. The ln (initial rate) vs ln[SA] plot given in Figure 6-39b is linear (R^2>0.95) with a slope of 0.8 ± 0.17 (not significantly different to 1; at a 5% confidence level (t = 1.63; f=2)). The y-intercept, converted to seconds (3.7 x 10^{-4} s^{-1}) gives the pseudo-rate constant k' with respect to surface area concentration. This would indicate a pseudo-first-order rate dependence of [SA]. This is in agreement with the AO 7 observations (Section 6.4.3) and other Mn oxide mediated organic oxidation investigations (Zhang and Huang, 2003; Khan et al., 2004; Kumar and Khan, 2005), and it seems sensible that increasing the surface area will increase the number of reactive sites available for reaction with the organic reductant, therefore increasing the reaction rate. The pseudo first order rate constant with respect to surface area for the reaction of AY 36 is (1.7 x 10^{-4} s^{-1}) substantially higher than that of AO 7 under the same reaction conditions (1.8 x $10^{-6}s^{-1}$) suggesting the initial oxidation of AY 36 is inherently faster than AO 7.

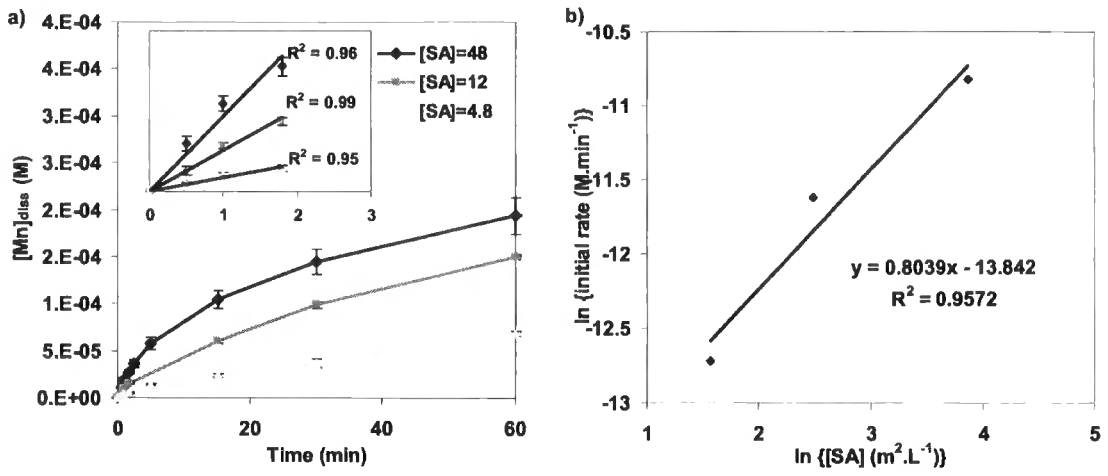

Figure 6-39 Plots of a) $[Mn]_{diss}$ (M) as a function of time for three surface area concentrations ([SA]) with inset showing initial rate plots for the three curves and b) ln(initial rate) vs ln[SA] for AY 36 oxidation

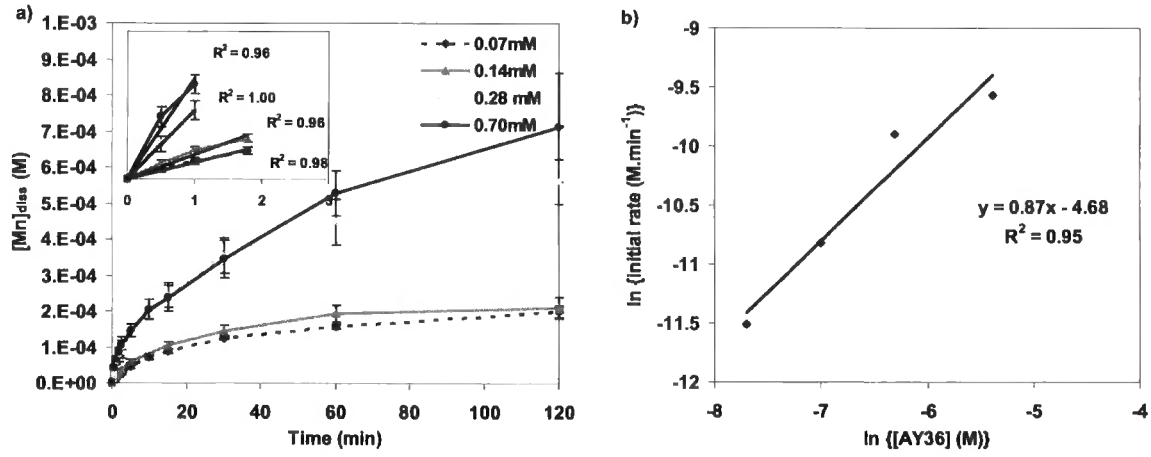

Figure 6-40 Plots of a) $[Mn]_{diss}$ (M) as a function of time for three AY 36 concentrations ([AY 36]) with inset showing initial rate plots for the three curves and b) ln(initial rate) vs ln[AY 36] for AY 36 oxidation

Figure 6-40a shows $[Mn]_{diss}$ as a function of time and the initial rate for three dye concentrations reacted at constant [SA] and pH. The linear (R^2>0.95) ln (initial rate) vs ln [AY 36] plot, with a slope of 0.9 ±0.15 (not significantly different to 1 at a confidence level of 5% (t = 1.2; f = 4)) (Figure 6-40b), suggests that the reaction, unlike AO 7, has a pseudo-first-order dependence on dye concentration. This infers that surface chemical reactions are not as rate limiting for AY 36 as for AO 7.

6.7. Factors influencing oxidative decolorisation of AY 36 and AO 7

Since textile effluents are usually complex mixtures of dyes, organic acids and fixing agents (European Commission, 2003) the effect of these auxiliary chemicals as well as other environmental parameters, such as light, on the oxidative breakdown of dyes was established.

6.7.1. The effect of light on decolorisation reactions

As many redox reactions are affected by light the influence of natural laboratory light (fluorescent tubes) on the dye oxidation reactions was established. The decolorisation reactions were carried out in the presence and absence of light (laboratory) for both AY 36 and AO 7. The data is shown in Figure 6-41. There was no significant difference observed for AY 36 and AO 7 decolorisation reactions conducted under laboratory light and dark conditions. The experiment was repeated under UV radiation, again no difference in decolorisation for either dye was observed (Appendix E: Figure E-2). Liu and Tang (2000) observed enhanced oxidation of 'direct light red' by a natural Mn(IV) oxide when the reaction was conducted under illuminated conditions. These authors suggested this could be a consequence of increasing the rate of electrons excited to the valence band, thereby increasing the reactivity of the oxide. Oxidation of the dyes by the tailings was unaffected by light, which may be a result of the domination of Mn(III) oxides which are not expected to experience such valence band excitations. Additionally the mixed slurry is dark due to the presence of the oxide thus light penetration is limited.

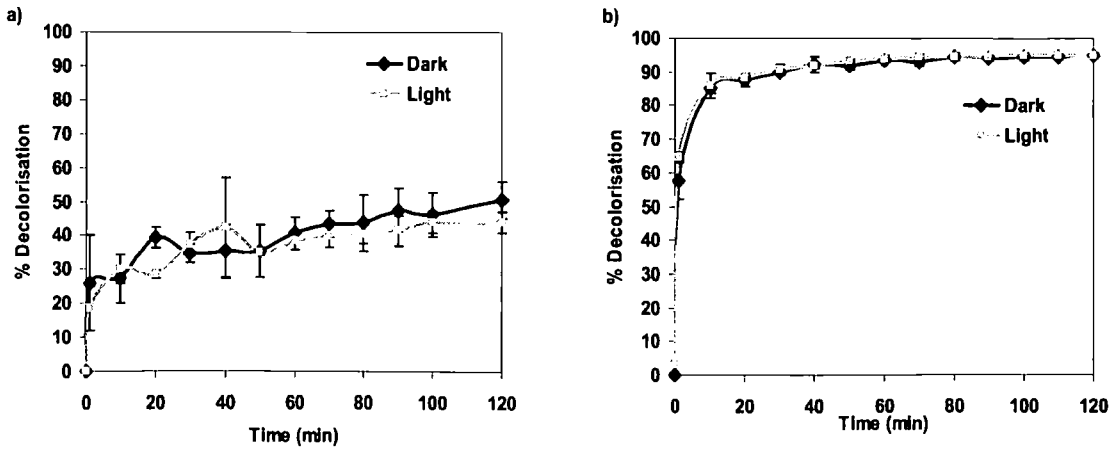

Figure 6-41 Percentage decolorisation at pH 4 as a function of time under light and dark reaction conditions for a) AO 7 and b) AY 36.

6.7.2. The effect of acetate buffer strength

Organic buffers, such as acetate, are commonly present in industrial dye effluent and may interfere with the reaction between the acid dye and the Mn oxide surface by changing the solution pH, blocking reactive surface sites and forming Mn-complexes. To establish the effect of acetate buffer concentration on the decoloristion of AO 7 and AY 36, the dyes were reacted with the tailings in pH 4 acetate buffers of varying strengths. The strong alkali buffering of the tailings resulted in pH drift in the lower buffer concentrations. The final pH was 4.5, 4.3 and 4.0 for the 100, 200 and 500 mM buffer solutions, respectively. To establish the effect of buffer concentration without the complications of pH drift, purchased Mn_2O_3 was also included in the reactions. The pH of the acetate buffers varied no more than ±0.04 units after addition of the synthetic Mn_2O_3. For comparison the dyes were reacted with the HT tailings and purchased Mn_2O_3 in DI, the pH of these samples in DI was 9.0 and 5.0, respectively. The results are given in Figure 6-42.

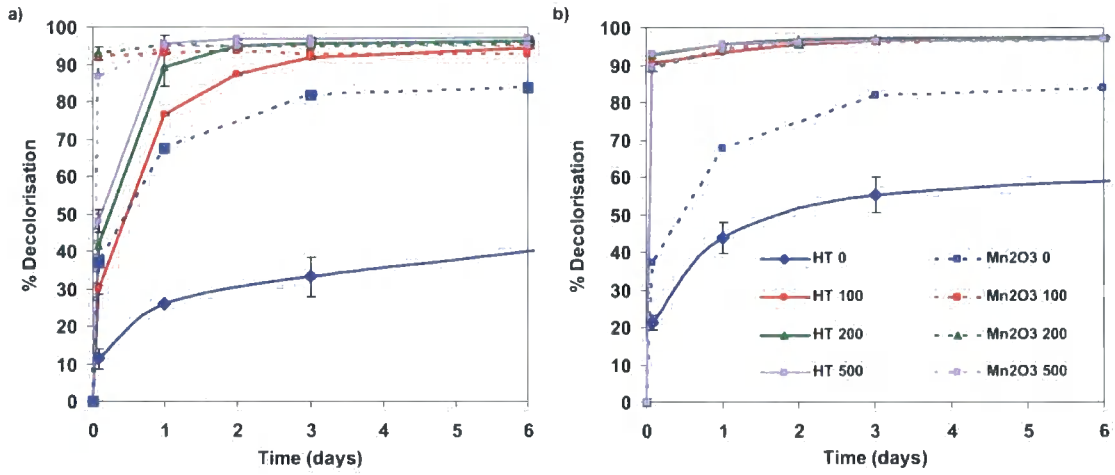

Figure 6-42 Percentage decolouration of a) AO 7 and b) AY 36 reacted with the HT tailings and purchased Mn_2O_3 (dashed lines) using a range (0, 100, 200 and 500 mM) of pH 4 acetate buffer concentrations (S:L 1:20).

The reaction of AO 7 with the tailings is notably affected by the acetate buffer concentration, with decolorisation being lowest for the unbuffered treatment and increasing with increasing

buffer strength (Figure 6-42a) over the measured time period. Even after 45 days the unbuffered AO 7 solution had only achieved 74% decolourisation (data not shown). The AO 7 decolorisation by the purchased Mn_2O_3 would appear less affected by acetate concentration with 89% decoloristion obtained within 2 hours of reaction for all acetate concentrations. In the unbuffered solutions (i.e. in DI) the Mn_2O_3 sample obtained a higher degree of colour removal than the unbuffered tailings sample, however, this is likely to be due to the differing reaction pH in these two samples (pH 5.0 and 9.0, respectively).

Decolourisation of AY 36 is lowest in the unbuffered solution and increases substantially in the buffered solutions (Figure 6-42b). There was little difference between the buffer concentrations with 90% AY 36 colour removal observed within 2 hours for all acetate concentrations in both the tailings and the Mn_2O_3 samples. As with AO 7 the unbuffered Mn_2O_3 sample showed higher colour removal efficiency than the unbuffered tailings sample, which is likely to result from the difference in reaction pH. This data suggests that the buffer strength indirectly influences the decolorisation reactions by regulating the pH. As shown in section 6.4.1, AO 7 oxidation is more sensitive to pH changes below pH 5 than AY 36, which would explain the correlation between buffer strength and decolorisation of AO 7. The presence of any Mn(III)-acetate complexes was discounted on the basis of a negative tetramethylbenzidine test (Bartlett, 1999).

From this data it would appear that buffer concentration has little direct effect on oxidation capacity of Mn_2O_3 or the tailings but pH drift in the lower concentration buffers, slightly reduces the decolourisation rate of AO 7 reacted with the tailings. Continual addition of fresh buffer, as would occur in a reactor, would reduce the pH as the carbonate fraction of the tailings is gradually exhausted. This issue is discussed later in this section.

6.7.3. The effect of salt type and concentration

The effect of salt type and concentration, on the oxidative dye decolorisation, was investigated with and without an acetate buffer. In the absence of the acetate buffer no pH adjustments were made. Figure 6-43 shows the decolorisation of a series of 0.14 mM AO 7 and AY 36 solutions containing 0, 30 and 100 mM Na_2SO_4, that were reacted with the tailings materials (HT) and quartz powder. Quartz treatments were included to observe any

salt induced changes on an 'inert' surface. Control dye solutions containing the same concentration of salt used in the experiment were prepared to establish if any salt-induced flocculation occurred. These solutions remained stable for the duration of the reaction period.

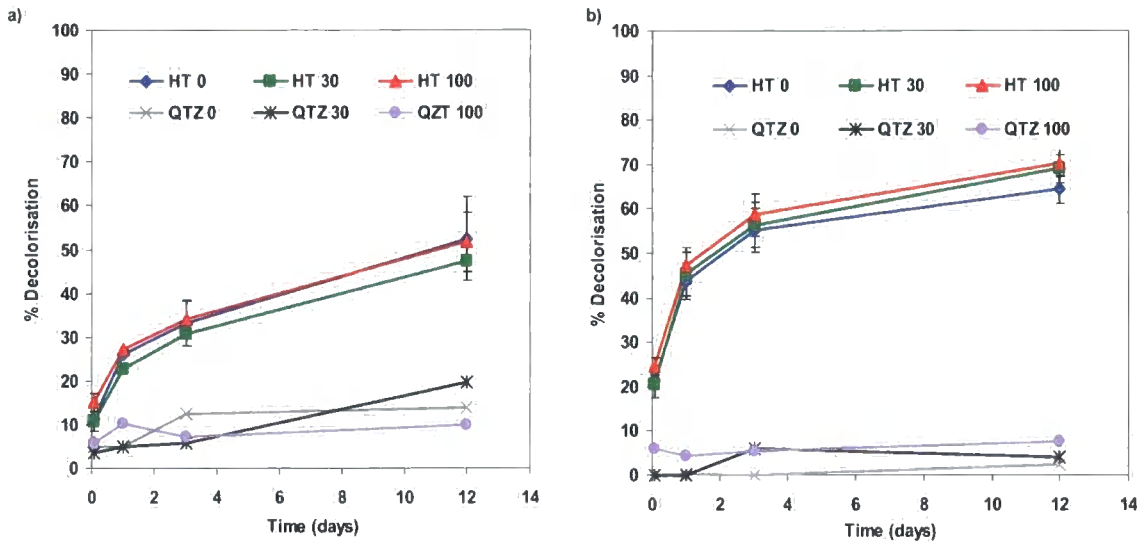

Figure 6-43 Percentage decolorisation of a) AO 7 and b) AY 36 reacted with the HT tailings (HT) in 0, 30 and 100 mM Na_2SO_4 solutions. Quartz (QTZ) samples where run as a controls.

In the absence of an acetate buffer Na_2SO_4 had little effect on the oxidative decolorisation reactions between the tailings and the two dyes (Figure 6-43). The quartz samples showed a slight increase in decolorisation over time and the quartz powder attained the yellow and orange colours of the two dyes over the reaction period. This would suggest that a certain amount of dye was adsorbing to the quartz surface, but the decolorisation in the tailings treatments was substantially higher.

To establish salt effects in the presence of an acetate buffer 100 mM NaCl and Na_2SO_4 were added to acetate buffered dye solutions.

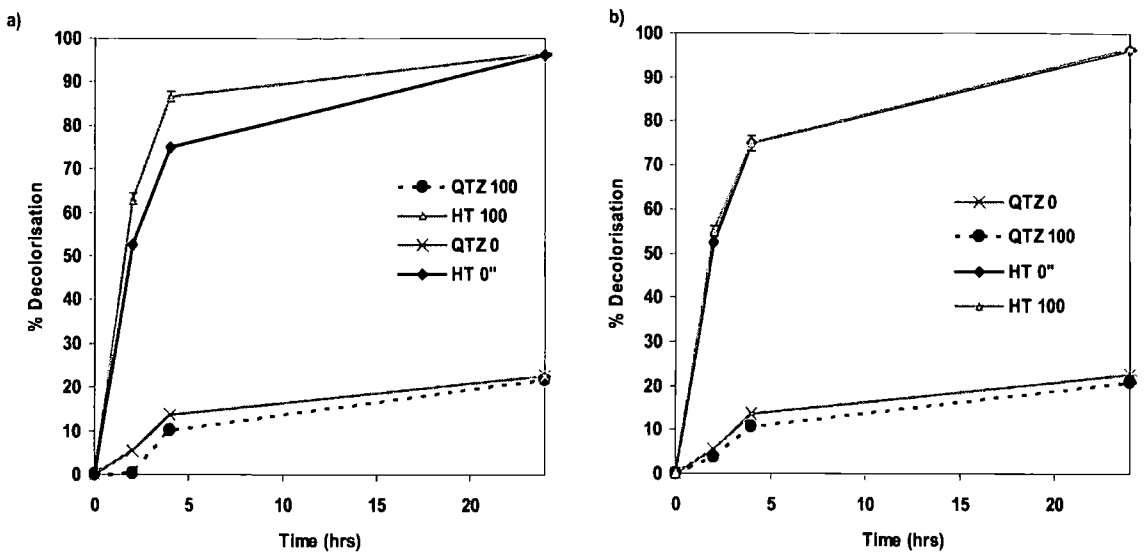

Figure 6-44 Percentage decolorisation of AO 7 reacted with the HT tailings (HT) and quartz (QTZ) in a 0.2 M, pH 4 acetate buffer containing no salt (0) and 100 mM (100) a) Na_2SO_4 and b) NaCl. Certain error bars maybe smaller than symbols.

Figure 6-44 shows the percentage decolorisation of AO 7 as a function of time in the presence and absence of Na_2SO_4 and NaCl. Addition of Na_2SO_4 significantly ($P = 0.0002$) increases the initial (< 4 hours) decolorisation of AO 7, however, after 24 hours of reaction there was no difference in decolorisation between the samples with and without Na_2SO_4. Increasing the concentration of NaCl had no significant influence on the initial or final decolorisation compared to the reaction in deionised water (Figure 6-44b). Both quartz controls showed a small amount of decolorisation over time, which again is likely to be a result of sorption.

The same experiment was repeated for AY 36, however, the clay phase of the Mn tailings became highly dispersed in the Na_2SO_4 treatment and even with filtration a clear supernatant could not be obtained. The turbidity persisted right through the 48 hour reaction period making decolorisation difficult to measure. Addition of NaCl did not have the same effect on the turbidity and no difference could be observed in AY 36 decolorisation between the salt treatment and the acetate buffer containing no salt (Appendix E; Figure E-3).

The initial decolorisation of AO 7 (after 2 hours reaction time) was established as a function of Na_2SO_4 and NaCl concentration (Figure 6-45). Due to the dispersion of AY 36 only AO 7 was considered. Increasing the Na_2SO_4 concentration above 50 mM had a positive effect on the initial decolorisation of AO 7, while no correlation could be observed in the NaCl treatments .

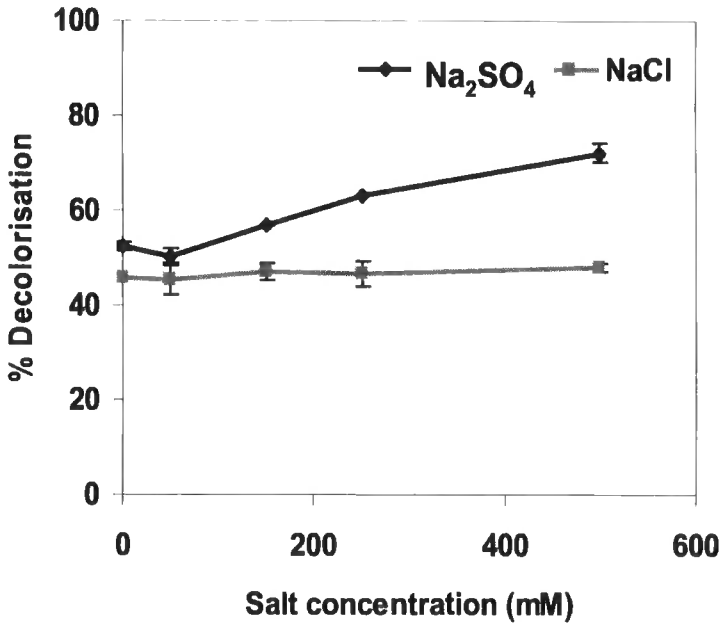

Figure 6-45 Percentage decolorisation of AO 7 as a function of salt concentration after 2 hrs reaction with the tailings

From this data it would appear that in the absence of a buffer (pH 9) Na_2SO_4 has little effect on dye decolorisation, but in the presence of a buffer (pH 4) the salt has a positive effect on decolorisation. Sodium chloride on the other hand had no significant influence in either scenario. Interestingly decolorisation via ozonation is also influenced by salt type, with the addition of both NaCl and Na_2SO_4 increasing decolorisation time, but conversely the effect is more pronounced for NaCl (Muthukumar and Selvakumar, 2004).

The effect of electrolyte on dye sorption and oxidation has been studied by a number of workers (Bandara et al., 1999a; Liu and Qu, 2002; Ge and Qu, 2003). Bandara et al. (1999a) observed suppression of AO 7 sorption on goethite surfaces in the presence of sulphate ions

and suggested that this was due to competition of sulphate ions for sorption sites on the oxide surface. The same conclusion was drawn for the observed suppressed sorption of acid red B on a $MnO\text{-}Fe_2O_3$ oxide (Wu et al., 2005). These workers used this observation to add evidence to their proposal of an inner-sphere sorption of the sulfonate group to the metal centre. Anions such as Cl^-, NO_3^- and SO_4^{2-} suppressed acid dye decolorisation by Mn oxides (Ge and Qu, 2003), even at very low concentrations. This was also attributed to competition of these anions for sorption sites on the oxide surface. Liu et al. (2000) observed an increase in the oxidation of 'direct light red' by Mn oxides in the presence of $NaNO_3$. This enhanced oxidation was proposed to result from the compacting of the double diffuse layer (DDL) in the presence of $NaNO_3$. Compressing the DDL has the effect of allowing the dye molecule to get into closer contact with the oxide surface and therefore enhancing oxidation. The conflicting affect of counter ions, may relate to differences between inner-sphere and outer-sphere adsorption. The presence of anions like sulfate, which are known to form inner-sphere complexes with oxide surfaces (Hug, 1997; Eggleston et al., 1998) may compete with the sulfonate group for sorption sites, thus hindering mineral-dye contact. However, if the oxidation reaction proceeds via an outer-sphere complex, addition of electrolyte would compact the DDL bringing the dye and oxide surface closer together. The increased decolorisation of AO 7 in the presence of sulphate would therefore support the observation made in the ATR study (section 6.5.2) that the sulfonate group of AO 7 forms a predominantly outer-sphere complex with the Mn tailings. The difference between NaCl and Na_2SO_4 in the above decolorisation reactions, cannot be rationalised on the basis of a simple DDL effect as concentration-dependent increase in oxidation with both salts would be expected. Another issue which may limit the interpretation of the results in terms of the DDL theory is the fact that Na_2SO_4 had no influence on oxidation at pH 9, where the charge on the oxide surface will be predominantly negative.

The dispersion of the clay fraction when AY 36 was reacted with Na_2SO_4 containing acetate buffer is difficult to explain. The dispersed solution could not be flocculated with $CaCl_2$ which would be expected to flocculate and negative colloids. Dispersion of negative colloids would also be expected at higher pH not at lower pH. If the dispersion of positive colloids was responsible for the turbidity, then SO_4^{2-} ions should assist in flocculation. The dispersion was only observed for AY 36 which may suggest that it could be a surface interaction with

the AY 36 oxidation intermediates that results in this clay phase dispersion. It was interesting to note that after a prolonged settling time (64 hours) the colloidal phase had settled, providing more evidence that it is the interaction between the intermediates and the clay fraction which causes the dispersion.

6.7.4. Continuous batch reactions

To establish how long the Mn tailings (HT) can sustain colour removal, a batch experiment was conducted in which the dye solution was replenished daily. The UV absorption, pH and Mn concentration were measured throughout the 60 day reaction period. After 2 days of AY 36 replenishment the tailings became highly dispersed and separating the solid and liquid phase became difficult so the experiment was only continued with AO 7. The decolorisation of AO 7 and AY 36 as a function of time is shown in Figure 6-46 a and b, respectively.

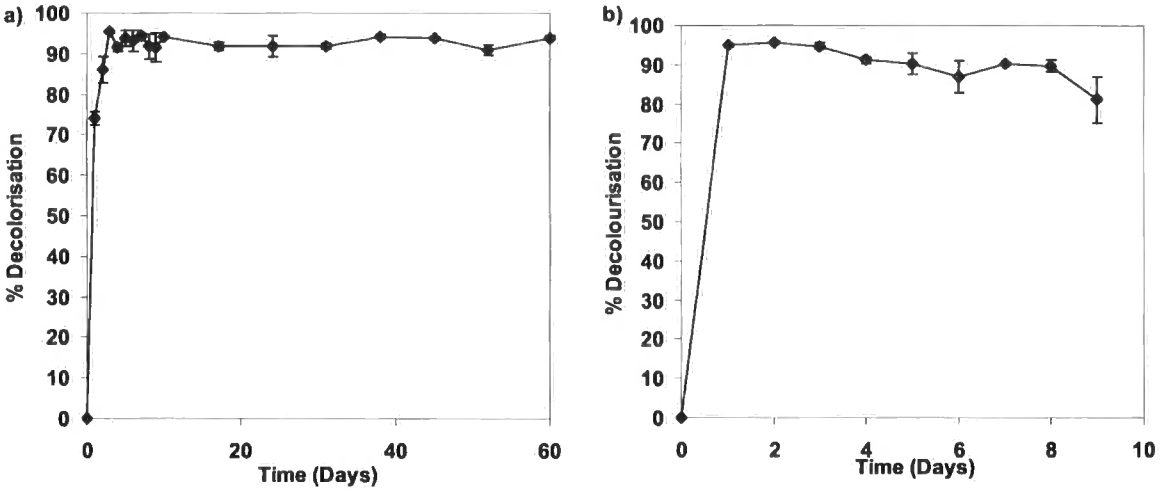

Figure 6-46 Percentage decolorisation of a) AO 7 and b) AY 36 over time after sequential reactions with fresh dye solution.

Due to the alkali buffering of the tailings the pH in the acetate buffer solutions had drifted upward (from pH 4.0 to pH 4.7) during the first 24 hour reaction period. The pH of the supernatants decreased daily as the replenished buffered solutions gradually depleted the buffer capacity of the tailings and the pH eventually stabilised at the pH of the buffer (pH 4) after day 3.

Maximum decolorisation of AY 36 was achieved on day 1 (Figure 6-46b), after this the sample became increasingly turbid and thus decolorisation became more difficult to measure. No dispersion was observed in the blank solutions or the AO 7 treatments. Thus it would appear that colloid dispersion is related to AY 36 or its breakdown products.

Decolorisation of AO 7 increases from 78% on day 1 to 96% on day 3 at which it stabilises (Figure 6-46a). The increase in colour removal coincides with the lowering of the pH in successive dye/acetate washings, as mentioned above. After 60 days of continual replenishment 95% decolorisation was still being achieved within the 24 hr reaction period, illustrating the longevity of the oxidative capacity of the tailings.

Manganese release was monitored over the course of the experiment (Figure 6-47). There is a daily incremental increase in the Mn release from both dye treatments and the blank until day 3, after which Mn release drops and stabilises at an average of 65 $mg.L^{-1}$ for the blank and 85 $mg.L^{-1}$ for the AO 7 treatment. Manganese release from the blank solution follows a similar pattern as the dye treatments, but is consistently lower. Reasons for the Mn release in the acetate buffer have been discussed earlier. The initial spike in Mn release, coincides with the progressive drop in pH. This could represent an easily reducible or labile Mn phase which is sensitive to change in pH. It would appear that this labile phase is quickly exhausted as the Mn release drops and stabilises after 4 days.

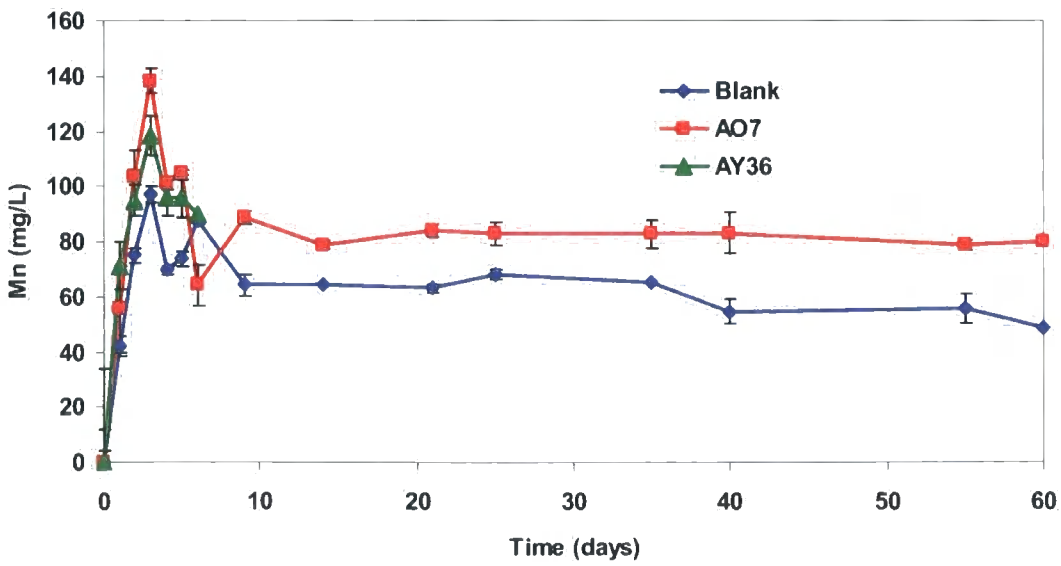

Figure 6-47 Manganese release measured in the supernatants of reacted blank and dye solutions as a function of time.

It is assumed that the difference in Mn concentration between the blank and the reacted sample represents dye-related Mn release. The average difference between the Mn released in the blank and the AO 7 treatment was calculated and gives a reaction stiochiometry of 1:3. This supports the reaction mechanism proposed in section 6.4.2 in which three one-electron transfers are involved in the oxidation of AO 7, assuming Mn(III) oxides predominate the tailings (Chapter 5).

Accumulation of Mn^{2+} on reactive sites has been shown to slow down reactions between Mn oxides and organic molecules (Klausen et al., 1997), however, data from this investigation shows that prolonged reaction and Mn release did not reduce the efficiency of the reaction. The reaction conditions used in this study i.e. agitation followed by complete removal of the supernatant, are very favourable for mixing and the data may represent an inflated decolorisation potential, but it provides a benchmark for what decolorisation can be achieved using a single measure of tailings.

The dispersion of the clay fraction after reaction with AY 36 may be a hindrance to treatment of such a dye. As noted above after a long enough reaction period the flocculation of the material occurred. Thus longer residence time of the dye in a reactor may be necessary to achieve efficient flocculation.

6.8. The use of Mn tailings as a possible dye decolorisation technology.

The results in this chapter have shown that the Mn tailings have the capacity to oxidise and decolorise two dye solutions. This oxidative breakdown is unaffected by the chemical environment present in most dye effluents (salts, organic acids) and the reaction is long lived. Thus the tailings appear to be an appealing treatment technology. The decolorisation capacity of the MT tailings was lower than the HT and WT tailings, and the former released more Mn in the acetate buffer solution. This would suggest that the HT and WT may be better suited for dye treatment.

The reaction mechanisms proposed in this study for the Mn tailings appear to be very similar to those of white rot fungi and other peroxidase catalysed reactions. The benefits of the Mn tailings over white rot fungi include the capacity of the tailings to withstand harsh chemical conditions, avoiding the need for 'initiating' conditions i.e. organic ligands, Mn^{2+} and primary substrates, and finally the contact time between the oxidant and the dye can be controlled via filtration which may prevent undesired coupling compounds forming as observed with enzyme mediated oxidations (Zille et al., 2005).

There are some important drawbacks to using the tailings as there would be in any treatment system. The major breakdown products are quinone-type compounds and hydroxybenzenesulfonate species. Quinone type compounds are light yellow to brown in colour and this would explain why 100% colour removal was never achieved. To attain 100% colour removal the quinone-type compounds would need to be removed. Quinone formation is one of two pathways followed during the oxidation of phenolic groups. The alternative pathway involves the coupling of two phenoxy radicals to form humic acid polymers in what is essentially a composting reaction (Huang, 2000). This latter pathway has many benefits compared to quinone formation as potentially ecotoxic quinone species are converted to non-toxic stable macromolecules. Despite the coupling reaction having a lower activation energy than electron transfer (Chang and Allan, 1971), it would appear in the chemical environment present in the dye decolorisation reactions, quinone formation prevails. The oxidation of phenols is known to be complex and usually results in a mixture of products. Early studies into phenol oxidation established that pH plays a key role in determining which pathway phenol oxidation would follow, with a low to neutral pH favouring the formation of quinones and alkaline conditions favoring coupling reactions (Waters, 1971). It is thus likely that in the acidic acetate solutions, used in this study, quinone formation is the dominant phenol oxidation pathway. If the reaction pH could be manipulated such that polymerisation reactions occurred, 100% decolorisation may be achieved making the tailings a highly feasibly decolorisation technology.

Lopez et al. (2004) assessed the toxicity of effluent generated after enzymatic oxidation of AO 7. This effluent contained the two major breakdown products identified in the current study i.e. 4-hydroxybenzensulfonate and 1,2 naphthoquinone. Although the effluent from the

enzymatic degradation showed no toxic effects, isolated assessment of 1,2 naphthoquinone showed that this compound is toxic towards aquatic organisms. This reiterates the need to remove quinone type compounds after treatment. Treatment of real textile effluent with white rot fungi reduced cytotoxicity by 70% compared to a 10% obtained for ozonation (Vanhulle et al., 2008). These workers found the most efficient reduction in cyctotoxicity (90%) when ozonation was used in conjunction with white rot fungi treatment. Considering the similarities between the oxidation mechanisms of white rot fungi and the tailings, equivalent detoxification after reaction with tailings would be expected.

Manganese release is an important issue that needs to be resolved before this technology can be implemented. There are many studies addressing the issue of Mn removal from waters (McBride, 1979; Junta and Hochella, 1994; Phillips et al., 1995; Johnson et al., 2005). One successful method of removing Mn from water is adsorbing and reoxidising Mn^{2+} ions on Mn oxides, in a process which is known as autooxidation (Ross and Bartlett, 1981). The Mn tailings with their high pH, and abundant carbonate component would offer three mechanisms of Mn^{2+} removal i) precipitation of Mn carbonate minerals, ii) provision of a high pH surface which would facilitate the oxidation and precipitation of Mn^{2+} ions and finally iii) autooxidation of Mn^{2+} on the Mn oxide phase of the tailings. Thus the tailings themselves may provide a suitable substrate for soluble Mn removal from treatment waters. These aspects are being investigated in a current parallel study. Another option would be to harness the soluble Mn^{2+} on an ion exchange resin. This harnessed Mn^{2+} may have an industrial application, such as Mn metal plating.

7. Results and discussion: Polycyclic aromatic hydrocarbons

Anthracene was chosen to represent the PAH contaminant group for reasons mentioned in Section 1.5. It has been highlighted in Chapter 3 that contact between the hydrophobic organic compounds and mineral surfaces depends on surface hydration. The effects of mineral surface hydration and pH on the oxidation of anthracene by the tailings are presented in this chapter.

7.1. Anthracene-mineral interactions under moist and dried conditions

Tailings (HT, WT and MT), quartz (QTZ), calcite (CC) and purchased Mn_2O_3 (MO) were reacted with anthracene under moist and dried (evaporative) conditions. As a control, anthracene-spiked water was evaporated from a clean glass surface. The pH of the mineral slurries were unadjusted. The concentration of anthracene (calculated as a % of the original anthracene spike i.e. % recovery) extracted from these samples after 7 days is given in Figure 7.1.

Anthracene recovery from the moist controls and samples was good for all treatments (>89%) (Figure 7-1a), some of the lost of recovery may have been attributed to volatilisation, but certain samples showed 100% recovery thus volatilisation was considered minimal. Drying resulted in decreased anthracene recovery from the control and all samples (Figure 7-1b). Volatilisation may have contributed to the loss of recovery but it was difficult to measure due to the reaction of the control (see later). The dried QTZ sample showed a similar recovery to that of the dried control (78%). The lowest and most variable recovery was observed in the dried HT (30%) and MT (40%) tailings, followed by dried CC. The large variation in anthracene recovery cannot be explained, repeat experiments gave consistently variable results. Chromatograms of the moist and dried HT and CC treatments are shown in Figure 7-2 and Figure 7-3, respectively.

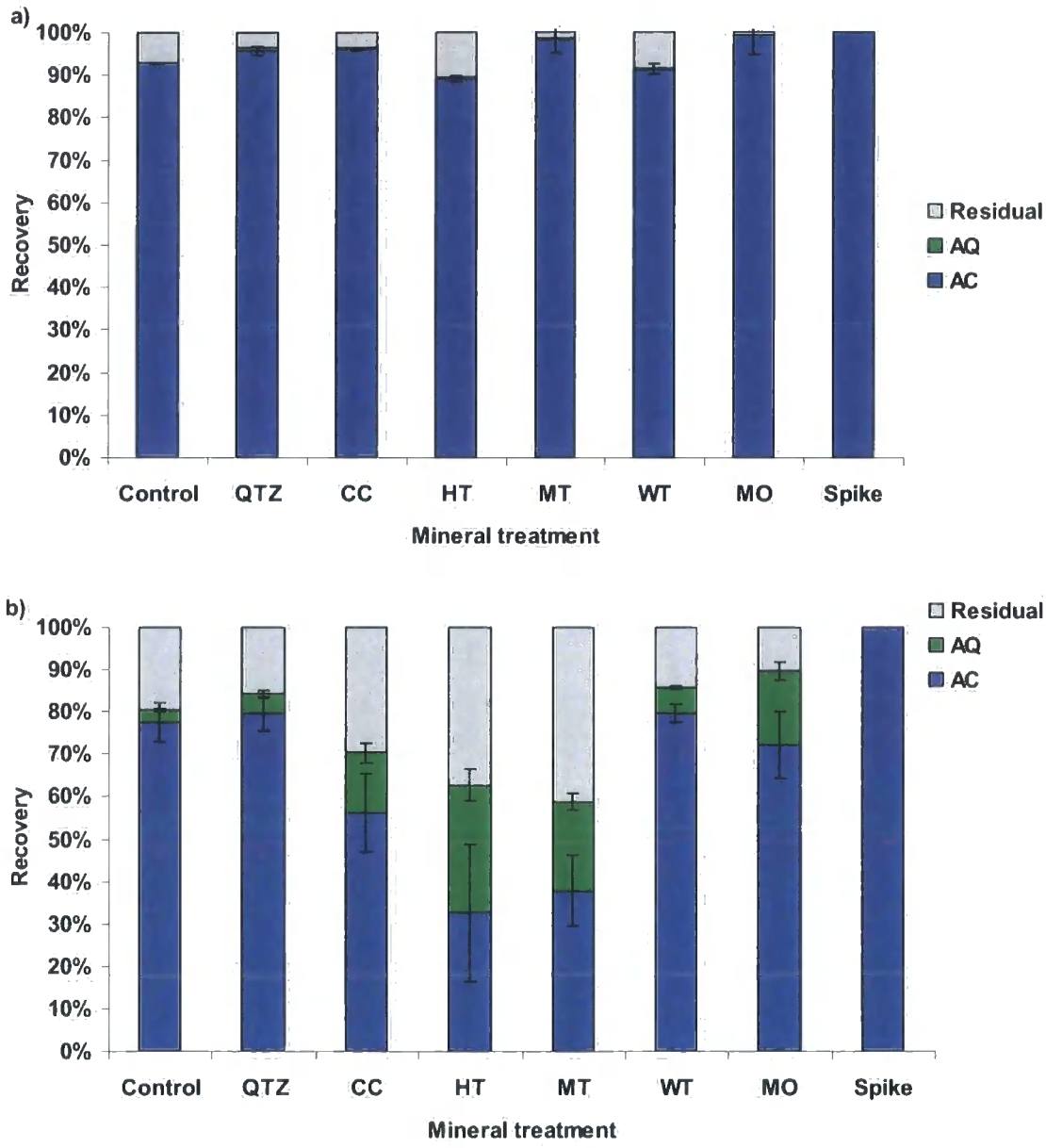

Figure 7-1 Percentage recovery (mole based) of anthracene (AC) and anthraquinone (AQ) in extracts from a) moist and b) air-dried controls, quartz (QTZ), calcite (CC), Hotazel type (HT), Mamatwan type (MT), Wessels type (WT) tailings and purchased Mn_2O_3 (MO) samples spiked with anthracene. No adjustment to pH was made.

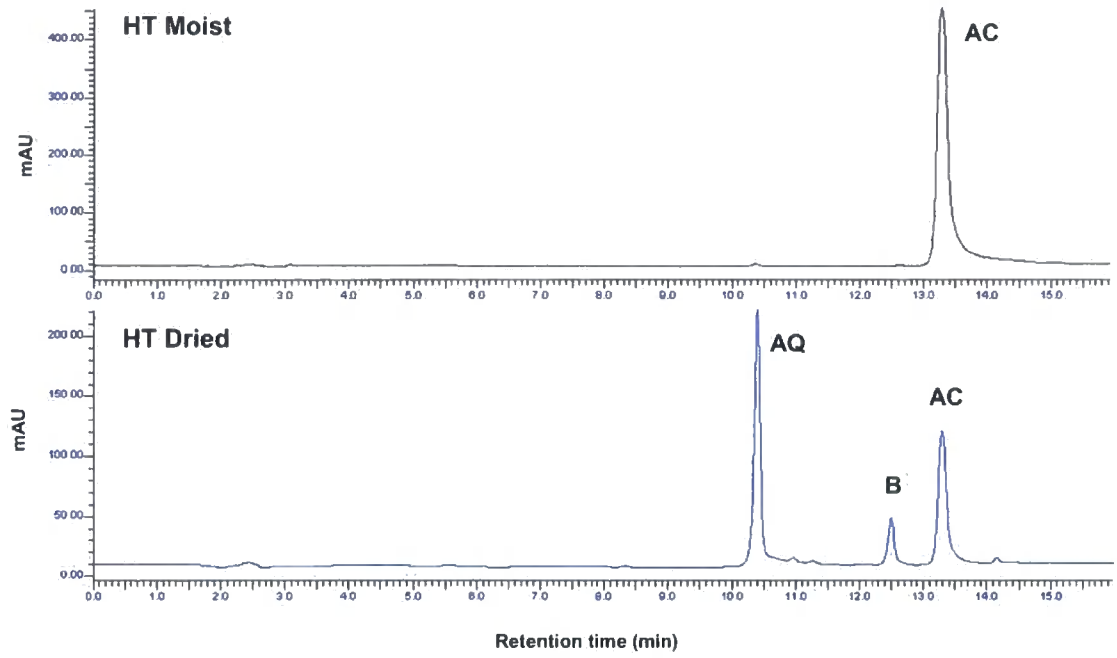

Figure 7-2 Chromatograms of cyclohexane extracts from moist and dried Hotazel tailings spiked with anthracene, showing peaks representing anthracene (AC), anthraquinone (AQ) and an unknown compound B.

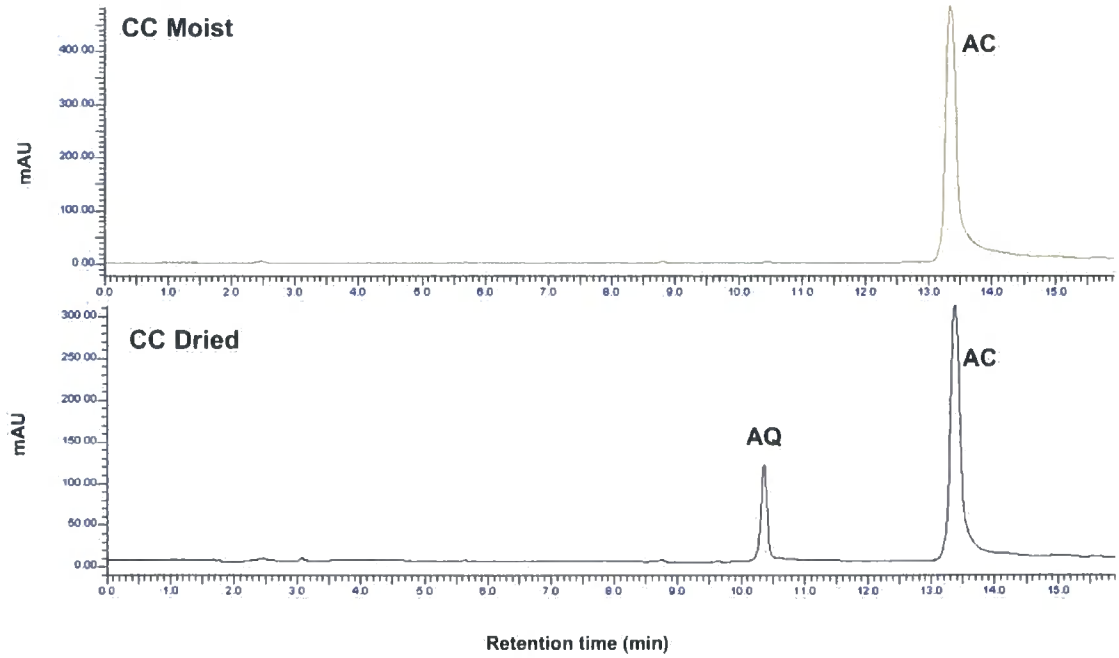

Figure 7-3 Chromatograms of cyclohexane extracts from moist and dried calcite samples spiked with anthracene, showing peaks representing anthracene (AC) and anthraquinone (AQ).

The peak at 13.4 minutes represents anthracene. The additional peak observed at 10.4 minutes in the dried CC and HT treatments suggests the formation of a new compound. This peak was identified as anthraquinone and was identified in the dried control and all dried mineral treatments. A third peak (peak B) is evident in the dried HT chromatogram at 12.5 min. Peak B was present in all the dried tailings treatments (Appendix E; Figure E-4 and E-5), but not in the control, QTZ, CC or MO. This peak could not be identified, but it suggests that there may be differences in the reactions occurring on the tailings and the other mineral phases.

The concentration of anthraquinone extracted from the moist and dried samples is presented in Figure 7-1b. Anthraquinone was detected in the dried control and all the dried mineral treatments. Oxidation of anthracene in the dried control would suggest that a limited amount of anthracene oxidation occurs as water is evaporated from a clean glass surface. Similar concentrations (4.5%) of anthraquinone were detected in the dried quartz treatment. The dried HT and MT tailings showed the highest anthraquinone concentrations (30 and 21%, respectively) followed by dried MO (17%). The CC treatment also showed substantial anthraquinone concentration (14%). Trace concentrations of anthraquinone were detected in the moist HT, MT, WT and QTZ treatments. It was observed in these samples that a small degree of mineral drying had occurred around the edges of the vial.

To assess the total recovery of organic compounds the residual (100-[anthraquinone+ anthtacene]) was plotted (Figure 7-1). Drying increases the residual in the control and all dried treatments. The dried HT chromatogram in Figure 7-2, and chromatograms from the dried WT and MT tailings (not shown), show peak B, suggesting there is an additional product to anthracene forming. This additional, unidentified compound, which was more prevalent in the dried HT and MT treatments may account for the reduced total recovery observed in these dried tailings samples.

The results from the drying experiments have given some anomalous results. It would appear that simple air-drying causes a limited amount of oxidation in the control and the quartz treatments. Calcite which was originally included as a control, oxidised an appreciable proportion of added anthracene with drying. This oxidation by a non-redox active mineral is

difficult to justify. There are large differences in the oxidation of anthracene by the tailings, with the HT and MT tailing oxidising the most anthracene and the WT tailings oxidising less (6%) than calcite. The purchased Mn oxide oxidised substantial amounts (17%) of anthracene. These results suggest that it may be the actual process of drying on a mineral surface, rather than electron transfer to the Mn oxides, which results in anthracene oxidation. It has been shown that short-range silica can catalyse the oxidation of polyphenols (Ziechmann, 1959). Ground quartz has been shown to have a disturbed layer which is short-range in nature (Iler, 1979) and thus it has been proposed that quartz may have similar polymerising capacity (Huang, 2000). Borosilicate glass has also shown the capacity to catalyse organic transformation reactions (Stanton, 1987), thus the reactions in the 'controls' may be explained by surface phenomena and the extreme environment of drying mineral surfaces.

7.1.1. The importance of the drying process

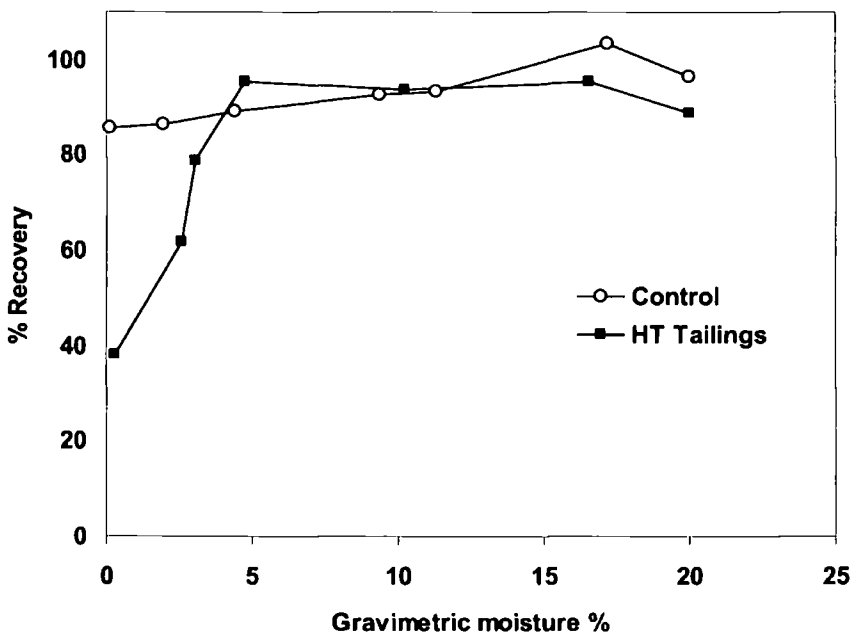

Figure 7-4 Anthracene recovery from hydrated, spiked HT and control samples allowed to dry to different degrees

In order to establish the dependence of anthracene oxidation on moisture content, a series of moist, spiked HT samples were dried to different degrees before extraction in cyclohexane. Figure 7-4 shows anthracene concentration as a function of gravimetric moisture content for HT tailings and control samples. Anthracene concentration in the control decreases slightly as water is evaporated but anthracene loss is substantially larger in the HT tailings treatment, especially as the water content drops below 5%. This would imply that the oxidation occurs on a drying but not necessarily dry surface.

The amount of anthracene initially added to the tailings was 0.028 mg, which would largely be insoluble in the small volume of hydrating water (0.4 mL). The substantial removal of added anthracene by the dried minerals suggests that more anthracene has been oxidised than is water soluble (0.07 $mg.L^{-1}$). This would imply that significant contact between the tailings and anthracene is achieved in the drying system. Sorption of HOC vapours on mineral surfaces is highly dependent on surface moisture content (Chiou and Shoup, 1985; Goss, 1992), which is considered to be largely a result of the displacement of sorbed organic compounds by water molecules. Sorption of organic molecules is most significantly affected when the moisture content is below one monolayer of water coverage, but there is still an exponential decrease in sorption up until 10 water monolayers (Chiou and Shoup, 1985; Goss, 1992; Goss, 1993; Goss and Eisenreich, 1996; Goss and Schwarzenbach, 2002). This would suggest that mineral surfaces may still impart an influence even while significantly hydrated.

Evaporation of water from a mineral surface has been shown to be an acidifying process (Mortland and Raman, 1968; Dowding et al., 2005), thus increased surface acidity of the mineral may play a role in the anthracene oxidation reaction. This drying-induced acidification is known to occur due to the hydrolysis of the last remaining water molecules surrounding exchangeable cations on the mineral surface (Mortland and Raman, 1968). As the clay surface becomes drier the Brønsted acidity increases and protons are concentrated in a smaller volume of water resulting in extreme surface acidity. If this was the cause of the anthracene oxidation, it would be expected that evaporation of spiked cyclohexane, instead of spiked water would not result in the same oxidisation. Thus the drying experiments were repeated with the HT and CC treatments, replacing the water with cyclohexane (i.e.

evaporation of a spiked cyclohexane-mineral slurry). To ensure that all the moisture was removed before the evaporation of cyclohexane, the samples were oven-dried (104°C) prior to the reaction. The results are given in Figure 7-5. Anthraquinone was detected in both the CC and HT treatments evaporated from cyclohexane (Figure 7-5). Interestingly no anthraquinone was observed in the control (spiked cyclohexane evaporated from the glass vial). The oxidation of anthracene on the mineral phases would imply that the hydrolysis of water molecules may not be responsible for the observed oxidation. The stability of anthracene at pH 1 was demonstrated by addition of anthracene to 0.1 M HCl. No conversion to anthraquinone was observed (data not shown), although its has been reported that acidities on drying mineral surfaces can reach an acidity equivalent to 6 M HCl in solution (McBride, 1994).

As mentioned above the samples were oven-dried prior to evaporation of the spiked organic solvent. This drying may have created surface acidity, which was not altered by the addition of cyclohexane and therefore still available for anthracene oxidation. If this were the case then similar oxidation would be observed in samples reacted in cyclohexane without evaporation of the organic solvent.

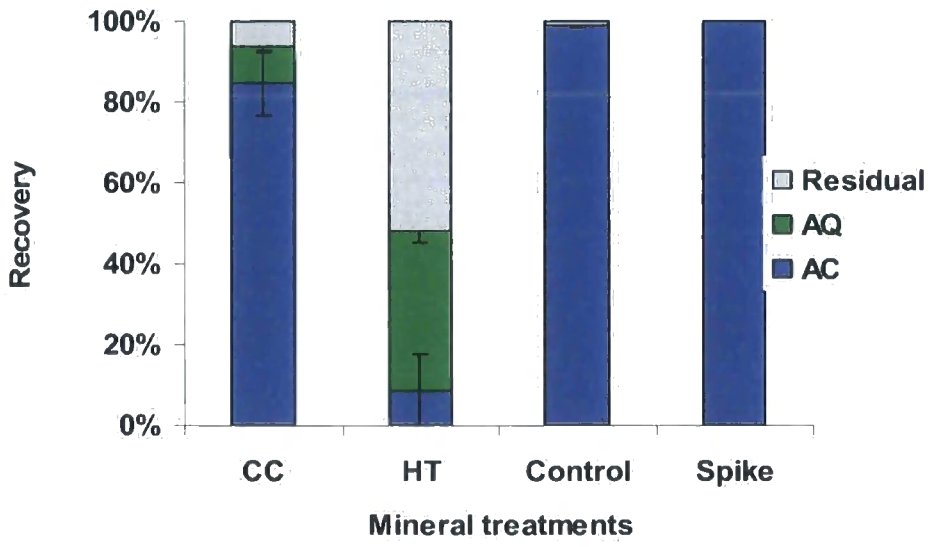

Figure 7-5 Recovery (%) of anthracene (AC) and anthraquinone (AQ) in extracts from spiked calcite (CC) and Hotazel type (HT) tailings after evaporating cyclohexane.

To assess this, oven-dried calcite and HT tailings were reacted with anthracene in cyclohexane, without any evaporation. The anthracene concentrations after reaction with the CC and HT tailings in cyclohexane are shown in Figure 7-6. Anthracene conversion to anthraquinone appears to be limited in the presence of an organic solvent, with only trace amounts of anthraquinone detected in the HT and CC treatments. Anthracene has been shown to oxidise on the surface of dried montmorillonite when an anthracene spike was added to the dry clay in dichloromethane (Karimi-Lotfabad et al., 1996). These authors suggested that exchangeable transition metals on the exchange sites were responsible for the oxidation of anthracene via a one electron transfer mechanism and the formation of a radical species. It is not possible to directly compare the current study to that of Karimi-Lotfabad et al. (1996), but enhancing the solubility of anthracene may be expected to facilitate any Mn oxide mediated anthracene oxidation, especially if surface acidity had been generated on the mineral surface during oven-drying. It is acknowledged that caution needs to be taken when interpreting these results but the limited reaction observed in an organic solvent and the oxidation observed during evaporation of a non-polar solvent would suggest that neither mineral-organic contact nor the generation of drying-induced acidity are the sole driving forces behind anthracene oxidation on the dried mineral surfaces. An important factor that needs to be taken into consideration when interpreting these data, is that in the moist samples, the reaction pH was that of the calcite or the tailings i.e. pH 8.3 and 9.0, respectively. It will be demonstrated later that the oxidation of anthracene by the Mn tailings is affected by pH.

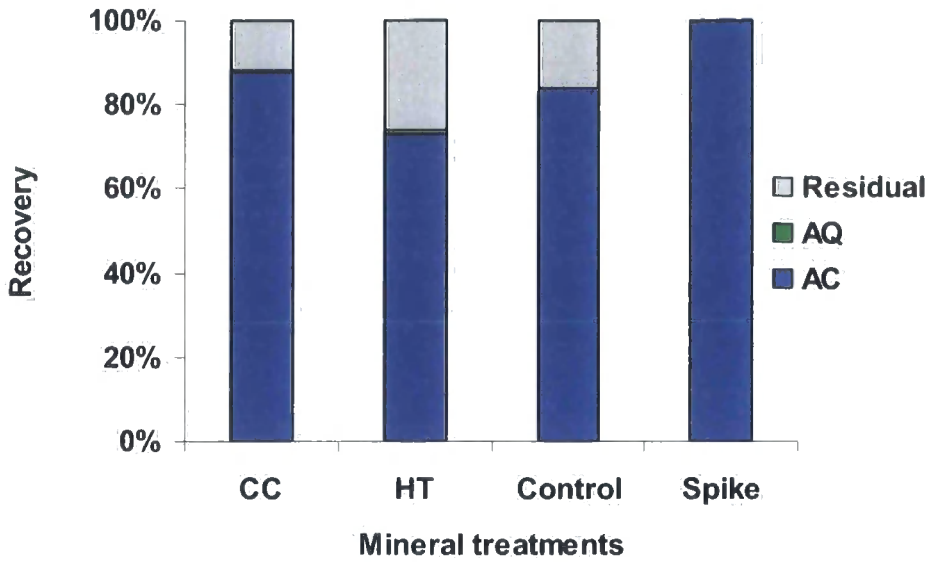

Figure 7-6 Percentage anthracene (AC) and anthraquinone (AQ) recovery after reacting anthracene with HT tailings and CC in cyclohexane solvent, calculated on a molar basis.

The above data would suggest that the oxidation of anthracene occurs as spiked polar and non-polar solvents are evaporated from the mineral surface. One of the changes that would occur during solvent evaporation is enhanced availability of oxygen on the mineral surface. Adsorbed O_2 molecules are seen to be partially responsible for hydroquinone oxidation by clay minerals (Thompson and Moll, 1973). To establish the effect of oxygen, the drying reactions were conducted under a nitrogen purge (Figure 7-7). Unfortunately work could not be conducted in an anaerobic chamber as the facilities were not available so these data are not conclusive. Anthracene oxidation was apparent in both CC and HT treatments, dried under N_2. The large variation in these samples makes the effect of O_2 on oxidation difficult to speculate.

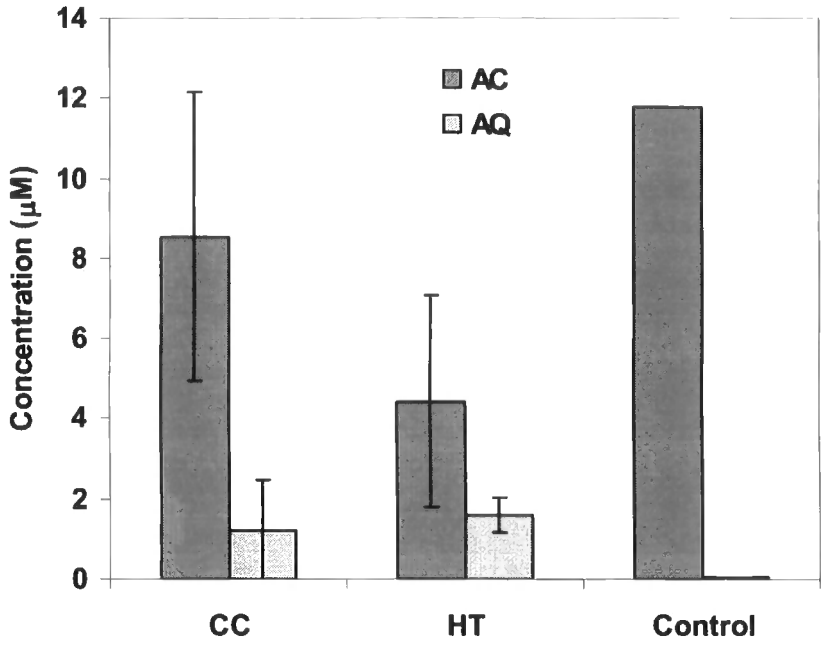

Figure 7-7 Anthracene (AC) and anthraquinone (AQ) concentrations of spiked CC and HT samples allowed to dry under nitrogen.

The data from the drying experiments does not provide any clear mechanism for the drying-induced oxidation of anthracene on the mineral surfaces. From the data presented in Figure 7-1 it would appear that anthracene is oxidised to a limited extent just through evaporation of water from an inert surface (glass or quartz) but this oxidation is substantially enhanced on calcite, the tailings and synthetic Mn oxide surfaces. At the ambient, pH (>5) of the calcite, tailings and purchased Mn oxide, limited oxidation was observed without evaporation of the water. Exchanging the evaporating solvent from water to cyclohexane makes little difference to the oxidation reaction on the calcite or the tailings surfaces, however, only limited oxidation is observed when anthracene is reacted with previously dried calcite and tailings samples in cyclohexane without evaporation. Thus it would appear that evaporation of both polar and non-polar solvents result in the anthracene oxidation on the tailings and calcite surfaces.

7.2. The influence of pH on anthracene oxidation in fully hydrated conditions

The effect of pH on oxidation of organic molecules by Mn oxides is well established (Stone and Morgan, 1984a; Laha and Luthy, 1990; Klausen et al., 1997; Matocha et al., 2001; Ge and Qu, 2003; Zhang and Huang, 2005). If electron transfer were to take place between the Mn tailings and anthracene it would be most likely to occur at low pH. Thus anthracene was reacted with the tailings in a series of pH adjusted acetate buffers under fully hydrated conditions. The results for the HT tailings are shown in Figure 7-8.

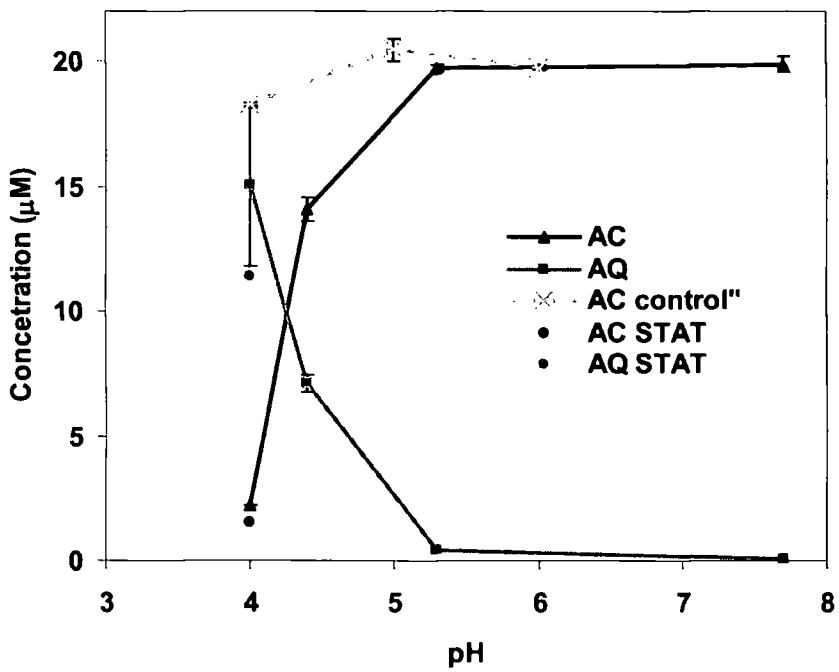

Figure 7-8 Anthracene (AC) and anthraquinone (AQ) concentrations after reacting anthracene with the HT tailings in a series of pH adjusted acetate buffers. Grey and black closed circles represent samples reacted at pH 4 in DI using 0.1 M HCl to control pH.

The cyclohexane extracts from the lower pH treatments (4.5 and 4.0) show a decrease in anthracene concentration and a corresponding increase in AQ concentration. Anthracene concentration in the quartz control showed no apparent decreases even below pH 4. The pH

treatments were repeated for the WT and MT tailings, the same pH dependent oxidation was observed (Appendix E: Figure A-6).

It has been shown that Mn(III)-acetate complexes can oxidise PAHs (Cremonesi et al., 1986). Tetramethylbenzidine was used to test for the presence of any Mn(III)-acetate complexes (Bartlett, 1999). At the buffer concentration used in this experiment (0.2 M) no Mn(III)-complexes were observed, thus it would suggest that oxidation was occurring between the solid phase and anthracene.

The amount of anthracene initially added (2 $mg.L^{-1}$) to the pH treatments far exceeds the aqueous anthracene solubility limit (0.07 $mg.L^{-1}$) yet substantial transformation (75%) to anthraquinone was observed in the pH 4 treatment (Figure 7-8). This would suggest that sufficient anthracene mineral contact was obtained in the acetate buffer. Acetate may be expected to slightly increase the solubility of anthracene as is observed with DOC (Raber et al., 1998). To establish if similar oxidation would occur in the absence of an organic buffer, the reaction with the HT tailings was repeated in DI using 0.1 M HCl to maintain the pH at 4. The results, shown in Figure 7-8, illustrate a substantial (50%) amount of anthracene has been oxidised in the HCl treated solution. Thus it would appear that appreciable tailings-anthracene contact is also achieved in the inorganic reaction medium. Considering the poor aqueous solubility of anthracene, the complete conversion of anthracene in solution is unanticipated. The 'hydrophobic effect' describes the partitioning out of hydrophobic organic compounds onto surfaces (Schwarzenbach, 1993). It has been that established that hydrophobicity and surface area are the most important aspects that govern partitioning of organic molecules onto the mineral surfaces. For a given system, however, sorption increases slightly with decreasing pH (Schlautman and Morgan, 1994) but this cannot account for the degree of mineral-anthracene contact necessary to oxidise the quantity of anthracene observed here.

It has been shown that the sorption of a range of PAHs onto the surfaces of alumina, kaolin and silica is complete within about 10 hours and that isotherms are linear up until the solubility limit of the organic compound is reached (Backhus, 1990). This suggests that of the anthracene added only a limited amount can be involved in the sorption and thus oxidation

reactions at a given time. It may be possible that the continual oxidation of anthracene on the mineral surface, keeps the activity of anthracene in solution below its aqueous solubility limit which would allow for progressive depletion of the non-soluble phase until almost total anthracene conversion has taken place. The reaction solutions were continually stirred over the 5 day period which would aid in removal of the formed anthraquinone, replenishing reactive surface for further anthracene sorption.

To establish if anthraquinone is broken down further by the tailings, anthraquinone was reacted with the tailings in a pH 3.7 acetate buffer. The percentage anthraquinone recovered after the reaction is shown in Figure 7-9. No significant change was observed in the anthraquinone concentration in the tailings or quartz treatments after 5 days reaction time. Thus it would appear that anthraquinone is the terminal product of anthracene oxidation by the tailings. Anthraquinone was determined to be the dead-end product of anthracene oxidation by white rot fungi (Field et al., 1992; Bezalel et al., 1996) thus further oxidation by the tailings would not be expected.

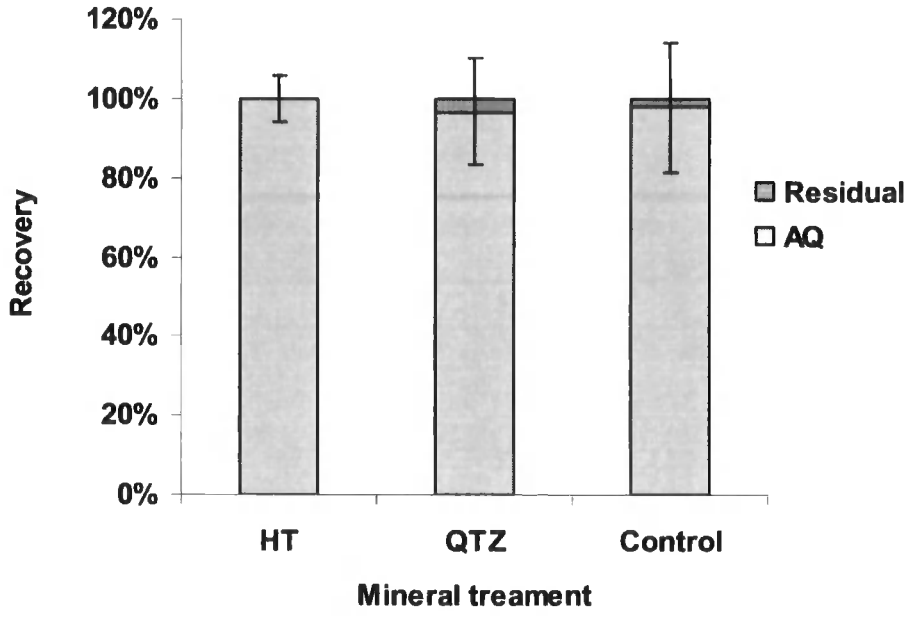

Figure 7-9 Percentage recovery of anthraquinone after reaction with the HT tailings and quartz (QTZ) in a pH 3.7 acetate buffer, presented with a control reacted in acetate buffer alone.

7.3. Possible mechanisms for anthracene oxidation at mineral surfaces

The mechanism of anthracene oxidation to anthraquinone has been established for peroxidase mediated reactions. The hydroxylation of anthracene is thought to occur by radical formation followed by nucleophilic attack of water molecules. The hydroxyl groups are then further oxidised to quinone moieties (Hammel et al., 1986). All of these steps involve one-electron transfers from the organic molecule to the metal centre. Other products identified in peroxidase oxidation include 9,10-dihydroxyanthracene and 1,2-dihydroxyanthracene (Hammel, 1995). It is possible that one of these compounds could account for the additional peak (peak B) observed in the chromatograms of the dried tailings treatments, but this was never verified.

The catalytic activity of mineral surfaces has been implicated in the polymerisation of PAHs during low temperature thermal treatment of contaminated sediment samples (Kopinke and Remmler, 1995; Remmler and Kopinke, 1995). These polymerisation reactions are assumed to proceed via radical pathways. It was proposed that the thermal treatment of the sediment resulted in the oxidation of Mn and Fe oxides which catalysed the radical formations of the PAHs (Remmler and Kopinke, 1995). In pure mineral studies, Remmler and Kopinke (1995) established that acid activated clays had the highest conversion rates of PAHs and that acid activation plays a more important role in the polymerising capacity of a surface than high surface area. Minerals such as calcite, kaolinite and pyrite are catalysts in the isomerisation, aromatization and cracking reactions of hydrocarbons under high temperatures (Regtop et al., 1985; Regtop et al., 1986). It is possible that drying the mineral surfaces of the tailings and calcite can activate the surface in such a manner that radical abstraction can take place from the sorbed organic molecule.

The transformation of anthracene to anthraquinone on the non-redox active calcite surface, implies that electron transfer from anthracene to the Mn centre of the tailings, as the only oxidation mechanism, is debatable. The only evidence that the reaction on the surface of the tailings may be different to that on the calcite surface is the additional peak present in the chromatograms of the dried tailings, which is not present in the dried calcite treatment.

However, this peak was not evident in the purchased Mn oxide sample so the data is inconclusive.

7.4. Applications of the tailings to treat PAHs

Anthraquinone has been identified as the terminal reaction product in the reaction of anthracene with the tailings. Anthraquinone is more bioavailable than anthracene and is therefore easier to biodegrade (Mueller et al., 1989). Hence oxidation of anthracene is considered a beneficial step in PAH degradation.

The results from this study appear to raise more questions surrounding PAH degradation by the tailings than answers. A very important issue is raised and that is; what is the effect of soil drying on the fate and behaviour of organic contaminants? Drying experiments were repeated on Al_2O_3 and kaolinite, with similar results to those observed with calcite. While this avenue of research is potentially very important it fell outside the focus of this study and thus was not further pursued.

The surface properties of the tailings showed the capacity to oxidise anthracene after drying. The HT and MT tailings show good anthracene conversion while the WT tailings appear less reactive. If cracking-type reactions are occurring on the surface of these tailings under the mild conditions used in this study, then these tailings may provide suitable cracking catalysts in more extreme conditions. This is an avenue which warrants further research.

The substantial conversion of anthracene, added in quantities exceeding its water solubility, to anthraquinone in an acidic (pH < 4.5) fully hydrated system is an encouraging result because water solubility is considered one of the properties responsible for the recalcitrance of PAHs and a limitation to biodegradation (Zhang et al., 1995; Eibes et al., 2005). Thus for PAH contaminated water, the tailings may provide a viable treatment option, provided the reaction pH is low enough. As discussed in Chapter 6, provision would need to be made to ensure the retention of any Mn released into solution.

8. Conclusions and further work

The overall aim of this project was to establish the capacity of the South African Mn oxide containing mine tailings to oxidatively breakdown organic pollutants found in soils and water. This is the first study to assess the remedial potential of the Mn tailings for treating organic contaminants and for this reason the study encompassed both hydrophobic (PAHs) and hydrophilic (azo dyes) contaminants. The main research focus centered on azo dyes.

The scope of the work ranges from mechanistic studies detailing reaction mechanisms, sorption phenomena and kinetics to more applied issues which deal with how treatment systems may work in the real world.

8.1. Conclusions

1. It was established that there is a similarity between the Mamatwan and Gloria tailings, collectively known as the Mamatwan type tailings; and the Nchwaning and Wessels tailings, collectively known as the Wessels type tailings. Hotazel type tailings are best characterised as a separate tailings group. These distinctions were based mainly on mineral and chemical composition. The Mamatwan type tailings are more carbonate-rich, while the Wessels and Hotazel type tailings are more Mn oxide-enriched. The net Mn oxidation state of the tailings follows the order Hotazel type > Wessels type >Mamatwan type. The total reducible Mn was highest for the Wessels type tailings (34 to 42%) followed by the Hotazel type tailings (33%) and then the Mamawatan type tailings (20 to 28%). The reactive 'easily reducible' Mn phase was highest in the Hotazel type tailings (3%). The Mamatwan type tailings release 2.5 times more Mn than the Wessels and Hotazel type tailings in acid solutions (pH 4) making the last two tailing types more suitable for dye waste water treatment. The concentrations of trace elements in the tailings are low, most being below the Worldwide mean for soils and U.S.EPA soil screening guidelines. All trace metal concentrations in the tailings were below those stipulated for sewage sludge applications to agricultural soils in South Africa. This means that additions of the waste to soils would be viable, provided that the target soils were not acidic (>pH 5) to prevent large scale Mn dissolution.

2. Decolorisation of azo dyes using the Mn tailings showed promising results. Only the most recalcitrant azo dye, acid yellow 9, was not decolorised by the tailings. This particular dye has also shown resistance to many bioremediation techniques. The dye decolorisation potential of the tailings is a result of the Mn oxide content, with synthetic Mn oxides showing similar decolorisation capacities. Dye decolorisation by the tailings was shown to be inversely proportional to pH, which probably relates to increased sorption and thermodynamic favorability of the reactions under acid conditions.

3. The reaction mechanism proposed for the oxidation of acid orange 7, by the Mn tailings is essentially the same as that proposed in numerous white rot fungi degradation studies. Successive one electron transfers, initiated on the phenolic group, results in a carbocation forming on the C housing the azo bond. Nucleophilic attack by water molecules, results in the formation of an unstable tetrahedral complex which leads to asymmetric cleavage of the azo bond. The terminal oxidation products were identified as 1,2 naphthoquinone and 4-hydroxybenzensulfonate.

4. Attenuated total reflectance Fourier transform infrared studies revealed that sorption of acid orange 7 onto a manganite (a common Mn mineral found in the tailings) surface is pH dependent and initial sorption is outer-sphere. A pronounced lag phase was observed between the initial sorption of the dye to the oxide surface and the initiation of oxidation. This lag phase can indicate that either the transfer of the initial electron is rate limiting or that correct and time consuming orientation of the molecule prior to inner-sphere complexation is necessary before oxidation can take place.

5. The reaction mechanism proposed for the oxidation of acid yellow 36 is initiated by successive one electron transfers from the amino moiety of the dye to the Mn oxide. The reaction pathway involves the formation of a number of intermediate products, some of which hydrolyse in a Mn oxide-independent step. The terminal oxidation products were observed to be *p*-benzoquinone and 3-hydroxybenzene sulfonate.

6. Tentative reaction rates and orders were determined for both dye oxidations. At pH 4 the initial oxidation of acid orange 7 is substantially slower (3.8×10^{-6} $mol.s^{-1}.m^{-2}$)

than the initial oxidation of acid yellow 36 (2.5 x 10^{-5} $mol.s^{-1}.m^{-2}$). Both dye oxidations were shown to be pseudo-first order with respect to Mn tailings surface area concentration. The initial oxidation of acid yellow 36 was shown to be pseudo first order with respect to dye concentration while acid orange 7 showed a fractional order with respect to dye concentration. This fractional rate order supports the ATR-FTIR observations of a rate-limiting surface reaction between the Mn oxide surface and AO 7.

7. The effects of auxiliary compounds, usually present in textile effluents, on dye oxidation were investigated. The consequence of salt addition and increased buffer strength enhanced acid orange 7 decolorisation, however, addition of salt affected the colloid stability of the Mn tailings in the acid yellow 36 reaction. The continual reaction between fresh acid orange 7 and a single measure of tailings showed longevity with 90% decolorisation still being achieved after 60 days of dye replenishment. Colloid stability problems were encountered during similar continual dye replenishment reactions with acid yellow 36. The reason for the colloid dispersion was never established, but it is thought to pertain to an interaction between one of the intermediates and the clay phase. This dispersion problem may be overcome by adjusting the residence time of the dye solution in contact with the tailings (see further work point vii).

8. The reaction mechanisms and the terminal products, which form during reactions of azo dyes with the Mn tailings, largely parallel that of enzymatic dye breakdown observed with white rot fungi peroxidases. There is a wealth of research that has been conducted on xenobiotic oxidations involving white rot fungi. Results from this study have shown there is a lot of overlap between oxidation capacity of the extracellular enzymes and the Mn tailings. Textile effluents treated with peroxidases have shown a substantial decrease in cytotoxicity. As with white rot fungi, the tailings only achieved approximately 90% decolorisation of the dye solutions. This was largely due to the formation of coloured quinone type compounds. The use of white rot fungi for the treatment of textile effluent has been identified as an attractive remediation technology. The current research has shown that the Mn tailings have decolorisation

capacities similar to white rot fungi, without the chemical constraints associated with peroxidase production and stability.

9. Oxidation of anthracene to anthraquinone was observed during the evaporation of anthracene spiked water from the surface of the tailings (up to 30% oxidation), a synthetic Mn oxide (17%), calcite (14%), quartz (5%) and a clean glass surface (3%). Limited oxidation was observed without evaporation of the water. Various attempts were made to elucidate the transformation reactions on the mineral surfaces, but no conclusive mechanism was obtained. It could not be established whether electron transfer was occurring between the Mn oxide phase of the tailings and the anthracene or whether the transformation was solely a surface meditated phenomenon. Anthraquinone was identified as the major transformation product in the drying reaction. Conversion of anthracene to anthraquinone on drying mineral surfaces has positive ramifications for soil remediation, as anthraquinone is more biodegradable than anthracene due to its higher water solubility. The substantial conversion of anthracene on the Hotazel type and Mamatwan type tailings under mild drying conditions, may indicate that these materials have good cracking capacity under more extreme temperatures (see further work point i).

10. The effect of pH on anthracene oxidation was investigated in fully hydrated systems. The tailings oxidised 75% of added anthracene to anthraquinone at pH 4, despite the amount added substantially exceeding the aqueous solubility of anthracene. It is proposed that the continual oxidation of anthracene maintains the concentration below its solubility limit thereby depleting and oxidising the majority of added anthracene. This has important implications in the treatment of PAHs as one of the main factors which contribute to their recalcitrance is their poor aqueous solubility. Anthracene was observed to be stable in acid solutions in the absence of the tailings. Anthraquinone did not react further with the tailings and thus is considered the terminal oxidation product.

11. The overall conclusion that propagates from the current study is that there are promising avenues for utilising the South African Mn oxide containing tailings for

organic contaminant remediation purposes, especially in the treatment of textile effluents. However, certain problems need to be addressed, probably the most important being the sequestration of released, soluble Mn.

8.2. Further work

These conclusions and other work conducted in this study have highlighted a number of possibilities for further work. These are listed below.

i) Assessing the cracking catalyst capacities of the Mn tailings. Mechanochemical reactions might also warrant some investigation, as dry surfaces are involved in organic contaminant breakdown by such techniques. It would also be interesting to assess the oxidative breakdown of hydrophobic compounds under mild heating conditions (40-50°C).

ii) Drying reactions, performed in an anaerobic chamber would establish the role O_2 plays in the drying induced oxidation of anthracene on the mineral surfaces.

iii) The role of mineral dehydration in organic contaminant breakdown needs to be established. The mechanism of the oxidation reactions also needs to be elucidated.

iv) Further research needs to be conducted to characterize any biological activity associated with the tailings. The unique chemical environment of the tailings may have resulted in some interesting and potentially useful biotic-abiotic interactions

v) Treatment of a real dye-house effluent needs to be tested on the tailings in a continuous flow stirred reaction vessel to optimise tailings-dye reaction times and solid-liquid ratios.

vi) The influence of sonication, electrochemistry, heating and addition of hydrogen peroxide on the tailings mediated decolorisation reactions should be established. These inputs may result in more effective dye breakdown.

vii) One of the observed problems with the oxidized dye solutions was the presence of coloured quinone-type compounds. Manipulation of reaction times and intercepting

the reaction at appropriate intervals may result in preferential formation of phenolic coupling products, which may improve decolorisation of treated dye solutions. Unwanted coupling products, formed between unreacted dye and breakdown products, may also be avoided by manipulating reaction times.

viii) If the tailings are to be used in water treatment processes it is essential that soluble Mn, released in the reactions, be sequestered. Manganese oxides are commonly referred to as catalysts due to their capacity to regenerate Mn oxide surfaces through a process know as autooxidation. It is possible that by placing two reactors, containing Mn tailings, in series the soluble Mn generated during the oxidation of the organic could be precipitated out in the second reactor, thus completing the catalytic cycle. The functioning of such a system would need further investigation.

ix) It was observed during this study that when the tailings were washed with pyrophosphate, citric, oxalic, malonic and tartaric acid, Mn(III)-complexes formed and remained stable for hours to days, depending on the complexing ligand used. Manganese (III)-complexes are central to the oxidative behaviour of certain white rot fungi, but generating them involves harvesting sufficient enzyme. The formation of the Mn(III) complexes after washing the tailings with organic ligands may provide a way to bypass the fungi and all the complications that occur with enzyme generation and stability. This is an avenue of research which should definitely warrant further investigation.

9. References

Alcalde, M., T. Bulter and F. H. Arnold (2002). "Colorimetric Assays for Biodegradation of Polycyclic Aromatic Hydrocarbons by Fungal Laccases." *Journal of Biomolecular Screening* **7**(6): 547-553.

Andreozzi, R., V. Caprio, A. Insola and R. Marotta (1999). "Advanced oxidation processes (AOP) for water purification and recovery." *Catalysis Today* **53**(1): 51-59.

Andrews, J. E., P. Brimblecombe, T. D. Jickells, P. S. Liss and B. J. Reid (2004). An introduction to environmental geochemistry. Padstow, Cornwall, Blackwell Publishing.

Appelo, C. A. J. and D. Postma (2005). Geochemistry, groundwater and pollution. Second Edition. Leiden, The Netherlands, A.A Balkema Publishers.

Backhus, D. A. (1990). Ph. D Dissertation, Massachusetts Institute of Technology. Cambrige, MA

Baiocchi, C., M. C. Brussino, E. Pramauro, A. B. Prevot, L. Palmisano and G. Marci (2002). "Characterization of methyl orange and its photocatalytic degradation products by HPLC/UV-VIS diode array and atmospheric pressure ionization quadrupole ion trap mass spectrometry." *International Journal of Mass Spectrometry* **214**(2): 247-256.

Ball, S., T. W. Goodwin and R. A. Morton (1948). "Studies on Vitamin-a .5. the Preparation of Retinene Vitamin-a Aldehyde." *Biochemical Journal* **42**(4): 516-523.

Balon, M., P. Guardado, C. Carmona, J. Hidalgo and M. A. Munoz (1993). "Influence of the Acidity on the Kinetics of Diphenylamine Oxidation by Peroxodisulfate Anions." *Canadian Journal of Chemistry-Revue Canadienne De Chimie* **71**(2): 167-174.

Bamforth, S. M., D. A. C. Manning, I. Singleton, P. L. Younger and K. L. Johnson (2006). "Manganese removal from mine waters - investigating the occurrence and importance of manganese carbonates." *Applied Geochemistry* **21**(8): 1274-1287.

Bamforth, S. M. and I. Singleton (2005). "Bioremediation of polycyclic aromatic hydrocarbons: current knowledge and future directions." *Journal of Chemical Technology and Biotechnology* **80**(7): 723-736.

Banat, I. M., P. Nigam, D. Singh and R. Marchant (1996). "Microbial decolorization of textile-dye-containing effluents: A review." *Bioresource Technology* **58**(3): 217-227.

Bandara, J., J. A. Mielczarski and J. Kiwi (1999a). "1. Molecular mechanism of surface recognition. Azo dyes degradation on Fe, Ti, and Al oxides through metal sulfonate complexes." *Langmuir* **15**(22): 7670-7679.

Bandara, J., J. A. Mielczarski and J. Kiwi (1999b). "2. Photosensitized degradation of azo dyes on Fe, Ti, and Al oxides. Mechanism of charge transfer during the degradation." *Langmuir* **15**(22): 7680-7687.

Banerjee, D. and H. W. Nesbitt (2001). "XPS study of dissolution of birnessite by humate with constraints on reaction mechanisms." *Geochimica Cosmochima Acta* **65**: 1703-1714.

Bartlett, R. J. (1981). "Nonmicrobial nitrate to nitrite transformation in soils." *Soil Science Society of America Journal* **45**: 1054-1058.

Bartlett, R. J. (1988). Manganese redox reactions and organic interactions in soils. Manganese in soils and plants. D. G. Graham and et al. Netherlands, Kluwer Academic Publishers: 59-73.

Bartlett, R. J. (1999). Characterizing soil redox reactions. Soil physical chemistry. D. L. Sparks. Baco Raton, Florida, CRC Press: 371-397.

Bartlett, R. J. and B. R. James (1979). "Behaviour of chromium in soils: III. Oxidation." *Journal of Environmental Quality* **8**: 31-35.

Bartlett, R. J. and B. R. James (1980). "Studying, dried stored soil samples - some pitfalls." *Soil Science Society of America Journal* **44**: 721-724.

Bartlett, R. J. and B. R. James (1994). "Redox chemistry in soils." *Advances in Agronomy* **50**: 151-208.

Bauer, C., P. Jacques and A. Kalt (1999). "Investigation of the interaction between a sulfonated azo dye (AO7) and a TiO2 surface." *Chemical Physics Letters* **307**(5-6): 397-406.

Bezalel, L., Y. Hadar, P. P. Fu, J. P. Freeman and C. E. Cerniglia (1996). "Initial Oxidation Products in the Metabolism of Pyrene, Anthracene, Fluorene, and Dibenzothiophene by the White Rot Fungus Pleurotus ostreatus." *Applied Environmental Microbiology* **62**(7): 2554-2559.

Bhatnagar, I. and M. V. George (1968). "Oxidation with Metal Oxides .3. Oxidation of Diamines and Hydrazines with Manganese Dioxide." *Journal of Organic Chemistry* **33**(6): 2407-&.

Bogan, B. W., R. T. Lamar, W. D. Burgos and M. Tien (1999). "Extent of humification of anthracene, fluoranthene, and benzo[a]pyrene by Pleurotus ostreatus during growth in PAH-contaminated soils." *Letters in Applied Microbiology* **28**(4): 250-254.

Borda, M. J., D. R. Strongin and M. A. Schoonen (2003). "A novel vertical attenuated total reflectance photochemical flow-through reaction cell for Fourier transform infrared spectroscopy." *Spectrochimica Acta* **59**: 1103-1106.

Bourikas, K., M. Stylidi, D. I. Kondarides and X. E. Verykios (2005). "Adsorption of acid orange 7 on the surface of titanium dioxide." *Langmuir* **21**(20): 9222-9230.

Brinch, U. C., F. Ekelund and C. S. Jacobsen (2002). "Method for Spiking Soil Samples with Organic Compounds." *Applied Environmental Microbiology* **68**(4): 1808-1816.

Brown, G. S., L. L. Barton and B. M. Thomson (2003). "Permanganate oxidation of sorbed polycyclic aromatic hydrocarbons." *Waste Management* **23**(8): 737-740.

Brown, M. A. and S. C. Devito (1993). "Predicting Azo-Dye Toxicity." *Critical Reviews in Environmental Science and Technology* **23**(3): 249-324.

Bryant, J. R., J. E. Taves and J. M. Mayer (2002). "Oxidations of hydrocarbons by manganese(III) tris(hexafluoroacetylacetonate)." *Inorganic Chemistry* **41**(10): 2769-2776.

Bumpus, J. A. (1989). "Biodegradation of Polycyclic Aromatic-Hydrocarbons by Phanerochaete-Chrysosporium." *Applied and Environmental Microbiology* **55**(1): 154-158.

Bumpus, J. A., M. Tien, D. Wright and S. D. Aust (1985). "Oxidation of Persistent Environmental-Pollutants by a White Rot Fungus." *Science* **228**(4706): 1434-1436.

Chang, H. M. and G. Allan (1971). Oxidation. Lignins. K. Sarkanen and C. Ludwig. New York, New York, Wiley Interscience.

Chao, T. T. (1972). "Selective dissolution of manganese oxides from soils and sediments with acidified hydroxylamine hydrochloride." *Soil Science Society of America Proceedings* **36**: 764-768.

Chiou, C. T., P. E. Porter and D. W. Schmedding (1983). "Partition Equilibria of Non-Ionic Organic-Compounds between Soil Organic-Matter and Water." *Environmental Science & Technology* **17**(4): 227-231.

Chiou, C. T. and T. D. Shoup (1985). "Soil Sorption of Organic Vapors and Effects of Humidity on Sorptive Mechanism and Capacity." *Environmental Science & Technology* **19**(12): 1196-1200.

Chivukula, M., J. T. Spadaro and V. Renganathan (1995). "Lignin Peroxidase-Catalyzed Oxidation of Sulfonated Azo Dyes Generates Novel Sulfophenyl Hydroperoxides." *Biochemistry* **34**(23): 7765-7772.

Coen, J. J. F., A. T. Smith, L. P. Candeias and J. Oakes (2001). "New insights into mechanisms of dye degradation by one-electron oxidation processes." *Journal of the Chemical Society-Perkin Transactions 2*(11): 2125-2129.

Concise International Chemical Assessment Document (2004). "Manganese and its compounds environmental aspects. Available at http://www.inchem.org/documents/cicads/cicads/cicad63.htm. Accessed 1/12/2005."

Couper, J. (1837). "On the effects of black oxide of manganese when

inhaled into the lungs." *BRIT ANN MED PHARM* **1**: 41-42.

Cremonesi, P., E. Cavalieri and E. Rogan (1986). "One-Electron Oxidation of 6-Substituted Benzo(a)Pyrenes by Manganic Acetate." *Abstracts of Papers of the American Chemical Society* **192**: 11-ORGN.

Cremonesi, P., E. Rogan and E. Cavalieri (1992). "Correlation Studies of Anodic Peak Potentials and Ionization-Potentials for Polycyclic Aromatic-Hydrocarbons." *Chemical Research in Toxicology* **5**(3): 346-355.

Daly, A. R. (1907). "The oxidation of napthalene to pthalonic acid by alkaline solutions of permanganate." *Journal of Organic Chemistry*(11): 93-106.

DeVilliers (1965). The Mineralogy of the Kalahari manganese-field north of Sishen, Cape Province.PhD thesis. Department of Geology. Pretoria, University of Pretoria.

Dion, H. G. and P. J. G. Mann (1946). "Three-valent manganese in soils." *Journal of Agricultural Science* **36**: 239-245.

Dixon, J. B. (1988). Todorokite, birnessite and lithiophorite as indicator minerals in soils. Manganese Symposium,Adelaide.

Dixon, J. B. and G. N. White (2002). Manganese oxides. Soil mineralogy with environmental applications. J. B. Dixon and D. G. Schulze. Madison, Wisconsin, Soil Science Society of America: 367-388.

Dohse, D. M. and L. W. Lion (1994). "Effect of Microbial Polymers on the Sorption and Transport of Phenanthrene in a Low-Carbon Sand." *Environmental Science & Technology* **28**(4): 541-548.

Doick, K. J., P. H. Lee and K. T. Semple (2003). "Assessment of spiking procedures for the introduction of a phenanthrene-LNAPL mixture into field-wet soil." *Environmental Pollution* **126**(3): 399-406.

Dorman, D. C., M. F. Struve and B. A. Wong (2002). "Brain manganese concentrations in rats following manganese tetroxide inhalation are unaffected by dietary manganese intake." *Neurotoxicology* **23**(2): 185-195.

dos Santos, A. B., F. J. Cervantes and J. B. van Lier (2007). "Review paper on current technologies for decolourisation of textile wastewaters: Perspectives for anaerobic biotechnology." *Bioresource Technology* **98**(12): 2369-2385.

Dowding, C. E. (2004). "Morphology, mineralogy and surface chemistry of manganiferous oxisols near Graskop, Mpumalanga Province, South Africa [MSc thesis] University of Stellenbosch, South Africa."

Dowding, C. E., M. J. Borda, M. V. Fey and D. L. Sparks (2005). "A new method for gaining insight into the chemistry of drying mineral surfaces using ATR-FTIR." *Journal of Colloid and Interface Science* **292**(1): 148-151.

Duckworth, O. W. and S. T. Martin (2001). "Surface complexation and dissolution of hematite by C_1-C_6 dicarboxylic acids at pH = 5.0." *Geochimica Cosmochima Acta* **65**: 4289-4301.

Duckworth, O. W. and G. Sposito (2005). "Siderophore-manganese(III) interactions II. Manganite dissolution promoted by desferrioxamine B." *Environmental Science & Technology* **39**(16): 6045-6051.

Duckworth, O. W. and G. Sposito (2007). "Siderophore-promoted dissolution of synthetic and biogenic layer-type Mn oxides." *Chemical Geology* **242**(3-4): 497-508.

Eggleston, C. M., S. Hug, W. Stumm, B. Sulzberger and M. Dos Santos Afonso (1998). "Surface Complexation of Sulfate by Hematite Surfaces: FTIR and STM Observations." *Geochimica et Cosmochimica Acta* **62**(4): 585-593.

Eibes, G., T. Lu-Chau, G. Feijoo, M. T. Moreira and J. M. Lema (2005). "Complete degradation of anthracene by Manganese Peroxidase in organic solvent mixtures." *Enzyme and Microbial Technology* **37**(4): 365-372.

European Commission (2003). Intergrated pollution prevention and control (IPPC) Reference document on best available techniques for the textiles industry. E. Commission.

Evans, D. A. D., J. Gutzmer, N. J. Beukes and J. L. Kirschvink (2001). "Paleomagnetic constraints on ages of mineralization in the Kalahari manganese field, South Africa." *Economic Geology and the Bulletin of the Society of Economic Geologists* **96**(3): 621-631.

Fatiadi, A. J. (1986). The oxidation of organic compounds by active manganese dioxide. Organic syntheses by oxidation with metal compounds. W. J. Mijs and C. R. H. I. DE Jonger. New York, Plenum P.

Field, J. A., E. Dejong, G. F. Costa and J. A. M. Debont (1992). "Biodegradation of Polycyclic Aromatic-Hydrocarbons by New Isolates of White Rot Fungi." *Applied and Environmental Microbiology* **58**(7): 2219-2226.

Fisher, J. A., M. J. Scarlett and A. D. Stott (1997). "Accelerated Solvent Extraction: An Evaluation for Screening of Soils for Selected U.S. EPA Semivolatile Organic Priority Pollutants." *Environmental Science & Technology* **31**(4): 1120-1127.

Flotron, V., J. Houessou, A. Bosio, C. Delteil, A. Bermond and V. Camel (2003). "Rapid determination of polycyclic aromatic hydrocarbons in sewage sludges using microwave-assisted solvent extraction: Comparison with other extraction methods." *Journal of Chromatography A* **999**(1-2): 175-184.

Frank, H. S. and M. W. Evans (1945). "Free Volume and Entropy in Condensed Systems .3. Entropy in Binary Liquid Mixtures - Partial Molal Entropy in Dilute Solutions - Structure and Thermodynamics in Aqueous Electrolytes." *Journal of Chemical Physics* **13**(11): 507-532.

Frondel, C. and L. H. Bauer (1955). "Kutnahorite: a manganese dolomite, $CaMn(CO_3)_2$." *American Mineralogist* **40**: 748-760.

Gambrell, R. C. and W. H. Patrick (1982). Manganese. Methods of Soil Analysis, Part 2. Chemical and Microbiological Properties. A. L. Page, R. H. Miller and D. R. Keeney. Madison, USA, ASA-SSSA: 263-273.

Ge, J. T. and J. H. Qu (2003). "Degradation of azo dye acid red B on manganese dioxide in the absence and presence of ultrasonic irradiation." *Journal of Hazardous Materials* **100**(1-3): 197-207.

Gianutsos, G. and M. T. Murray (1982). "Alterations in Brain Dopamine and Gaba Following Inorganic or Organic Manganese Administration." *Neurotoxicology* **3**(3): 75-82.

Gilkes, R. J. and R. M. McKenzie (1988). Geochemistry and mineralogy of manganese in soils. Manganese in soils and plants. R. D. G. e. al. Netherlands, Kluwer Academic Publishers.

Gold, M. H., H. Wariishi and K. Valli (1989). "Extracellular Peroxidases Involved in Lignin Degradation by the White Rot Basidiomycete Phanerochaete-Chrysosporium." *Acs Symposium Series* **389**: 127-140.

Goncalves, I. C., C. Dowding, K. Johnson and A. Brown (2007). "Remediation of azo dyes by natural manganese oxides." *Geochimica Et Cosmochimica Acta* **71**: A341-A341.

Gordon, G. and H. Taube (1962). "Oxygen Tracer Experiments on Oxidation of Aqueous Uranium(Iv) with Oxygen-Containing Oxidizing Agents." *Inorganic Chemistry* **1**(1): 69-&.

Goss, K. U. (1992). "Effects of Temperature and Relative-Humidity on the Sorption of Organic Vapors on Quartz Sand." *Environmental Science & Technology* **26**(11): 2287-2294.

Goss, K. U. (1993). "Effects of Temperature and Relative-Humidity on the Sorption of Organic Vapors on Clay-Minerals." *Environmental Science & Technology* **27**(10): 2127-2132.

Goss, K. U. and S. J. Eisenreich (1996). "Adsorption of VOCs from the gas phase to different minerals and a mineral mixture." *Environmental Science & Technology* **30**(7): 2135-2142.

Goss, K. U. and R. P. Schwarzenbach (2002). "Adsorption of a diverse set of organic vapors on quartz, CaCO3, and alpha-Al2O3 at different relative humidities." *Journal of Colloid and Interface Science* **252**(1): 31-41.

Goszczynski, S., A. Paszczynski, M. B. Pastigrigsby, R. L. Crawford and D. L. Crawford (1994). "New Pathway for Degradation of Sulfonated Azo Dyes by Microbial Peroxidases of Phanerochaete-Chrysosporium and Streptomyces-Chromofuscus." *Journal of Bacteriology* **176**(5): 1339-1347.

Gray, M. R., D. K. Banerjee, P. M. Fedorak, A. Hashimoto, J. H. Masliyah and M. A. Pickard (1994). "Biological Remediation of Anthracene-Contaminated Soil in Rotating Bioreactors." *Applied Microbiology and Biotechnology* **40**(6): 933-940.

Guest, C. A., D. G. Schulze, I. A. Thompson and D. M. Huber (2002). "Correlating manganese X-ray absorption near-edge structure spectra with extractable soil manganese." *Soil Science Society of America Journal* **66**: 1172-1181.

Gutowska, A., J. Kaluzna-Czaplinska and W. K. Jozwiak (2007). "Degradation mechanism of Reactive Orange 113 dye by H_2O_2/Fe^{2+} and ozone in aqueous solution." *Dyes and Pigments* **74**(1): 41-46.

Gutzmer, J. and N. J. Beukes (1996). "Mineral paragenesis of the Kalahari managanese field, South Africa." *Ore Geology Reviews* **11**(6): 405-428.

Hammel, K. E. (1995). "Mechanisms for polycyclic aromatic hydrocarbon degradation by ligninolytic fungi." *Environmental Health Perspectives* **103**: 41-43.

Hammel, K. E., K. A. Jensen, M. D. Mozuch, L. L. Landucci, M. Tien and E. A. Pease (1993). "Ligninolysis by a Purified Lignin Peroxidase." *Journal of Biological Chemistry* **268**(17): 12274-12281.

Hammel, K. E., B. Kalyanaraman and T. K. Kirk (1986). "Oxidation of Polycyclic Aromatic-Hydrocarbons and Dibenzo[P]-Dioxins by Phanerochaete-Chrysosporium Ligninase." *Journal of Biological Chemistry* **261**(36): 6948-6952.

Healy, T. W., A. P. Herring and D. W. Fuerstenau (1966). "The effect of crystal structure on the surface properties of a series of manganese dioxides." *Journal of Colloid and Interface Science* **21**: 435-444.

Herbes, S. E. and L. R. Schwall (1978). "Microbial Transformation of Polycyclic Aromatic-Hydrocarbons in Pristine and Petroleum-Contaminated Sediments." *Applied and Environmental Microbiology* **35**(2): 306-316.

Hofrichter, M. (2002). "Review: lignin conversion by manganese peroxidase (MnP)." *Enzyme and Microbial Technology* **30**(4): 454-466.

Holcapek, M., P. Jandera and J. Prikryl (1999). "Analysis of sulphonated dyes and intermediates by electrospray mass spectrometry." *Dyes and Pigments* **43**(2): 127-137.

Holcapek, M., P. Jandera and P. Zderadicka (2001). "High performance liquid chromatography-mass spectrometric analysis of sulphonated dyes and intermediates." *Journal of Chromatography A* **926**(1): 175-186.

Holcapek, M., K. Volna and D. Vanerkova (2007). "Effects of functional groups on the fragmentation of dyes in electrospray and atmospheric pressure chemical ionization mass spectra." *Dyes and Pigments* **75**(1): 156-165.

Holmgrén, G. G. S. (1967). "A rapid citrate-dithionite extractable iron procedure." *Soil Science Society of America Proceedings* **31**: 210-211.

Huang, P.-K. C. and E. M. Kosower (1968). "Diazenes. III. Properties of phenyldiazene." *J. Am. Chem. Soc.* **90**(9): 2367-2376.

Huang, P. M. (2000). Abiotic Catalysis. Handbook of Soil Science. M. E. Sumner. Boca Raton, Florida, CRC Press.

Hug, S. J. (1997). "In SituFourier Transform Infrared Measurements of Sulfate Adsorption on Hematite in Aqueous Solutions." *Journal of Colloid and Interface Science* **188**(2): 415-422.

Hunter, R. J. (1981). Zeta potential in colloid science, principles and applications. Sydney, Academic Press.

Iler, R. K. (1979). The chemistry of silica. New York, New York, John Wiley and Sons.

Johnson, K. L., A. Baker and D. A. C. Manning (2005). "Passive treatment of Mn-rich mine water: Using fluorescence to observe microbiological activity." *Geomicrobiology Journal* **22**(3-4): 141-149.

Johnson, S. B., G. E. Brown, T. W. Healy and P. J. Scales (2005). "Adsorption of organic matter at mineral/water interfaces. 6. Effect of inner-sphere versus outer-sphere adsorption on colloidal stability." *Langmuir* **21**(14): 6356-6365.

Junta, J. and M. F. Hochella (1994). "Manganese(II) Oxidation at Mineral Surfaces - a Microscopic and Spectroscopic Study." *Geochimica Et Cosmochimica Acta* **58**(22): 4985-4999.

Kabata-Pendias, A. and H. Pendias (2001). Trace elements in soils and plants. Boca Raton, CRC Press.

Karimi-Lotfabad, S., M. A. Pickard and M. R. Gray (1996). "Reactions of polynuclear aromatic hydrocarbons on soil." *Environmental Science & Technology* **30**(4): 1145-1151.

Khan, Z., P. Kumar and D. Kabir ud (2004). "Kinetics and mechanism of the reduction of colloidal manganese dioxide by d-fructose." *Colloids and Surfaces A: Physicochemical and Engineering Aspects* **248**(1-3): 25-31.

Kim, J. G., J. B. Dixon, C. C. Chusuei and Y. Deng (2002). "Oxidation of chromium(III) to (VI) by manganese oxides." *Soil Science Society of America Journal* **66**: 306-315.

Klausen, J., S. B. Haderlein and R. P. Schwarzenbach (1997). "Oxidation of substituted anilines by aqueous MnO_2: Effect of co-solutes on initial and quasi-steady-state kinetics." *Environmental Science & Technology* **31**(9): 2642-2649.

Klewicki, J. K. and J. J. Morgan (1999). "Dissolution of β-MnOOH particles by ligands: Pyrophosphate, ethylenediaminetetraacetate, and citrate." *Geochimica Cosmochima Acta* **63**: 3017-3024.

Kleyenstuber, A. S. E. (1984). "The mineralogy of the manganese-bearing Hotazel Formation of the Proterozoic Transvaal Sequence in Griqualand West, South Africa." *Transactions of the Geologocal Society of South Africa* **87**: 257-272.

Kohler, T., T. Armbruster and E. Libowitzky (1997). "Hydrogen Bonding and Jahn-Teller Distortion in Groutite,[alpha]-MnOOH, and Manganite,[gamma]-MnOOH, and Their Relations to the Manganese Dioxides Ramsdellite and Pyrolusite." *Journal of Solid State Chemistry* **133**(2): 486-500.

Konstantinou, I. K. and T. A. Albanis (2004). "TiO_2-assisted photocatalytic degradation of azo dyes in aqueous solution: kinetic and mechanistic investigations: A review." *Applied Catalysis B: Environmental* **49**(1): 1-14.

Kopinke, F.-D. and M. Remmler (1995). "Reactions of hydrocarbons during thermodesorption from sediments." *Thermochimica Acta* **263**: 123-139.

Kosower, E. M., P.-K. C. Huang and T. Tsuji (1969). "Diazenes. V. Aryldiazenes." *Journal of the American Chemical Society* **91**(9): 2325-2329.

Krauss, M. and W. Wilcke (2001). "Predicting Soil-Water Partitioning of Polycyclic Aromatic Hydrocarbons and Polychlorinated Biphenyls by Desorption with Methanol-Water Mixtures at Different Temperatures." *Environmental Science & Technology* **35**(11): 2319-2325.

Kumar, P. and Z. Khan (2005). "Oxidation of gum arabic by soluble colloidal MnO_2." *Carbohydrate Research* **340**(7): 1365-1371.

Laha, S. and R. G. Luthy (1990). "Oxidation of Aniline and Other Primary Aromatic-Amines by Manganese-Dioxide." *Environmental Science & Technology* **24**(3): 363-373.

Lasaga, A. C. (1981). Rate laws of chemical reactions. Kinetics of geochemical processes. Reviews in mineralogy, Vol. 8. A. C. Lasaga and R. J. Kirkpatrick. Washington, DC., Mineralogical Society America: p 1-68.

Li, G. T., J. H. Qu, X. W. Zhang, H. J. Liu and H. N. Liu (2006). "Electrochemically assisted photocatalytic degradation of Orange II: Influence of initial pH values." *Journal of Molecular Catalysis a-Chemical* **259**(1-2): 238-244.

Liu, H. J. and J. H. Qu (2002). "Decolorization of reactive bright red K2G dye: electrochemical process catalyzed by manganese mineral." *Water Science and Technology* **46**(11-12): 133-138.

Liu, R. X. and H. X. Tang (2000). "Oxidative decolorization of direct light red F3B dye at natural manganese mineral surface." *Water Research* **34**(16): 4029-4035.

Long, G. M. (1993). "Clean up hydrocarbon contamination effectively." *Chemical Engineering Progress*: 58-67.

Lopez-Avila, V., R. Young, J. Benedicto, P. Ho, R. Kim and W. F. Beckert (1995). "Extraction of organic pollutants from solid samples using microwave energy." *Analytical Chemistry* **67**(13): 2096-2102.

Lopez, C., A. G. Valade, B. Combourieu, M. Mielgo, B. Bouchon and J. M. Lema (2004). "Mechanism of enzymatic degradation of the azo dye Orange II determined by ex situ H-1 nuclear magnetic resonance and electrospray ionization-ion trap mass spectrometry." *Analytical Biochemistry* **335**(1): 135-149.

Lu, Y. P. and I. Hardin (2006). "Analysis of sulfonated azo dyes degraded by white rot fungus Pleurotus ostreatus." *Aatcc Review* **6**(1): 31-36.

Lucarelli, L., V. Nadtochenko and J. Kiwi (2000). "Environmental photochemistry: Quantitative adsorption and FTIR studies during the Ti-O_2 - photocatalysed degradation of Orange II." *Langmuir* **16**: 1102-1108.

Manceau, A., A. I. Gorshkov and V. A. Drits (1992). "Structural chemistry of Mn, Fe, Co, and Ni in manganese hydrous oxides: Part II. Information from EXAFS spectroscopy and electron and X-ray diffraction." *American Mineralogist* **77**: 1144-1157.

Manceau, A., S. Llorca and G. Calas (1987). "Crystal chemistry of cobalt and nickel in lithiophorite and asbolane from New Caledonia." *Geochimica Cosmochima Acta* **51**: 105-113.

Manceau, A., N. Tamura, R. S. Celestre, A. A. Macdowell, N. Geoffroy, G. Sposito and H. A. Padmore (2003). "Molecular-scale speciation of Zn and Ni in soil ferromanganese nodules from loess soils of the Mississippi basin." *Environmental Science and Technology* **37**: 75-80.

Manilal, V. B. and M. Alexander (1991). "Factors Affecting the Microbial-Degradation of Phenanthrene in Soil." *Applied Microbiology and Biotechnology* **35**(3): 401-405.

Matocha, C. J., D. L. Sparks, J. E. Amonette and R. K. Kukkadapu (2001). "Kinetics and mechanism of birnessite reduction by catechol." *Soil Science Society of America Journal* **65**(1): 58-66.

Maynard, J. B. (2004). Manganiferrous sediments, rocks and ores. Sediments, diagenesis and sedimentary rocks: Treaties on Geochemistry, Volume 7. F. T. Mckenzie. Amsterdam, Elsevier-Pergamon.

McArdell, C. S., A. T. Stone and J. Tian (1998). "Reaction of EDTA and related aminocarboxylate chelating agents with $Co^{III}OOH$ (heterogenite) and $Mn^{III}OOH$ (manganite)." *Environmental Scence and Technoogy.* **32**: 2923-2930.

McBride, M. B. (1979). "Chemisorption and Precipitation of Mn^{2+} at $CaCO_3$ Surfaces." *Soil Science Society of America Journal* **43**(4): 693-698.

McBride, M. B. (1994). Environmental Chemistry of Soils. New York, Oxford University Press.

McFarland, M. J. and R. C. Sims (1991). "Thermodynamic Framework for Evaluating PAH Degradation in the Subsurface." *Ground Water* **29**(6): 885-896.

McKenzie, R. M. (1980). "The adsorption of lead and other heavy metals on oxides of manganese and iron." *Australian Journal of Soil Research* **18**: 61-73.

McNally, D. L., J. R. Mihelcic and D. R. Lueking (1998). "Biodegradation of three- and four-ring polycyclic aromatic hydrocarbons under aerobic and denitrifying conditions." *Environmental Science & Technology* **32**(17): 2633-2639.

Means, J. C. (1995). "Influence of salinity upon sediment-water partitioning of aromatic hydrocarbons." *Marine Chemistry* **51**(1): 3-16.

Mentasti, E., E. Pelizzetti, E. Pramauro and G. Giraudi (1975). "Redox reaction of 1,2-dihydroxybenzene with Mn(III) in aqueous perchlorate media. Kinetics and mechanism." *Inorganica Chimica Acta* **12**(1): 61-65.

Mihelcic, J. R. and R. G. Luthy (1988). "Degradation of Polycyclic Aromatic Hydrocarbon Compounds under Various Redox Conditions in Soil-Water Systems." *Applied and Environmental Microbiology* **54**(5): 1182-1187.

Mittal, A., V. K. Gupta, A. Malviya and J. Mittal (2008). "Process development for the batch and bulk removal and recovery of a hazardous, water-soluble azo dye (Metanil Yellow) by adsorption over waste materials (Bottom Ash and De-Oiled Soya)." *Journal of Hazardous Materials* **151**(2-3): 821-832.

Mokrini, A., D. Ousse and E. Esplugas (1997). "Oxidation of aromatic compounds with UV radiation/ozone/hydrogen peroxide." *Water Science and Technology* **35**(4): 95-102.

Mortland, M. M. and K. V. Raman (1968). "Surface acidity of smectites in relation to hydration, exchangeable cation and structure." *Clays and Clay Minerals* **16**: 393-398.

Mueller, J. G., P. J. Chapman and P. H. Pritchard (1989). "Action of a Fluoranthene-Utilizing Bacterial Community on Polycyclic Aromatic Hydrocarbon Components of Creosote." *Applied and Environmental Microbiology* **55**(12): 3085-3090.

Murdoch, M. H., P. M. Chapman, D. M. Norman and V. M. Quintino (1997). "Spiking sediment with organochlorines for toxicity testing." *Environmental Toxicology and Chemistry* **16**(7): 1504-1509.

Murphy, E. M., J. M. Zachara and S. C. Smith (1990). "Influence of Mineral-Bound Humic Substances on the Sorption of Hydrophobic Organic-Compounds." *Environmental Science & Technology* **24**(10): 1507-1516.

Murray, J. W. (1974). "The surface chemistry of hydrous manganese dioxide." *Journal of Colloid and Interface Science* **46**: 357-371.

Murray, J. W., L. S. Balistrieri and B. Paul (1984). "The oxidation state of manganese in marine sediments and ferromanganese nodules." *Geochimica Cosmochima Acta* **48**: 1237-1247.

Murray, J. W. and J. G. Dillard (1979). "The oxidation of cobalt(II) adsorbed on manganese dioxide." *Geochimica Cosmochima Acta* **43**: 781-787.

Muruganandham, M. and M. Swaminathan (2006). "Photocatalytic decolourisation and degradation of Reactive Orange 4 by TiO_2-UV process." *Dyes and Pigments* **68**(2-3): 133-142.

Muthukumar, M. and N. Selvakumar (2004). "Studies on the effect of inorganic salts on decolouration of acid dye effluents by ozonation." *Dyes and Pigments* **62**(3): 221-228.

Nakamoto, K. (1997). Infrared and Raman Spectra of Inorganic and Coordination Compounds. Part B., John Wiley & Sons, New York, USA. .

Napola, A., M. D. R. Pizzigallo, P. Di Leo, M. Spagnuolo and P. Ruggiero (2006). "Mechanochemical approach to remove phenanthrene from a contaminated soil." *Chemosphere* **65**(9): 1583-1590.

Neaman, A., B. Waller, F. Mouele, F. Trolard and G. Bourrie (2004). "Improved methods for selective dissolution of manganese oxides from soils and rocks." *European Journal of Soil Science* **55**: 47-54.

Negra, C., D. S. Ross and A. Lanzirotti (2005). "Oxidizing behavior of soil manganese: Interactions among abundance, oxidation state, and pH." *Soil Science Society of America Journal* **69**(1): 87-95.

Neta, P. (1981). "Redox Properties of Free-Radicals." *Journal of Chemical Education* **58**(2): 110-113.

Nico, P. S. and R. J. Zasoski (2000). "Importance of Mn(III) availability on the rate of Cr(III) oxidation on delta-MnO_2." *Environmental Science & Technology* **34**(16): 3363-3367.

Nico, P. S. and R. J. Zasoski (2001). "Mn (III) center availability as a rate controlling factor in the oxidation of phenol and sulfide on delta-MnO_2." *Environmental Science & Technology* **35**(16): 3338-3343.

Northcott, G. L. and K. C. Jones (2001). "Partitioning, Extractability, and Formation of Nonextractable PAH Residues in Soil. 1. Compound Differences in Aging and Sequestration." *Environmental Science & Technology* **35**(6): 1103-1110.

Oakes, J. and P. Gratton (1998). "Kinetic investigations of the oxidation of Methyl Orange and substituted arylazonaphthol dyes by peracids in aqueous solution." *Journal of the Chemical Society-Perkin Transactions 2*(12): 2563-2568.

Parikh, S. J., B. J. Lafferty and D. L. Sparks (2008). "An ATR-FTIR spectroscopic approach for measuring rapid kinetics at the mineral/water interface." *Journal of Colloid and Interface Science* **320**(1): 177-185.

Pasti-Grigsby, M. B., A. Paszczynski, S. Goszczynski, D. L. Crawford and R. L. Crawford (1992). "Influence of Aromatic-Substitution Patterns on Azo Dye Degradability by Streptomyces Spp and Phanerochaete-Chrysosporium." *Applied and Environmental Microbiology* **58**(11): 3605-3613.

Pekkuz, H., I. Uzun and F. Guezel (2008). "Kinetics and thermodynamics of the adsorption of some dyestuffs from aqueous solution by poplar sawdust." *Bioresource Technology* **99**: 2009-2017.

Pena, J., O. W. Duckworth, J. R. Bargar and G. Sposito (2007). "Dissolution of hausmannite (Mn_3O_4) in the presence of the trihydroxamate siderophore desferrioxamine B." *Geochimica Et Cosmochimica Acta* **71**(23): 5661-5671.

Perez-Benito, J. F., C. Arias and E. Amat (1996). "A kinetic study of reduction of colloidal manganese dioxide by oxalic acid." *Journal of Colloid and Interface Science* **177**: 288-297.

Petrie, R. A., P. R. Grossl and R. C. Sims (2002). "Oxidation of pentachlorophenol in manganese oxide suspensions under controlled E-h and pH environments." *Environmental Science & Technology* **36**(17): 3744-3748.

Phillips, P., J. Bender, R. Simms, S. Rodriguezeaton and C. Britt (1995). "Manganese Removal from Acid Coal-Mine Drainage by a Pond Containing Green-Algae and Microbial Mat." *Water Science and Technology* **31**(12): 161-170.

Pizzigallo, M. D. R., A. Napola, M. Spagnuolo and P. Ruggiero (2004). "Mechanochemical removal of organo-chlorinated compounds by inorganic components of soil." *Chemosphere* **55**(11): 1485-1492.

Post, J. E. (1999). Manganese oxide minerals: Crystal structures and economic and environmental significance. Geology, Mineralogy and Human Welfare. Proceedings of the National Academy of Science ,Irvine, CA. **96:** 3447-3454.

Post, J. E. and D. L. Bish (1988). "Rietveld refinement of the todorokite structure." *American Mineralogist* **78**: 861-869.

Raber, B., I. Kogel-Knabner, C. Stein and D. Klem (1998). "Partitioning of polycyclic aromatic hydrocarbons to dissolved organic matter from different soils." *Chemosphere* **36**(1): 79-97.

Rafols, C. and D. Barcelo (1997). "Determination of mono- and disulphonated azo dyes by liquid chromatography atmospheric pressure ionization mass spectrometry." *Journal of Chromatography A* **777**(1): 177-192.

Ramstedt, M., B. M. Andersson, A. Shchukarev and S. Sjoberg (2004). "Surface properties of hydrous manganite (gamma-MnOOH). A potentiometric, electroacoustic, and X-ray photoelectron spectroscopy study." *Langmuir* **20**(19): 8224-8229.

Raveh, A. and Y. Avnimelech (1978). "The effect of drying on the colloidal properties of humic compounds." *Plant and Soil* **50**: 545-552.

Reddy, G. V. B., M. D. S. Gelpke and M. H. Gold (1998). "Degradation of 2,4,6-trichlorophenol by Phanerochaete chrysosporium: Involvement of reductive dechlorination." *Journal of Bacteriology* **180**(19): 5159-5164.

Regtop, R. A., P. T. Crisp, J. Ellis and C. J. R. Fookes (1986). "1-Pristene as a precursor for 2-pristene in pyrolysates of oil shale from Condor, Australia." *Organic Geochemistry* **9**(5): 233-236.

Regtop, R. A., J. Ellis, P. T. Crisp, A. Ekstrom and C. J. R. Fookes (1985). "Pyrolysis of model compounds on spent oil shales, minerals and charcoal : Implications for shale oil composition." *Fuel* **64**(12): 1640-1646.

Reid, B. J., G. L. Northcott, K. C. Jones and K. T. Semple (1998). "Evaluation of Spiking Procedures for the Introduction of Poorly Water Soluble Contaminants into Soil." *Environmental Science & Technology* **32**(20): 3224-3227.

Remmler, M. and F. D. Kopinke (1995). "Thermal conversion of hydrocarbons on solid matrices." *Thermochimica Acta* **263**: 113-121.

Riu, J., I. Schonsee, D. Barcelo and C. Rafols (1997). "Determination of sulphonated azo dyes in water and wastewater." *TrAC Trends in Analytical Chemistry* **16**(7): 405-419.

Ross, D. S. and R. J. Bartlett (1981). "Evidence for nonmicrobial oxidation of manganese in soil." *Soil Science* **132**: 153-160.

Ross, D. S., H.C. Hales, G. C. Shea-McCarthy and A. Lanzirotti (2001a). "Sensitivity of soil manganese oxides: Drying and storage cause reduction." *Soil Science Society of America Journal* **65**: 736-743.

Russell, G. A. and R. F. Bridger (1963). "Reactivity of Phenyl Radicals toward Molecular Oxygen." *Journal of the American Chemical Society* **85**(23): 3765-&.

Schlautman, M. A. and J. J. Morgan (1994). "Sorption of Perylene on a Nonporous Inorganic Silica Surface - Effects of Aqueous Chemistry on Sorption Rates." *Environmental Science & Technology* **28**(12): 2184-2190.

Schwarz, F. P. and S. P. Wasik (1976). "Fluorescence Measurements of Benzene, Naphthalene, Anthracene, Pyrene, Fluoranthene, and Benzo[E]Pyrene in Water." *Analytical Chemistry* **48**(3): 524-528.

Schwarzenbach, R. P. (1993). Environmental organic chemistry. New York ; Chichester, Wiley.

Shaul, G. M., T. J. Holdsworth, C. R. Dempsey and K. A. Dostal (1991). "Fate of Water-Soluble Azo Dyes in the Activated-Sludge Process." *Chemosphere* **22**(1-2): 107-119.

Shigwedha, N., Z. Z. Hua and J. Chen (2006). "Immobilizing TiO_2 allows H_2O_2 to be present at the start and enhances the photodegradation of acid yellow 36 (AY-36)." *Journal of Chemical Engineering of Japan* **39**(4): 475-480.

Shindo, H. and P. M. Huang (1984). "Catalytic Effects of Manganese(IV), Iron(III), Aluminum, and Silicon-Oxides on the Formation of Phenolic Polymers." *Soil Science Society of America Journal* **48**(4): 927-934.

Shindo, H. and P. M. Huang (1985). "Catalytic polymerization of hydroquinone by primary minerals." *Soil Science* **139**: 505-511.

Sleiman, M., D. Vildozo, C. Ferronato and J.-M. Chovelon (2007). "Photocatalytic degradation of azo dye Metanil Yellow: Optimization and kinetic modeling using a chemometric approach." *Applied Catalysis B: Environmental* **77**(1-2): 1-11.

Spadaro, J. T. and V. Renganathan (1994). "Peroxidase-Catalyzed Oxidation of Azo Dyes - Mechanism of Disperse Yellow-3 Degradation." *Archives of Biochemistry and Biophysics* **312**(1): 301-307.

Sparks, D. L. (2003). Environmental soil chemistry. Orlando, Florida, Academic Press.

Sperline, R. P., Y. Song and H. Freiser (1994). "Fourier-Transform Infrared Attenuated Total-Reflection Linear Dichroism Study of Sodium Dodecylbenzenesulfonate Adsorption at the Al2O3/Water Interface Using Al2O3-Coated Optics." *Langmuir* **10**(1): 37-44.

Stanton, D. T. (1987). "Glass-catalysed decomposition of oxycarboxin in aqueous solution." *Journal of Agricultural and Food Chemistry* **35**: 856-859.

Stone, A. T. (1986). "Adsorption of organic reductants and subsequent electron transfer on metal oxide surfaces." *ACS Symposia Ser.* **323**: 446-461.

Stone, A. T. (1987a). "Microbial metabolites and the reductive dissolution of manganese oxides: oxalate and pyruvate." *Geochimica Cosmochima Acta* **51**: 919-925.

Stone, A. T. (1987b). "Reductive Dissolution of Manganese(III/IV) Oxides by Substituted Phenols." *Environmental Science & Technology* **21**(10): 979-988.

Stone, A. T. and J. J. Morgan (1984a). "Reduction and dissolution of manganese(III) and manganese(IV) oxides by organics.1 Reaction with hydroquinone." *Environmental Science and Technology* **18**: 450-456.

Stone, A. T. and J. J. Morgan (1984b). "Reduction and dissolution of manganese(III) and manganese(IV) oxides by organics.2 Survey of the reactivity organics." *Environmental Science and Technology* **18**: 617-624.

Stylidi, M., D. I. Kondarides and X. E. Verykios (2003). "Pathways of solar light-induced photocatalytic degradation of azo dyes in aqueous TiO2 suspensions." *Applied Catalysis B-Environmental* **40**(4): 271-286.

Sweeney, E. A., J. K. Chipman and S. J. Forsythe (1994). "Evidence for Direct-Acting Oxidative Genotoxicity by Reduction Products of Azo Dyes." *Environmental Health Perspectives* **102**: 119-122.

Taylor, R. M., R. M. McKenzie and K. Norrish (1964). "The mineralogy and chemistry of manganes in some Australian soils." *Australian Journal of Soil Research* **2**: 235-248.

Tebo, B. M., J. R. Bargar, B. G. Clement, G. J. Dick, K. J. Murray, D. Parker, R. Verity and S. M. Webb (2004). "Biogenic manganese oxides: Properties and Mechanisms of Formation." *Annual Review of Earth and Planetary Sciences* **32**(1): 287-328.

Thompson, T. D. and W. F. Moll (1973). "Oxidative power of smectites measured by hydroquinone " *Clays and Clay Minerals* **21**: 337-350.

Tokashiki, Y., T. Hentona, M. Shimo and L. P. Vidhana Arachchi (2003). "Improvement of the successive selective dissolution procedure for the separation of birnessite, lithiophorite and goethite in soil manganese nodules." *Soil Science Society of America Journal* **67**: 837-834.

Tokashiki, Y., J.B. Dixon and D. C. Golden (1986). "Manganese oxide analysis in soils by combined X-ray diffraction and selective dissolution methods." *Soil Science Society of America Journal* **50**: 1079-1084.

Tombacz, E., C. Csanaky and E. Illes (2001). "Polydisperse fractal aggregate formation in clay mineral and iron oxide suspensions, pH and ionic strength dependence." *Colloid and Polymer Science* **279**(5): 484-492.

Tremblay, L., S. D. Kohl, J. A. Rice and J.-P. Gagne (2005). "Effects of temperature, salinity, and dissolved humic substances on the sorption of polycyclic aromatic hydrocarbons to estuarine particles." *Marine Chemistry* **96**(1-2): 21-34.

Tsikos, H. and J. M. Moore (2005). "Sodic metasomatism in the Palaeoproterozoic Hotazel iron-formation, Transvaal Supergroup, South Africa: implications for fluid-rock interaction in the Kalahari manganese field." *Geofluids* **5**(4): 264-271.

U.S.EPA (1996). "Manganese. Integrated Risk Information System (IRIS). U.S Environmental Protection Agency. Available from http://www.epa.gov/iris.Accessed 1/11/2005."

U.S.EPA (2003). "Health Effects Support Document for Manganese. U.S. Environmental Protection Agency. Available at http://www.epa.gov/safewater/ccl/pdf/manganese.pdf. Accessed 9/7/2005."

Ulrich, H. J. and A. T. Stone (1989). "Oxidation of Chlorophenols Adsorbed to Manganese Oxide Surfaces." *Environmental Science & Technology* **23**(4): 421-428.

Valli, K. and M. H. Gold (1991). "Degradation of 2,4-Dichlorophenol by the Lignin-Degrading Fungus Phanerochaete-Chrysosporium." *Journal of Bacteriology* **173**(1): 345-352.

Vanhulle, S., M. Trovaslet, E. Enaud, M. Lucas, S. Taghavi, D. Van Der Lelie, B. Van Aken, M. Foret, R. C. A. Onderwater, D. Wesenberg, S. N. Agathos, Y. J. Schneider and A. M. Corbisier (2008). "Decolorization, cytotoxicity, and genotoxicity reduction during a combined ozonation/fungal treatment of dye-contaminated wastewater." *Environmental Science & Technology* **42**(2): 584-589.

Viljoen, M. J. and W. U. Reimold (1999). An introduction to South Africa's geological and mining heritage. Johannesburg, South Africa, Mintek.

Vinodgopal, K., D. E. Wynkoop and P. V. Kamat (1996). "Environmental photochemistry on semiconductor surfaces: Photosensitized degradation of a textile azo dye, acid orange 7, on TiO_2 particles using visible light." *Environmental Science & Technology* **30**(5): 1660-1666.

Volkering, F., A. M. Breure, A. Sterkenburg and J. G. Vanandel (1992). "Microbial-Degradation of Polycyclic Aromatic-Hydrocarbons - Effect of Substrate Availability

on Bacterial-Growth Kinetics." *Applied Microbiology and Biotechnology* **36**(4): 548-552.

Wang, A. M., J. H. Qu, H. J. Liu and P. J. Lei (2006). "Dyes wastewater treatment by reduction-oxidation process in an electrochemical reactor packed with natural manganese mineral." *Journal of Environmental Sciences-China* **18**(1): 17-22.

Wariishi, H., L. Akileswaran and M. H. Gold (1988). "Manganese Peroxidase from the Basidiomycete Phanerochaete-Chrysosporium - Spectral Characterization of the Oxidized States and the Catalytic Cycle." *Biochemistry* **27**(14): 5365-5370.

Wariishi, H., K. Valli and M. H. Gold (1991). "Invitro Depolymerization of Lignin by Manganese Peroxidase of Phanerochaete-Chrysosporium." *Biochemical and Biophysical Research Communications* **176**(1): 269-275.

Wariishi, H., K. Valli and M. H. Gold (1992). "Manganese(Ii) Oxidation by Manganese Peroxidase from the Basidiomycete Phanerochaete-Chrysosporium - Kinetic Mechanism and Role of Chelators." *Journal of Biological Chemistry* **267**(33): 23688-23695.

Waters, W. A. (1971). "Mechanism of One-Electron Oxidation of Phenols - Fresh Interpretatioon of Oxidative Coupling Reactions of Plant Phenols." *Journal of the Chemical Society B-Physical Organic*(10): 2026-2029.

Weissenfels, W. D., H. J. Klewer and J. Langhoff (1992). "Adsorption of Polycyclic Aromatic-Hydrocarbons (Pahs) by Soil Particles - Influence on Biodegradability and Biotoxicity." *Applied Microbiology and Biotechnology* **36**(5): 689-696.

Wesenberg, D., I. Kyriakides and S. N. Agathos (2003). "White-rot fungi and their enzymes for the treatment of industrial dye effluents." *Biotechnology Advances* **22**(1-2): 161-187.

Whelan, G. and R. C. Sims (1995). "Mn-catalyzed oxidation of naphthalenediol." *Hazardous Waste & Hazardous Materials* **12**(4): 381-394.

Wiese, G. R. and T. W. Healy (1975). "Coagulation and Electrokinetic Behavior of TiO_2 and Al_2O_3 Colloidal Dispersions." *Journal of Colloid and Interface Science* **51**(3): 427-433.

Willumsen, B., M. R. Gray and M. J. Dudas (1997). "Biological degradation of anthracene in soil after sorption from non-aqueous phase liquids." *Environmental Technology* **18**(7): 755-762.

Wu, R. C., J. H. Qu and Y. S. Chen (2005). "Magnetic powder MnO-Fe_2O_3 composite - a novel material for the removal of azo-dye from water." *Water Research* **39**(4): 630-638.

Xyla, A. G., B. Sulzberger, G. W. Luther, J. G. Hering, P. Van Cappellen and W. Stumm (1992). "Reductive dissolution of manganese (III,IV) (hydr)oxides by oxalate: The effect of pH and light." *Langmuir* **8**: 95-103.

Zhang, H. C. and C. H. Huang (2003). "Oxidative transformation of triclosan and chlorophene by manganese oxides." *Environmental Science & Technology* **37**(11): 2421-2430.

Zhang, H. C. and C. H. Huang (2005). "Oxidative transformation of fluoroquinolone antibacterial agents and structurally related amines by manganese oxide." *Environmental Science & Technology* **39**(12): 4474-4483.

Zhang, H. C. and C. H. Huang (2005). "Reactivity and transformation of antibacterial N-oxides in the presence of manganese oxide." *Environmental Science & Technology* **39**(2): 593-601.

Zhang, S. J., H. Q. Yu and Q. R. Li (2005). "Radiolytic degradation of Acid Orange 7: A mechanistic study." *Chemosphere* **61**(7): 1003-1011.

Zhang, W., E. Bouwer, L. Wilson and N. Durant (1995). "Biotransformation of aromatic hydrocarbons in subsurface biofilms." *Water Science and Technology* **31**(1): 1-14.

Zhao, X., Y. Lu and I. Hardin (2005). "Determination of biodegradation products from sulfonated dyes by Pleurotus ostreatususing capillary electrophoresis coupled with mass spectrometry." *Biotechnology Letters* **27**(1): 69-72.

Zhao, X., Y. Lu, D. R. Phillips, H.-M. Hwang and I. R. Hardin (2007). "Study of biodegradation products from azo dyes in fungal degradation by capillary electrophoresis/electrospray mass spectrometry." *Journal of Chromatography A* **1159**(1-2): 217-224.

Ziechmann, W. (1959). "Die Darstellung von Huminsauren im heterogenen systen mit neutraler Reaktion." *Zeitschrift fur Pflanzenernaehrung Duenger* **84**: 155-159.

Zille, A., B. Gornacka, A. Rehorek and A. Cavaco-Paulo (2005). "Degradation of Azo Dyes by Trametes villosa Laccase over Long Periods of Oxidative Conditions." *Appl. Environ. Microbiol.* **71**(11): 6711-6718.

Zinder, B., G. Furrer and W. Stumm (1986). "The coordination chemistry of weathering: II. Dissolution of Fe(III) oxides." *Geochimica Cosmochima Acta* **50**: 1861-1869.

Appendix A.Manganese in waste and the environment

A.1. Manganese in the environment

A.1.1. Rocks and soils

Manganese is the twelfth most abundant element in the lithosphere comprising about 0.1% of the earths crust (Dixon and White, 2002; Concise International Chemical Assessment Document (CICADS), 2004). The Mn concentration in crustal rocks ranges from 350 to 2000 ppm (Kabata-Pendias and Pendias, 2001) and is generally highest in mafic rocks (Gilkes and McKenzie, 1988) and certain sedimentary rocks like dolomite. Manganese is present in minerals as Mn^{2+}, Mn^{3+} and Mn^{4+} ions. In primary minerals the dominant species is Mn^{2+}. Weathering and oxidation of primary minerals often result in the formation of Mn^{4+} and Mn^{3+} oxide minerals. Manganese oxides are the most common Mn bearing minerals in soils.

The Mn content of soils is quoted as ranging from <1 to 4000 mg/kg with mean values between 300-600 mg/kg (CICADS, 2004). The geochemistry of Mn in soils is similar to that of iron with Mn mobility being largely dependent on the pH and redox potential. Thus Mn is likely to be removed from acidic, organic rich soils and horizons and accumulate in alkaline, organic poor soils and horizons. Manganese concentration gradients commonly occur down soil profiles with the Mn from the topsoil being mobilized and redistributed to the lower part of the profile.

Manganese oxides are one of the most redox reactive constituents in soils. Their small particle size and large surface area allow them to impart a larger influence on soil chemistry than would be expected by their relative abundance (Bartlett, 1988). Manganese oxides have been implicated in the removal of harmful free radicals in soils (Bartlett, 1999) and in non-microbial oxidation of NH_4^+ to nitrate (Bartlett, 1981). Manganese oxides have been shown to act as catalysts for the breakdown and humification of organic matter (Shindo and Haung, 1984) and play an important role in

the formation of topsoils (Bartlett and James, 1994). The affinity for many trace elements is another important attribute of Mn oxides. Trace elements such as Ba, Cu, Co, Pb, Zn and Ni have been shown to be sequestered by Mn oxides (Mckenzie, 1980). This can have positive implications for contaminated soils and negative consequences for plant nutrition where important trace metals become unavailable. Manganese oxides have the capacity to oxidize inorganic ions such as Se, U, Cr, As and Co and organic molecules such as phenols and aromatic amines to quinone-type or polymeric products. These interactions can be favourable, as in the case of many organics and As, and unfavorable as in the case of Cr and U, which are rendered more mobile through oxidation.

There is little information on the concentration ranges of Mn in South African soils. An investigation into trace element compositions of a variety of soils from the Mpumalanga province showed Mn ranges of between 311 and 711 mg/kg (Steyn and Herselman, 2006). Soils derived from Chunniespoort dolomite are arguably some of the most Mn enriched soils in the world having Mn contents of up to 16% (Dowding, 2004). This manganiferous dolomite forms part of the Transvaal supergroup occurring along parts of the eastern escarpment and stretching from north of Zeerust to the western Witwatersrand. Although not all of the soils along this dolomite band have been investigated, studies on western Witwatersrand (Beukes et al., 1999) show that these soils are significantly enriched in Mn.

A.1.2. Plants

Manganese is an essential element in plant nutrition and can be present in soils at both deficient and phytotoxic concentrations. Manganese plays a pivotal role in photosynthesis and has been described by Bartlett (1999) as being the 'key to life' due to its involvement in the oxidation of H_2O and the generation of oxygen in the chloroplast.

For Mn to be available to plants it needs to be present in its soluble, divalent form. Plants vary greatly in their sensitivity to Mn concentration in solution with a sensitive species such as oat grass showing toxicity symptoms at 5 mg/L while marsh bent grass remains unaffected at 200 mg/L (Kabata-Pendias and Pendias, 2001). The uptake of Mn from the

soil also differs greatly amongst species; Loneragan (1996) showed that for the same soil the dry weight (DW) average of Mn ranged from 30 ppm for *Medicago trunculata* to 500 ppm (DW) in *Lupinus albus*. Worldwide background concentrations of Mn range from 17 to 334 ppm (DW) for grasses and from 25-119 ppm in clovers (Kabata-Pendias and Pendias, 2001). Plant foodstuffs contain variable amounts of Mn being the highest in beetroots (36 to 113 ppm). Cereal grains have a worldwide range of averages between 15 and 85 ppm (Kabata Pendias and Pendias, 2001). Members of the *Ericaceae* family, which includes blueberries, are regarded as Mn accumulators. There are numerous reports of foliar Mn levels in excess of 2000–4000 ppm, particularly for *Vaccinium angustifolium* and *V. vitis-idaea* (Korcak, 1988).

A.1.3. Water

Manganese is only readily soluble in its divalent state thus the Mn^{2+} ion is likely to be the dominant species found in surface and groundwaters. Factors that influence the solubility of Mn in water are the same that govern its solubility in soils. Surface freshwater data suggest that higher Mn concentrations occur during periods of higher stream flow, such as spring runoff, and lower concentrations tend to occur downstream of lakes that act as settling areas for sediment (CICAD, 2004). Acid mine waters often have high concentrations of soluble Mn while hard, carbonate rich waters are likely to have low Mn concentrations. The concentration of Mn in natural waters ranges between 0.01 to 10 mg/L but rarely exceeds 0.2 mg/L (CICADS 2004).

There is little data available on natural Mn concentrations in SA waters. Sanders et al. (1998) showed the level of Mn in the Potchefstroom dam, which is considered to be uncontaminated, to range between < 0.002 and 0.02 mg/L. The Germiston lake, which has a history of metal pollution, was shown to have an annual Mn range of <0.002 to 0.065 mg/L. The annual range of Mn in the Witbank dam is between 0.050 and 0.250 mg/L (Nussey et al., 2000). The higher concentrations in the Witbank dam are likely to be due to the impacts of surrounding industry.

A.2. Human toxicology

Manganese is an essential element for physiological health with adverse health effects observed with Mn deficiencies as well as toxicities. The most common route of human exposure to Mn is through food ingestion. The United States Environmental Protection Agency (U.S.EPA) suggests an appropriate Reference Dose (RfD) of 10mg Mn/day (U.S.EPA, 1996). Other channels of exposure to Mn are through drinking Mn rich water, inhalation of Mn dust and ingestion of soil containing Mn compounds.

It is thought that inhalation of excessive amounts of Mn dust has the most serious adverse health effect, and at comparable doses it has been shown that more Mn reaches the brain following inhalation than following ingestion (Gianutsos et al., 1992; Dorman et al., 2002). Chronic inhalation of Mn containing particulate has been associated with nervous system disorders in a Parkinson-like disease known as manganism (Couper, 1837). In comparison Mn ingested orally has low toxicity and reports of adverse effects by this route are rare (U.S.EPA, 2003b). There is limited data available on the effects of orally ingested Mn. One study in Greece (Kondakis et al., 1989) suggested that some neurological symptoms and Mn retention were apparent for people over 50 years old who had consumed water with 2 mg/L Mn over a lifetime. However, other exposure routes were not investigated in this study. In Germany a long-term drinking water study found no neurological effects in people over 50 who had ingested water with Mn concentrations of 0.3 to 2 mg/L for 10 years (Vieregge et al., 1995). In an extreme case a small Japanese community was exposed to drinking water with Mn concentrations as high as 29 mg/L for three months. Symptoms included lethargy, increased muscle tonus, tremor, mental disturbances and even death. The elderly were most severely affected, while 6 children (age 1-10) were not intoxicated (Kawamura et al., 1941).

Recently it has been suggested that inhalation of Mn containing water through the olfactory system during showering may be an important route for Mn to reach the central nervous system (Elsner and Spangler, 2005). These speculations are based on the extrapolation of data from the investigation of Brenneman et al. (2000) where rats were exposed to aerosolised water containing 277 mg/L $MnCl_2.H_2O$ (107 Mn mg/L). Using

this data Elsner and Spangler (2005) calculated that a daily 10 minute shower in water with a concentration of 0.5 mg/L Mn may lead to excessive Mn concentration entering the brain tissue. While the review of Elsner and Spangler (2005) raises some very important questions, an investigation using more relevant Mn concentrations would be needed to validate these extrapolations.

There is no information available on the carcinogenic effects of Mn and the U.S.EPA classifies Mn as a non-carcinogenic (2003b).

A.3. Ecotoxicology

Most ecotoxicological data is based on the aqueous Mn^{2+} ion. There is little published information on colloidal or complexed Mn but it is assumed that toxicity of the soluble species will be greater in most cases (CICAD, 2004).

The EC/LC_{50} for some of the most sensitive organisms according to the CICAD for Mn (CICAD, 2004) are listed in Table A-1. It is often observed that ecotoxicity is the greatest in soft waters, additions of lime or organic complexes can significantly reduce the ecotoxicity of Mn (CICAD, 2004). For this reason a range of EC/LC_{50} are given for certain organisms. From this data it would appear that the most sensitive organism is *Daphnia magna* (water flea) which has an EC_{50} range of between 0.8 mg/L to 76.3 mg/L depending on the water hardness (Riemer, 1999). Embryos of the yellow crab also appear to be sensitive to Mn concentration. Concentrations of between 0.01 and 10 mg/L resulted in 27 to 45% embryo mortality, however, the response was not concentration-dependent (Macdonald et al., 1988).

Ecotoxicity to plants in the terrestrial environment is highly variable, with critical dry plant tissue values ranging from 100 to 5000 mg/kg, and greatly influenced by the background concentration of Mn (CICAD, 2004).

Table A-1 Toxicity of Mn to aquatic species (taken from CICADS 2004)

Organism	Habitat	End-point	Mn concentration (mg/L)	Reference
Diatom (*Ditylum brightwelli*)	Marine	5-day EC_{50} (Growth inhibition)	1.5	Canterford & Canterford (1980)
Alga (*Scenedesmus quadricauda*)	Freshwater	12-day EC_{50} (Growth inhibition)	5	Fargašová et al. (1999)
Sea Urchin (*Heliocidaris tuberculata*)	Marine	72-h EC_{50} (abnormal larvae)	5.2	Doyle et al. (2003)
Daphnid (*Daphnis magna*)	Freshwater	48-h LC_{50}	0.8-76.3[a]	Reimer (1999)
Coho salmon (*Oncorhynchus kisutch*)	Freshwater	96-h LC_{50}	2.4-17.4[a]	Reimer (1999)

Setting a single guidance value for Mn in the various environments is recognized as having limited value due to the variety of parameters that have to be taken into account in association with Mn concentration in order to ascertain its toxicity (CICAD, 2004). Overall guidance values have been created using a problematic approach. An overall guidance value for the protection of 95% of marine species with 50% confidence was derived at 0.3 mg/L. The guidance value for freshwater species in soft waters is 0.2 mg/L. No guidance value is given for the terrestrial environment as it is recognized that background concentrations need to be taken into account.

A.4. Threshold levels of Mn in assessing contaminated land and waters

A.4.1. Land

Currently in South Africa there are no guidelines for the assessment of contaminated land. For this reason contaminated land studies are usually conducted using the various international guidelines as a reference. Sometimes the Acceptable Environmental Risk (AER) levels for compounds, as given in the Department of Water and Forestry's Minimum Requirements for the Handling, Classification and Disposal of Hazardous Waste (1998), are used to give guidance when assessing contaminated land. The AER

level for Mn is 0.3 mg/L in a leachate but this is non-enforceable as it is not a soil specific guideline.

In the USA the U.S.EPA's soil screening levels (SSLs) provide guidelines designed for making decisions on which sites need further attention and which sites do not. They have been conservatively compiled, with the vision of residential land use. There are two approaches to applying the SSL levels to soils: The more stringent generic SSLs can be used to assess a site making some conservative, default assumptions. Alternatively a more site specific approach can be employed whereby SSLs can be generated for each site using a specific risk based approach. Currently there is no generic SSL for Mn.

A set of eco-soil screening levels have been drawn up by the U.S.EPA (2003) with the aim of protecting terrestrial organisms, that are in contact with the soil, against exposure to certain contaminants. Manganese appears as one of the 17 metals being considered for inclusion; however, at present the specific guidelines surrounding Mn are pending.

In the United Kingdom risk to humans from contaminated land is characterised using the Contaminated Land Exposure Assessment (CLEA). The CLEA model uses a number of Soil Guideline Values (SGVs) which are given for priority contaminants. In compiling the list of contaminants it is stated that while it is recognized that any substance can be toxic given adequate quantities, only contaminants which are likely to pose a risk in relation to toxicity and abundance are listed. Manganese is not present in the current list of 10 metals which includes Ba, Be, Cd, Cr, Cu, Pb, Hg, Ni, V and Zn. The rationale for the omission of Mn from the list is stated as 'Soil Mn contamination may present a risk to the water environment because it may have deleterious effect on water supply due to colour and precipitation. It is not included because its moderate toxicity to human health in a contaminated land context would not often represent a significant hazard'.

No target or intervention level is given for Mn within the Dutch soil guidelines. Manganese is not listed within the Danish guidelines for contaminants and the French guidelines offer no numerical value for Mn. The Australian soil guidelines give a health investigation level of 1500 mg/kg for soils proposed for standard residential use and an interim ecotoxicological level of 500 mg/kg.

A.4.2. Water

The presence of Mn in waters can be problematic because of its tendency to precipitate and stain. This has often resulted in the guideline value for Mn being lower than that which will result in adverse health affects.

The target threshold levels for Mn given in the South African Water Quality guidelines are shown in Table A-2. The target levels for both domestic and industrial water use are set at the level for maintaining aesthetic water quality (Department of Water Affairs and Forestry, 1996 a and b), while the threshold for irrigation water is based on the accumulation of Mn to phytotoxic levels in the top 15 cm of the soil (Department of Water Affairs and Forestry, 1996c).

Table A-2 South African Water Quality Guideline Mn target threshold values for different water uses

Water use	Aquatic Environment	Aquaculture	Domestic	Industry	Livestock	Irrigation
Target threshold values ($mg.L^{-1}$)	0.18	0.1	0.05	0.05	10	0.02

Manganese levels in the various international drinking water quality guidelines are given in Table A-3. Manganese is listed on the U.S.EPA secondary drinking water standards. The secondary drinking water standards unlike the primary standards are non-enforceable guidelines regulating contaminants that may cause cosmetic effects (such as skin or tooth discoloration) or aesthetic effects (such as taste, odour, or colour) in drinking water. The secondary drinking water standard for Mn is 0.05mg/L, while the health reference level is 0.3 mg/L (U.S.EPA 2003b).

Table A-3 International drinking water quality guidelines

Standard	Concentration $mg.L^{-1}$
World Health Organization	0.5
European Union	0.05
U.S.EPA secondary drinking water standard	0.05
U.S.EPA Health based level	0.3
Australia	0.1

A.5. Waste characterisation and management

A.5.1. Sampling and mobility testing

Sampling and mobility testing of wastes is an important part of the waste characterization process. Artifacts can arise within the sampling and testing process that can result in misleading results. This is particularly important when analyzing samples for Mn. Manganese oxides are known to react to changes in their environment. When soils are air dried from their field moist state the amount of exchangeable Mn has been shown to increase significantly (Fujimoto and Sherman, 1945; Bartlett and James, 1979; Bartlett and James, 1980; Goldberg and Smith, 1984; Berndt, 1988; Haynes and Swift, 1991; Ross et al., 1994; Bunzl et al., 1999; Makino et al., 2000; Ross et al., 2001). Figure A-1 shows the increase in exchangeable Mn as a function of time and moisture content in soils left on the lab bench to dry for 7 days. This figure shows the significant influence soil moisture content has on the release of exchangeable Mn.

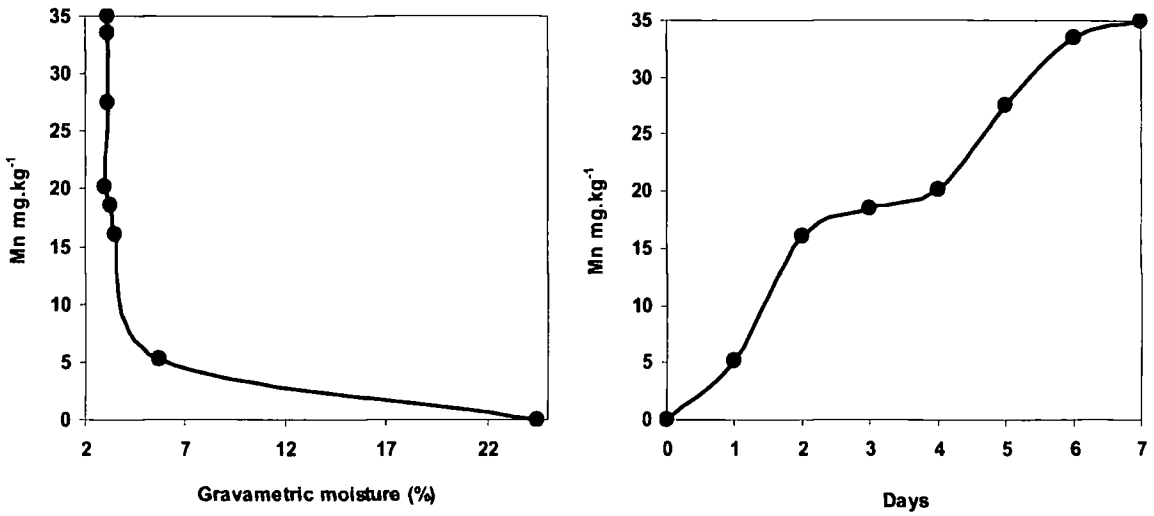

Figure A-1 Increase in exchangeable Mn, measured in 0.5 M $CaCl_2$, in air-dried soils as a function of time and gravimetric moisture content (taken from Dowding, 2004))

Sample crushing is also known to increase the concentration of exchangeable Mn in soils (Bartlett, 1980). While this phenomenon is well documented, many standard laboratory procedures require that soils be air dried, crushed and sieved prior to analysis. These procedures are also used by laboratories performing standard leaching procedures such as the TCLP (U.S.EPA 1311) and acid rain leach (Minimum Requirements for Handling, Classification and Disposal of Hazardous Waste, 1998). This drying phenomenon could result in erroneous, elevated concentrations of Mn in leachate studies. In ionic solutions such as a TCLP solution much of this drying induced exchangeable Mn may be released, which could possibly explain why the TCLP is often observed to be particularly aggressive towards Mn.

A.5.2. Overview of the South African Waste Management strategy

The South African Environmental Conservation Act requires that all wastes must be classified and disposed of according to the procedures outlined in the Department of Water Affairs and Forestry's "Minimum Requirements for the Handling, Classification and Disposal of Hazardous Waste". This document outlines the guidelines for determining if a waste classifies as 'general' or 'hazardous'. The 1998 guidelines have

recently been updated to a third edition, however, only a draft of the third edition (Minimum Requirements for the Handling, Classification and Disposal of Hazardous Wastes Draft (2005)) was available at the time of this review. This document will hereafter be referred to as Minimum Requirements.

A.5.2.1. Minimum Requirements for the Handling, Classification and disposal of Hazardous Wastes Draft (2005)

Within the minimum requirements the first approach to waste classification is to identify potentially hazardous wastes, from the generating process or industry. Potentially hazardous wastes are defined as:

- Products used in service industries that are classified as hazardous substances, e.g., solvents, grease and oil.
- Putrescible organic wastes, e.g., waste arising from production of edible oils, skins and other animal based products.
- Poisonous or toxic chemicals utilised in agriculture, forestry and related industries.
- Packaging materials contaminated with hazardous substances.
- Waste arising from hospitals, medical clinics, veterinary services and similar services.
- Pharmaceutical wastes.
- Residues such as ash, slags and leachate.
- Waste designated as Hazardous by the authorities.

A potentially hazardous waste then needs to be characterised and tested to determine if it has hazardous properties. The waste must be classified according to the nine hazard characteristics of the South African Bureau of Standards (SABS) Code 0228 "The Identification and Classification of Dangerous Substances and Goods". The hazard rating of the waste can then be determined based on the toxicity of the material. The hazard rating determines the type of landfill to which a waste can be disposed.

The SABS Code 0228 is a system for classifying hazardous substances for transport purposes. In the Code hazardous substances are given an identification number and divided into nine classes:

Class 1, Explosives

Class 2, Gases

Class 3, Flammable Liquids

Class 4, Flammable Solids

Class 5, Oxidising Substances and Organic Peroxides

Class 6, Toxic and Infectious Substances

Class 7, Radioactive Substances

Class 8, Corrosive Substances and

Class 9, Miscellaneous Dangerous Substances

In an environmental context Class 6: Toxic and Infectious substances must include acute mammalian toxicity (LD_{50}) as well as acute ecotoxicity (LC_{50}) data. The hazard rating of a waste is determined by its classification within Class 6. In the published guidelines (Minimum Requirements for the Handling, Classification and Disposal of Hazardous Waste, 1998) it was assumed that aquatic organisms are likely to be the most sensitive to contaminants therefore the hazard rating was determined by LC_{50} ranges. The short coming of this was certain compounds, like arsenic, were regulated at doses (0.4 mg/L) toxic to humans. In contrast, the Draft edition identifies that both humans and the environment need to be treated as end receptors. The values for the LD_{50} are generated from a Reference Dose (RfD) or a Tolerance Daily Intake (TDI). The subclasses of Class 6 together with the LC_{50} and LD_{50} are given in Table A-4.

Table A-4 Toxcity criteria used in determining the hazard rating of wastes according to the Minimum Requirements for the Handling, Classification and Disposal of Hazardous Waste (2005 draft)

Class 6 hazard status	Hazard Rating	Mammalian toxicity mg/kg	Ecotoxicity ranges for fish (96hr) in mg/L
Extreme Hazardous	HR1	$5>LD_{50}$	$1>LC_{50}$
High Hazardous	HR2	$5<LD_{50}<50$	$1<LC_{50}<10$
Moderate Hazardous	HR3	$50<LD_{50}<500$	$10<LC_{50}<100$
Low Hazard	HR4	$500<LD_{50}<5000$	$100<LC_{50}<1000$

The hazard rating, determined from the above table, is used to determine the type of landfill needed for disposal of the waste. Hazard ratings 1 and 2 can only be disposed of in H:H landfills while wastes with hazard ratings of 3 and 4 can be disposed of in either H:H or h:H landfills. The design and pollution control measures of H:H landfills are more stringent than that of h:H landfills.

The Acceptable Environmental Risk level of the 1998 guidelines is likely superseded by the Acceptable Exposure to the aquatic environment and Acceptable Exposure to human health (proposed in the draft guidelines). The Acceptable Exposure to the aquatic environment is calculated as being one tenth of the LC_{50} whilst the Acceptable Exposure to human health is calculated on the basis of the RfD or TDI using the formula:

$$\text{Acceptable Exposure to human health} = \text{TDI or RfD} \times \frac{70kg}{2l}$$

For Mn the LC_{50} is 3 mg/L and the RfD is 0.14 mg/kg thus the hazard rating (based on both the LC_{50} and LD_{50}) for Mn is HR 2. The acceptable exposure to the aquatic environment and to human health is 0.3 and 4.9 mg/L, respectively. The most conservative exposure concentration becomes the threshold therefore the acceptable exposure level for Mn is 0.3 mg/L. This threshold level is the same as the published value in the 1998 guidelines.

The estimated environmental concentration (EEC) represents the exposure by a hazardous substance should it leach into an underlying water body. The EEC of all compounds in a waste stream need to be determined and compared with Acceptable Exposure values to determine whether or not a waste exceeds a threshold concentration.

The EEC can be calculated in one of two ways: The first is to apply a generic equation based on a fixed, so called 'worst case', scenario where it is assumed that all hazardous substances in a waste will be leached into a water body 15 cm below the surface. It works on the assumption that ecosystems can handle a certain maximum load applied at a certain rate. Thus the equation for the EEC in µg/L is:

$$EEC(ppb) = \frac{dose(g/ha/month)}{Weight\ of\ \ underground\ \ body\ \ of\ water}$$

This simplifies to the formula:

$$EEC(ppb) = dose(g/ha/month) \times 0.66$$

where the dose represents the total amount in grams of a substance in the waste that can be disposed of on one hectare of the disposal site per month.

A site specific EEC can also be generated whereby site specific attenuation factors, such as waste treatment, mode of site operation, climatic conditions and engineering attributes in the form of covers, liners and leachate interception are taken into consideration.

If the EEC is calculated to be less than the lowest Acceptable Exposure level (AEL), 300 ppb for Mn, the waste can be delisted to a lower hazard rating. If the EEC exceeds the lowest AEL the waste remains in its hazard group and needs to be disposed of accordingly. The total amount of a constituent that can be disposed of per month can be calculated from the lowest AEL/0.66. For Mn this is 455 g/ha/month. The EEC is calculated using the total concentration of the constituent in the waste. Leaching tests such as the Toxicity Characteristic Leaching Procedure (TCLP) of the U.S.EPA and the Acid Rain test can be used if a particular waste is proved to be insoluble. The concentration of the constituent in the leachate is then used to calculate the EEC. The TCLP leach is used when the waste is proposed to be co-disposed with domestic waste, in which organic acids may be generated. The Acid Rain test is used when inorganic wastes are disposed of in a dedicated site and the likelihood of organic acids is low.

In an outline of the Draft 2005 guidelines it was made note of that the current mobility tests were being reviewed due to the apparent selectivity of the TCLP test for Mn. However, no mention of this was made in the Draft 2005 edition.

A.5.3. Overview of international waste management strategies

A.5.3.1. United States Environmental Protection Agency

The first federal law to address hazardous wastes in the USA was the Resource Conservation and Recovery Act (RCRA). The U.S. Environmental Protection Agency (U.S.EPA) developed a regulatory program to implement the RCRA. This resulted in U.S.EPA regulating waste generators, transporters, treatment, storage, and disposal facilities by implementing a three tiered approach to waste disposal. The Landfill Disposal Restrictions (LDR) regulations ensures that hazardous waste cannot be placed on the land until the waste meets specific treatment standards to reduce the mobility or toxicity of the hazardous constituents. The U.S.EPA expresses treatment standards either as required treatment technologies that must be applied to the waste or contaminant concentration levels that must be met. The Landfill Disposal Unit (LDU) regulations and Groundwater monitoring are the final two tiers of the regulatory programme. Only the LDR will be considered in this review.

To be considered as a hazardous waste a substance needs to fall within the definition of a solid waste which is defined as:

"Any garbage, refuse, sludge from a wastewater treatment plant, or air pollution control facility, and other discarded material, including solid, liquid, semisolid, or contained gaseous material, resulting from industrial, commercial, mining, and agricultural operations and from community activities."

A solid waste is considered hazardous if the following two conditions are met: first, solid wastes are hazardous wastes if they are listed by U.S.EPA as hazardous wastes in 40 CFR Part 261 Subpart D. Second, solid wastes are also hazardous wastes if they exhibit any of the following characteristics: ignitable, corrosive, reactive or toxic (based on the toxicity

leaching procedure). A waste that has been identified as hazardous must comply with the LDR regulations before being land filled. Since the physical and chemical composition of a waste significantly impacts the effectiveness of a given treatment technology, U.S.EPA divides the treatment standard for each waste code into two categories: wastewaters and non-wastewaters. The Agency defines these two categories based on the percentages of total organic carbon (TOC) and total suspended solids (TSS) present in a waste, since these factors commonly impact the effectiveness of treatment methods. Wastewaters contain less than one percent TOC by weight and less than one percent TSS by weight. Non-wastewaters include wastes that do not meet the definition of wastewater.

For metal containing wastes the toxicity characteristic is most relevant. There are only twelve metals which are listed on the Toxicity Characteristic list of contaminants. Manganese is not present in this list and therefore wastes will not be characterized as hazardous based on their Mn content.

In 2000, the U.S.EPA proposed listing a titanium dioxide non-wastewater stream in the inorganic chemicals industry, with Mn as one of the constituents for which it would be listed (65 FR55684-55782, September 14, 2000). Furthermore the U.S.EPA proposed that Mn be listed as a hazardous constituent and thus be added to the Treatment Standard for hazardous wastes and the Universal Treatment Standard (UTS) at concentrations of 17.1 mg/L for wastewaters and 3.6 mg/L (TCLP) for non-wastewaters. However, when the proposed rule was opened for public comment there was strong objection against the listing of Mn as a hazardous constituent. The various stakeholders opposed the proposal on the following grounds amongst others:

- The ubiquitous nature of Mn in the environment. With background levels of 40 to 900 mg/kg and an approximate mean of 300 mg/kg the U.S.EPA would be proposing a treatment standard that is well below concentration that Mn occurs in many natural soils.
- In contrast to inhaled Mn, ingested Mn has rarely been associated with toxicity. When ingested, Mn is considered to be among the least toxic of the trace elements and the proposed UTS for non-wastewaters of 3.6 mg/L TCLP is well below the

established safe threshold for human exposure represented by the RfD of 0.14 mg/kg-day (or 10 mg/day for the average 70 kg adult).

- Manganese does not appear to be a major chemical of concern for Superfund cleanups. The U.S.EPA's "Generic Soil Screening Levels (SSLs)" do not include a SSL for Mn. There are SSLs for 14 other metals, including antimony, arsenic, barium, beryllium, cadmium, chromium (total, III and VI), cyanide, lead, nickel, selenium, silver, thallium, vanadium and zinc, which demonstrates the low toxicity and lack of historical concern for Mn by the Agency at Superfund sites.
- There are no recommended values or ranges of dissolved Mn in the U.S.EPA's water quality standards.
- The proposed regulatory actions relevant to Mn would have far-reaching economic impacts not addressed in U.S.EPA's economic impact analysis.

The strong objections raised against the listing of Mn as a hazardous constituent resulted in the U.S.EPA deferring all decisions regarding Mn (Federal Register Vol 66 No 244, 20 November 2001). No further proposals to list Mn as a hazardous constituent have been made by the U.S.EPA.

A.5.3.2. European Union

The Hazardous Waste Directive (HWD, Council Directive 91/689/EC) was drawn up by the European Union to establish a European-wide definition of hazardous waste. The starting point of the HWD is to establish whether a waste is classified as hazardous or non-hazardous. The HWD defines hazardous waste as wastes featuring on a list drawn up by the European Commission, because they possess one or more of the 14 hazardous properties set out in the HWD. These properties are listed in Table A-5.

Table A-5 Fourteen hazardous waste properties of the European Hazardous Waste Directory

Hazard	Property
H1	Explosive
H2	Oxidising
H3A	Highly flammable
H3B	Flammable
H4	Irritant
H5	Harmful
H6	Toxic
H7	Carcinogenic
H8	Corrosive
H9	Infectious
H10	Toxic for reproduction
H11	Mutagenic
H12	Release toxic or very toxic gasses
H13	Substances and preparations capable by any means after disposal of yielding another substance e.g. Leachate, which possess any of the characteristics listed above
H14	Ecotoxic

To aid in decision making a comprehensive list of wastes was compiled which is known as the European Waste Catalogue (EWC). The latest revisions to the EWC were made in 2002 (EWC 2002). The EWC 2002 is intended to be a catalogue of all wastes, grouped according to generic industry, process or waste type. A number of wastes covered by hazardous entries on the EWC 2002 are deemed to be hazardous regardless of their composition or the concentration of any "dangerous substance" within the waste. Such entries have been termed "absolute entries". Wastes that have the potential to be either hazardous or non-hazardous depending on their actual composition and the concentrations of "dangerous substances" within the waste are known as "mirror entries": A "mirror entry" waste can be classified as hazardous if the threshold limit for a particular risk phrase is exceeded. Risk phrases are a classification given in the Approved Supply List (ASL), which prescribes hazard information and classification for many common chemicals.

Hazard rating for Mn

The most pertinent hazardous properties for Mn containing wastes are Hazards 5, 6, 13 and 14. The process of assigning a hazard class in these hazardous property groups needs to be understood to establish the hazard status of Mn containing wastes.

Hazards 5 and 6 are determined together and wastes can fall under the categories: Acutely toxic; Toxic; and Harmful. The characterization is based on toxicological data and each category has different risk phrases and threshold levels as summarized in Table A-6.

Table A-6 Limits for assigning hazards to Harmful and Toxic categories taken from the Environment Agency Technical Guidance WM2 (2005) Appendix C

Classification	Risk phrase	Thresholds for classification as hazardous	Limits for assigning hazard	
			H5: Harmful	H6: Toxic
Very toxic	R26, R27, R28 and combined risk phrases with or without R39	≥0.1%	0.1% ≤ total conc. < 7%	≥7%
Toxic	R23, R24, R25 and combined risk phrases with or without R39 or R48	≥3%	3% ≤ total conc. < 7%	≥25%
Harmful	R20, R21, R22, R65, Xn R68 and combined risk phrases with or without R48	≥25%	≥25%	n/a

n/a not applicable

For certain substances and preparations the limiting concentrations for hazard H13, may be calculated from the expected reaction and the likely concentration or production rate of new substance, like leachate, that will be produced. This can then be assessed against the available limits for hazards H1 to H12. Hazard 13 does not cover reactions that yield materials which are ecotoxic (H14).

Hazard 14 falls into four categories: Very toxic to aquatic organisms; Toxic to aquatic organisms; Harmful to aquatic organisms; and May cause long-term effects in the aquatic environment. The risk phrases and ecotoxicological data are summarized in Table A-7.

Table A-7 Classification for the aquatic environment as described in Environment Agency Technical Guidance WM2 (2005) Appendix C

Classification	Risk phrase	Ecotoxicological data
Very toxic to aquatic organisms	R50	96 hr LC50 (for fish): <1 mg/L; or 48 hr EC50 (for daphnia): <1 mg/L; or 72 hr IC50 (for algae): <1 mg/L
Toxic to aquatic organism	R51	96 hr LC50 (for fish): 1 mg/L < $LC_{50} \leq 10$ mg/L; or 48 hr EC50 (for daphnia): 1 mg/L < $EC_{50} \leq 10$ mg/L; or 72 hr IC50 (for algae): 1 mg/L < $IC_{50} \leq 10$ mg/L
Harmful to aquatic organisms	R52	96 hr LC50 (for fish): 10 mg/L < LC50 <100 mg/L; or 48 hr EC50 (for daphnia): 10 mg/L < EC50 < 100 mg/L; or 72 hr IC50 (for algae): 10 mg/L < IC50 < 100 mg/L
May cause long-term effects in the aquatic environment	R53	The substance is not readily degradable; or the log Pow ≥ 3.0 (unless the experimentally determined BCF ≤ 100)

Some of the risk phrases associated with aquatic toxicity are additive i.e. the concentrations of substances with the same and/or different risk phrases need to be added together to determine the correct classification for a preparation and subsequently the threshold concentration for determining whether the waste is hazardous by ecotoxicity. For example a substance with a risk phrase N: R50-R53 would be very toxic to aquatic organisms and may cause long term effects in the aquatic environment. Thus thresholds of additive risks must be complied. These are given in Table A-8.

Table A-8 Classification Criteria for classifying a waste as ecotoxic on the basis of aquatic toxicity taken from Environment Agency Technical Guidance WM2 (2005) Appendix C

Classification	Hazardous waste classification thresholds
Acute aquatic toxicity and long-term adverse effects	$\frac{\sum N:R50-R53}{0.25}+\frac{\sum N:R51-53}{2.5}+\frac{\sum R52-R53}{25}\geq 1$
Acute toxicity	$\sum N:R50-R53+\sum N:R50\geq 25$
Long-term adverse effects	$\sum N:R50-R53+\sum N:R51-R53+\sum R52-R53+\sum R53\geq 25$
Aquatic toxicity	$\sum R52\geq 25$

According to the ASL, Mn dioxide has the risk phrase R20/R22, Harmful: if inhaled or swallowed. According to Table A-6 a waste would need to contain 25% MnO_2 for it to be classified as hazardous. The system recognises no ecotoxicological risk associated with MnO_2.

In contrast Mn sulfate has two risk phrases: R48/R20/R22, Harmful: danger of severe damage to health by prolonged exposure through inhalation and if swallowed and R51/53: Toxic to aquatic organisms, may cause long-term adverse effects in the aquatic environment. According to Table A-6 a waste would only be considered as harmfully hazardous if the waste contained 25% Mn sulfate. The ecotoxic risk phrase for $MnSO_4$ falls within the toxic category with a LC_{50} of between 1 and 10 mg/L, it is also considered a persistent substance and so is allocated the risk phrase for long-term adverse effects. From Table A-8 it can be seen that Mn sulfate containing wastes can qualify as hazardous due to acute toxicity or through long-term adverse effects. For it to qualify for acute toxicity a waste needs to have a concentration of 2.5% $MnSO_4$ and to classify as hazardous with regard to long-term effects it needs to have a concentration of 25%; therefore the threshold for Mn sulfate concentration is 2.5% i.e. 25000 mg/kg (9105 mg $Mn.kg^{-1}$).

A.5.3.3. Basel Convention

The Basel Convention on the control of trans-boundary movements of hazardous wastes and their disposal was adopted in 1989 in response to concerns about toxic waste from industrialized countries being dumped in developing countries and countries with

economies in transition. In recent years the convention has focused on providing guidance for the management of hazardous wastes.

Wastes are generally classified on the basis of three waste lists given in Annex III, VIII and IX of the Basel Convention. Wastes contained in Annex VIII are characterized as hazardous, wastes under Annex IX are characterized as non-hazardous and Annex III is a list of hazardous characteristics which need to be considered even if a waste classifies as an Annex VIII or IX waste.

Manganese is not one of the nine listed metals in Annex VII that constitute to a waste being hazardous and none of the wastes streams in Annex VII are listed due to the presence of Mn. Metallic Mn scrap and spent Mn catalysts are amongst the waste listed in Annex IX which classify as non-hazardous. This means that the hazard status of Mn containing wastes will be determined by one or more of the 14 hazard characteristics listed in Appendix III.

The fourteen hazard characteristics in Annex III are essentially the same as those listed under the HWD of the European Union (Table A-5): H1- Explosive; H3- Flammable liquids; H4.1- Flammable solids; H4.2-substances prone to spontaneous combustion; H4.3 Substances, which in contact with water emit flammable gases; H5.1 Oxidising; H5.2 organic peroxides; H6.1 Poisonous (Acute); H6.2 Infections substances; H8 corrosive; H10 Substances which liberate toxic gasses in contact with water; H11 Toxic; H12 Ecotoxic and H13 Capable, by any means, after disposal, of yielding another material, e.g. leachate, which possess any of the characteristics listed above.

The most relevant to Mn containing materials are Hazard Characteristics H11- Toxic; H12:-Ecotoxic and H13-Capable of generating substances that display one or more of the 13 Hazardous Characteristics.

For hazards H11 and H12 a similar approach to the European Hazardous Waste Directive is taken using the same risk phrase and risk phrase thresholds. Thus Mn oxide will be classified as R20/R22/R48 and Mn sulfate as R20/R22/R48 and R51/R53. Under the

Basel Convention Mn sulfate will classify under H12 (ecotoxic) as chronic category 2, with the concentration threshold of 2.5% w/w.

The classification of a metal as persistent (R53) and therefore as chronically ecotoxic is based on the bioavailability of the metal in the aqueous environment (OECD, 2001). A metal that is rapidly removed from solution though sorption, precipitation etc will be less bioavailable than a metal that does not undergo rapid partitioning between the solid and aqueous phase. Divalent Mn is very soluble which is likely to account for its classification as persistent (R53) and therefore as chronically ecotoxic. Manganese oxide does not have a risk phrase for ecotoxicology.

The hazard group H13 is a relatively new addition to the hazard characteristics of Annex III. The capacity of a waste to generate hazardous leachate is one such scenario that would result in a waste being classified as hazardous under H13 category. There is no harmonized protocol laid out by the Basel Convention on how to analyse for hazardous leachates or threshold concentrations for constituents in the leachate. The approaches and leachate threshold concentrations of various countries are given in the interim guidelines on hazard characteristic H13 (Interim guidelines on hazard characteristic H13 of Annex III to the Basel Convention, 2005). The threshold leachate contaminant concentrations in guidelines from Canada, Thailand, Austria, Australia and Costa Rica are given as interim guidance. None of these countries list Mn as a contaminant. Both the Canadian and Australian approach is to apply a dilution attenuation factor (DAF) to drinking water guidelines to give concentration threshold values for TCLP leachate contaminants. In most cases the DAF is 100 so the maximum concentration of the toxic constituent in the waste can be one hundred times the drinking water standard or less without posing a hazard to human health due to the dilution that takes place before the water is consumed. It has been suggested that using the World Health Organization (WHO) drinking water standards may be appropriate to base an approach for harmonizing the threshold levels of contaminants in leachate. Applying a 100 DAF to these guideline values would result in the cut-off threshold concentration for Mn in a leachate being 50 mg/L.

A.6. Comparative approaches to Mn waste classification

The classification of Mn containing wastes differs significantly in the various international waste classification strategies. The Minimum Requirements of South Africa are by far the most conservative with relation to Mn. According to the U.S.EPA, wastes are not classified as hazardous on the basis of their Mn content. When Mn was being considered as a possible hazardous constituent the proposed threshold level for non-wastewaters was 3.6 mg/L in a TCLP test, which is 12 times higher than the Minimum Requirements Acceptable Exposure for the aquatic environment of 0.3 mg/L. The strong opposition against the listing of Mn resulted in the U.S.EPA deferring their decision on Mn and no further proposals have been made by the U.S.EPA.

The EU Directive classifies wastes based on their specific risk phrase. Unlike the U.S.EPA and the Minimum Requirement guidelines the EU directive recognizes the importance of speciation when determining the classification of Mn with $MnSO_4$ being more conservatively classified than Mn oxide. According to the risk phrase of $MnSO_4$ it is acutely toxic to aquatic organisms with long term effects. This corresponds to the LC_{50} of Mn falling between 1 and 10 mg/L and the fact that Mn^{2+} is fairly soluble. With this classification it is recommended that the maximum amount of Mn as $MnSO_4$ allowed in a waste before it is termed hazardous is 9105 mg/kg. Direct comparison of this value with the Minimum Requirements specification of 0.3 mg/L cannot be made easily because of the different units; however, supposing that the 0.3 mg/L is applied to a leachate concentration, using a 1:20 soil solution ratio, a value of 455 mg/L can be calculated from the European threshold for the same ratio assuming all the Mn was rendered soluble. While direct comparison of the two threshold concentrations should be made with some caution, it would appear that the EU Directive is significantly more lenient with respect to Mn.

Manganese is not one of the nine metals listed in Annex III of the Basel Convention or the EWC that render a waste hazardous. The Basel convention has only established interim guidelines for assessing the generation of hazardous leachate from waste. These guidelines are based on the approach of Austria, Australia, Canada, Thailand and Costa

Rica. None of these countries include Mn in their list of hazardous leachate constituents and if the WHO drinking water value for Mn were to be applied together with a DAF of 100 the allowable concentration of Mn in a leachate would be 50 mg/L. This again is significantly more lenient than the 0.3 mg/L given by Minimum Requirements.

A.7. Discussion and conclusions

Manganese is ubiquitous and can be present at both deficient and toxic concentrations in the environment. It is a difficult element to regulate because acceptable concentration thresholds are often exceeded in nature.

The harmful effects of inhaled Mn are well recognized but the effects of Mn ingestion are less understood. The possibility of Mn being inhaled through Mn laden shower water is an aspect of Mn toxicity that needs to be confirmed. The aquatic organisms appear to be the most sensitive to dissolved Mn but this sensitivity is highly dependent on factors such as total organic carbon and water hardness, which makes a single guideline value difficult to generate unless the worst case scenario is always assumed.

In the light of international guidelines, the South African approach towards Mn appears conservative, despite using universal ecotoxicological data. Minimum Requirements guidelines do not apply a dilution attenuation factor in devising threshold concentrations. Current Minimum Requirements guidelines would protect sensitive aquatic species if they were to be exposed to undiluted TCLP or acid rain leachate. According to the Acceptable Exposure Value of 300 ppb for Mn the maximum amount of Mn that can be disposed of in a leachate-controlled landfill is 454.5 g/ha/month. If the mean Mn concentration in natural soils is taken to be 300 mg/kg (CICAD, 2004) this maximum limit would only allow 1.5 tons of soil to be disposed of in a leachate-controlled landfill per month; a higher load would need to be disposed of in a H:H waste dump. While it is understood that when dealing with potential contaminants it is sensible to stand on the side of caution, the fate of Mn in the vadose zone and groundwater should be modeled to establish whether it is reasonable to accept 0.3 mg/L in a leachate as the limit to which an organism will be exposed.

A.8. References

Bartlett, R.J. 1981. Nonmicrobial nitrate to nitrite transformation in soils. Soil Science Society of America Journal. 45: 1054-1058.

Bartlett, R.J. 1988. Manganese redox reactions and organic interactions in soils, p. 59-73. In: D.G. Graham and et al. (eds.). Manganese in soils and plants. Kluwer Academic Publishers, Netherlands.

Bartlett, R.J. 1999. Characterizing soil redox reactions, p. 371-397. In: D.L. Sparks (ed.). Soil physical chemistry. CRC Press, Baco Raton, Florida.

Bartlett, R.J.and B.R. James. 1979. Behaviour of chromium in soils: III. Oxidation. Journal of Environmental Quality. 8: 31-35.

Bartlett, R.J.and B.R. James. 1980. Studying, dried stored soil samples - some pitfalls. Soil Science Society of America Journal. 44: 721-724.

Bartlett, R.J.and B.R. James. 1994. Redox chemistry in soils. Advances in Agronomy. 50: 151-208.

Berndt, G.F. 1988. Effect of drying and storage conditions upon extractable soil manganese. Journal of the Science of Food and Agriculture. 45: 119-130.

Beukes, N.J., H.S. van Niekerk, and J. Gutzmer. 1999. Post Gondwana African land surface and pedogenetic ferromanganese deposits on the Witwatersrand at the West Wits gold mine, South Africa. South African Journal of Geology. 102: 65-82.

Brenneman, K.A., B.A. Wong, M.A. Buccellato, E.R. Costa, E.A. Gross, and D.C. Dorman. 2000. Direct olfactory transport of inhaled manganese ($(MnCl_2)$-Mn-54) to the rat brain: Toxicokinetic investigations in a unilateral nasal occlusion model. Toxicology and Applied Pharmacology. 169: 238-248.

Bunzl, K., W. Schimmack, P. Schramel, and M. Suomela. 1999. Effects of sample drying and storage time on extraction of fallout Pu239+240, Cs-137 and natural Pb-210 as well as of stable Cs, Pb and Mn from soils. Analyst. 124: 1383-1387.

Canterford, G.S.and D.R. Canterford. 1980. Toxicity of Heavy-Metals to the Marine Diatom Ditylum-Brightwellii (West) Grunow - Correlation between Toxicity and Metal Speciation. Journal of the Marine Biological Association of the United Kingdom. 60: 227-242. Concise International Chemical

Assessment Document. 2004. Manganese and its compounds environmental aspects. Available at http://www.inchem.org/documents/cicads/cicads/cicad63.htm. Accessed 1/12/2005.

Couper, J. 1837. On the effects of black oxide of manganese when inhaled into the lungs. BRIT ANN MED PHARM. 1: 41-42.

Department of Water Affairs and Forestry. 1996 a. South African Water Quality Guidelines (second edition). Volume 1: Domestic Use.

Department of Water Affairs and Forestry. 1996 b. South African Water Quality Guidelines (second edition), Volume 3: Industrial Use.

Department of Water Affairs and Forestry. 1996c. South African Water Quality Guidelines (second edition). Volume 4: Agricultural Use: Irrigation.

Department of Water Affairs and Forestry. 1998. Waste Management Series. Minimum Requirements for the Handling, Classification and Disposal of Hazardous Waste.

Department of Water Affairs and Forestry. 2005. Waste Management Series. Minimum Requirements for the Handling, Classification and Disposal of Hazardous Waste.

Dixon, J.B.and G.N. White. 2002. Manganese oxides, p. 367-388. In: J.B. Dixon and D.G. Schulze (eds.). Soil mineralogy with environmental applications. Soil Science Society of America, Madison, Wisconsin.

Dorman, D.C., M.F. Struve, and B.A. Wong. 2002. Brain manganese concentrations in rats following manganese tetroxide inhalation are unaffected by dietary manganese intake. Neurotoxicology. 23: 185-195.

Dowding, C.E. 2004. Morphology, mineralogy and surface chemistry of manganiferous oxisols near Graskop,Mpumalanga Province, South Africa [MSc thesis] University of Stellenbosch, South Africa.

Doyle, C.J., F. Pablo, R.P. Lim, and R.V. Hyne. 2003. Assessment of metal toxicity in sediment pore water from Lake Macquarie, Australia. Archives of Environmental Contamination and Toxicology. 44: 343-350.

Elsner, R.J.F.and J.G. Spangler. 2005. Neurotoxicity of inhaled manganese: Public health danger in the shower? Medical Hypotheses. 65: 607-616.

Environment Agency. 2005. Technical Guidance WM2:Interpretation of the definition and classification of hazardous waste (Second Edition) available from http://publications.environment-agency.gov.uk/pdf/GEHO0603BIRB-e-e.pdf/. Accessed 30/11/2005.

Fargašová, A., B. A, and H. E. 1999. Ecotoxicological effects and uptake of metals (Cu+, Cu2+, Mn^{2+}, Mo^{6+}, Ni^{2+}, V^{5+}) in freshwater alg. Scenedesmus quadricauda. Chemosphere. 38: 1165-1173.

Fujimoto, C.K.and D. Sherman. 1945. The effect of drying, heating, and wetting on the level of exchangeable manganese in Hawaiian soils. Soil Science Society of America Proceedings. 10: 107-112.

Gianutsos, G.and M.T. Murray. 1982. Alterations in Brain Dopamine and Gaba Following Inorganic or Organic Manganese Administration. Neurotoxicology. 3: 75-82.

Gilkes, R.J.and R.M. McKenzie. 1988. Geochemistry and mineralogy of manganese in soils. In: R.D. Graham (ed.). Manganese in soils and plants. Kluwer Academic Publishers, Netherlands.

Goldberg, S.P.and K.A. Smith. 1984. Soil manganese: E Values, distribution of manganese-54 among soil fractions, and effects of drying. Soil Science Society of America Journal. 48: 559-564.

Haynes, R.J.and R.S. Swift. 1991. Concentrations of extractable Cu, Zn, Fe, and Mn in a group of soils as influenced by air-drying and oven-drying and wetting. Geoderma. 49: 319-333.

Kabata-Pendias, A.and H. Pendias. 2001. Trace elements in soils and plants. CRC Press, Boca Raton.

Kawamura, C.L., H. IKuta, and S. Fukuzimi. 1941. Intoxication be manganese in well water. Kitasato Arch. Exp. Med. 18: 145-169.

Kondakis, X.G., N. Makris, M. Leotsinidis, M. Prinou, and T. Papapetropoulos. 1989. Possible Health-Effects of High Manganese Concentration in Drinking-Water. Archives of Environmental Health. 44: 175-178.

Korcak, R.F. 1988. Response of Blueberry Species to Excessive Manganese. Journal of the American Society for Horticultural Science. 113: 189-193.

Loneragan, J.F. 1996. Mineral nutrition of higher plants, second edition : Horst Marschner. Academic Press, London. Field Crops Research. 46: 184-185.

Macdonald, J.M., J.D. Shields, and R.K. Zimmerfaust. 1988. Acute Toxicities of 11 Metals to Early Life-History Stages of the Yellow Crab Cancer-Anthonyi. Marine Biology. 98: 201-207.

Makino, T., S. Hasegawa, Y. Sakurai, S. Ohno, H. Maejima, and K. Momohara. 2000. Influence of soil-drying under field conditions on exchangeable manganese, colbalt, and copper contents. Soil Science and Plant Nutrition. 46: 581-590.

McKenzie, R.M. 1980. The adsorption of lead and other heavy metals on oxides of manganese and iron. Australian Journal of Soil Research. 18: 61-73.

Nussey, G., J.H.J. van Vuren, and H.H. du Preez. 2000. Bioaccumulation of chromium, manganese, nickel and lead in the tissues of the moggel, Labeo umbratus (Cyprinidae), from Witbank Dam, Mpumalanga. Water SA. 26: 269-284.

OECD Guidelines for testing and assessment Paris. 2001. Harmonised integrated classification system for human health and environmental hazards of chemical substances and mixtures. Available from http://www.oecd.org/ehs/. Accessed 15/11/05.

Reimer, P.S. 1999. Environmental effects of manganese and proposed freshwater guidelines to protect aquatic life in British Columbia [MSc thesis]. Vancouver, B.C., University of British Columbia [Cited by CICAD, 2004].

Ross, D.S., H.C. Hales, G.C. Shea-McCarthy, and A. Lanzirotti. 2001. Sensitivity of soil manganese oxides: Drying and storage cause reduction. Soil Science Society of America Journal. 65: 736-743.

Ross, D.S., T.R. Wilmot, and J. Larsen. 1994. Testing sugarbush soils- effects of sampling storage and drying. Communications in Soil Science and Plant Analysis. 25: 2899-2908.

Sanders, M.J., H.H. Du Preez, and J.H.J. Van Vuren. 1998. The freshwater river crab, Potamonautes warreni, as a bioaccumulative indicator of iron and manganese pollution in two aquatic systems. Ecotoxicology and Environmental Safety. 41: 203.

Shindo, H.and P.M. Huang. 1984. Catalytic Effects of Manganese(iv), Iron(iii), Aluminum, and Silicon-Oxides on the Formation of Phenolic Polymers. Soil Science Society of America Journal. 48: 927-934.

U.S.EPA. 1996. Manganese. Integrated Risk Information System (IRIS). U.S Environmental Protection Agency. Available from http://www.epa.gov/iris Accessed 1/11/2005.

U.S.EPA. 2003a. Guidance for Developing Ecological Soil Screening Levels. U.S Environmental Protection Agency. OSWER Directive 9285.7-55.

U.S.EPA. 2003b. Health Effects Support Document for Manganese. U.S. Environmental Protection Agency. Available at http://www.epa.gov/safewater/ccl/pdf/manganese.pdf. Accessed 9/7/2005.

Vieregge, P., B. Heinzow, G. Korf, H.M. Teichert, P. Schleifenbaum, and H.U. Mosinger. 1995. Long-Term Exposure to Manganese in Rural Well Water Has No Neurological Effects. Canadian Journal of Neurological Sciences. 22: 286-289.

Appendix B.X-ray diffraction patterns

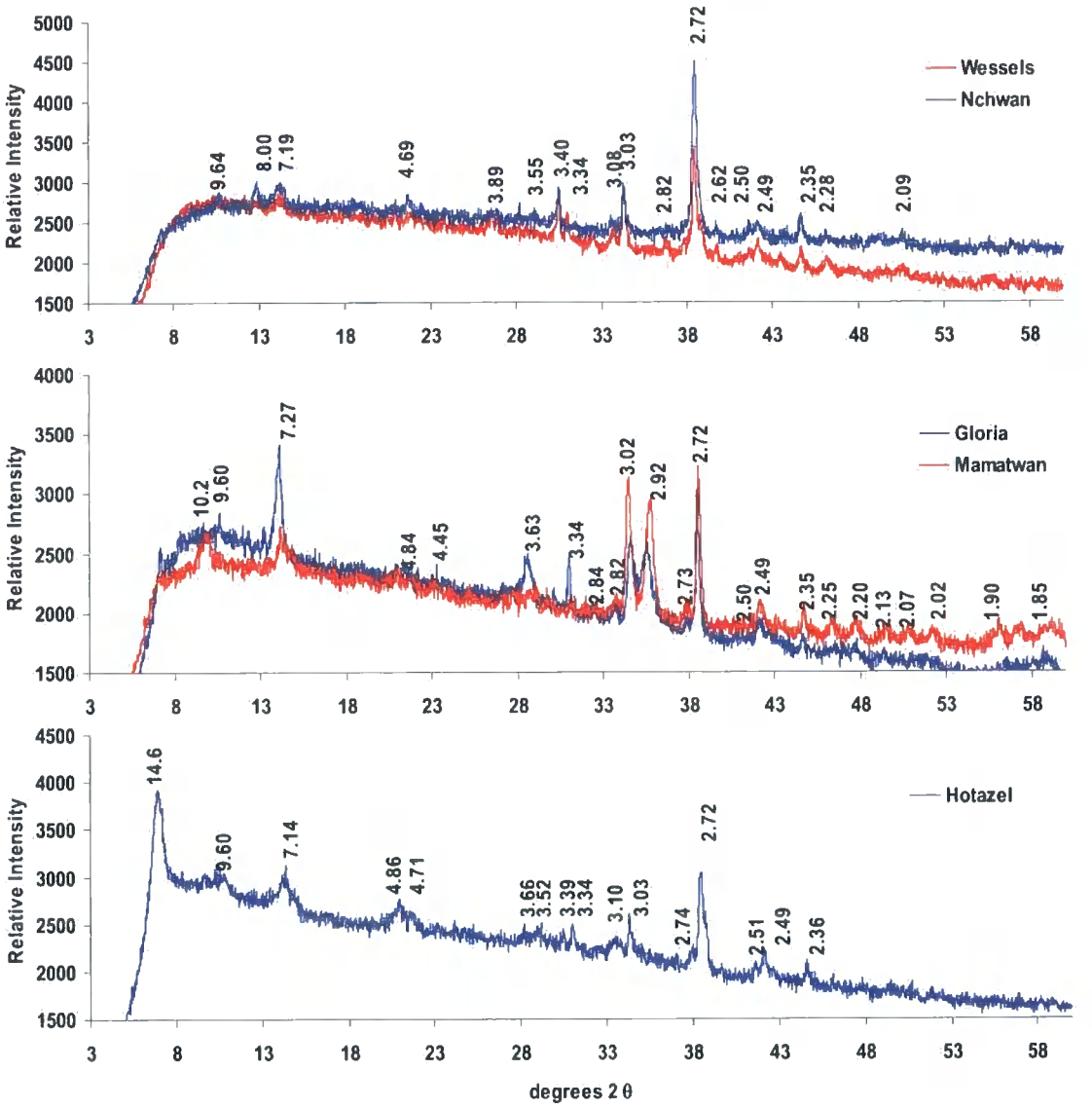

Figure B-1 X-ray diffraction patterns of the clay fraction from the Wessels type (Wessels and Nchwaning), Mamatwan type (Mamatwan and Gloria) and Hotazel type tailings.

Appendix C.Manganite characterization

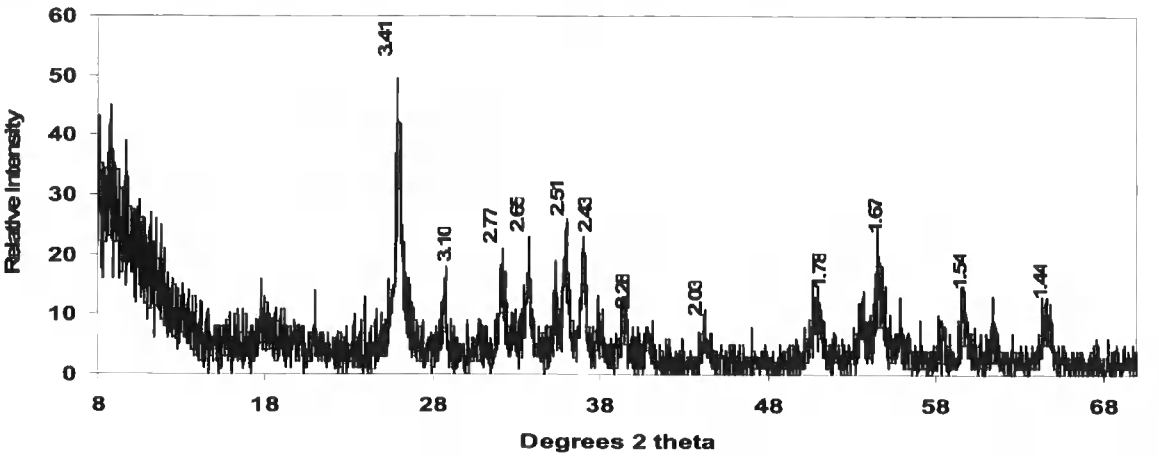

Figure C-1 X-ray diffraction pattern of synthetic manganite, peaks labelled with d-distances (Å)

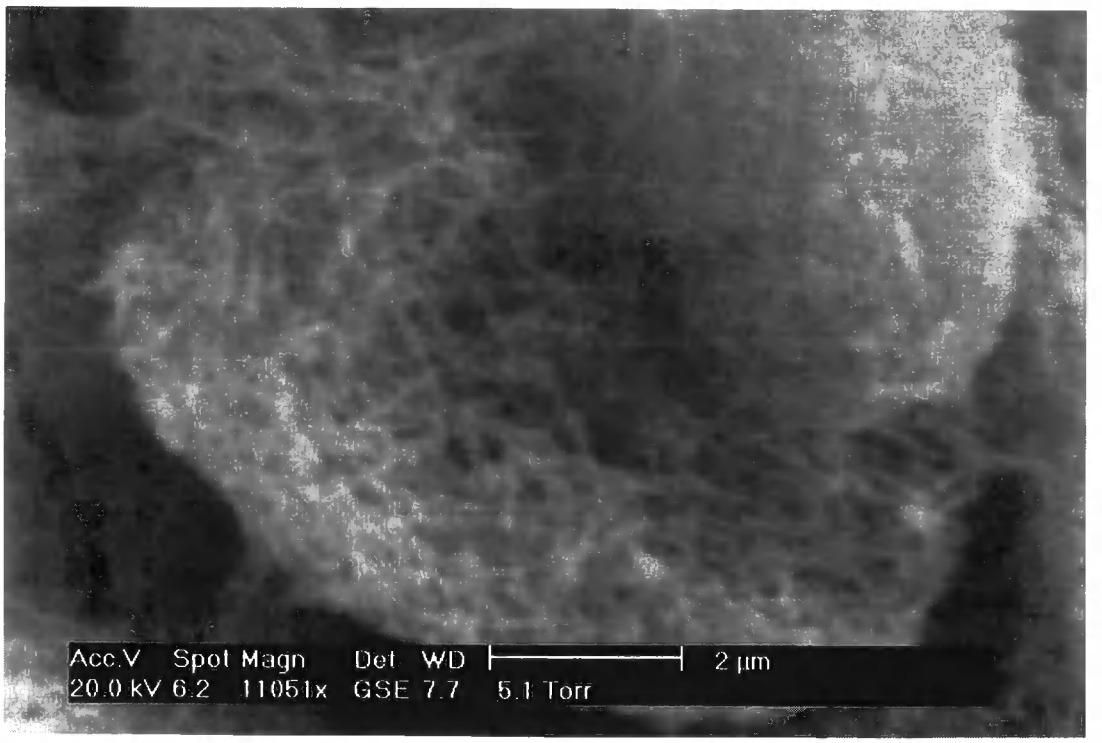

Figure C-2 Environmental scanning electron image of freeze dried synthetic manganite

Appendix D.Kinetic data

Table D-1 Average Mn concentrations (of three replicates) measured after reaction of HT tailings with pH 4, 0.14 mM AO 7 and pH 4 acetate blanks using surface area concentrations [SA] of 4.8, 12 and 48 $m^2.L^{-1}$. $[Mn]_{diss}$ calculated as difference between Mn released in dye treatments and Mn released in blank samples (s = standard deviation)

Time (min)	Dye (mM)	s	Blank (mM)	s	$[Mn]_{diss}$ (M)	s
[SA] = 48						
0.0	0.00E+00	0.00E+00	0.00E+00	0.00E+00	0.00E+00	0.00E+00
0.5	9.45E-03	5.14E-05	8.01E-03	1.26E-03	1.44E-06	1.26E-06
1.0	1.50E-02	2.19E-04	1.10E-02	1.40E-03	3.91E-06	1.42E-06
1.8	1.91E-02	2.57E-04	1.34E-02	1.12E-03	5.70E-06	1.15E-06
15.0	5.68E-02	3.99E-04	3.50E-02	1.52E-03	4.79E-05	1.57E-06
30.0	8.29E-02	4.47E-03	5.25E-02	3.95E-03	8.29E-05	5.97E-06
60.0	1.35E-01	1.94E-03	7.97E-02	5.82E-03	1.40E-04	6.13E-06
120.0	2.20E-01	6.31E-03	1.42E-01	1.18E-02	2.08E-04	1.34E-05
[SA] = 12						
0.0	0.00E+00	0.00E+00	0.00E+00	0.00E+00	0.00E+00	0.00E+00
0.5	3.13E-03	5.55E-04	2.47E-03	5.18E-04	6.55E-07	7.59E-07
1.0	4.72E-03	1.09E-03	3.99E-03	2.83E-04	7.33E-07	1.12E-06
1.8	5.80E-03	1.03E-03	5.16E-03	3.82E-04	6.36E-07	1.09E-06
30.0	3.41E-02	1.84E-03	1.87E-02	1.02E-03	1.54E-05	2.11E-06
60.0	5.56E-02	3.11E-03	2.83E-02	9.30E-04	2.73E-05	3.24E-06
120.0	8.94E-02	3.16E-03	3.47E-02	8.49E-03	5.48E-05	9.06E-06
[SA] = 4.8						
0.0	0.00E+00	0.00E+00	0.00E+00	0.00E+00	0.00E+00	0.00E+00
0.5	1.42E-03	1.82E-04	1.11E-03	0.00E+00	3.09E-07	1.82E-07
5.0	4.55E-03	7.19E-04	4.00E-03	5.09E-04	5.52E-07	8.81E-07
15.0	9.39E-03	8.47E-04	6.33E-03	9.28E-04	3.05E-06	1.26E-06
30.0	1.37E-02	9.56E-04	8.76E-03	1.15E-03	4.93E-06	1.49E-06
60.0	2.51E-02	4.82E-03	1.41E-02	1.94E-03	1.10E-05	5.19E-06
120.0	4.49E-02	2.81E-03	2.22E-02	2.76E-03	2.26E-05	3.94E-06

Table D-2 Average Mn concentrations (of three replicates) measured after reaction of HT tailings with pH 4, 0.14 mM AY 36 and pH 4 acetate blanks using surface area concentrations [SA] of 4.8, 12 and 48 $m^2.L^{-1}$. $[Mn]_{diss}$ calculated as difference between Mn released in dye treatments and Mn released in blank samples (s = standard deviation)

Time (min)	Dye (mM)	s	Blank (mM)	s	$[Mn]_{diss}$ (M)	s
[SA] = 48						
0.0	0.00E+00	0.00E+00	0.00E+00	0.00E+00	0.00E+00	0.00E+00
0.5	1.85E-02	1.10E-03	8.01E-03	1.26E-03	1.05E-05	1.67E-06
1.0	3.03E-02	8.63E-04	1.10E-02	1.40E-03	1.92E-05	1.65E-06
1.8	4.07E-02	1.75E-03	1.34E-02	1.12E-03	2.73E-05	2.08E-06
2.5	5.13E-02	3.72E-03	1.58E-02	1.60E-03	3.55E-05	4.04E-06
5.0	7.86E-02	6.50E-03	2.07E-02	8.66E-04	5.79E-05	6.56E-06
15.0	1.39E-01	8.99E-03	3.50E-02	1.52E-03	1.04E-04	9.12E-06
30.0	1.97E-01	1.31E-02	5.25E-02	3.95E-03	1.45E-04	1.37E-05
60.0	2.73E-01	1.85E-02	7.97E-02	5.82E-03	1.94E-04	1.94E-05
120.0	3.53E-01	1.64E-02	1.42E-01	1.18E-02	2.11E-04	2.02E-05
[SA] = 12						
0.0	0.00E+00	0.00E+00	0.00E+00	0.00E+00	0.00E+00	0.00E+00
0.5	6.96E-03	8.65E-04	2.47E-03	5.18E-04	4.49E-06	1.01E-06
1.0	1.40E-02	5.72E-04	3.99E-03	2.83E-04	1.00E-05	6.39E-07
1.8	2.05E-02	6.32E-04	5.16E-03	3.82E-04	1.54E-05	7.39E-07
15.0	6.99E-02	1.62E-03	1.02E-02	7.93E-04	5.97E-05	1.80E-06
30.0	1.17E-01	2.74E-03	1.87E-02	1.02E-03	9.84E-05	2.92E-06
60.0	1.78E-01	2.37E-03	2.83E-02	9.30E-04	1.50E-04	2.55E-06
120	2.66E-01	1.75E-02	3.47E-02	8.49E-03	2.31E-04	1.94E-05
[SA] = 4.8						
0	0.00E+00	0.00E+00	0.00E+00	0.00E+00	0.00E+00	0.00E+00
0.5	3.05E-03	0.00E+00	1.11E-03	0.00E+00	1.95E-06	0.00E+00
1	5.28E-03	3.40E-04	1.79E-03	4.31E-04	3.48E-06	5.49E-07
1.8	7.13E-03	5.83E-04	2.16E-03	4.11E-04	4.96E-06	7.13E-07
5	1.77E-02	6.88E-04	4.00E-03	5.09E-04	1.37E-05	8.56E-07
15	3.03E-02	1.83E-03	6.33E-03	9.28E-04	2.40E-05	2.05E-06
30	4.55E-02	4.92E-03	8.76E-03	1.15E-03	3.68E-05	5.05E-06
60	8.24E-02	1.02E-03	1.41E-02	1.94E-03	6.84E-05	2.19E-06
120	1.40E-01	2.32E-02	2.22E-02	2.76E-03	1.18E-04	2.34E-05

Table D-3 Average Mn concentrations (of three replicates) measured after reaction of HT tailings with pH 4, 0.07, 0.28 and 0.7 mM AO 7 and pH 4 acetate blanks; [SA] = 48 $m^2.L^{-1}$. $[Mn]_{diss}$ calculated as difference between Mn released in dye treatments and Mn released in blank samples (s = standard deviation)

Time (min)	Dye (M)	s	Blank (M)	s	$[Mn]_{diss}$ (M)	s
0.07 mM						
0.0	0.00E+00	0.00E+00	0.00E+00	0.00E+00	0.00E+00	0.00E+00
0.5	1.31E-05	8.28E-07	9.78E-06	6.56E-08	3.36E-06	8.30E-07
1.0	1.77E-05	5.01E-07	1.39E-05	1.03E-07	3.82E-06	5.11E-07
1.8	2.15E-05	8.92E-07	1.73E-05	7.32E-07	4.28E-06	1.15E-06
2.5	2.49E-05	1.18E-06	2.05E-05	0.00E+00	4.37E-06	1.18E-06
5.0	3.44E-05	8.88E-07	2.48E-05	1.27E-06	9.62E-06	1.55E-06
10.0	4.75E-05	1.67E-06	3.34E-05	1.50E-06	1.41E-05	2.25E-06
15.0	5.82E-05	1.82E-06	4.09E-05	1.65E-06	1.73E-05	2.46E-06
30.0	8.74E-05	2.32E-06	5.92E-05	1.74E-06	2.82E-05	2.90E-06
60.0	1.60E-04	5.10E-05	9.15E-05	2.74E-06	6.80E-05	5.10E-05
120.0	2.24E-04	2.79E-05	1.36E-04	7.31E-06	8.83E-05	2.88E-05
240.0	3.35E-04	5.10E-05	2.19E-04	1.18E-05	1.16E-04	5.23E-05
1080.0	9.46E-04	2.19E-05	7.04E-04	1.16E-05	2.42E-04	2.48E-05
0.28 (mM)						
0.0	0.00E+00	0.00E+00	0.00E+00	0.00E+00	0.00E+00	0.00E+00
0.5	1.17E-05	7.67E-07	9.78E-06	6.56E-08	1.88E-06	7.70E-07
1.0	1.69E-05	7.20E-07	1.39E-05	1.03E-07	3.02E-06	7.27E-07
1.8	2.15E-05	5.18E-07	1.73E-05	7.32E-07	4.27E-06	8.97E-07
2.5	2.51E-05	1.10E-06	2.05E-05	0.00E+00	4.55E-06	1.10E-06
5.0	3.83E-05	3.49E-06	2.48E-05	1.27E-06	1.35E-05	3.72E-06
15.0	6.82E-05	1.06E-05	4.09E-05	1.65E-06	2.73E-05	1.07E-05
30.0	1.07E-04	2.10E-05	5.92E-05	1.74E-06	4.76E-05	2.10E-05
60.0	1.81E-04	3.00E-05	9.15E-05	2.74E-06	8.96E-05	3.02E-05
120.0	2.64E-04	4.70E-05	1.36E-04	7.31E-06	1.28E-04	4.76E-05
240.0	4.41E-04	1.17E-04	2.19E-04	1.18E-05	2.22E-04	1.18E-04
360.0	5.89E-04	1.49E-04	3.15E-04	2.51E-05	2.74E-04	1.51E-04
1080.0	1.47E-03	3.28E-04	7.04E-04	1.16E-05	7.69E-04	3.28E-04
0.7 (mM)						
0.0	0.00E+00	0.00E+00	0.00E+00	0.00E+00	0.00E+00	0.00E+00
0.5	1.33E-05	7.71E-08	9.78E-06	6.56E-08	3.56E-06	1.01E-07
1.0	2.08E-05	2.01E-06	1.39E-05	1.03E-07	6.89E-06	2.01E-06
1.8	2.78E-05	4.06E-06	1.73E-05	7.32E-07	1.05E-05	4.13E-06
2.5	3.40E-05	5.63E-06	2.05E-05	0.00E+00	1.35E-05	5.63E-06
5.0	5.21E-05	8.28E-06	2.48E-05	1.27E-06	2.73E-05	8.38E-06
15.0	1.03E-04	1.27E-05	4.09E-05	1.65E-06	6.17E-05	1.28E-05
30.0	1.65E-04	1.53E-05	5.92E-05	1.74E-06	1.06E-04	1.54E-05
60.0	2.40E-04	2.01E-06	9.15E-05	2.74E-06	1.48E-04	3.39E-06
120.0	4.30E-04	0.00E+00	1.36E-04	7.31E-06	2.93E-04	7.31E-06

Table D-4 Average Mn concentrations (of three replicates)measured after reaction of HT tailings with pH 4, 0.07, 0.28 and 0.7 mM AO 7 and pH 4 acetate blanks; [SA] = 48 $m^2.L^{-1}$. $[Mn]_{diss}$ calculated as difference between Mn released in dye treatments and Mn released in blank samples (s = standard deviation)

Time (min)	Dye (M)	s	Blank (M)	s	$[Mn]_{diss}$ (M)	s
0.07(mM)						
0	0.00E+00	0.00E+00	0.00E+00	0.00E+00	0.00E+00	0.00E+00
0.5	1.66E-05	2.22E-06	9.78E-06	6.56E-08	6.87E-06	2.22E-06
1	2.78E-05	2.22E-06	1.57E-05	1.03E-07	1.21E-05	2.22E-06
1.8	3.63E-05	1.85E-06	1.73E-05	7.32E-07	1.91E-05	1.99E-06
2.5	4.54E-05	4.22E-06	1.96E-05	0.00E+00	2.58E-05	4.22E-06
5	7.20E-05	6.70E-06	2.48E-05	1.27E-06	4.72E-05	6.82E-06
10	1.07E-04	6.54E-06	3.34E-05	1.50E-06	7.31E-05	6.71E-06
15	1.30E-04	5.49E-06	4.09E-05	1.65E-06	8.92E-05	5.74E-06
30	1.85E-04	4.03E-06	5.92E-05	1.74E-06	1.26E-04	4.39E-06
60	2.50E-04	4.05E-06	9.15E-05	2.74E-06	1.59E-04	4.89E-06
120	3.35E-04	1.17E-05	1.36E-04	7.31E-06	1.99E-04	1.38E-05
0.14 (mM)						
0	0.00E+00	0.00E+00	0.00E+00	0.00E+00	0.00E+00	0.00E+00
0.5	1.85E-05	1.10E-06	8.01E-06	1.26E-06	1.05E-05	1.67E-06
1	3.03E-05	8.63E-07	1.10E-05	1.40E-06	1.92E-05	1.65E-06
1.8	4.07E-05	1.75E-06	1.34E-05	1.12E-06	2.73E-05	2.08E-06
2.5	5.13E-05	3.72E-06	1.58E-05	1.60E-06	3.55E-05	4.04E-06
5	7.86E-05	6.50E-06	2.07E-05	8.66E-07	5.79E-05	6.56E-06
15	1.39E-04	8.99E-06	3.50E-05	1.52E-06	1.04E-04	9.12E-06
30	1.97E-04	1.31E-05	5.25E-05	3.95E-06	1.45E-04	1.37E-05
60	2.73E-04	1.85E-05	7.97E-05	5.82E-06	1.94E-04	1.94E-05
120	3.53E-04	1.64E-05	1.42E-04	1.18E-05	2.11E-04	2.02E-05

Table 4-D continued

Time (min)	Dye (M)	sd	Blank (M)	sd	$[Mn]_{diss}$ (M)	sd
0.7 mM						
0	0.00E+00	0.00E+00	0.00E+00	0.00E+00	0.00E+00	0.00E+00
0.5	5.18E-05	6.90E-06	9.78E-06	6.56E-08	4.20E-05	6.90E-06
1	7.97E-05	5.93E-06	1.57E-05	1.03E-07	6.40E-05	5.94E-06
1.8	1.03E-04	1.03E-05	1.73E-05	7.32E-07	8.54E-05	1.03E-05
2.5	1.23E-04	1.29E-05	1.96E-05	0.00E+00	1.04E-04	1.29E-05
5	1.71E-04	1.80E-05	2.48E-05	1.27E-06	1.46E-04	1.81E-05
10	2.38E-04	2.71E-05	3.34E-05	1.50E-06	2.04E-04	2.71E-05
15	2.77E-04	3.38E-05	4.09E-05	1.65E-06	2.36E-04	3.38E-05
30	4.03E-04	5.08E-05	5.92E-05	1.74E-06	3.44E-04	5.08E-05
60	6.20E-04	5.87E-05	9.15E-05	2.74E-06	5.29E-04	5.87E-05
120	8.49E-04	1.43E-04	1.36E-04	7.31E-06	7.13E-04	1.44E-04
0.28 (mM)						
0	0.00E+00	0.00E+00	0.00E+00	0.00E+00	0.00E+00	0.00E+00
0.5	3.36E-05	5.10E-06	9.78E-06	6.56E-08	2.38E-05	5.10E-06
1	6.19E-05	6.39E-06	1.57E-05	1.03E-07	4.62E-05	6.39E-06
1.8	9.52E-05	1.92E-05	1.73E-05	7.32E-07	7.79E-05	1.92E-05
2.5	1.18E-04	2.99E-05	1.96E-05	0.00E+00	9.85E-05	2.99E-05
15	2.84E-04	3.32E-05	4.09E-05	1.27E-06	2.43E-04	3.32E-05
30	4.14E-04	4.81E-05	5.92E-05	1.50E-06	3.55E-04	4.81E-05
60	5.39E-04	6.10E-05	9.15E-05	1.65E-06	4.48E-04	6.10E-05
120	6.96E-04	6.02E-05	1.36E-04	1.74E-06	5.60E-04	6.02E-05

Table D-5 Average Mn concentrations (of three replicates) measured after reaction of HT tailings with pH 4, pH 5 and pH 6, 0.14 mM AY 36 solutions and the corresponding acetate blanks; [SA] = 48 $m^2.L^{-1}$. $[Mn]_{diss}$ calculated as difference between Mn released in dye treatments and Mn released in blank samples (s = standard deviation)

Time (min)	Dye (M)	s	Blank (M)	s	$[Mn]_{diss}$ (M)	s
pH 4						
0.0	0.00E+00	0.00E+00	0.00E+00	0.00E+00	0.00E+00	0.00E+00
0.5	1.85E-05	1.10E-06	5.00E-04	8.01E-06	1.26E-06	1.05E-08
1.0	3.03E-05	8.63E-07	1.00E-03	1.10E-05	1.40E-06	1.92E-08
1.8	4.07E-05	1.75E-06	1.80E-03	1.34E-05	1.12E-06	2.73E-08
2.5	5.13E-05	3.72E-06	2.50E-03	1.58E-05	1.60E-06	3.55E-08
5.0	7.86E-05	6.50E-06	5.00E-03	2.07E-05	8.66E-07	5.79E-08
15.0	1.39E-04	8.99E-06	1.50E-02	3.50E-05	1.52E-06	1.04E-07
30.0	1.97E-04	1.31E-05	3.00E-02	5.25E-05	3.95E-06	1.45E-07
60.0	2.73E-04	1.85E-05	6.00E-02	7.97E-05	5.82E-06	1.94E-07
120.0	3.53E-04	1.64E-05	1.20E-01	1.42E-04	1.18E-05	2.11E-07
pH 5						
0.0	0.00E+00	0.00E+00	0.00E+00	0.00E+00	0.00E+00	0.00E+00
0.5	5.74E-06	1.89E-06	4.60E-06	4.23E-07	1.14E-06	1.89E-06
1.0	1.18E-05	4.62E-07	6.78E-06	4.60E-07	5.07E-06	4.62E-07
2.0	1.50E-05	3.74E-07	8.04E-06	7.98E-07	7.01E-06	3.74E-07
2.5	2.15E-05	2.72E-07	9.70E-06	1.27E-06	1.18E-05	2.72E-07
5.0	2.88E-05	8.22E-07	1.14E-05	1.31E-06	1.74E-05	8.22E-07
10.0	4.24E-05	2.89E-06	1.40E-05	2.19E-06	2.84E-05	2.89E-06
15.0	5.52E-05	2.51E-06	1.76E-05	3.51E-06	3.76E-05	2.51E-06
30.0	8.47E-05	7.28E-06	2.76E-05	3.92E-06	5.71E-05	7.28E-06
60.0	1.21E-04	1.42E-05	4.11E-05	8.39E-06	7.95E-05	1.42E-05
120.0	1.64E-04	2.35E-05	6.69E-05	2.08E-05	9.66E-05	2.35E-05
pH 6						
0.0	0.00E+00	0.00E+00	0.00E+00	0.00E+00	0.00E+00	0.00E+00
0.5	2.21E-06	6.39E-08	2.21E-06	1.00E-07	6.06E-09	6.39E-08
1.0	4.20E-06	2.38E-07	3.08E-06	7.57E-08	1.12E-06	2.38E-07
2.0	5.29E-06	2.82E-07	3.59E-06	1.38E-07	1.70E-06	2.82E-07
2.5	5.65E-06	2.18E-07	3.85E-06	1.39E-07	1.81E-06	2.18E-07
10.0	8.95E-06	1.20E-06	5.70E-06	3.38E-07	3.25E-06	1.20E-06
15.0	1.16E-05	8.76E-07	5.98E-06	6.67E-07	5.58E-06	8.76E-07
30.0	1.53E-05	8.71E-07	7.33E-06	5.37E-07	7.94E-06	8.71E-07
60.0	2.11E-05	1.14E-06	9.02E-06	9.62E-07	1.21E-05	1.14E-06
120.0	3.01E-05	1.97E-06	1.27E-05	1.61E-06	1.74E-05	1.97E-06
360.0	4.69E-05	1.72E-06	2.10E-05	8.20E-07	2.59E-05	1.72E-06

Table D-6 Statistical data for testing the significance of the slope (rate order) for AO 7 reactions

[SA]

x	$(x_i-x_{av})^2$	y	ŷ	yi-ŷ	$(yi-ŷ)^2$	sy/x	sb	V'b	t-value (f=2)
1.569	1.151	-15.425	-15.488	0.063	0.004	0.131	0.080	0.003	3.367
2.485	0.025	-14.509	-14.402	-0.107	0.011				
3.871	1.512	-12.717	-12.759	0.042	0.002				
x_{av} =2.642		$\sum(x_i-x_{av})^2$ = 2.689				$\sum(yi-ŷ)^2$ =0.017			

[AO 7]

x	$(x_i-x_{av})^2$	y	ŷ	yi-ŷ	$(yi-ŷ)^2$	sy/x	sb	V'b	t-value (f=2)
-7.696	1.512	-13.816	-13.852	0.037	0.001	0.115	0.070	0.002	8.286
-5.394	1.151	-12.429	-12.485	0.056	0.003				
-6.310	0.025	-13.122	-13.029	0.093	0.009				
x_{av} =-6.467		$\sum(x_i-x_{av})^2$ = 2.689				$\sum(yi-ŷ)^2$ =0.0132			

Table D-7 Statistical data for testing the significance of the slope (rate order) for AY 36 reactions

[SA]

x	$(x_i-x_{av})^2$	y	ŷ	yi-ŷ	$(yi-ŷ)^2$	sy/x	sb	V'b	t-value (f=2)
1.569	1.151	-12.717	-12.581	-0.136	0.018	0.279	0.170	0.014	1.631
2.485	0.025	-11.618	-11.844	0.226	0.051				
3.871	1.512	-10.820	-10.730	0.090	0.008				
X_m = 2.641		$\sum(x_i-x_m)^2$ = 2.687				$\sum(yi-ŷ)^2$ =0.077			

[AY36]

x	$(x_i-x_m)^2$	y	ŷ	yi-ŷ	$(yi-ŷ)^2$	sy/x	sb	V'b	t-value (f=4)
-7.696	1.200	-11.513	-11.409	-0.104	0.011	0.252	0.148	0.011	1.206
-7.003	0.162	-10.820	-10.803	0.017	0.000				
-6.310	0.085	-9.903	-10.197	0.293	0.086				
-5.394	1.457	-9.567	-9.396	0.171	0.029				
X_m =-6.6007		$\sum(x_i-x_m)^2$ = 2.904				$\sum(yi-ŷ)^2$ =0.127			

pH

x	$(x_i-x_m)^2$	y	ŷ	yi-ŷ	$(yi-ŷ)^2$	sy/x	sb	V'b	t-value (f=2)
4.000	1.000	-4.699	-4.700	0.001	0.000	0.004	0.003	0.004	155.687
5.000	0.000	-5.398	-5.400	0.002	0.000				
6.000	1.000	-6.097	-6.100	0.003	0.000				
	X_m = 5.00	$\sum(x_i-x_m)^2$ = 2.000			$\sum(yi-ŷ)^2$ =0.127				

Equations

Standard deviation of the slope (s_b)

$$s_{x/y} = \sqrt{\frac{\Sigma(y_i - \hat{y})^2}{n-2}} \qquad s_b = \frac{s_{x/y}}{\sqrt{\Sigma(x_i - x_m)^2}}$$

Where y_i = the actual y- value; $\hat{y}$ = the y-value calculated from the regression equation, x_i = the individual x-values and x_m = the arithmetic mean of the x-values

Testing slope significance

$$V'_b = \frac{(s_{b1}^2 + s_{b2}^2)}{2} \qquad t = \frac{|b_1 - b2|}{\sqrt{V'_b}}$$

Were the V'b is the average variance and b_1 is slope 1 and b_2 is slope 2; f = 2x n-4 degrees of freedom

Appendix E. Supporting data

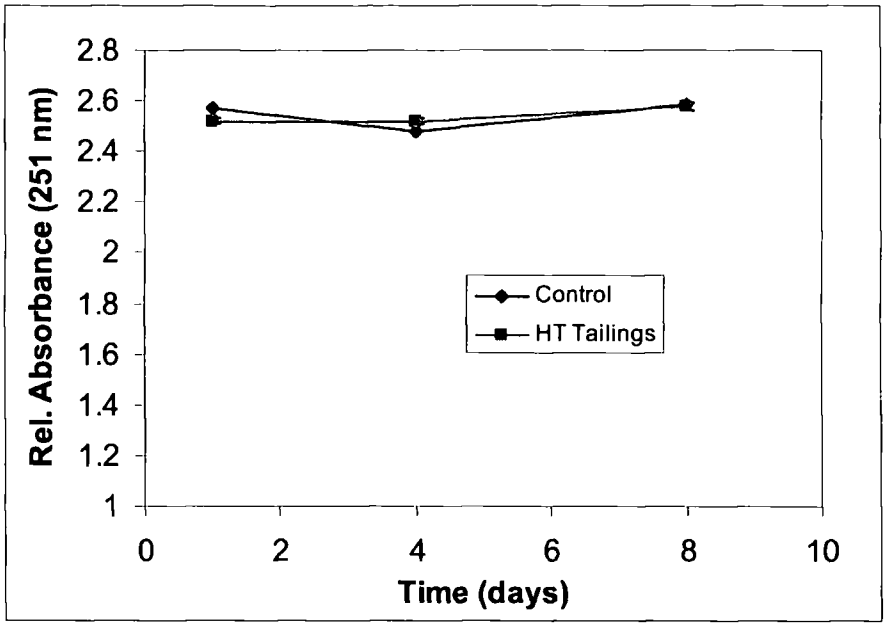

Figure E-1 Relative absorbance measured at 251 nm for control benzoquinone samples and those reacted with HT tailings for 8 days

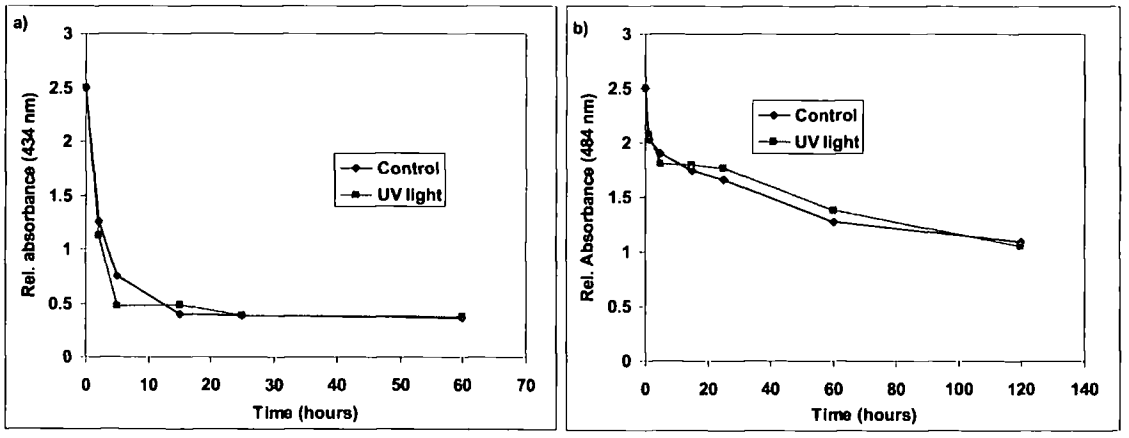

Figure E-2 Relative absorbance at a) 434 nm (AY 36) and b) 484 nm (AO 7) for samples reacted with the dye solution with under UV –light and in the dark (control)

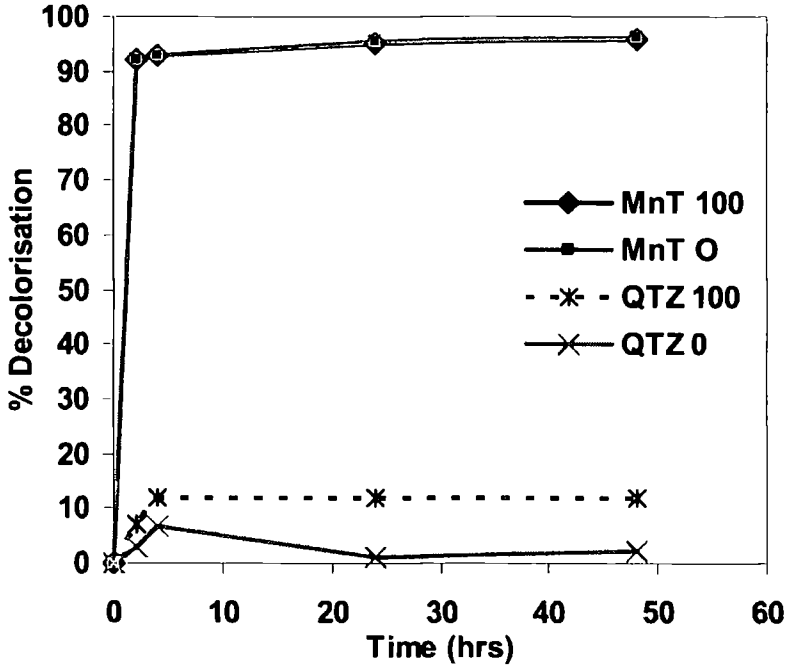

Figure E-3 Percentage decolourisation of AY 36 reacted with the Mn tailings (MnT) and a quartz control (QTZ) in a 0.2 M, pH 4 acetate buffer containing no salt (0) and 100 mM (100) NaCl. Error bars maybe smaller than symbols

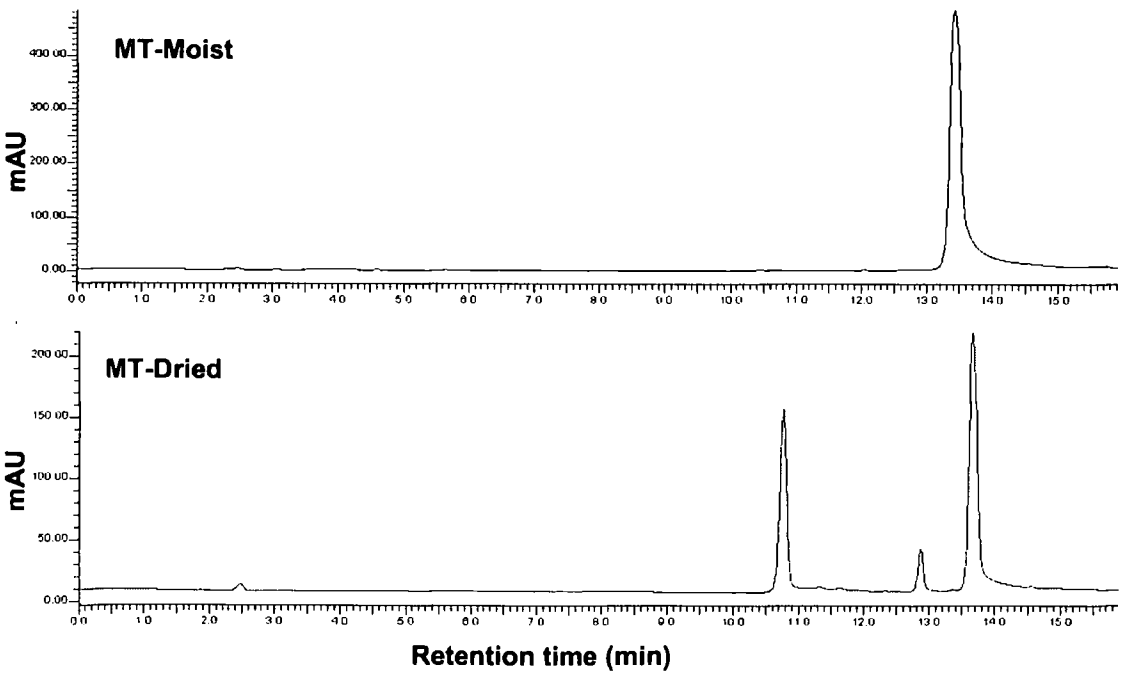

Figure E-4 Chromatograms of cyclohexane extracts from moist and dried MT tailings spiked with anthracene. showing peaks representing anthracene (AC) and anthraquinone (AQ).

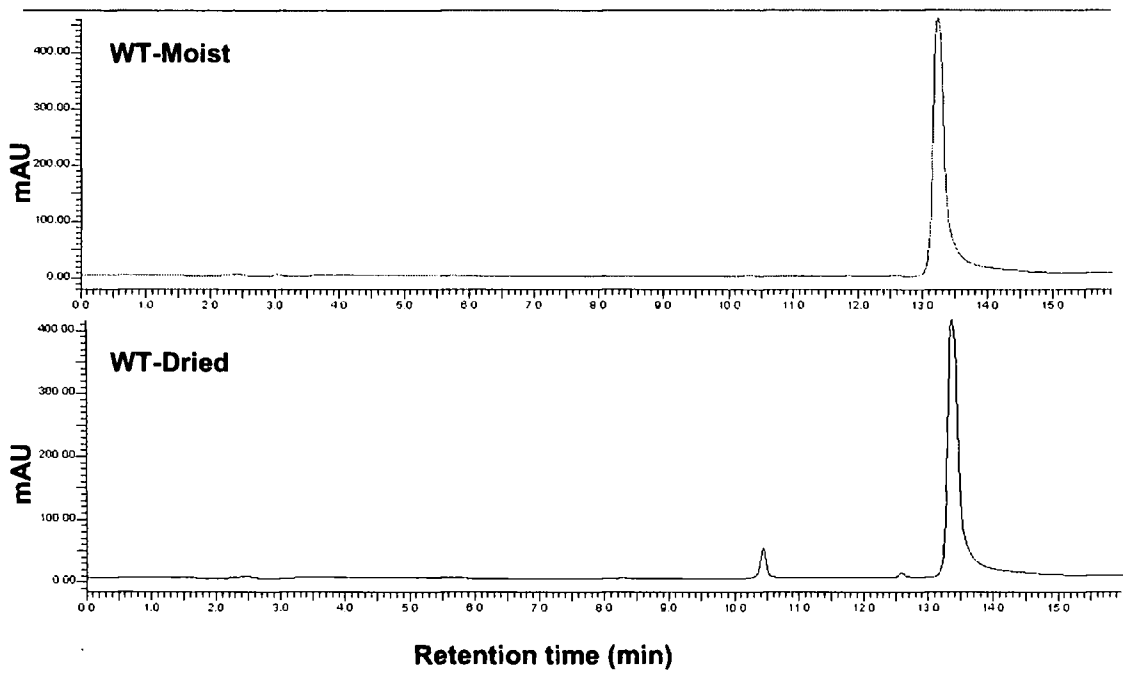

Figure E-5 Chromatograms of cyclohexane extracts from moist and dried WT tailings spiked with anthracene. showing peaks representing anthracene (AC) and anthraquinone (AQ).

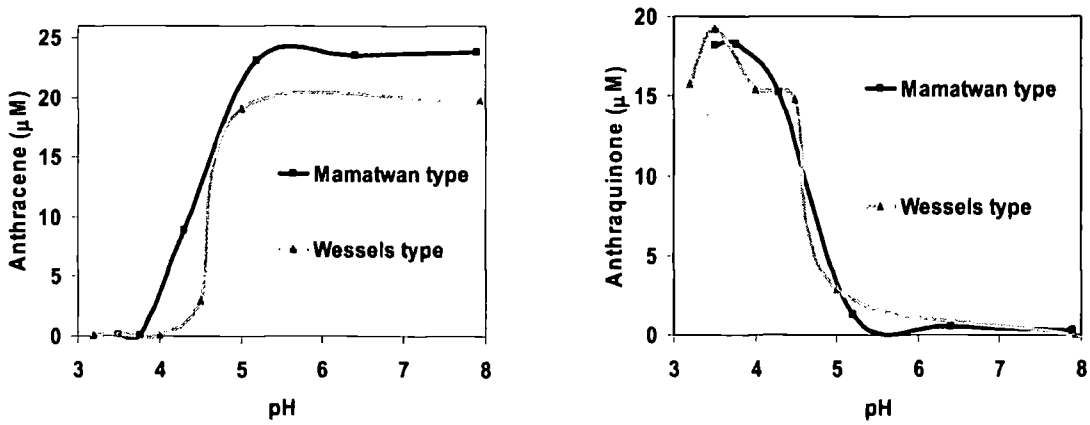

Figure E-6 a) Anthracene (AC) and b) anthraquinone (AQ) concentrations after reacting anthracene with the Mamatwan and Wessels type tailings in a series of pH adjusted acetate buffers.